Event Generators for FCC-ee

DESY. HELMHOLTZ

Universität Hamburg
DER FORSCHUNG | DER LEHRE | DER BILDUNG

CLUSTER OF EXCELLENCE
QUANTUM UNIVERSE

LoopFest XXIV

Hosted by Brookhaven National Laboratory
May 27–29, 2026

LOOPFEST 2026
BNL
BROOKHAVEN
NATIONAL LABORATORY

Jürgen R. Reuter

DESY.

(EW) Precision Program at FCC-ee

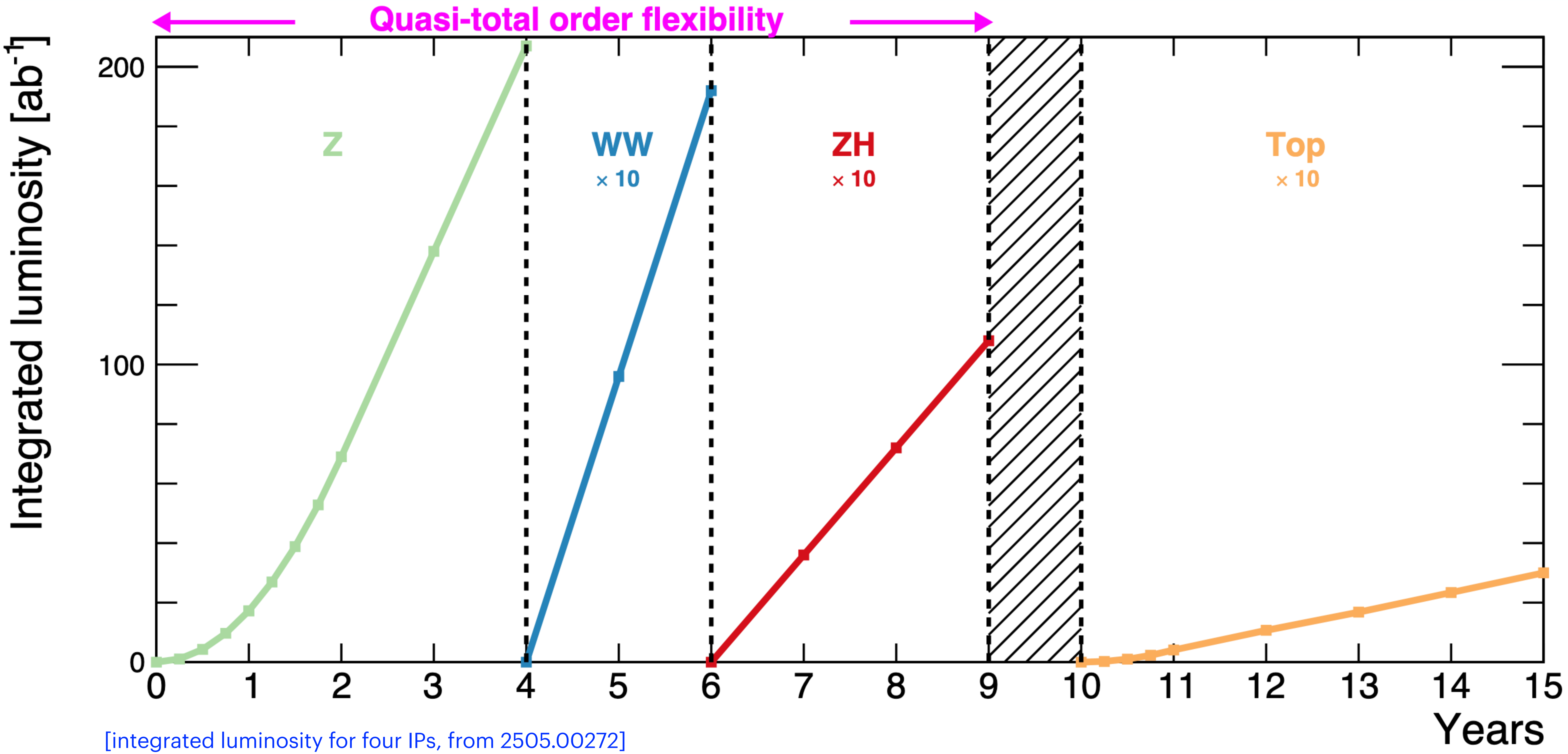

[integrated luminosity for four IPs, from 2505.00272]

Physics program to be simulated

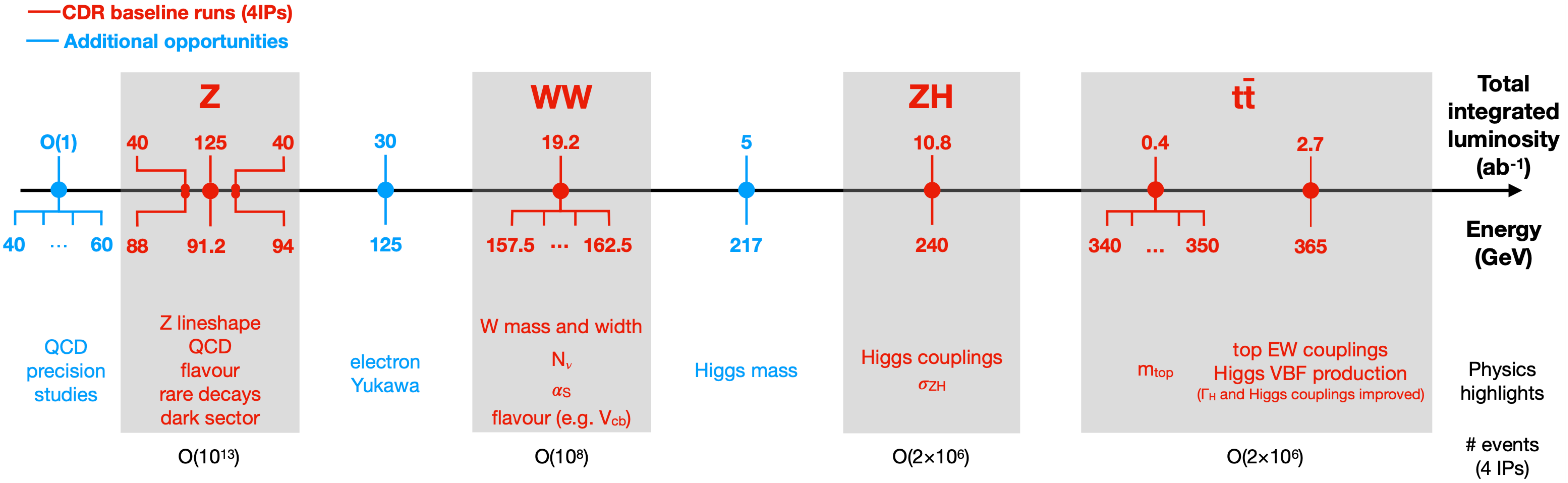

Why are event generators important? Because all our forward simulation chain depends on them!

Why are event generators non-trivial? Because they contain *all* our knowledge of particle physics!

Physics program to be simulated

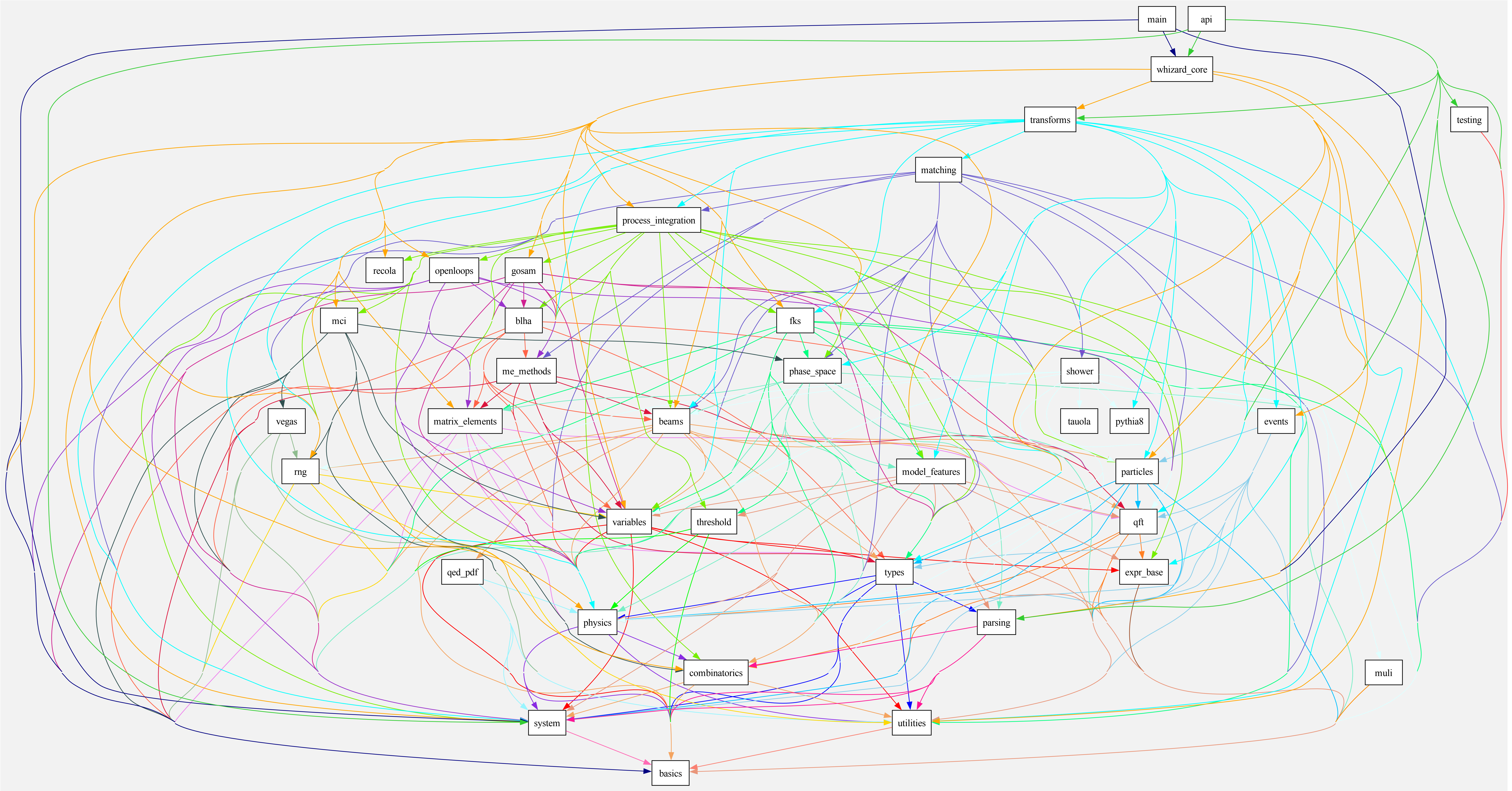

Disclaimer:

- Many different aspects cannot be covered in 25 min
- MC authors are often generalists, meaning not experts in anything

The importance of MC event generators

Why are event generators important? Because all our forward simulation chain depends on them!

Why are event generators non-trivial? Because they contain *all* our knowledge of particle physics!

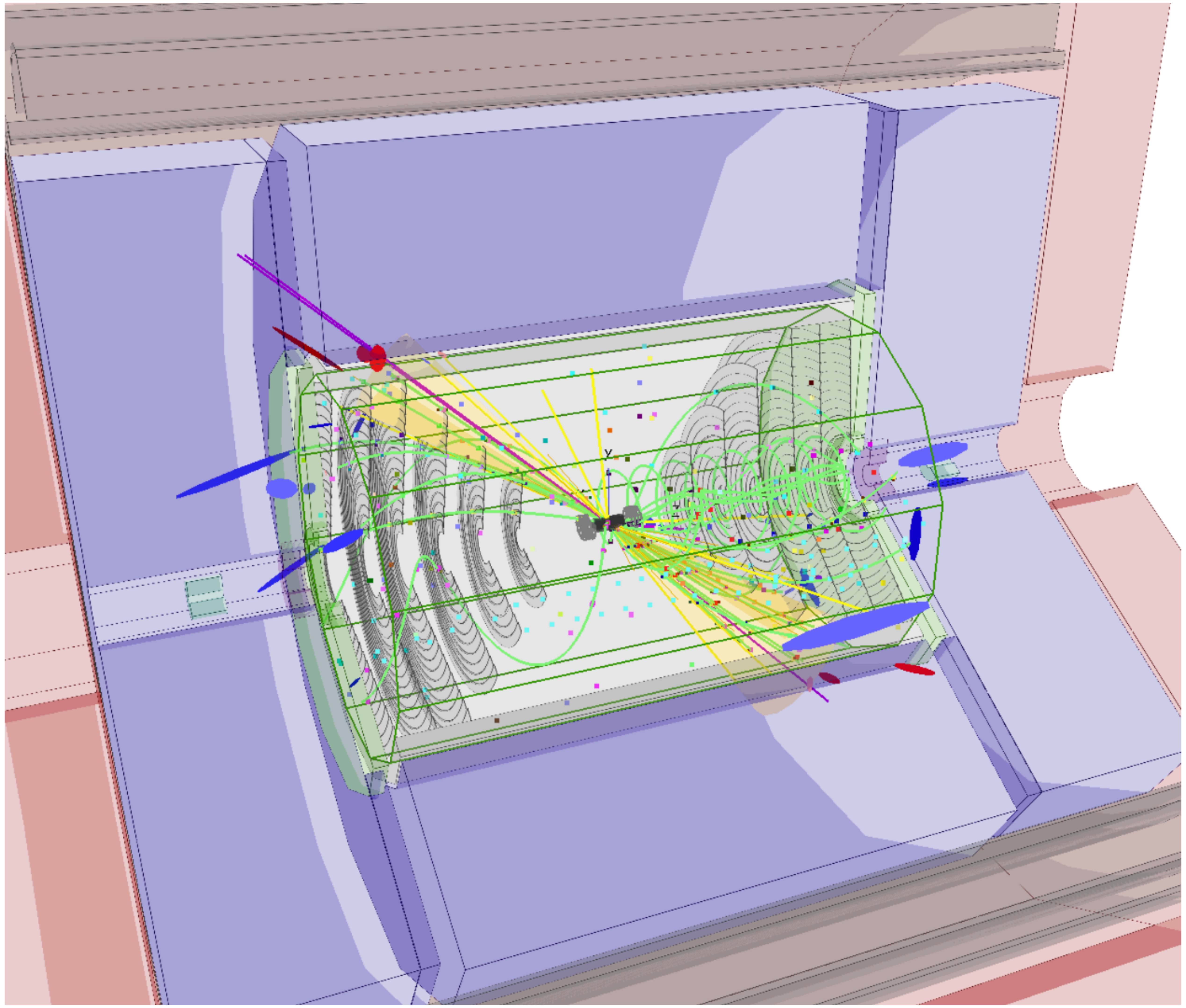

The importance of MC event generators

Why are event generators important? Because all our forward simulation chain depends on them!

Why are event generators non-trivial? Because they contain *all* our knowledge of particle physics!

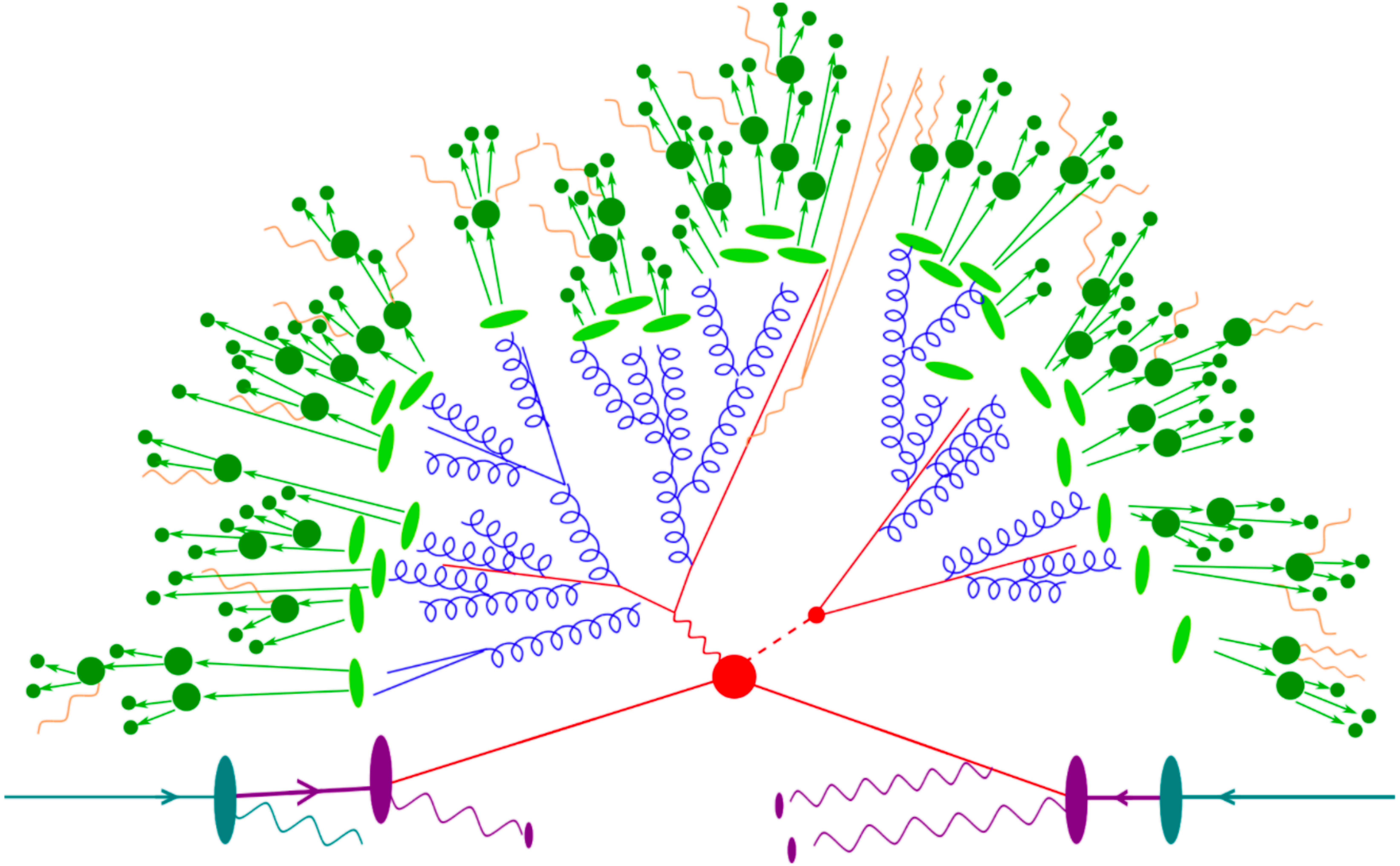

Image by Frank Siegert

The importance of MC event generators

Why are event generators important? Because all our forward simulation chain depends on them!

Why are event generators non-trivial? Because they contain *all* our knowledge of particle physics!

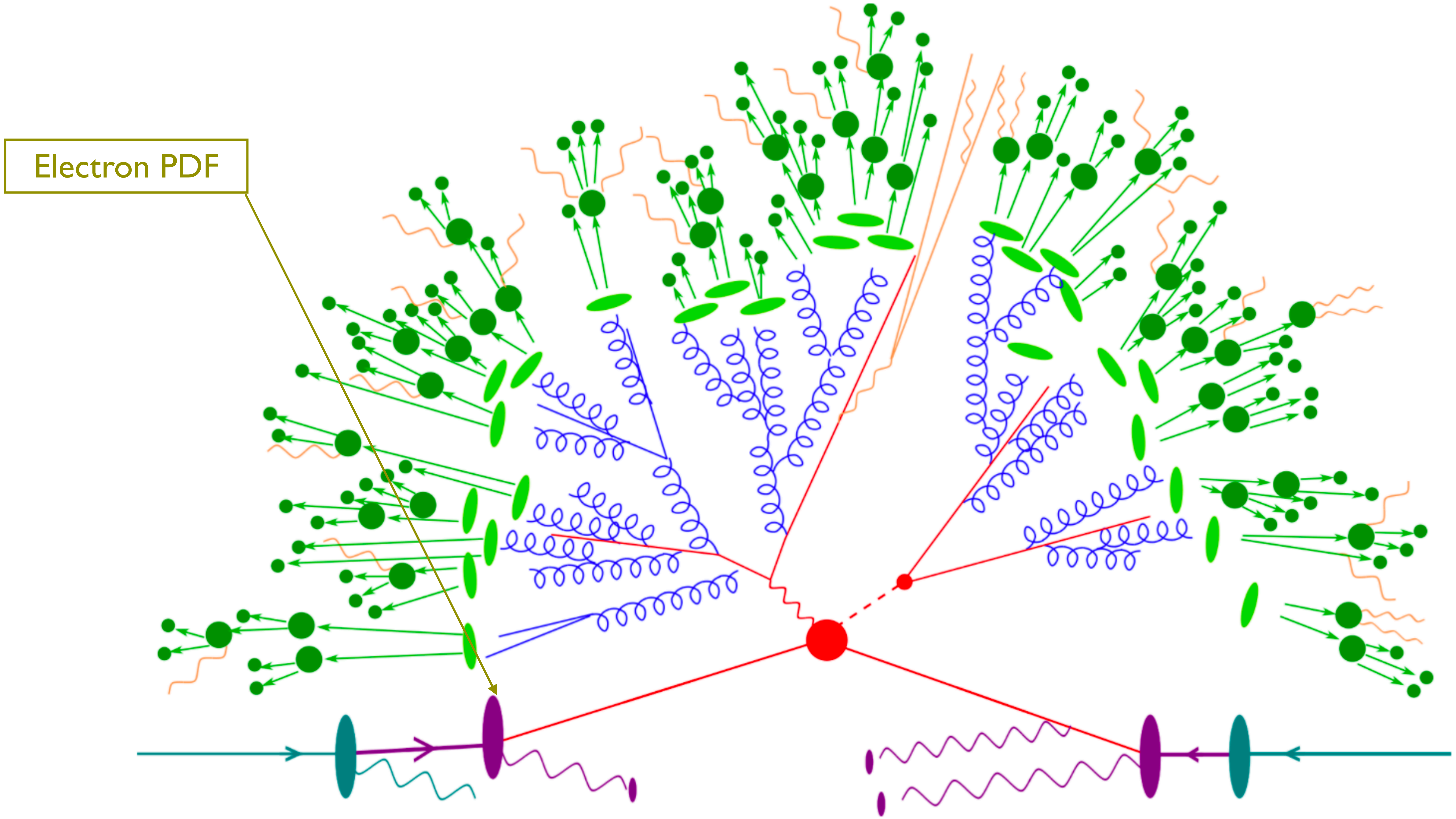

Image by Frank Siegert

The importance of MC event generators

Why are event generators important? Because all our forward simulation chain depends on them!

Why are event generators non-trivial? Because they contain *all* our knowledge of particle physics!

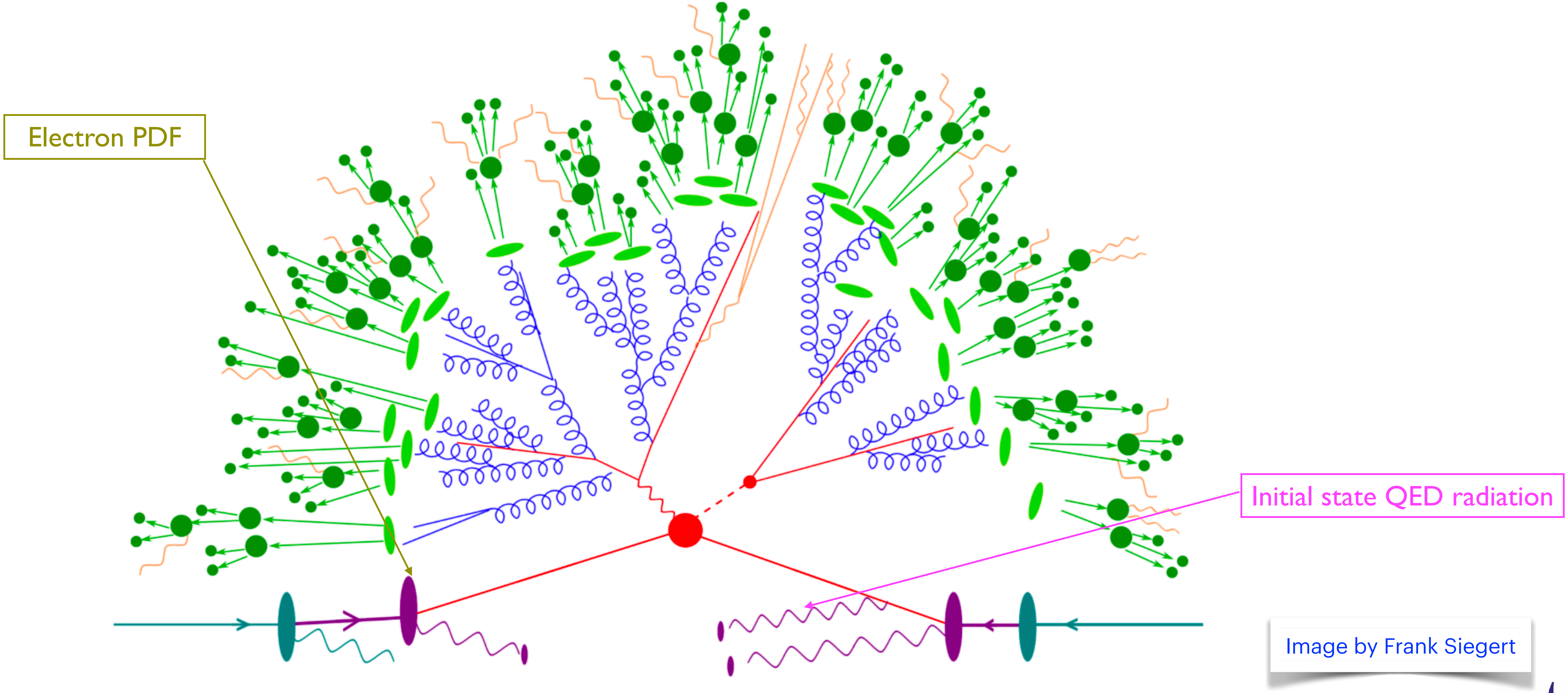

The importance of MC event generators

Why are event generators important? Because all our forward simulation chain depends on them!

Why are event generators non-trivial? Because they contain *all* our knowledge of particle physics!

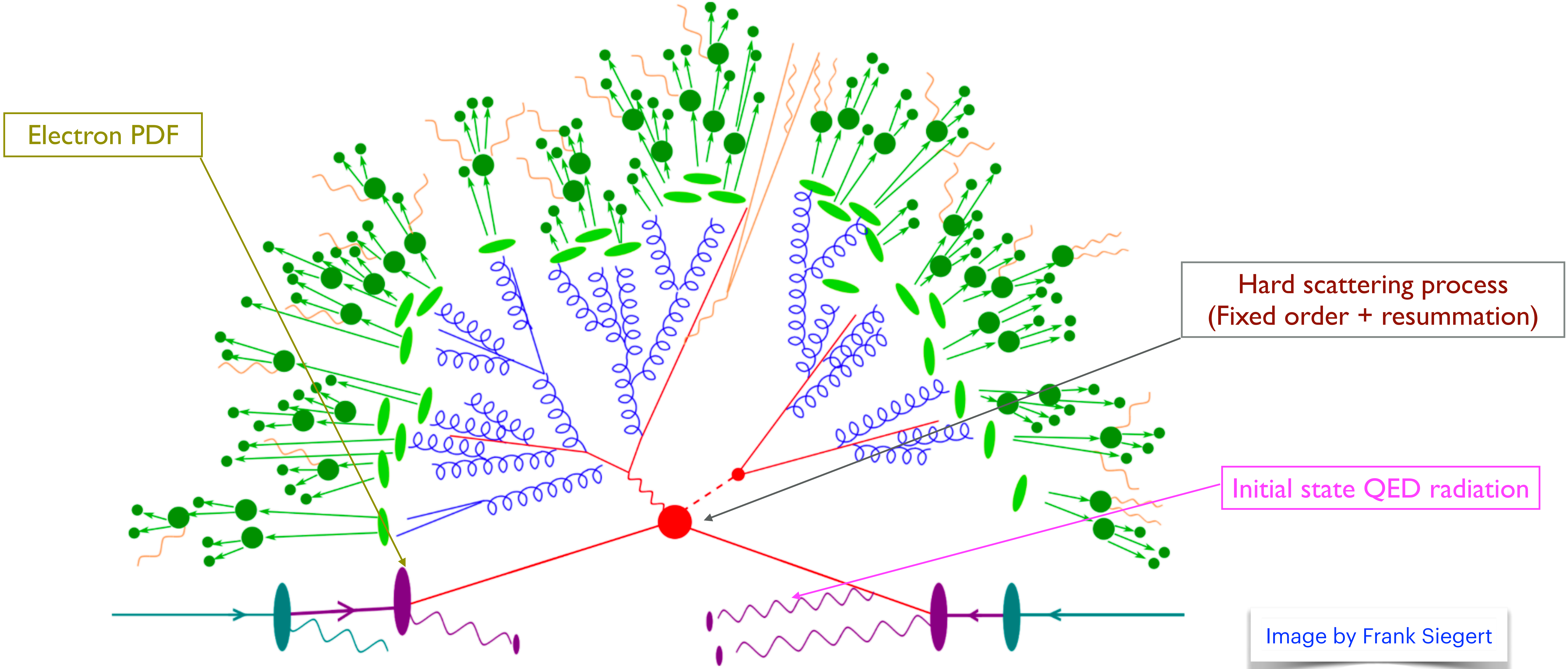

The importance of MC event generators

Why are event generators important? Because all our forward simulation chain depends on them!

Why are event generators non-trivial? Because they contain *all* our knowledge of particle physics!

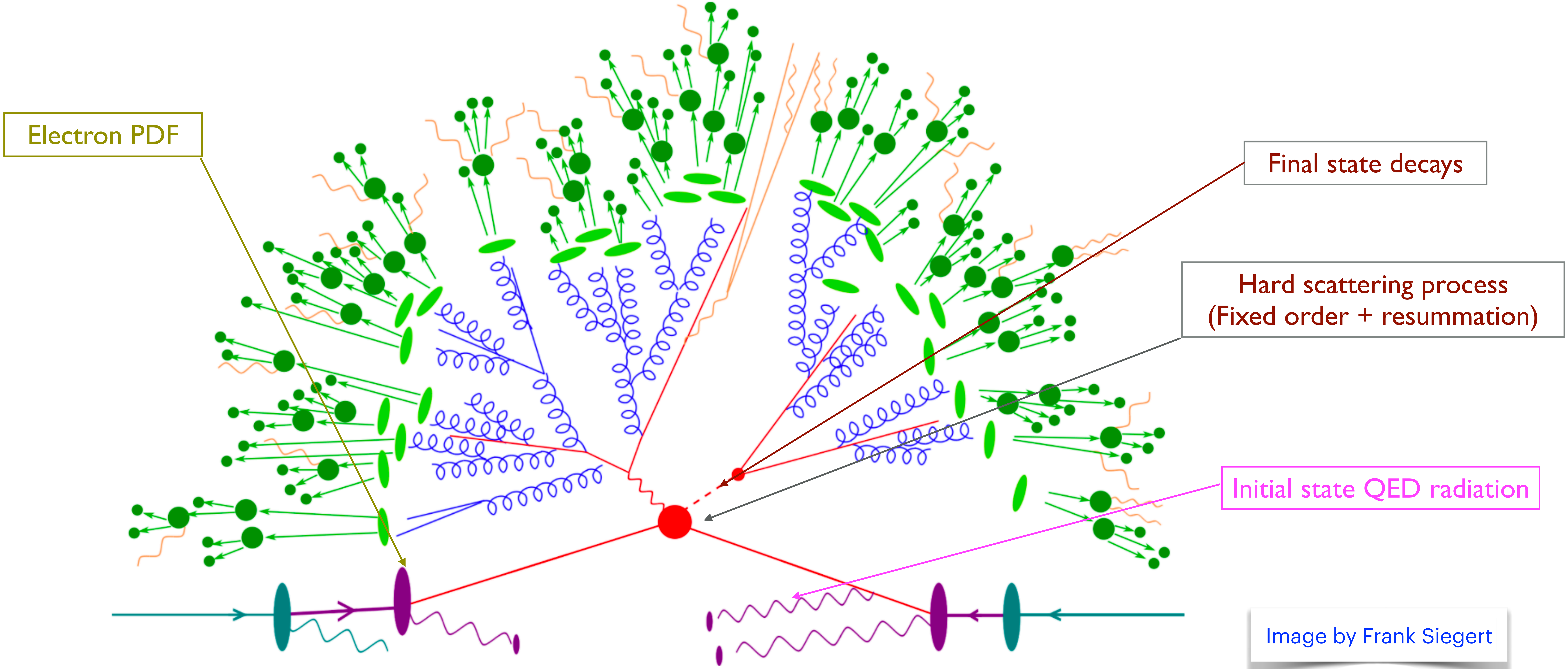

Image by Frank Siegert

The importance of MC event generators

Why are event generators important? Because all our forward simulation chain depends on them!

Why are event generators non-trivial? Because they contain *all* our knowledge of particle physics!

The importance of MC event generators

Why are event generators important? Because all our forward simulation chain depends on them!

Why are event generators non-trivial? Because they contain *all* our knowledge of particle physics!

The importance of MC event generators

Why are event generators important? Because all our forward simulation chain depends on them!

Why are event generators non-trivial? Because they contain *all* our knowledge of particle physics!

The importance of MC event generators

Why are event generators important? Because all our forward simulation chain depends on them!

Why are event generators non-trivial? Because they contain *all* our knowledge of particle physics!

The importance of MC event generators

Why are event generators important? Because all our forward simulation chain depends on them!

Why are event generators non-trivial? Because they contain *all* our knowledge of particle physics!

The importance of MC event generators

Why are event generators important? Because all our forward simulation chain depends on them!

Why are event generators non-trivial? Because they contain *all* our knowledge of particle physics!

Image by Frank Siegert

The importance of MC event generators

Why are event generators important? Because all our forward simulation chain depends on them!

Why are event generators non-trivial? Because they contain *all* our knowledge of particle physics!

Needs for MC generators for e^+e^-

- Experience from LEP, ILC TDR+250 GeV full simulation, CLIC + CEPC simulation samples towards FCC-ee
- ECFA Higgs / Top / EW factory study: MC effort, several dedicated workshops
- “FCC PED Physics WG for Reference Design Phase”, “Gearing up for FCC @ CERN”

Process Specific

RacoonWW

KKCM

YFSWW

TAUOLA

KoralW

BabaYaga@NLO

General Purpose MC

MadGraph5_aMC@NLO

SHERPA

PYTHIA

HERWIG7

WHIZARD

cf. also talks by Stefan Höche, Giovanni Stagnitto & Francesco Ucci

from Alan Price, 2nd ECFA HF WS, Paestum, 2023

The vice and virtue of FCC-ee

Observable	present value	±	uncertainty	FCC-ee Stat.	FCC-ee Syst.	Comment and leading uncertainty
m_Z (keV)	91 187 600	±	2000	**4**	100	From Z line shape scan Beam energy calibration
Γ_Z (keV)	2 495 500	±	2300	**4**	12	From Z line shape scan Beam energy calibration
$\sin^2\theta_W^{\text{eff}}$ ($\times 10^6$)	231,480	±	160	**1.2**	1.2	From $A_{FB}^{\mu\mu}$ at Z peak Beam energy calibration
$1/\alpha_{\text{QED}}(m_Z^2)$ ($\times 10^3$)	128 952	±	14	**3.9** **0.8**	small tbc	From $A_{FB}^{\mu\mu}$ off peak From $A_{FB}^{\mu\mu}$ on peak QED&EW uncert. dominate
R_ℓ^Z ($\times 10^3$)	20 767	±	25	**0.05**	0.05	Ratio of hadrons to leptons Acceptance for leptons
$\alpha_S(m_Z^2)$ ($\times 10^4$)	1 196	±	30	**0.1**	1	Combined R_ℓ^Z, Γ_{tot}^Z, σ_{had}^0 fit
σ_{had}^0 ($\times 10^3$) (nb)	41 480.2	±	32.5	**0.03**	0.8	Peak hadronic cross section Luminosity measurement
N_ν($\times 10^3$)	2 996.3	±	7.4	**0.09**	0.12	Z peak cross sections Luminosity measurement
R_b ($\times 10^6$)	216 290	±	660	**0.25**	0.3	Ratio of $b\bar{b}$ to hadrons
$A_{FB}^{b,0}$ ($\times 10^4$)	992	±	16	**0.04**	0.04	b-quark asymmetry at Z pole From jet charge
$A_{FB}^{\text{pol},\tau}$ ($\times 10^4$)	1 498	±	49	**0.07**	0.2	τ polarisation asymmetry τ decay physics
τ lifetime (fs)	290.3	±	0.5	**0.001**	0.005	ISR, τ mass
τ mass (MeV)	1 776.93	±	0.09	**0.002**	0.02	estimator bias, ISR, FSR
τ leptonic ($\mu\nu_\mu\nu_\tau$) BR (%)	17.38	±	0.04	**0.00007**	0.003	PID, π^0 efficiency
m_W (MeV)	80 360.2	±	9.9	**0.18**	0.16	From WW threshold scan Beam energy calibration
Γ_W (MeV)	2 085	±	42	**0.27**	0.2	From WW threshold scan Beam energy calibration
$\alpha_S(m_W^2)$ ($\times 10^4$)	1 010	±	270	**2**	2	Combined R_ℓ^W, Γ_{tot}^W fit
N_ν ($\times 10^3$)	2 920	±	50	**0.5**	small	Ratio of invis. to leptonic in radiative Z returns
m_{top} (MeV)	172 570	±	290	**4.2**	4.9	From $t\bar{t}$ threshold scan QCD uncert. dominate
Γ_{top} (MeV)	1 420	±	190	**10**	6	From $t\bar{t}$ threshold scan QCD uncert. dominate
$\lambda_{\text{top}}/\lambda_{\text{top}}^{\text{SM}}$	1.2	±	0.3	**0.015**	0.015	From $t\bar{t}$ threshold scan QCD uncert. dominate
ttZ couplings		±	30%	**0.5–1.5 %**	small	From $\sqrt{s} = 365$ GeV run

Tiny experimental uncertainties, improved by up to 3 orders of magnitude!!!

True bottleneck: theory uncertainties => disruptive advances needed

References and summaries, physics:

- FCC-ee Feasibility Study, Vol. 1, Physics etc., 2505.00272
- [LC Vision Report, 2503.19983]
- PPG Physics Briefing Book, 2511.03883, uncertainty Spreadsheet (link)
- Theory requirements for … precision @FCC-ee, Heinemeyer/Jadach/JRR, 2106.11802

References and summaries, MC generators:

- ECFA Higgs-Top-EW Factory Report, 2506.15390 , Sec. 3.2
- Encyclopedia of Particle Physics: MC gen., JRR, 2509.21611
- Snowmass Event Generator report, Campbell et al., 2203.11110
- HEP Primer on MC ecosystem: Bothmann et al., 2605.16036
- and many more …

General remarks

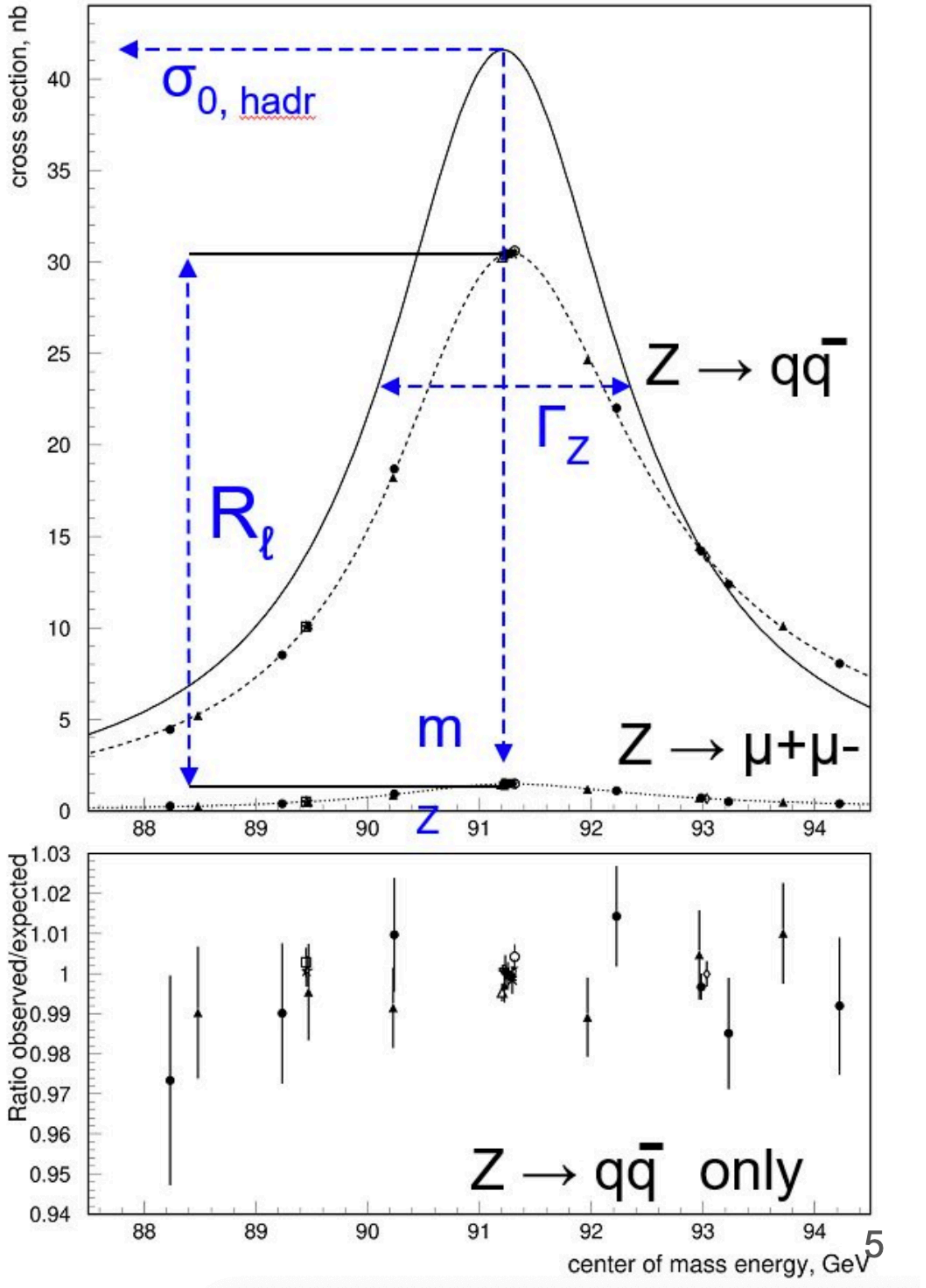

Differences to LHC:

- No triggers (!), all events recorded
- Z pole: in a single year 26x all of LHC data (!!!) with 40 nb signal cross section
- No shadowing of physics effects through proton PDFs
- Detectors are much more granular (ECAL photon accept./resol. better 400 MeV)
- Electroweak production: NNLO EW as or more important than NN(N)LO QCD
- All different signal + background processes interconnected through interference
- Thresholds with very large effects from QED (Z, W^+W^-) or QCD ($t\bar{t}$)

General remarks

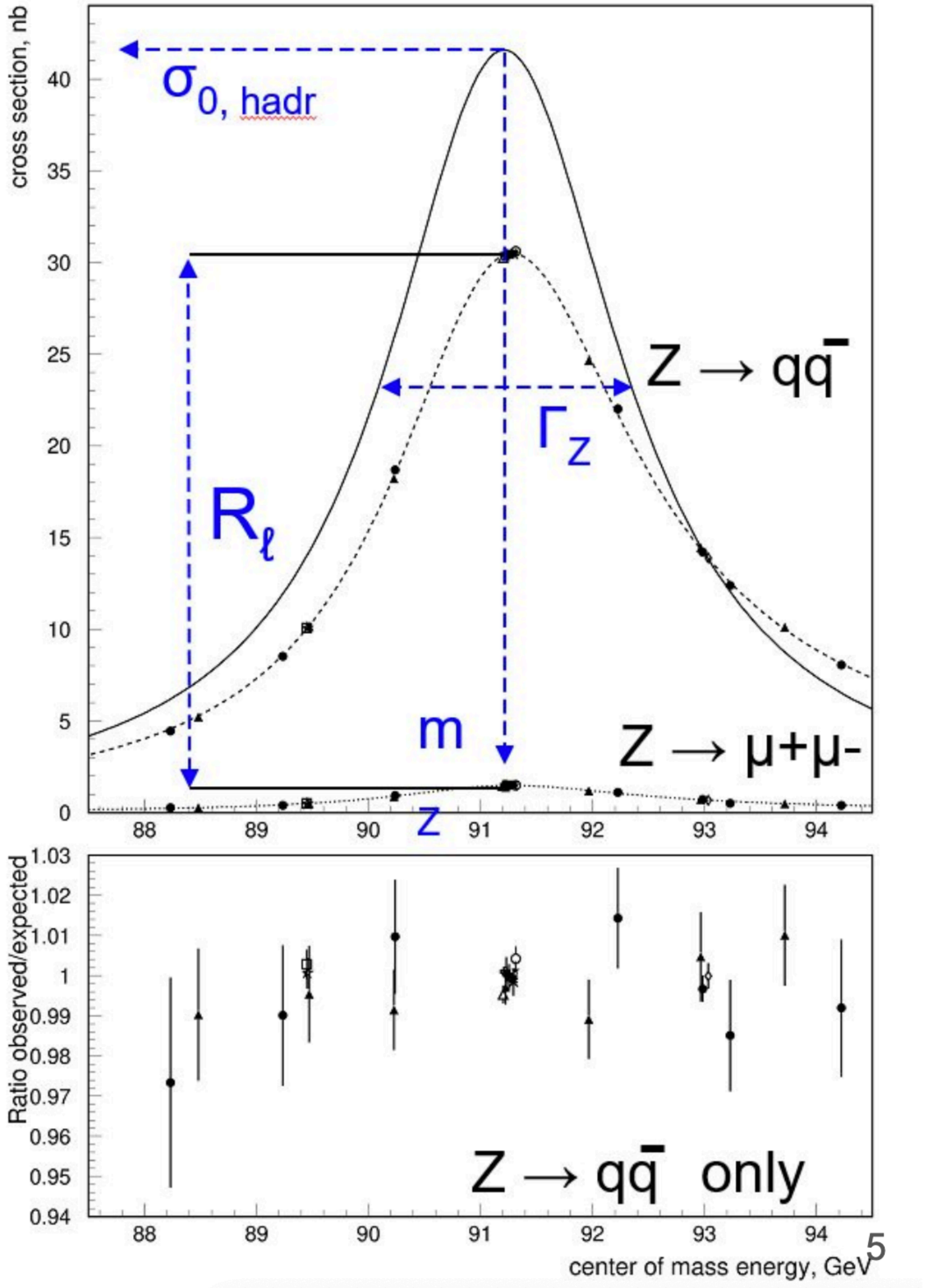

Differences to LHC:

- No triggers (!), all events recorded
- Z pole: in a single year 26x all of LHC data (!!!) with 40 nb signal cross section
- No shadowing of physics effects through proton PDFs
- Detectors are much more granular (ECAL photon accept./resol. better 400 MeV)
- Electroweak production: NNLO EW as or more important than NN(N)LO QCD
- All different signal + background processes interconnected through interference
- Thresholds with very large effects from QED (Z, W^+W^-) or QCD ($t\bar{t}$)

- LEP/SLC: theory predictions as "pseudo-observables (PO)" ("hard process")
- Relate PO to data via deconvolution/unfolding QED radiation
- Worked for LEP/SLC precision, [more] difficult for FCC-ee precision
- Very likely: "PO approach" & "MC approach"
- MC approach: include all higher/est order corrections in (cf. e.g. S. Frixione, FCC workshop Annecy 2024, MITP workshop on EW corrections, Mainz, May 2026)

MC: Fixed-Order Perturbation Theory

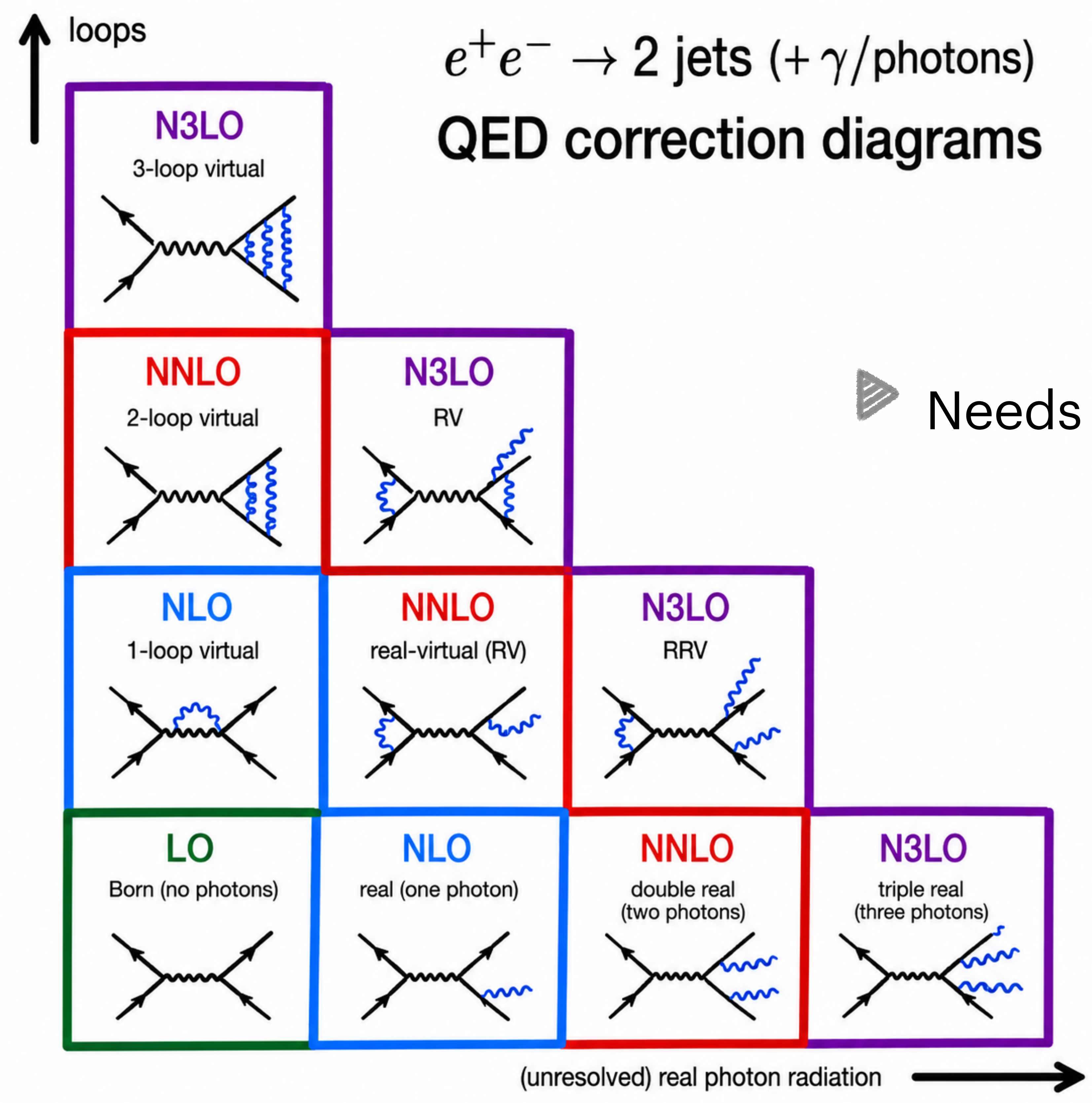

$e^+e^- \to$ 2 jets $(+\gamma/\text{photons})$

QED correction diagrams

- LHC progress: NLO QCD + EW automation: Sherpa, MG5, Whizard, ...
- One-Loop Providers: BlackHat, GoSam, MadLoop, OpenLoops, Recola
- Active work on NNLO [QCD] automation

▷ Needs $e^+e^- \to 2f, 3f, 4f, 5f, 6f, [7-10f]$ @ *NLO QCD* $\oplus$ *EW* (arbitr. cuts, fully differential)

	$\sigma_{\rm LO}$[fb]	$\sigma_{\rm NLO}$[fb]	K
$e^+e^- \to jj$	622.737(8)	639.39(5)	1.027
$e^+e^- \to jjj$	340.6(5)	317.8(5)	0.933
$e^+e^- \to jjjj$	105.0(3)	104.2(4)	0.992
$e^+e^- \to jjjjj$	22.33(5)	24.57(7)	1.100
$e^+e^- \to jjjjjj$	3.583(17)	4.46(4)	1.245
$e^+e^- \to t\bar{t}$	166.37(12)	174.55(20)	1.049
$e^+e^- \to t\bar{t}j$	48.12(5)	53.41(7)	1.110
$e^+e^- \to t\bar{t}jj$	8.592(19)	10.526(21)	1.225
$e^+e^- \to t\bar{t}jjj$	1.035(4)	1.405(5)	1.357

arXiv: 2104.11141

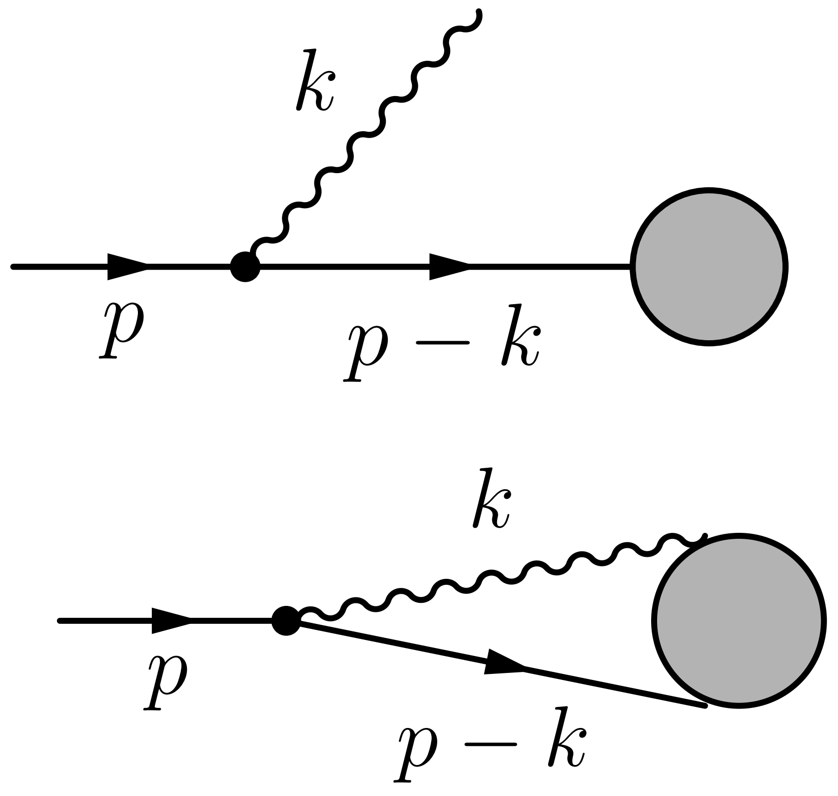

▷ IR singularities cancelled in MC numerically in subtraction formalism

FKS [Frixione/Kunszt/Signer, '96], CS-Dipoles [Catani/Seymour, '98]

IR divergencies in MC: subtraction formalisms

- General structure of NLO cross section:

$$d\sigma_n^{\rm NLO} = d\Phi_n \mathcal{B}_n \quad + \quad d\Phi_n \mathcal{V}_n \quad + \quad d\Phi_{n+1} \mathcal{R}_{n+1}$$

Born approximation — renormalized virtual correction, IR-divergent — real correction, IR-divergent

$$d\sigma_n^{\rm NLO} = d\Phi_n \left[\mathcal{B}_n + \mathcal{V}_n + \mathcal{B}_n \otimes S \right] + d\Phi_{n+1} \left[\mathcal{R}_{n+1} - \mathcal{B}_n \otimes dS \right]$$

IR divergencies in MC: subtraction formalisms

- General structure of NLO cross section:

$$d\sigma_n^{\rm NLO} = d\Phi_n \mathcal{B}_n \quad + \quad d\Phi_n \mathcal{V}_n \quad + \quad d\Phi_{n+1} \mathcal{R}_{n+1}$$

Born approximation — renormalized virtual correction, IR-divergent — real correction, IR-divergent

$$d\sigma_n^{\rm NLO} = d\Phi_n \left[\mathcal{B}_n + \mathcal{V}_n + \mathcal{B}_n \otimes S \right] + d\Phi_{n+1} \left[\mathcal{R}_{n+1} - \mathcal{B}_n \otimes dS \right]$$

Three major bottlenecks to go to NNLO

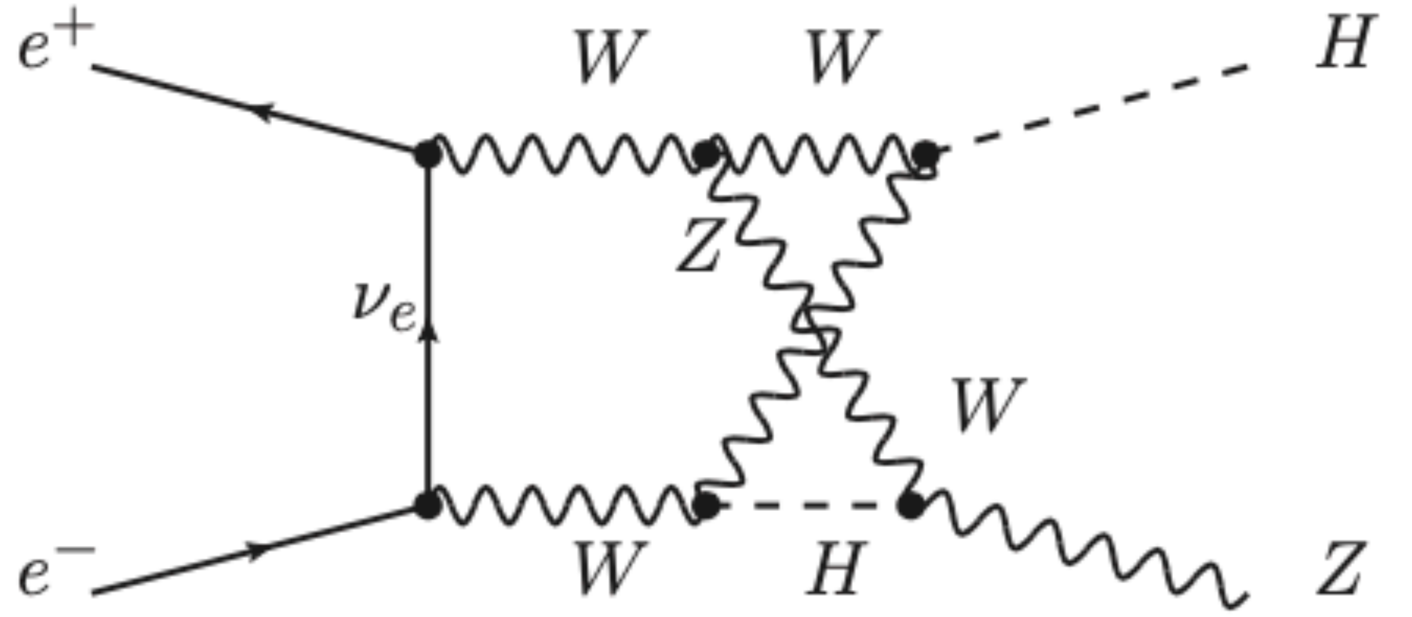

- Virtual integrals with many mass scales / off-shell legs
- Process-independent automated NNLO subtraction [for QCD in reach!]
  especially: full-fledged soft+collinear NNLO EW subtraction
- Negative weights: bad at NLO, worse at NNLO

... and, of course, efficiency and speed (numerical stability, quadruple precision [not liked by GPUs] ....)

Resonance mappings for NLO processes

- Amplitudes (except for pure QCD/QED) contain resonances (*Z, W, H, t*)
- In general: resonance masses *not* respected by modified kinematics of subtraction terms

- Algorithm to include resonance histories [Ježo/Nason, 1509.09071]
- Most important for narrow resonances ($H \to bb$)

  - $D_H^{\text{Born}} = \left[\left(\bar{p}_{bb}^2 - m_H^2\right)^2 + m_H^2\Gamma_H^2\right]^{-1},$
  - $D_H^{\text{Real}} = \left[\left(p_{bbg}^2 - m_H^2\right)^2 + m_H^2\Gamma_H^2\right]^{-1}$

$$p_{bbg}^2 = \bar{p}_{bb}^2 + \Delta_{bbg}^2 \qquad \frac{D_H^{\text{Born}}}{D_H^{\text{Real}}} \overset{\bar{p}_{bb}^2 \to m_H^2}{=} 1 + \frac{\Delta_{bbg}^4}{m_H^2\Gamma_H^2}$$

Resonance mappings for NLO processes

- Amplitudes (except for pure QCD/QED) contain resonances (*Z, W, H, t*)
- In general: resonance masses *not* respected by modified kinematics of subtraction terms

- Algorithm to include resonance histories [Ježo/Nason, 1509.09071]
- Most important for narrow resonances ($H \to bb$)

▸ $D_H^{\text{Born}} = \left[\left(\bar{p}_{bb}^2 - m_H^2\right)^2 + m_H^2\Gamma_H^2\right]^{-1}$,

▸ $D_H^{\text{Real}} = \left[\left(p_{bbg}^2 - m_H^2\right)^2 + m_H^2\Gamma_H^2\right]^{-1}$

$$p_{bbg}^2 = \bar{p}_{bb}^2 + \Delta_{bbg}^2 \qquad \frac{D_H^{\text{Born}}}{D_H^{\text{Real}}} \overset{\bar{p}_{bb}^2 \to m_H^2}{=} 1 + \frac{\Delta_{bbg}^4}{m_H^2\Gamma_H^2}$$

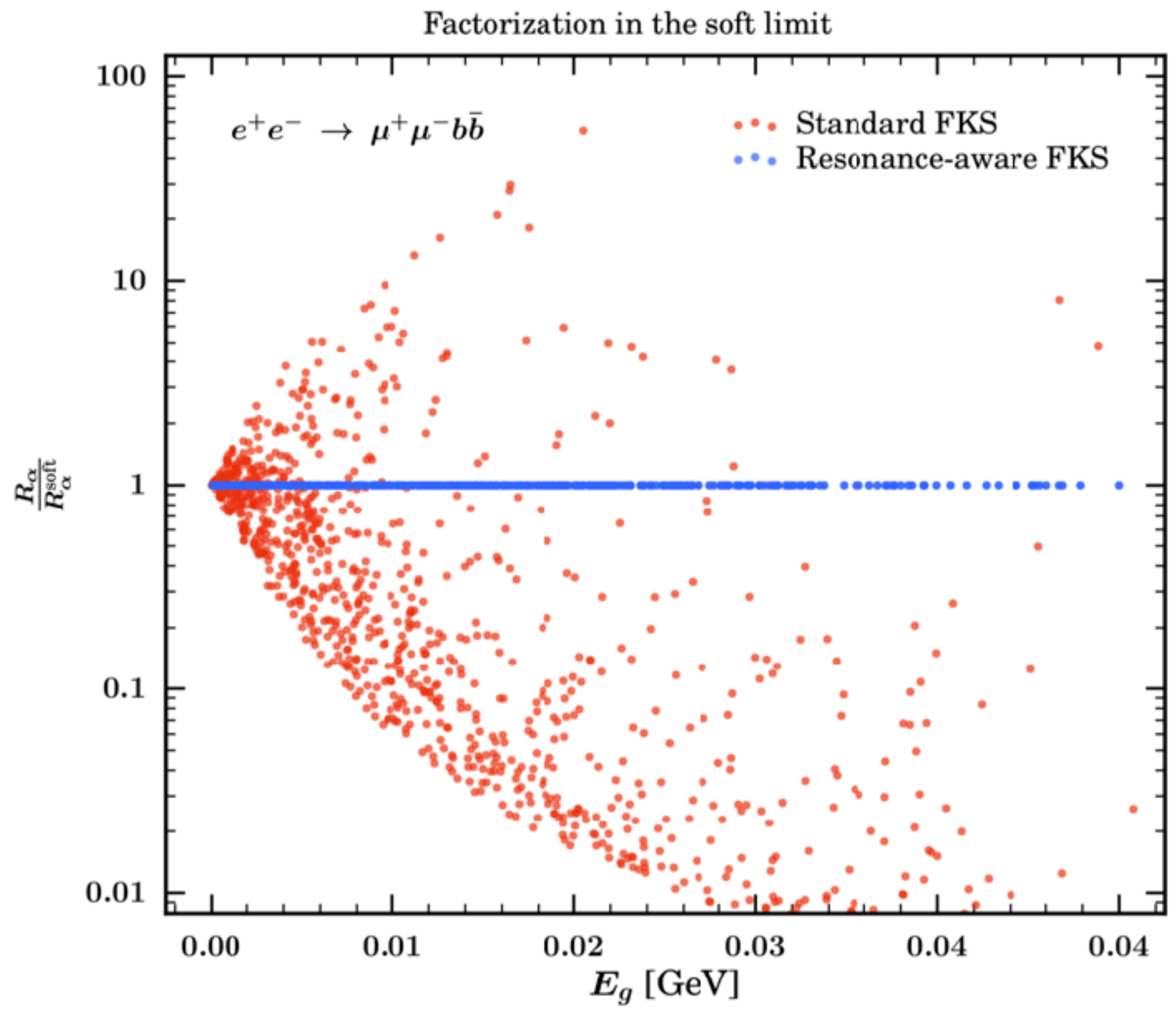

Resonance mappings for NLO processes

- Amplitudes (except for pure QCD/QED) contain resonances (*Z, W, H, t*)
- In general: resonance masses *not* respected by modified kinematics of subtraction terms

- Algorithm to include resonance histories [Ježo/Nason, 1509.09071]
- Most important for narrow resonances ($H \to bb$)

  - $D_H^{\text{Born}} = \left[\left(\bar{p}_{bb}^2 - m_H^2 \right)^2 + m_H^2 \Gamma_H^2 \right]^{-1},$
  - $D_H^{\text{Real}} = \left[\left(p_{bbg}^2 - m_H^2 \right)^2 + m_H^2 \Gamma_H^2 \right]^{-1}$

$$p_{bbg}^2 = \bar{p}_{bb}^2 + \Delta_{bbg}^2 \qquad \frac{D_H^{\text{Born}}}{D_H^{\text{Real}}} \overset{\bar{p}_{bb}^2 \to m_H^2}{=} 1 + \frac{\Delta_{bbg}^4}{m_H^2 \Gamma_H^2}$$

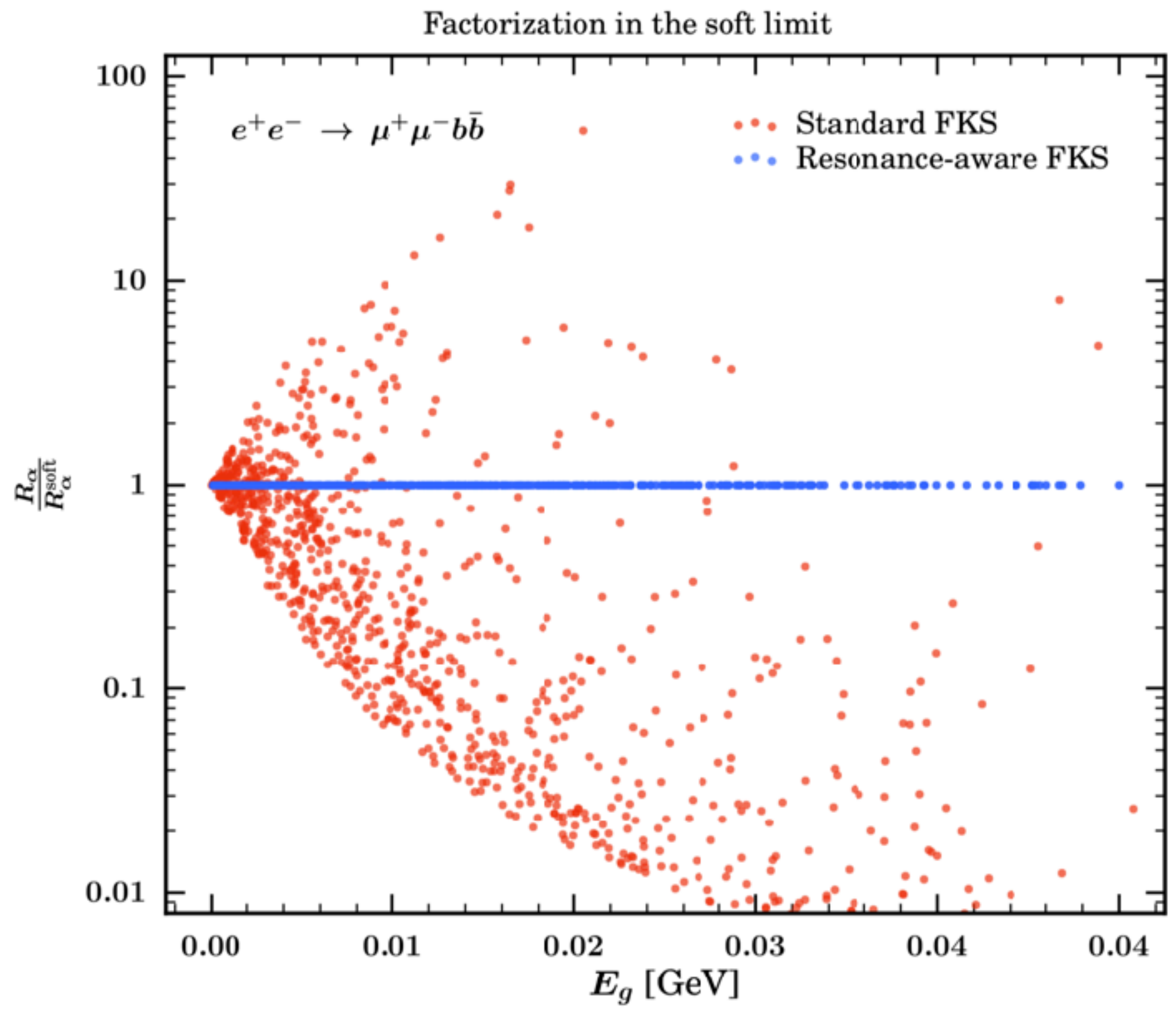

- Whizard complete automatic implementation: example $e^+e^- \to \mu^+\mu^- b\bar{b}$ (ZZ, ZH histories)

It	Calls	Integral[fb]	Error[fb]	Err[%]	Acc	Eff[%]	Chi2	N[It]
1	11988	9.6811847E+00	6.42E+00	66.30	72.60*	0.65		
2	11959	2.8539703E+00	2.35E-01	8.25	9.02*	0.69		
3	11936	2.4907574E+00	6.54E-01	26.25	28.68	0.35		
4	11908	2.7695559E+00	9.67E-01	34.91	38.09	0.30		
5	11874	2.4346151E+00	4.82E-01	19.80	21.57*	0.74		
5	59665	2.7539078E+00	1.97E-01	7.15	17.47	0.74	0.49	5

standard FKS

It	Calls	Integral[fb]	Error[fb]	Err[%]	Acc	Eff[%]	Chi2	N[It]
1	11988	2.9057032E+00	8.35E-02	2.87	3.15*	7.90		
2	11962	2.8591952E+00	5.20E-02	1.82	1.99*	10.91		
3	11936	2.9277880E+00	4.09E-02	1.40	1.52*	14.48		
4	11902	2.8512337E+00	3.98E-02	1.40	1.52*	13.70		
5	11874	2.8855399E+00	3.87E-02	1.34	1.46*	17.15		
5	59662	2.8842006E+00	2.04E-02	0.71	1.72	17.15	0.53	5

FKS with resonance mappings

It works "out of the (black) box" [most of the time]

ee @ 1 TeV, NLO QCD

Process	WHIZARD+OpenLoops σ_{LO} [fb]	WHIZARD+OpenLoops σ_{NLO} [fb]
$e^+e^- \to jj$	622.737(8)	639.39(5)
$e^+e^- \to jjj$	340.6(5)	317.8(5)
$e^+e^- \to jjjj$	105.0(3)	104.2(4)
$e^+e^- \to jjjjj$	22.33(5)	24.57(7)
$e^+e^- \to jjjjjj$	3.583(17)	4.46(4)

$e^+e^- \to t\bar{t}$	166.37(12)	174.55(20)
$e^+e^- \to t\bar{t}j$	48.12(5)	53.41(7)
$e^+e^- \to t\bar{t}jj$	8.592(19)	10.526(21)
$e^+e^- \to t\bar{t}jjj$	1.035(4)	1.405(5)
$e^+e^- \to t\bar{t}t\bar{t}$	$0.6388(8) \cdot 10^{-3}$	$1.1922(11) \cdot 10^{-3}$
$e^+e^- \to t\bar{t}t\bar{t}j$	$2.673(7) \cdot 10^{-5}$	$5.251(11) \cdot 10^{-5}$
$e^+e^- \to t\bar{t}H$	2.020(3)	1.912(3)
$e^+e^- \to t\bar{t}Hj$	$2.536(4) \cdot 10^{-1}$	$2.657(4) \cdot 10^{-1}$
$e^+e^- \to t\bar{t}Hjj$	$2.646(8) \cdot 10^{-2}$	$3.123(9) \cdot 10^{-2}$
$e^+e^- \to t\bar{t}Z$	4.638(3)	4.937(3)
$e^+e^- \to t\bar{t}Zj$	$6.027(9) \cdot 10^{-1}$	$6.921(11) \cdot 10^{-1}$
$e^+e^- \to t\bar{t}Zjj$	$6.436(21) \cdot 10^{-2}$	$8.241(29) \cdot 10^{-2}$
$e^+e^- \to t\bar{t}W^\pm jj$	$2.387(8) \cdot 10^{-4}$	$3.716(10) \cdot 10^{-4}$
$e^+e^- \to t\bar{t}HZ$	$3.623(19) \cdot 10^{-2}$	$3.584(19) \cdot 10^{-2}$
$e^+e^- \to t\bar{t}ZZ$	$3.788(6) \cdot 10^{-2}$	$4.032(7) \cdot 10^{-2}$
$e^+e^- \to t\bar{t}HH$	$1.3650(15) \cdot 10^{-2}$	$1.2168(16) \cdot 10^{-2}$
$e^+e^- \to t\bar{t}W^+W^-$	$1.3672(21) \cdot 10^{-1}$	$1.5385(22) \cdot 10^{-1}$

pp @ 13 TeV, NLO QCD

Process Vector boson (pair) plus jets	WHIZARD σ_{LO}[fb]	WHIZARD σ_{NLO}[fb]	K
$pp \to W^\pm$ *	$1.3749(8) \cdot 10^8$	$1.7696(10) \cdot 10^8$	1.29
$pp \to W^\pm j$ *	$2.046(3) \cdot 10^7$	$2.854(5) \cdot 10^7$	1.39
$pp \to W^\pm jj$	$6.856(12) \cdot 10^6$	$7.814(27) \cdot 10^6$	1.14
$pp \to W^\pm jjj$ †	$1.840(5) \cdot 10^6$	$1.978(7) \cdot 10^6$	1.07
$pp \to Z$	$4.2541(3) \cdot 10^7$	$5.4086(16) \cdot 10^7$	1.27
$pp \to Zj$	$7.215(4) \cdot 10^6$	$9.733(10) \cdot 10^6$	1.35
$pp \to Zjj$	$2.364(5) \cdot 10^6$	$2.676(7) \cdot 10^6$	1.13
$pp \to Zjjj$	$6.381(23) \cdot 10^5$	$6.85(3) \cdot 10^5$	1.07
$pp \to W^+W^-(4f)$	$7.352(10) \cdot 10^4$	$10.268(11) \cdot 10^4$	1.40
$pp \to W^+W^-j(4f)$	$2.853(7) \cdot 10^4$	$3.733(7) \cdot 10^4$	1.31
$pp \to W^+W^-jj(4f)$ *	$1.150(5) \cdot 10^4$	$1.372(6) \cdot 10^4$	1.19
$pp \to W^+W^+jj$ *	$1.506(5) \cdot 10^2$	$2.235(7) \cdot 10^2$	1.48
$pp \to W^-W^-jj$	$6.772(24) \cdot 10^1$	$9.982(28) \cdot 10^1$	1.47
$pp \to ZW^\pm$	$2.780(5) \cdot 10^4$	$4.488(4) \cdot 10^4$	1.61
$pp \to ZW^\pm j$	$1.609(4) \cdot 10^4$	$2.0940(28) \cdot 10^4$	1.30
$pp \to ZW^\pm jj$	$8.06(3) \cdot 10^3$	$9.02(4) \cdot 10^3$	1.12
$pp \to ZZ$ *	$1.0969(10) \cdot 10^4$	$1.4183(11) \cdot 10^4$	1.29
$pp \to ZZj$	$3.667(9) \cdot 10^3$	$4.807(8) \cdot 10^3$	1.31
$pp \to ZZjj$ *	$1.356(6) \cdot 10^3$	$1.684(8) \cdot 10^3$	1.24

pp @ 13 TeV, NLO QCD/EW mixed

$pp \to t\bar{t}W^+$	$\alpha_s^n\alpha^m$	σ^{tot} [fb] MUNICH$_{(\mathrm{CS})}$	σ^{tot} [fb] WHIZARD	σ^{sig} / *dev* MUNICH$_{(\mathrm{CS})}$-WHIZARD
LO$_{21}$	$\alpha_s^2\alpha$	$2.411403(1) \cdot 10^2$	$2.4114(1) \cdot 10^2$	0.72 / 0.003%
LO$_{12}$	$\alpha_s\alpha^2$	0.000	0.000	0.00 / 0.000%
LO$_{03}$	α^3	$2.31909(1) \cdot 10^0$	$2.3193(1) \cdot 10^0$	1.76 / 0.009%
δNLO$_{31}$	$\alpha_s^3\alpha$	$1.18993(2) \cdot 10^2$	$1.1905(5) \cdot 10^2$	1.06 / 0.048%
δNLO$_{22}$	$\alpha_s^2\alpha^2$	$-1.09511(9) \cdot 10^1$	$-1.0947(3) \cdot 10^1$	1.13 / 0.035%
δNLO$_{13}$	$\alpha_s\alpha^3$	$2.93251(3) \cdot 10^1$	$2.9334(8) \cdot 10^1$	1.14 / 0.030%
δNLO$_{04}$	α^4	$5.759(3) \cdot 10^{-2}$	$5.756(4) \cdot 10^{-2}$	0.58 / 0.049%

μμ @ 3 TeV, NLO EW

$\mu^+\mu^- \to X, \sqrt{s} =$	$\sigma_{\mathrm{LO}}^{\mathrm{incl}}$ [fb]	$\sigma_{\mathrm{NLO}}^{\mathrm{incl}}$ [fb]	δ_{EW} [%]
W^+W^-	$4.6591(2) \cdot 10^2$	$4.847(7) \cdot 10^2$	+4.0(2)
ZZ	$2.5988(1) \cdot 10^1$	$2.656(2) \cdot 10^1$	+2.19(6)
HZ	$1.3719(1) \cdot 10^0$	$1.3512(5) \cdot 10^0$	−1.51(4)
HH	$1.60216(7) \cdot 10^{-7}$	$5.66(1) \cdot 10^{-7}$ *	
W^+W^-Z	$3.330(2) \cdot 10^1$	$2.568(8) \cdot 10^1$	−22.9(2)
W^+W^-H	$1.1253(5) \cdot 10^0$	$0.895(2) \cdot 10^0$	−20.5(2)
ZZZ	$3.598(2) \cdot 10^{-1}$	$2.68(1) \cdot 10^{-1}$	−25.5(3)
HZZ	$8.199(4) \cdot 10^{-2}$	$6.60(3) \cdot 10^{-2}$	−19.6(3)
HHZ	$3.277(1) \cdot 10^{-2}$	$2.451(5) \cdot 10^{-2}$	−25.2(1)
HHH	$2.9699(6) \cdot 10^{-8}$	$0.86(7) \cdot 10^{-8}$ *	
$W^+W^-W^+W^-$	$1.484(1) \cdot 10^0$	$0.993(6) \cdot 10^0$	−33.1(4)
W^+W^-ZZ	$1.209(1) \cdot 10^0$	$0.699(7) \cdot 10^0$	−42.2(6)
W^+W^-HZ	$8.754(8) \cdot 10^{-2}$	$6.05(4) \cdot 10^{-2}$	−30.9(5)
W^+W^-HH	$1.058(1) \cdot 10^{-2}$	$0.655(5) \cdot 10^{-2}$	−38.1(4)
$ZZZZ$	$3.114(2) \cdot 10^{-3}$	$1.799(7) \cdot 10^{-3}$	−42.2(2)
$HZZZ$	$2.693(2) \cdot 10^{-3}$	$1.766(6) \cdot 10^{-3}$	−34.4(2)
$HHZZ$	$9.828(7) \cdot 10^{-4}$	$6.24(2) \cdot 10^{-4}$	−36.5(2)
$HHHZ$	$1.568(1) \cdot 10^{-4}$	$1.165(4) \cdot 10^{-4}$	−25.7(2)

ee @ .25 TeV, NLO EW, pol.av. + pol.

$\sqrt{s}$ [GeV]	MCSANCee[37] $\sigma_{\mathrm{LO}}^{\mathrm{tot}}$ [fb]	MCSANCee[37] $\sigma_{\mathrm{NLO}}^{\mathrm{tot}}$ [fb]	WHIZARD+RECOLA $\sigma_{\mathrm{LO}}^{\mathrm{tot}}$ [fb]	WHIZARD+RECOLA $\sigma_{\mathrm{NLO}}^{\mathrm{tot}}$ [fb]	WHIZARD+RECOLA δ_{EW} [%]	σ^{sig} (LO/NLO)
250	225.59(1)	206.77(1)	225.60(1)	207.0(1)	−8.25	0.4/2.1
500	53.74(1)	62.42(1)	53.74(3)	62.41(2)	+16.14	0.2/0.3
1000	12.05(1)	14.56(1)	12.0549(6)	14.57(1)	+20.84	0.5/0.5

arXiv: 2104.11141

arXiv: 2208.09438

It works "out of the (black) box" [most of the time]

AUTOMATION ≙ "WORKS AS LONG AS THE 1ST PROCESS CRASHES"

ee @ 1 TeV, NLO QCD

Process	WHIZARD+OpenLoops $\sigma_{\rm LO}$ [fb]	$\sigma_{\rm NLO}$ [fb]
$e^+e^- \to jj$	622.737(8)	639.39(5)
$e^+e^- \to jjj$	340.6(5)	317.8(5)
$e^+e^- \to jjjj$	105.0(3)	104.2(4)
$e^+e^- \to jjjjj$	22.33(5)	24.57(7)
$e^+e^- \to jjjjjj$	3.583(17)	4.46(4)

$e^+e^- \to t\bar{t}$	166.37(12)	174.55(20)
$e^+e^- \to t\bar{t}j$	48.12(5)	53.41(7)
$e^+e^- \to t\bar{t}jj$	8.592(19)	10.526(21)
$e^+e^- \to t\bar{t}jjj$	1.035(4)	1.405(5)
$e^+e^- \to t\bar{t}t\bar{t}$	$0.6388(8) \cdot 10^{-3}$	$1.1922(11) \cdot 10^{-3}$
$e^+e^- \to t\bar{t}t\bar{t}j$	$2.673(7) \cdot 10^{-5}$	$5.251(11) \cdot 10^{-5}$
$e^+e^- \to t\bar{t}H$	2.020(3)	1.912(3)
$e^+e^- \to t\bar{t}Hj$	$2.536(4) \cdot 10^{-1}$	$2.657(4) \cdot 10^{-1}$
$e^+e^- \to t\bar{t}Hjj$	$2.646(8) \cdot 10^{-2}$	$3.123(9) \cdot 10^{-2}$
$e^+e^- \to t\bar{t}Z$	4.638(3)	4.937(3)
$e^+e^- \to t\bar{t}Zj$	$6.027(9) \cdot 10^{-1}$	6.92[illegible]
$e^+e^- \to t\bar{t}Zjj$	$6.436(21) \cdot 10^{-2}$	[illegible]
$e^+e^- \to t\bar{t}W^{\pm}jj$	$2.387(8) \cdot 10^{-4}$	[illegible] $\cdot 10^{-4}$
$e^+e^- \to t\bar{t}HZ$	3.623(19)[illegible]	[illegible](19) $\cdot 10^{-2}$
$e^+e^- \to t\bar{t}ZZ$	3.78[illegible]	$4.032(7) \cdot 10^{-2}$
$e^+e^- \to t\bar{t}HH$	[illegible]	$1.2168(16) \cdot 10^{-2}$
$e^+e^- \to t\bar{t}W^+W^-$	[illegible] $\cdot 10^{-1}$	$1.5385(22) \cdot 10^{-1}$

pp @ 13 TeV, NLO QCD

Process Vector boson (pair) plus jets	WHIZARD $\sigma_{\rm LO}$[fb]	$\sigma_{\rm NLO}$[fb]	K
$pp \to W^{\pm}$ *	$1.3749(8) \cdot 10^8$	$1.7696(10) \cdot 10^8$	1.29
$pp \to W^{\pm}j$ *	$2.046(3) \cdot 10^7$	$2.854(5) \cdot 10^7$	1.39
$pp \to W^{\pm}jj$	$6.856(12) \cdot 10^6$	$7.814(27) \cdot 10^6$	1.14
$pp \to W^{\pm}jjj$ †	$1.840(5) \cdot 10^6$	$1.978(7) \cdot 10^6$	1.07
$pp \to Z$	$4.2541(3) \cdot 10^7$	$5.4086(16) \cdot 10^7$	1.27
$pp \to Zj$	$7.215(4) \cdot 10^6$	$9.733(10) \cdot 10^6$	1.35
$pp \to Zjj$	$2.364(5) \cdot 10^6$	$2.676(7) \cdot 10^6$	1.13
$pp \to Zjjj$	$6.381(23) \cdot 10^5$	$6.85(3) \cdot 10^5$	1.07
$pp \to W^+W^-(4f)$	$7.352(10) \cdot 10^4$	$10.268(11) \cdot 10^4$	[illegible]
$pp \to W^+W^-j(4f)$	$2.853(7) \cdot 10^4$	3.733(7) [illegible]	[illegible]
$pp \to W^+W^-jj(4f)$ *	$1.150(5) \cdot 10^4$	1.372[illegible]	[illegible]
$pp \to W^+W^+jj$ *	$1.506(5) \cdot 10^2$	2[illegible]	[illegible]
$pp \to W^-W^-jj$	$6.772(24) \cdot 10^1$	[illegible]	1.47
$pp \to ZW^{\pm}$	2.780(5) [illegible]	[illegible]	1.61
$pp \to ZW^{\pm}j$	1.609[illegible]	[illegible](28) $\cdot 10^4$	1.30
$pp \to ZW^{\pm}jj$	[illegible]	[illegible].02(4) $\cdot 10^3$	1.12
$pp \to ZZ$ *	[illegible]	$1.4183(11) \cdot 10^4$	1.29
$pp \to ZZj$	[illegible] 10^3	$4.807(8) \cdot 10^3$	1.31
$pp \to ZZjj$ *	[illegible](6) $\cdot 10^3$	$1.684(8) \cdot 10^3$	1.24

pp @ 13 T[illegible] QCD/EW mixed

$pp \to t\bar{t}W^+$	$\alpha_s^n \alpha^m$	[illegible] [fb] [illegible](CS)	WHIZARD	$\sigma^{\rm sig}$ / dev MUNICH$_{\rm (CS)}$-WHIZARD
LO$_{21}$	α^2[illegible]	[illegible]03(1) $\cdot 10^2$	$2.4114(1) \cdot 10^2$	0.72 / 0.003%
LO$_{12}$	[illegible]	0.000	0.000	0.00 / 0.000%
LO$_{03}$	[illegible]	$2.31909(1) \cdot 10^0$	$2.3193(1) \cdot 10^0$	1.76 / 0.009%
δNL[illegible]	[illegible]$_s\alpha$	$1.18993(2) \cdot 10^2$	$1.1905(5) \cdot 10^2$	1.06 / 0.048%
[illegible]	$\alpha_s^2\alpha^2$	$-1.09511(9) \cdot 10^1$	$-1.0947(3) \cdot 10^1$	1.13 / 0.035%
[illegible]	$\alpha_s\alpha^3$	$2.93251(3) \cdot 10^1$	$2.9334(8) \cdot 10^1$	1.14 / 0.030%
[illegible]LO$_{04}$	α^4	$5.759(3) \cdot 10^{-2}$	$5.756(4) \cdot 10^{-2}$	0.58 / 0.049%

μμ @ 3 TeV, NLO EW

$\mu^+\mu^- \to X, \sqrt{s} =$	$\sigma^{\rm incl}_{\rm LO}$ [fb]	$\sigma^{\rm incl}_{\rm NLO}$ [fb]	$\delta_{\rm EW}$ [%]
W^+W^-	$4.6591(2) \cdot 10^2$	$4.847(7) \cdot 10^2$	+4.0(2)
ZZ	$2.5988(1) \cdot 10^1$	$2.656(2) \cdot 10^1$	+2.19(6)
HZ	$1.3719(1) \cdot 10^0$	$1.3512(5) \cdot 10^0$	−1.51(4)
HH	$1.60216(7) \cdot 10^{-7}$	$5.66(1) \cdot 10^{-7}$ *	
W^+W^-Z	$3.330(2) \cdot 10^1$	$2.568(8) \cdot 10^1$	−22.9(2)
W^+W^-H	$1.1253(5) \cdot 10^0$	$0.895(2) \cdot 10^0$	−20.5(2)
ZZZ	$3.598(2) \cdot 10^{-1}$	$2.68(1) \cdot 10^{-1}$	−25.5(3)
HZZ	$8.199(4) \cdot 10^{-2}$	$6.60(3) \cdot 10^{-2}$	−19.6(3)
HHZ	$3.277(1) \cdot 10^{-2}$	$2.451(5) \cdot 10^{-2}$	−25.2(1)
HHH	$2.9699(6) \cdot 10^{-8}$	$0.86(7) \cdot 10^{-8}$ *	
$W^+W^-W^+W^-$	$1.484(1) \cdot 10^0$	$0.993(6) \cdot 10^0$	−33.1(4)
W^+W^-ZZ	$1.209(1) \cdot 10^0$	$0.699(7) \cdot 10^0$	−42.2(6)
W^+W^-HZ	$8.754(8) \cdot 10^{-2}$	$6.05(4) \cdot 10^{-2}$	−30.9(5)
W^+W^-HH	$1.058(1) \cdot 10^{-2}$	$0.655(5) \cdot 10^{-2}$	−38.1(4)
$ZZZZ$	$3.114(2) \cdot 10^{-3}$	$1.799(7) \cdot 10^{-3}$	−42.2(2)
$HZZZ$	$2.693(2) \cdot 10^{-3}$	$1.766(6) \cdot 10^{-3}$	−34.4(2)
$HHZZ$	$9.828(7) \cdot 10^{-4}$	$6.24(2) \cdot 10^{-4}$	−36.5(2)
$HHHZ$	$1.568(1) \cdot 10^{-4}$	$1.165(4) \cdot 10^{-4}$	−25.7(2)

[illegible]e @ .25 TeV, NLO EW, pol.av. + pol.

$\sqrt{s}$ [GeV]	MCSANCee[37] $\sigma^{\rm tot}_{\rm LO}$ [fb]	$\sigma^{\rm tot}_{\rm NLO}$ [fb]	WHIZARD+RECOLA $\sigma^{\rm tot}_{\rm LO}$ [fb]	$\sigma^{\rm tot}_{\rm NLO}$ [fb]	$\delta_{\rm EW}$ [%]	$\sigma^{\rm sig}$ (LO/NLO)
250	225.59(1)	206.77(1)	225.60(1)	207.0(1)	−8.25	0.4/2.1
500	53.74(1)	62.42(1)	53.74(3)	62.41(2)	+16.14	0.2/0.3
1000	12.05(1)	14.56(1)	12.0549(6)	14.57(1)	+20.84	0.5/0.5

arXiv: 2104.11141

arXiv: 2208.09438

BSM processes at NLO EW in MC

- BSM signal allow for lower precision than SM processes, *but:*
- NLO EW always necessary, sometimes even NNLO EW [exceptions: unique signatures like disappearing tracks etc.]
- OLP can / do provide 1-loop libraries for BSM models [difficult part: renormalization of BSM fields for all cases]
- Example: $e^+e^- \to H_{125}\nu\bar{\nu}$ for 2HDM @ NLO EW, 365 GeV [Bredt/Banno/Höfer/Iguro/Kilian/Ma/JRR/Zhang, PRL 136 (2026) 8, 081101]

BSM processes at NLO EW in MC

- BSM signal allow for lower precision than SM processes, *but:*
- NLO EW always necessary, sometimes even NNLO EW [exceptions: unique signatures like disappearing tracks etc.]
- OLP can / do provide 1-loop libraries for BSM models [difficult part: renormalization of BSM fields for all cases]
- Example: $e^+e^- \to H_{125}\nu\bar{\nu}$ for 2HDM @ NLO EW, 365 GeV [Bredt/Banno/Höfer/Iguro/Kilian/Ma/JRR/Zhang, PRL 136 (2026) 8, 081101]

  - ☑ Theoretical uncertainty 0.5% [EW scheme,missing NNLO EW] ⟹one of very few BSM calculations to match exp. prec.
  - ☑ Proofs that FCC-ee can distinguish SM and 2HDM at 5σ just from production

BSM processes at NLO EW in MC

- BSM signal allow for lower precision than SM processes, *but:*
- NLO EW always necessary, sometimes even NNLO EW [exceptions: unique signatures like disappearing tracks etc.]
- OLP can / do provide 1-loop libraries for BSM models [difficult part: renormalization of BSM fields for all cases]
- Example: $e^+e^- \to H_{125}\nu\bar{\nu}$ for 2HDM @ NLO EW, 365 GeV [Bredt/Banno/Höfer/Iguro/Kilian/Ma/JRR/Zhang, PRL 136 (2026) 8, 081101]

☑ Theoretical uncertainty 0.5% [EW scheme,missing NNLO EW] ⟹one of very few BSM calculations to match exp. prec.

☑ Proofs that FCC-ee can distinguish SM and 2HDM at 5σ just from production

	$\sqrt{s} = 365$ GeV	
	LO [fb]	NLO EW [fb]
SM	55.79	52.44(1)
2HDM	55.71	51.45(1)
Rel.Diff.	−0.1%	−1.9%
2HDM (aligned)	55.79	51.58(1)
Rel.Diff.	0.0%	−1.7%

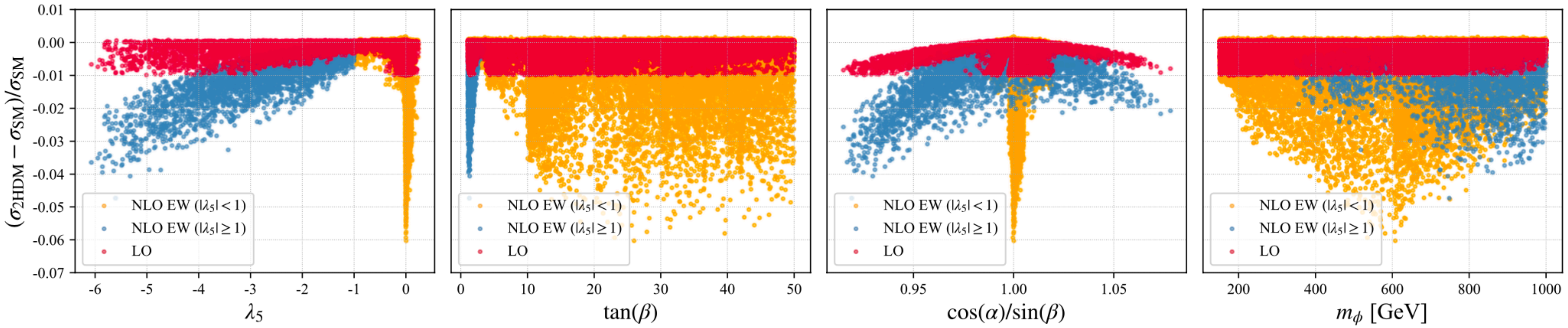

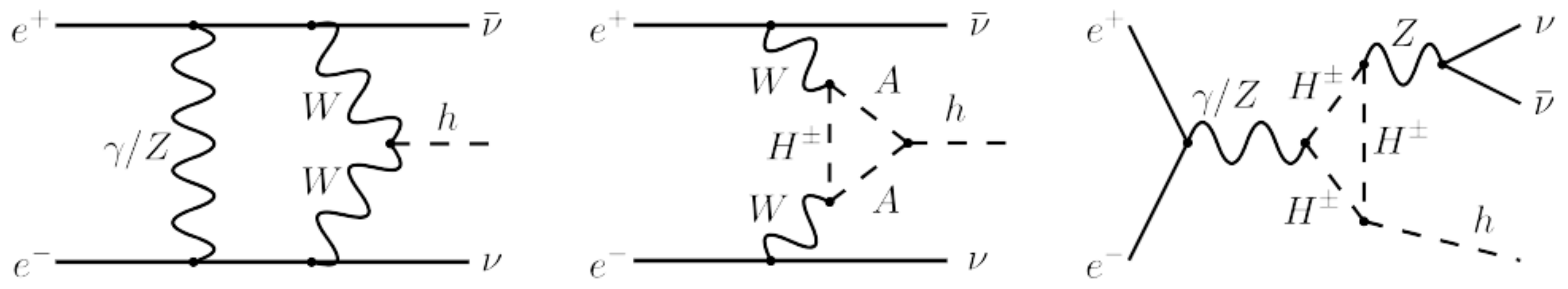

MC: differential (fixed order) distributions

$e^+e^- \to jjjjj$ @ 1 TeV, NLO QCD

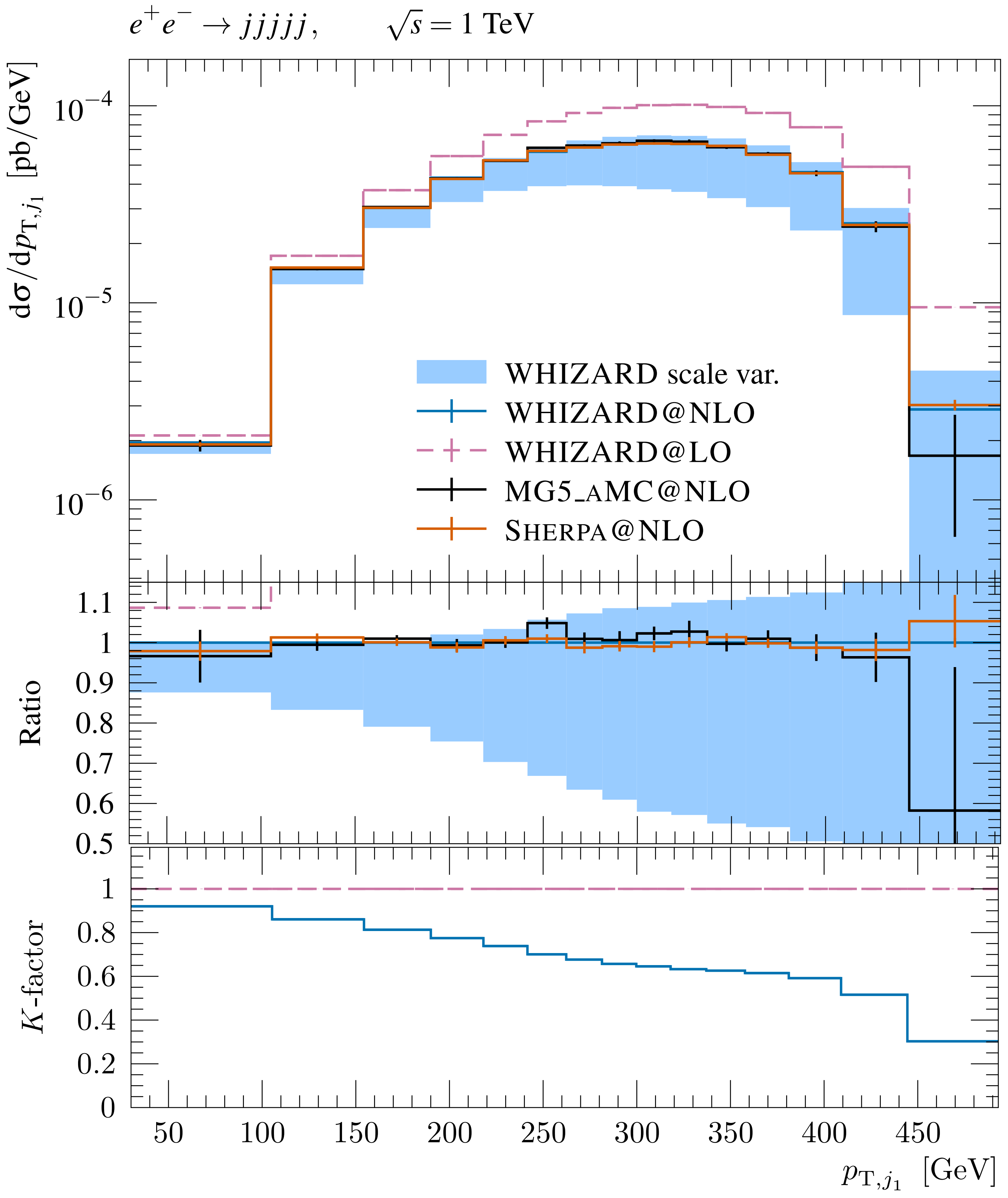

MC: differential (fixed order) distributions

$e^+e^- \to \ell_1^+\nu_1\ell_1^-\bar{\nu}_2 b\bar{b}$ @ 365 GeV, NLO QCD

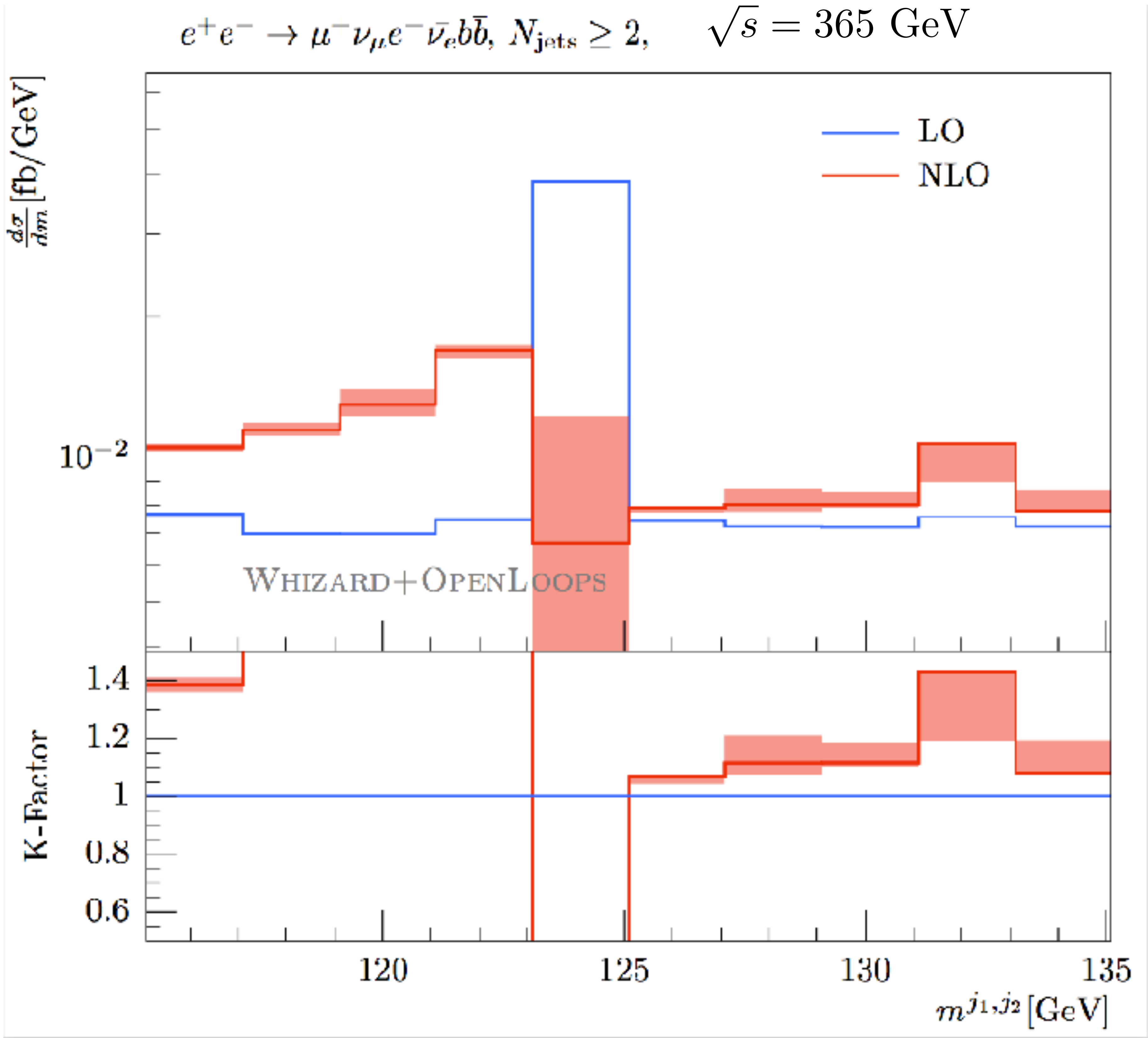

MC: differential (fixed order) distributions

$e^+e^- \to \ell_1^+\nu_1\ell_1^-\bar{\nu}_2 b\bar{b}$ @ 365 GeV, NLO QCD

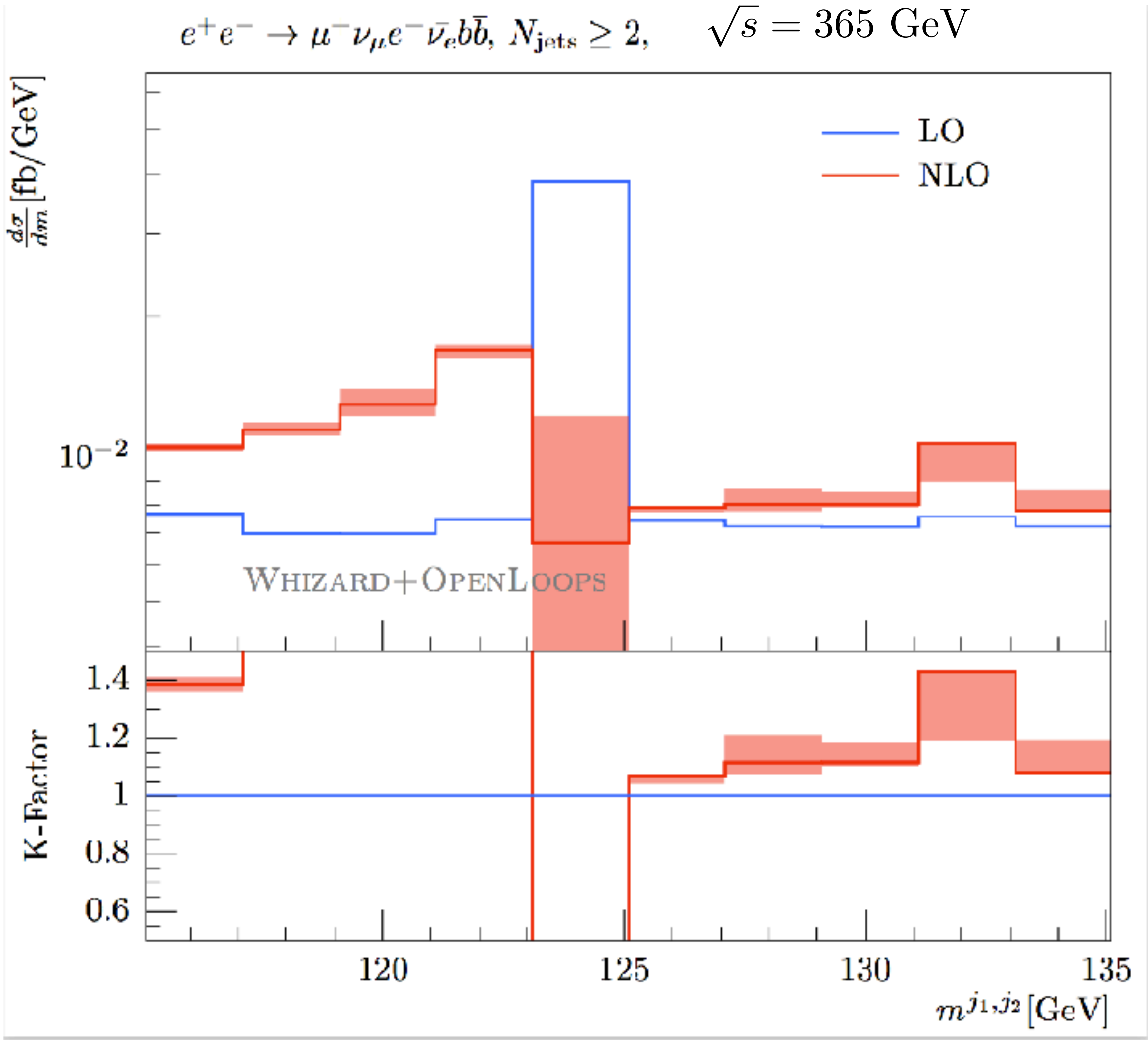

$e^+e^- \to H\nu\bar{\nu}$ 2HDM @ 365/550 GeV, NLO EW

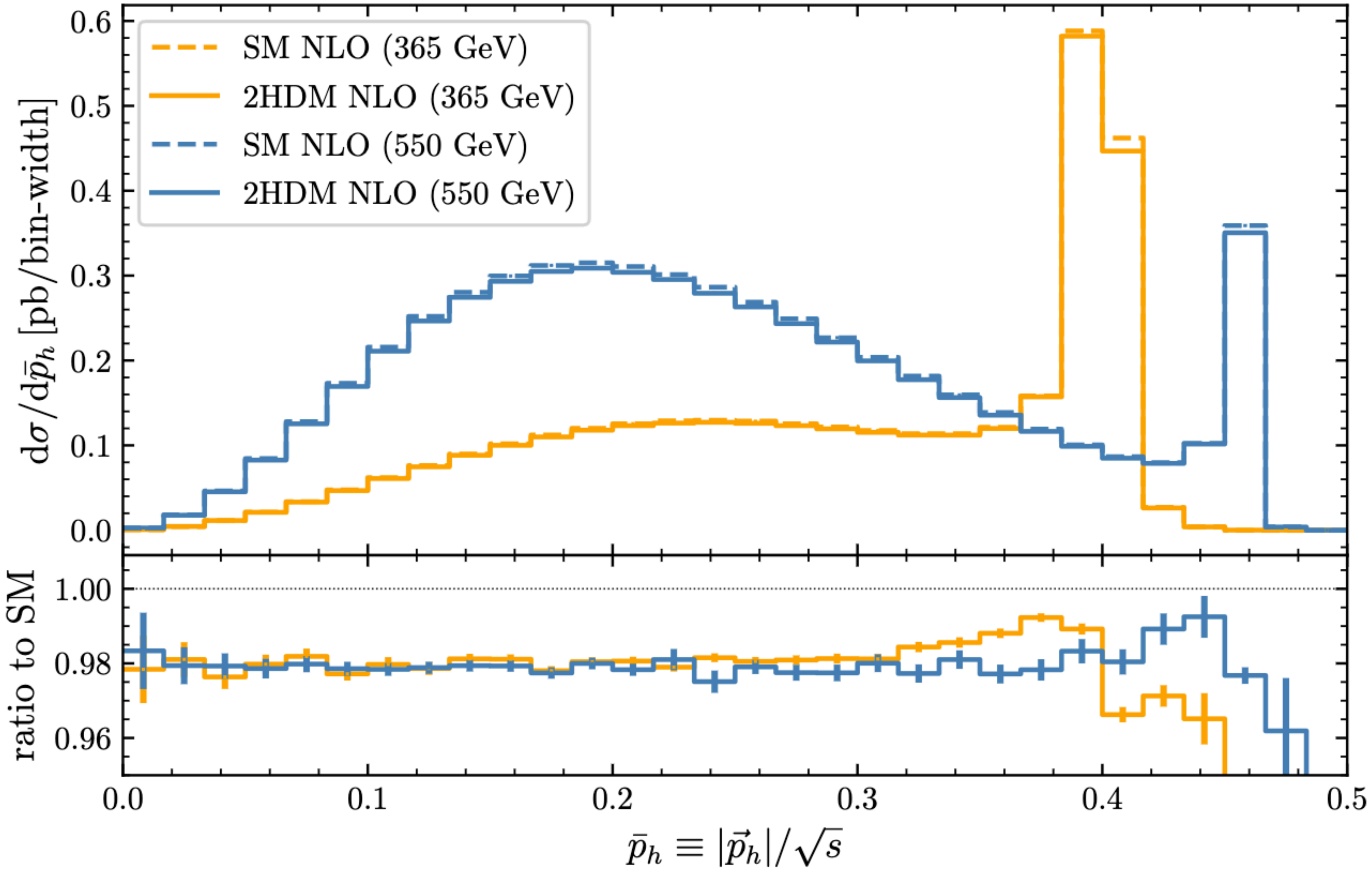

QCD showers, matching & hadronization

- Tremendous progress driven by LHC: QCD parton showers NLL (towards NNLL), spin effects, recoils, etc.
- Sophisticated matching procedures at NLO (MC@NLO, POWHEG, ...), NNLO (MINNLOPS, UNNLOPS, Geneva...) ....
- Increasing interplay between analytic resummation (inclusive) and parton showers (exclusive)
- Minuscule statistical uncertainties: hadronic (i.e. non-pert.) uncertainties Λ_{QCD}/Q likely dominant
- Need for analytic power correction calculations and maybe new hadronization models

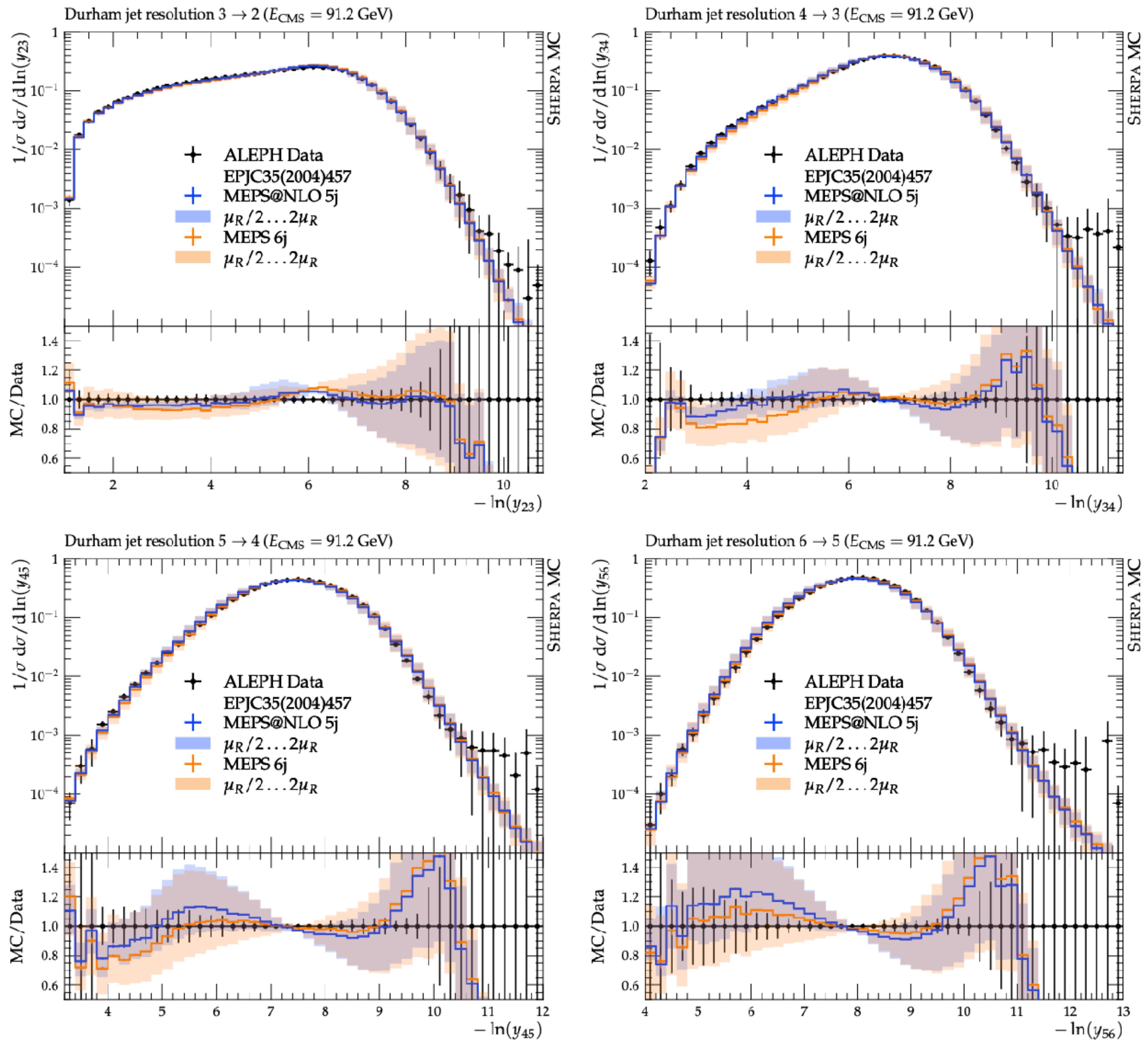

Höche/Krauss/Meinzinger/Reichelt, 2207.22837
cf. talks S. Höche & G. Stagnitto

- More topics: color reconnections, Bose-Einstein correlations, ...

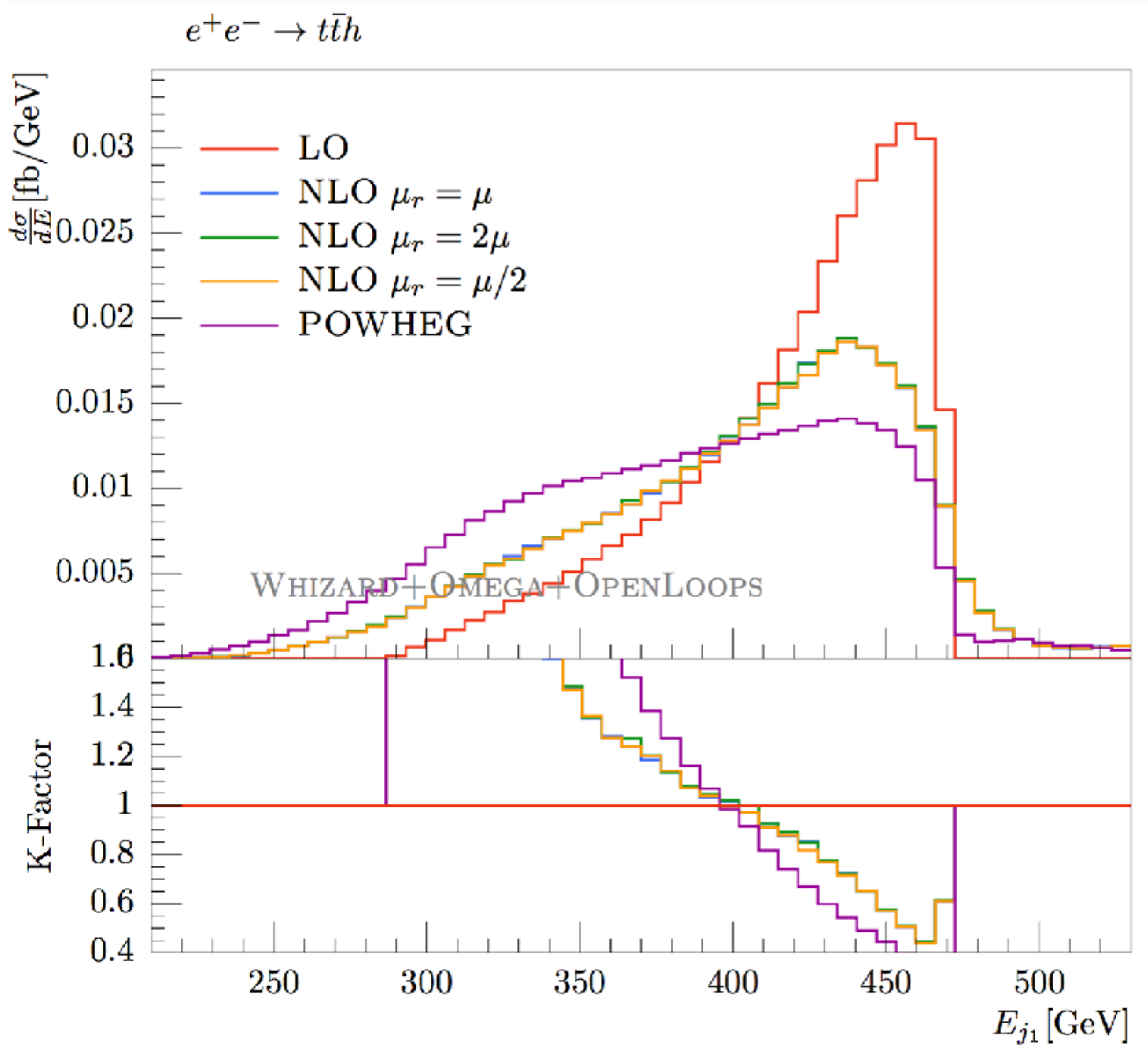

Chokoufé/Hoang/JRR et al., 1602.06270

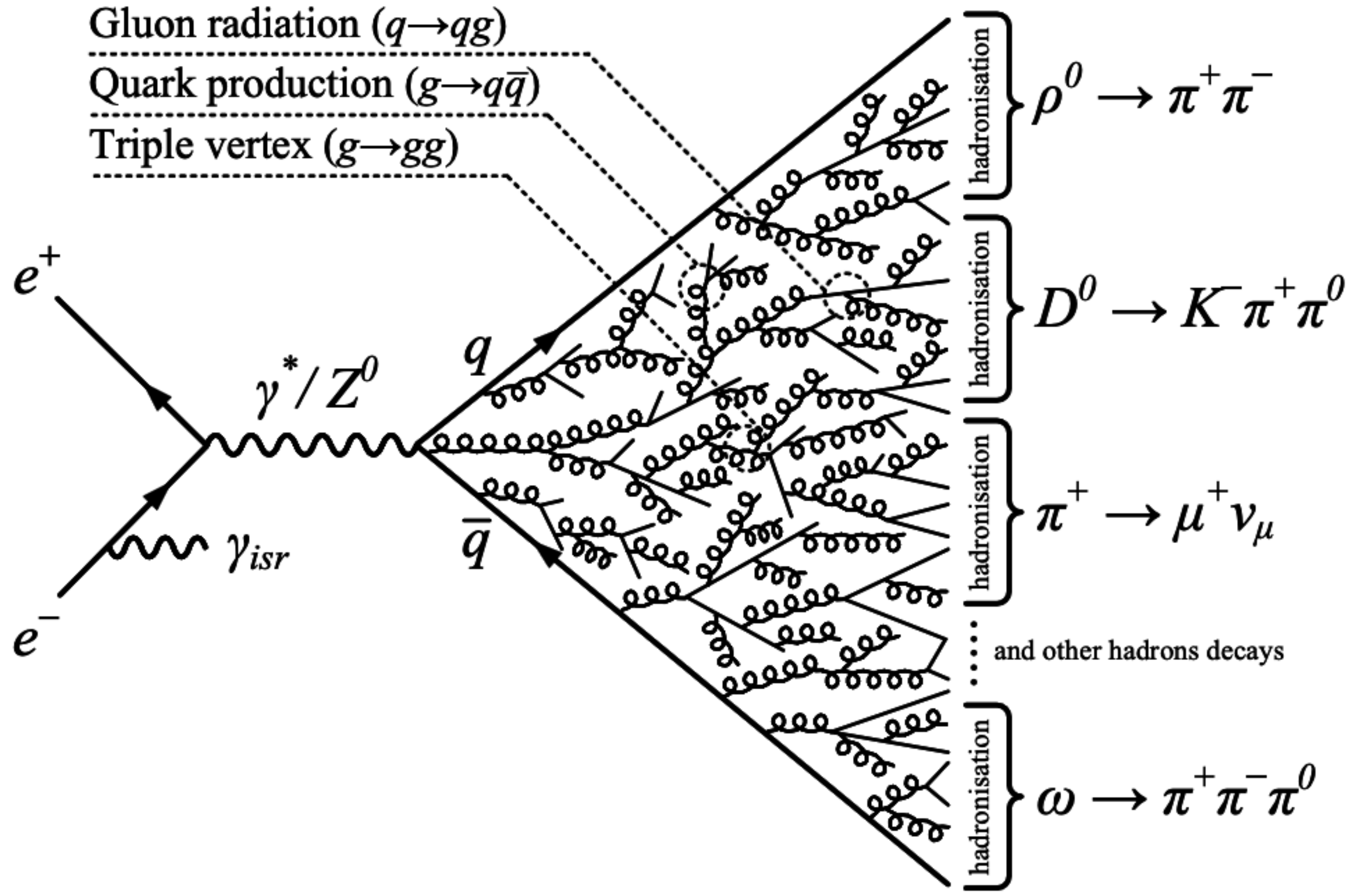

(Resonance) Matching to shower / hadronization


```
?resonance_history = true
resonance_on_shell_limit = 4
resonance_on_shell_turnoff = 1
resonance_background_factor = 1e-10
```

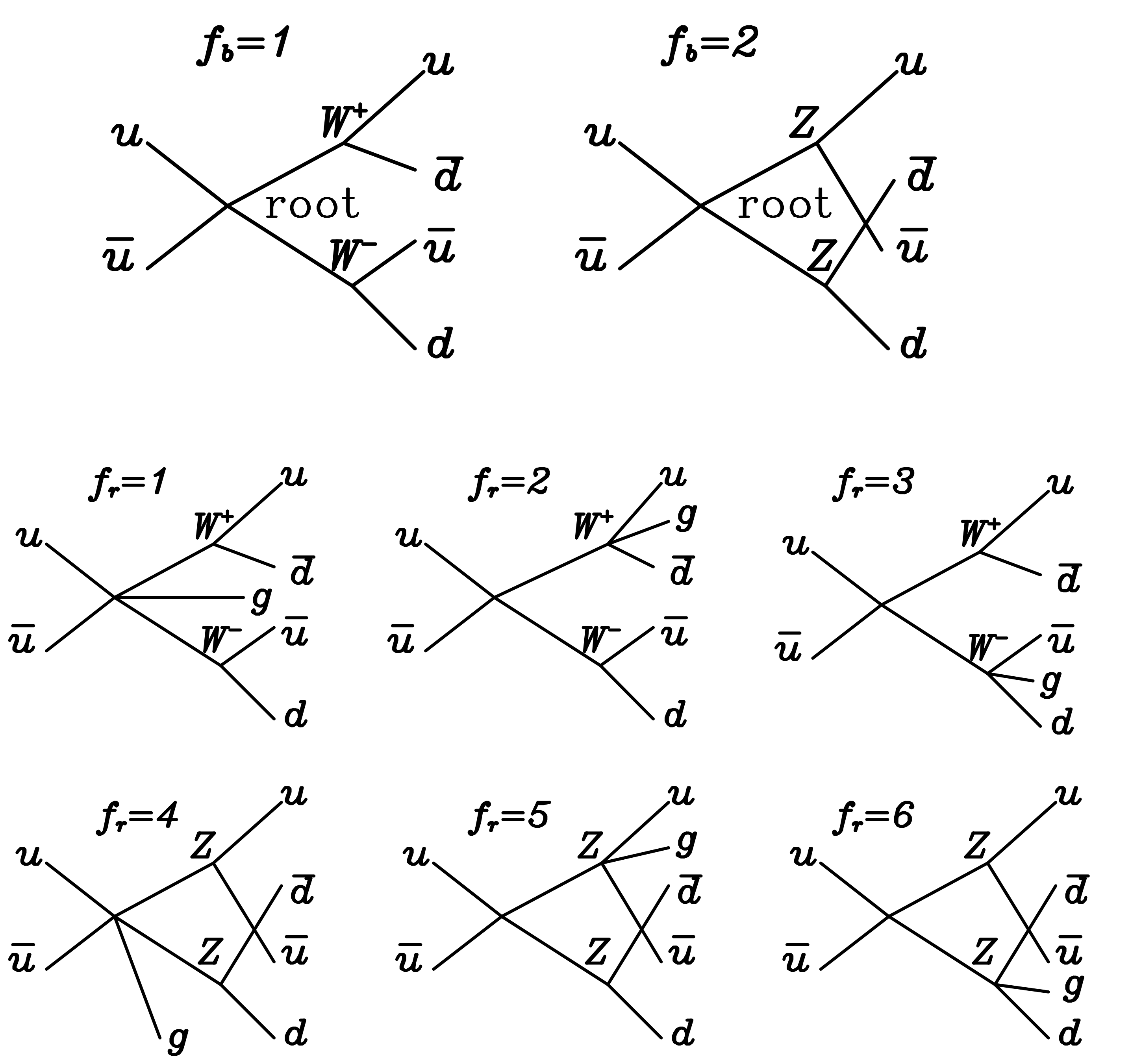

- Problem: $e^+e^- \to jjjj$ not dominated by highest α_s power,
  but by resonances $e^+e^- \to WW/ZZ \to (jj)(jj)$

  Solution, p. A: proper merging w/ resonant subprocesses by resonance histories

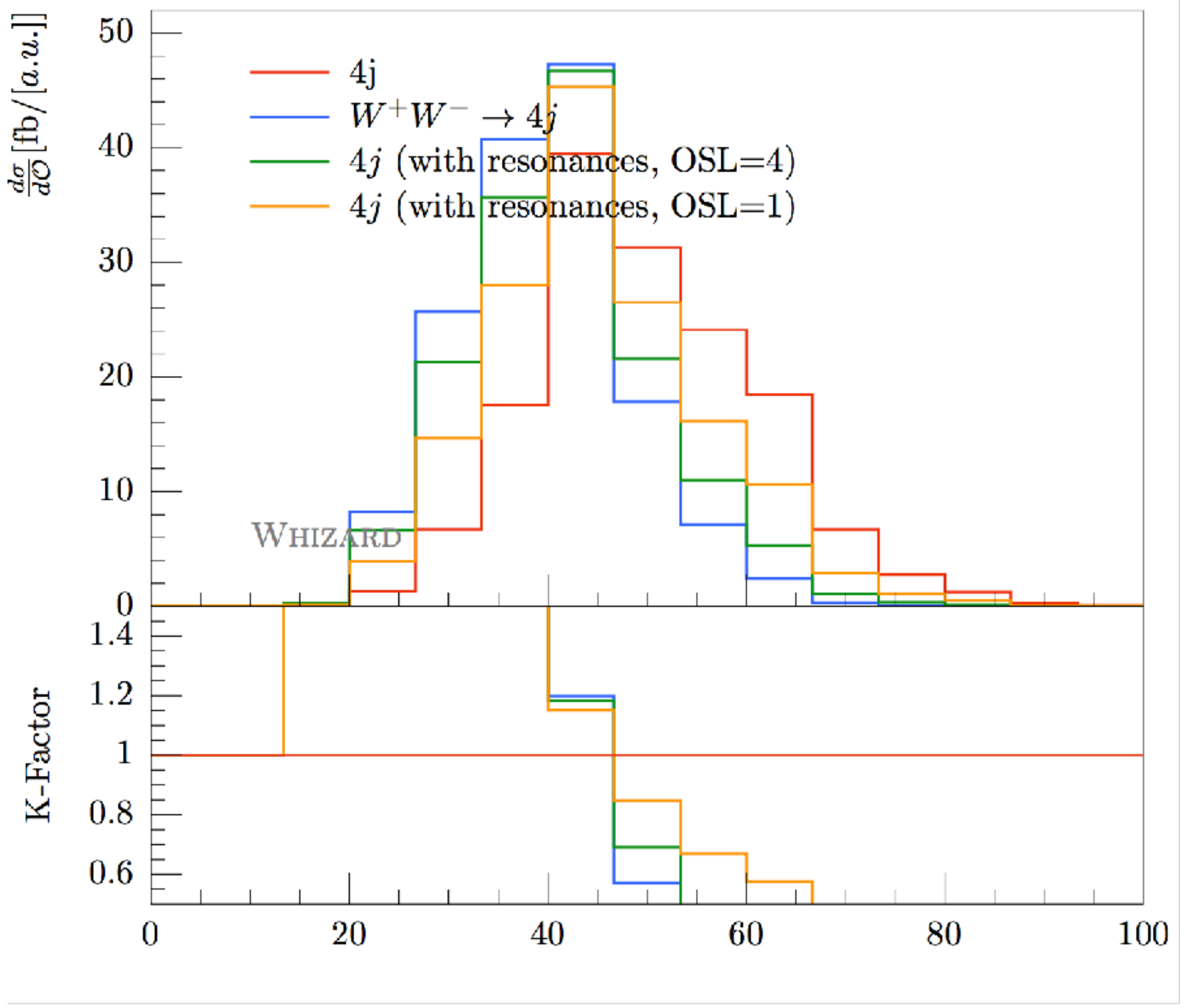

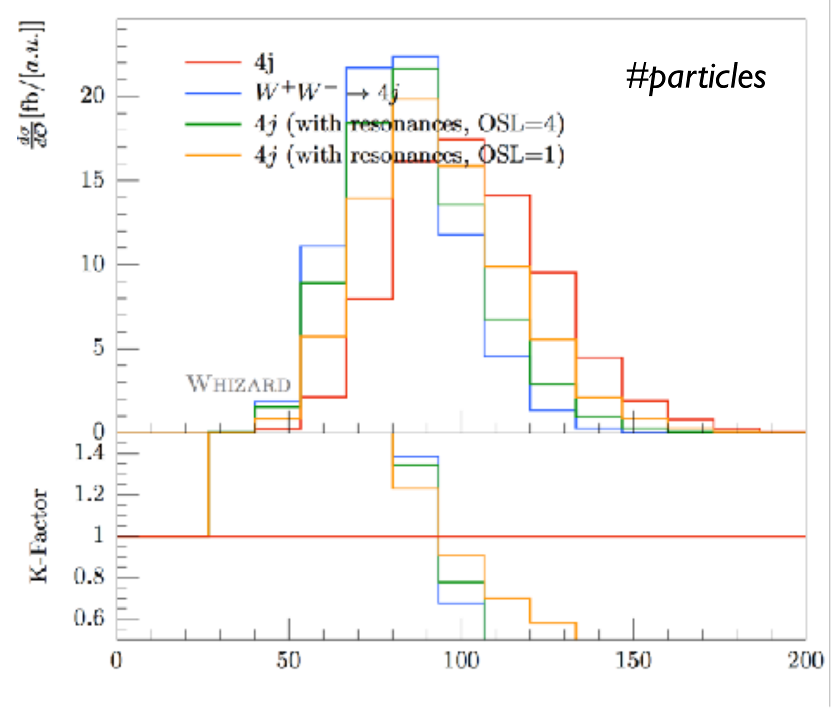

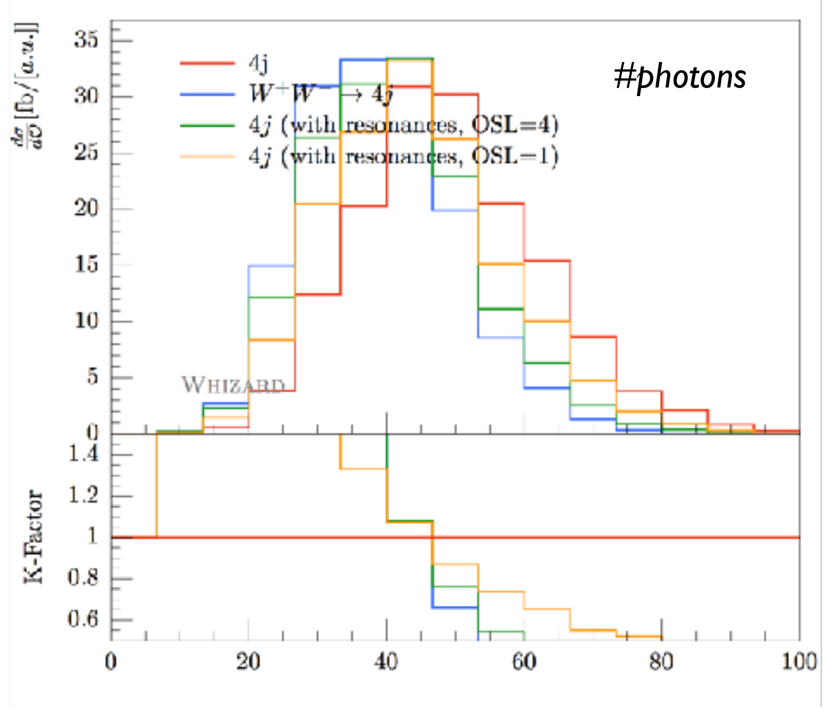

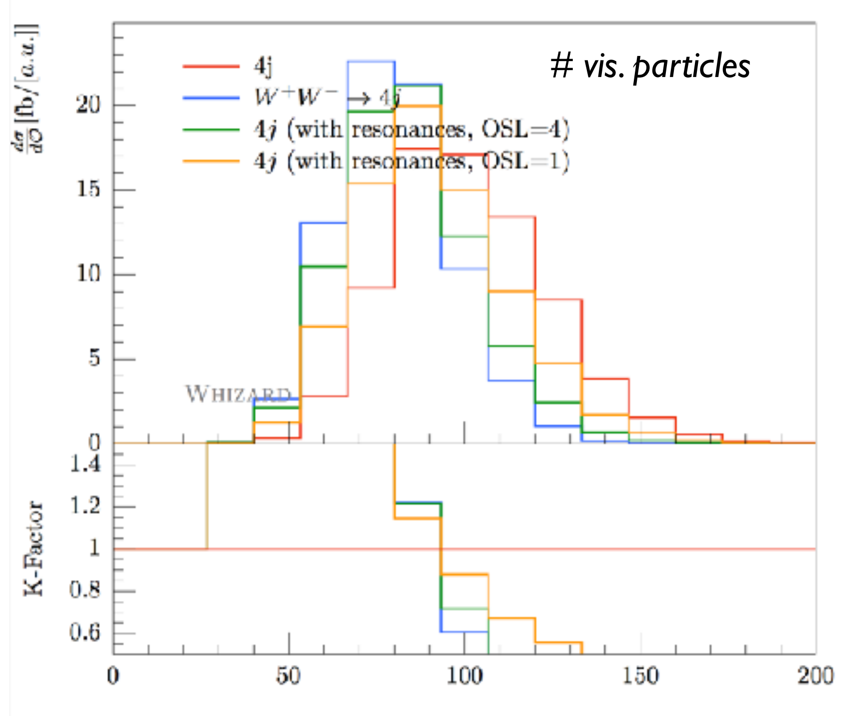

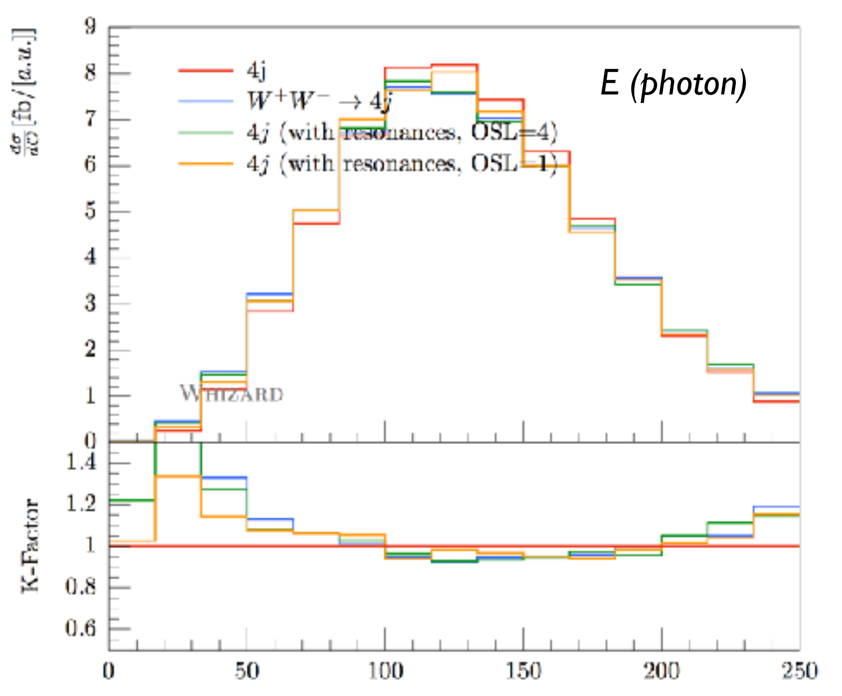

- Solution, p. B: resonance-aware parton showers Höche/Reichelt, 2604.13978 ↪ Talk by Stefan Höche

QED corrections / factorization

Collinear logarithms

$$L = \log \frac{Q^2}{m^2}$$

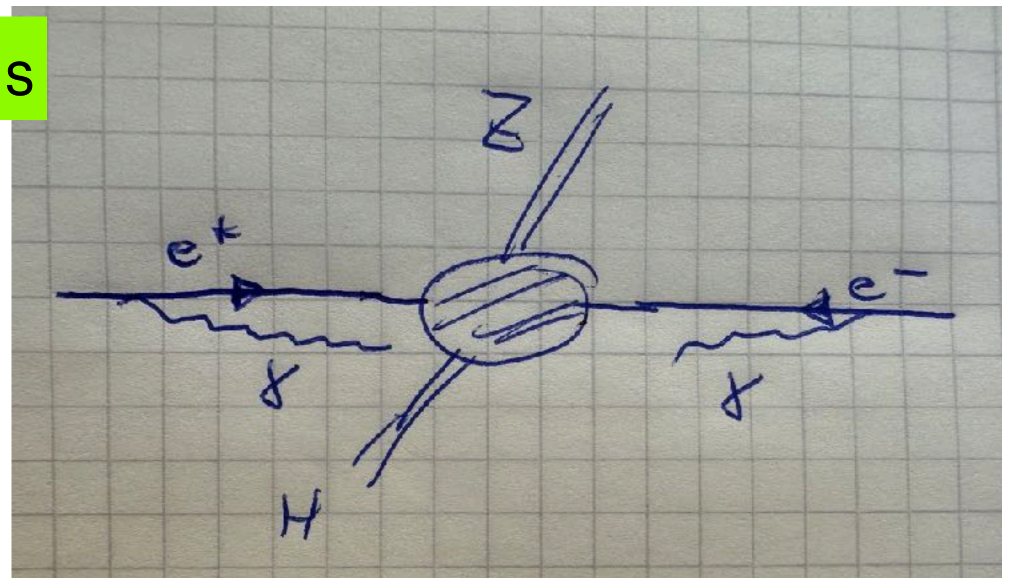

$$\sigma = \alpha^b \sum_{n=0}^{\infty} \alpha^n \sum_{i=0}^{n} \sum_{j=0}^{n} \varsigma_{n,i,j} L^i \ell^j$$

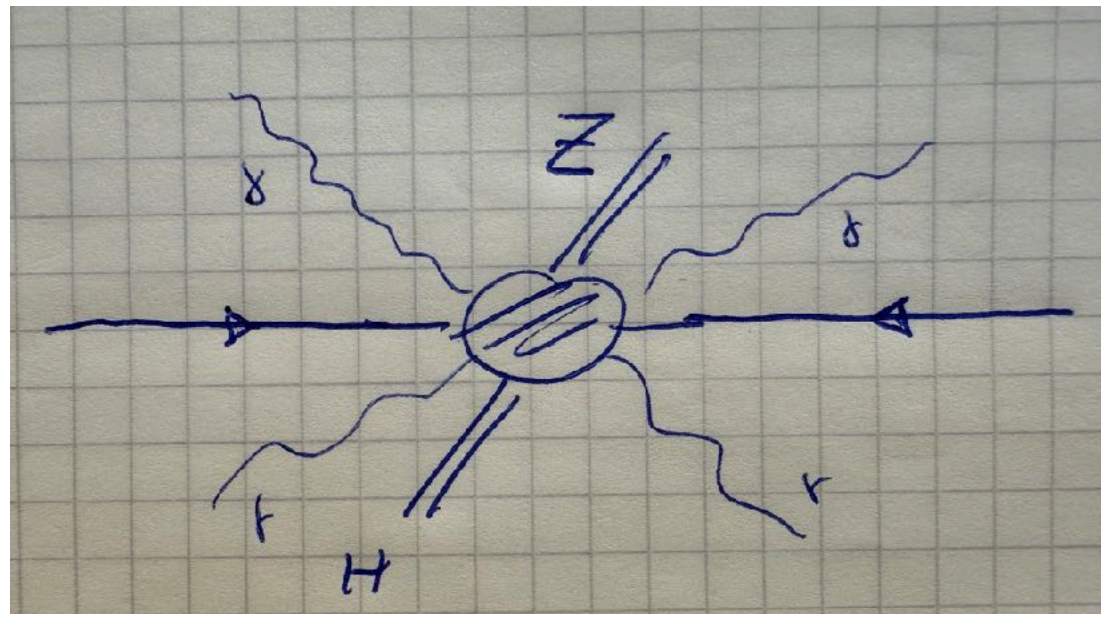

Soft logarithms

$$\ell = \log \frac{Q^2}{\langle E_\gamma \rangle^2}$$

- *Collinear factorization resums collinear logarithms*: collinear splittings, m_e dependence factorized into (collinear) ePDFs
- *Soft / eikonal factorization resums soft logarithms*: soft/eikonal splittings (a.k.a. as Yennie-Frautschi-Suura [YFS])
- Both resum soft-collinear logarithms that give rise to a integrable singularity at $z \to 1$
- Both approaches can be systematically improved; both have (different!!!) finite remainders and power corrections

$$d\sigma_{kl}(p_k, p_l) = \sum_{ij=e^+,e^-,\gamma} \int dz_+ dz_- \Gamma_{i/k}(z_+, \mu^2, m^2) \Gamma_{j/l}(z_-, \mu^2, m^2) \times d\hat{\sigma}_{ij}(z_+ p_k, z_- p_l, \mu^2) + \mathcal{O}\left(\left(\frac{m^2}{s}\right)^p\right)$$

$$d\sigma(L, \ell) = \mathcal{K}_{soft}(\ell; L)\beta(L)d\mu = e^{Y(p_1,p_2,p_X)} \sum_{n=0}^{\infty} \beta_n \left(\mathcal{R}p_1, \mathcal{R}p_2, \mathcal{R}p_X; \{k_i\}_{i=0}^n\right) d\mu_{X+n\gamma}$$

QED PDFs: physics & properties

- Soft-collinear resummation to all orders Gribov/Lipatov, 1972; Kuraev/Fadin, 1985
- Hard collinear radiation $\mathcal{O}(\alpha^2)$ Kuraev/Fadin, 1985 , $\mathcal{O}(\alpha^3)$ Skrzypek/Jadach, 1992
- LO boundary conditions, collinear evolution @ LL Skrzypek/Jadach, 1992; Cacciari/Deandrea/Montagna/Nicrosini, 1992
- NLO boundary conditions for NLL QED PDF evolution Frixione, 1909.03886
- NLO QED PDFs, collinear evolution @ NLL Bertone/Cacciari/Frixione/Stagnitto, 1911.12040 + 2207.03265
- NNLO QED PDFs Stahlhofen, 2508.16964; Szafron/Schnubel, 2509.09618

$$\frac{\partial \mathbb{E}_N(t)}{\partial t} = \frac{b_0 \alpha^2(\mu)}{\beta(\alpha(\mu))} \sum_{k=0}^{\infty} \left(\frac{\alpha(\mu)}{2\pi}\right)^k \mathbb{P}_N^{[k]} \mathbb{E}_N(t)$$
$$= \left[\mathbb{P}_N^{[0]} + \frac{\alpha(\mu)}{2\pi}\left(\mathbb{P}_N^{[1]} - \frac{2\pi b_1}{b_0}\mathbb{P}_N^{[0]}\right)\right] \mathbb{E}_N(t) + \mathcal{O}(\alpha^2)\,.$$

$$\Gamma_i^{[0]}(z,\mu_0^2) = \delta_{ie^-}\delta(1-z)\,,$$
$$\Gamma_{e^-}^{[1]}(z,\mu_0^2) = \left[\frac{1+z^2}{1-z}\left(\log\frac{\mu_0^2}{m^2} - 2\log(1-z) - 1\right)\right]_+ + K_{ee}(z)\,,$$
$$\Gamma_{\gamma}^{[1]}(z,\mu_0^2) = \frac{1+(1-z)^2}{z}\left(\log\frac{\mu_0^2}{m^2} - 2\log z - 1\right) + K_{\gamma e}(z)\,,$$
$$\Gamma_{e^+}^{[1]}(z,\mu_0^2) = 0\,,$$

$$\mathbb{P}_{\rm S} = \begin{pmatrix} P_{\Sigma\Sigma} & P_{\Sigma\gamma} \\ P_{\gamma\Sigma} & P_{\gamma\gamma} \end{pmatrix},$$
$$P_{\rm NS} = P_{e^\pm e^\pm} - P_{e^\pm e^\mp} \equiv P_{ee}^{\rm V} - P_{e\bar{e}}^{\rm V}\,.$$

Recent efforts in $e^+e^- \to f\bar{f}$ (2-loop, logarithmic corrections, radiator functions)
Blümlein/de Freitas/Raab/Schönwald, 1901.08018, 1910.05759, 2003.14283, 2004.04287 etc.

QED Full Factorization

- Fully factorized QED amplitudes for small/vanishing m_e Laenen et al. 2008.01736

QED PDFs: physics & properties

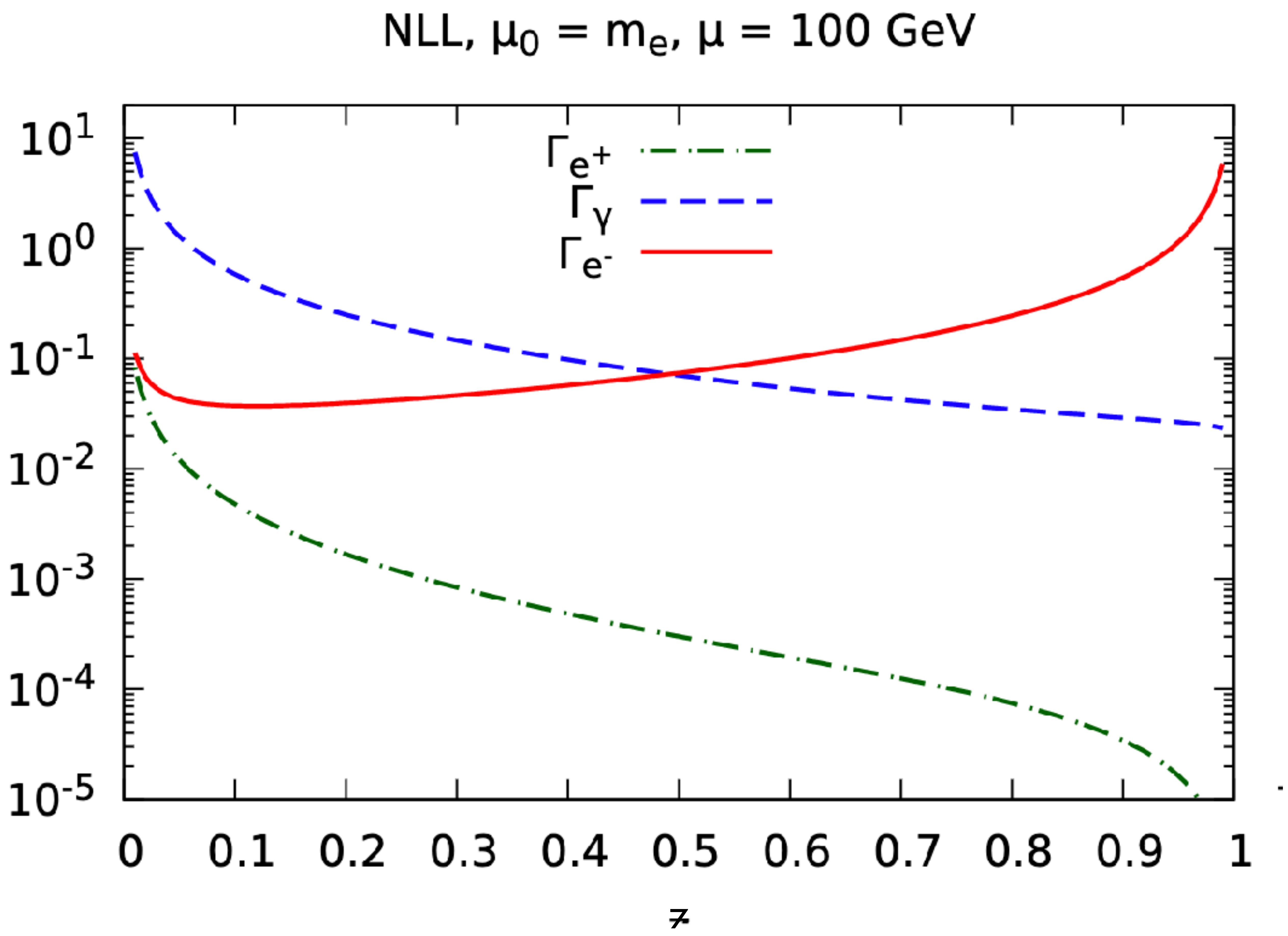

$$f_{e^\pm}(z,Q^2) = \beta \frac{\exp\left[-\gamma_E \beta + \frac{3}{4}\beta_S\right]}{\Gamma(1+\beta)}(1-z)^{\beta-1} + \beta_H \sum_{n=0}^{\infty} \beta_H^n \mathscr{H}_n(z)$$

Numerical stability for $z \to 1$,
also in ratio of Sudakov factor of ISR QED shower

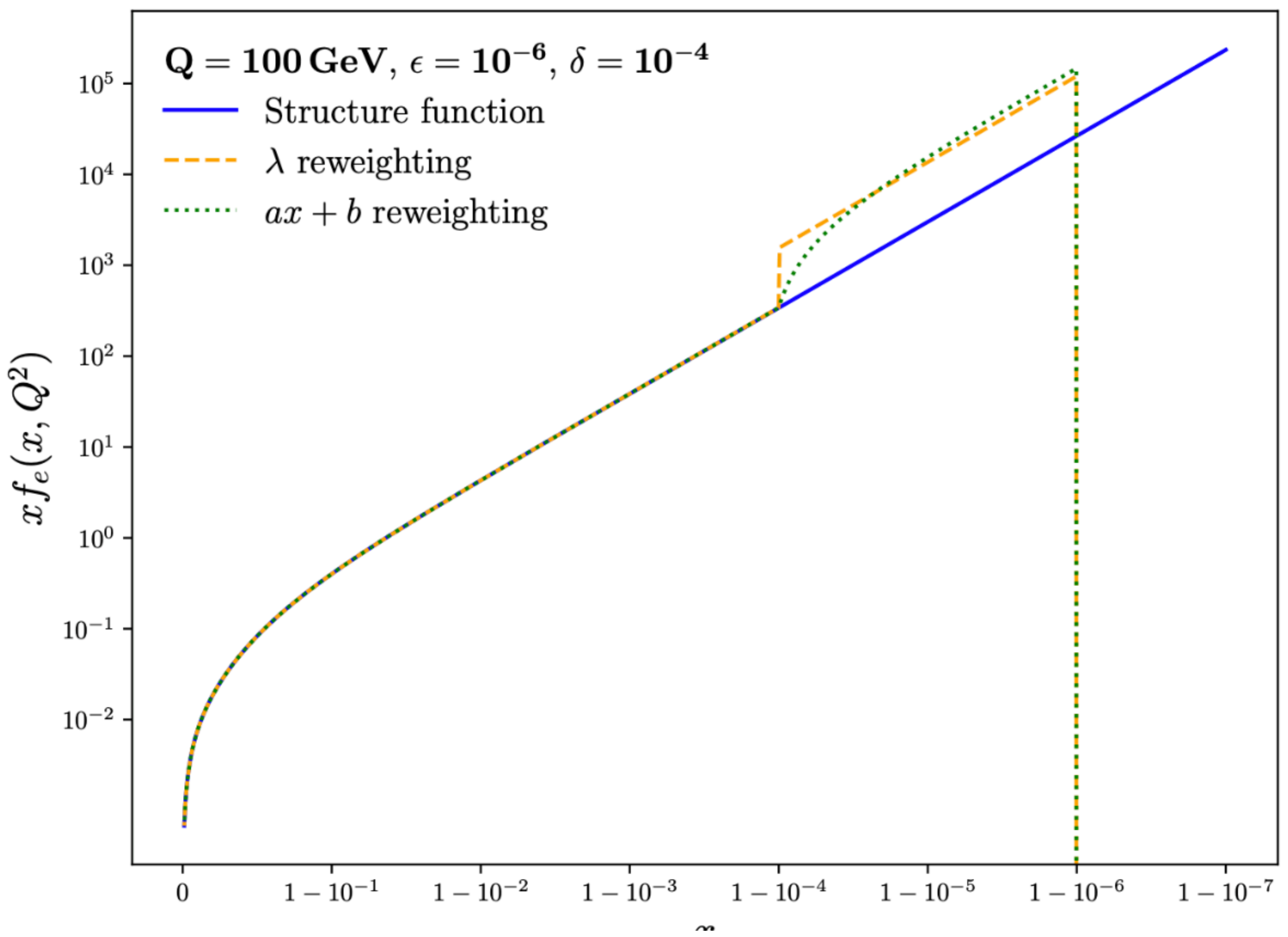

cf. e.g. Maxwell/Schönherr, 2603.05585

$$W_e = \begin{cases} f_e(x) & 0 \le x \le 1-\delta \\ w(x) f_e(x) & 1-\delta < x < 1-\epsilon \\ 0 & \text{else} \end{cases}$$

where $w(x)$ solves $\int_{1-\delta}^{1} W_e(x)dx = \int_0^1 f_e(x)dx\,.$

YFS: physics & properties

QED ISR [+FSR], exclusive part

- Exclusive ("coherent") resummation — Yennie/Frautschi/Suura, 1961
- Explicitly matches ME photons — Jadach/Ward/Yost, hep-ph/0103163+0104049+0211132+0602197, Piccinini ea.
- Exponentiated EW corrections (EEX) — Jadach ea., 1993-2001; Krauss/Price/Schönherr, 2203.10948; Kraus/Price, 2512.04959
- Coherent exponentiated EW corrections (CEEX) — Jadach/Ward/Wąs, hep-ph/0006359; 1409.4173
- Eikonal local subtraction scheme for soft singularities, collinear terms added constructively / process-dependent
- Provides MC algorithm for generation of exclusive multiple resolved (soft) photons

$$d\sigma = \sum_{n_\gamma=0}^{\infty} \frac{e^{Y(\Omega)}}{n_\gamma!} d\Phi_Q \left[\prod_{i=1}^{n_\gamma} d\Phi_i^\gamma \, \tilde{S}(k_i)\, \Theta(k_i,\Omega)\right] \left(\tilde{\beta}_0 + \sum_{j=1}^{n_\gamma} \frac{\tilde{\beta}_1(k_j)}{\tilde{s}(k_j)} + \sum_{\substack{j,k=1\\ j<k}}^{n_\gamma} \frac{\tilde{\beta}_2(k_j,k_k)}{\tilde{s}(k_j)\tilde{s}(k_k)} + \cdots\right)$$

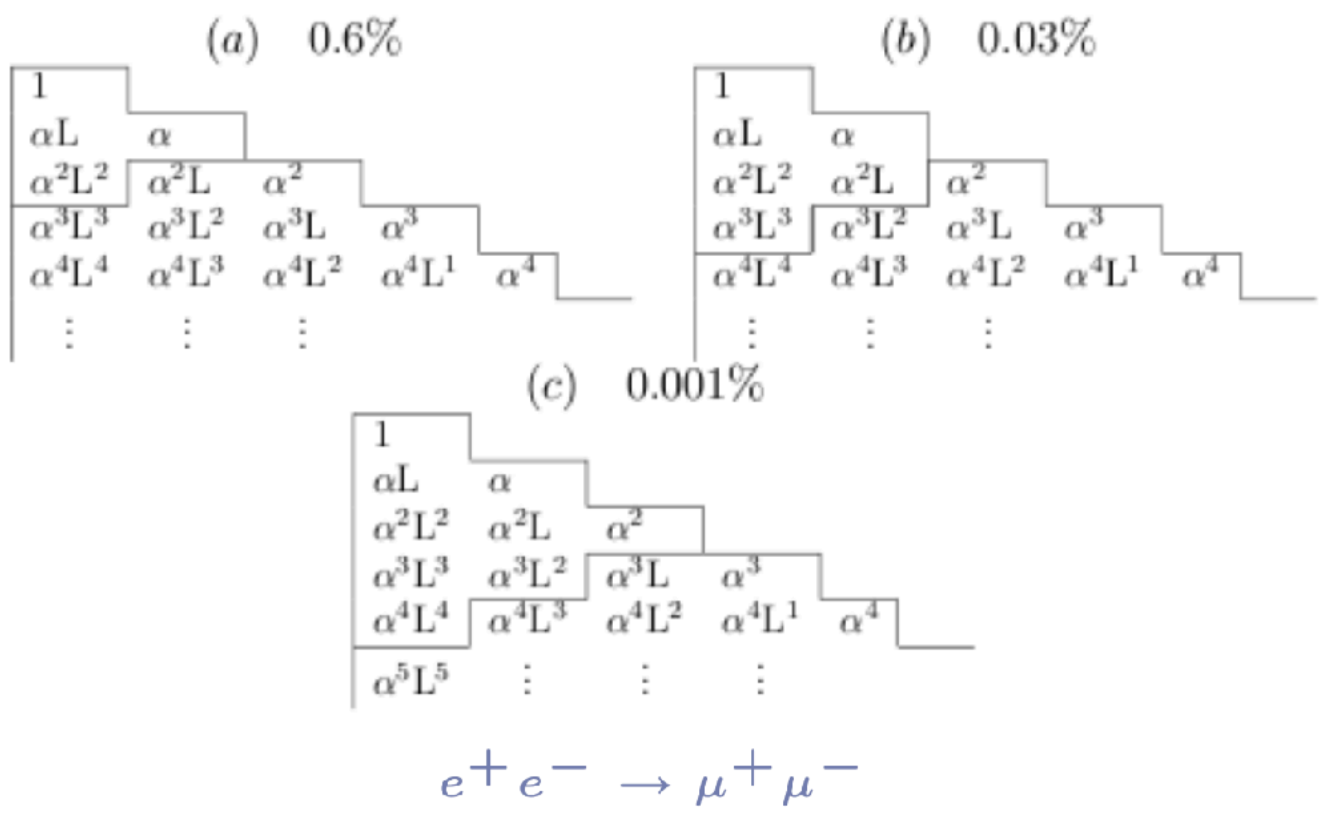

- $\mathcal{O}(\alpha L)$ and $\mathcal{O}(\alpha^2 L)$ in YFS *typically* mean the corresponding coefficients in the β_n terms
- $\mathcal{O}(\alpha L)$ and $\mathcal{O}(\alpha^2 L)$ in collinear factorisation mean the whole LL and NLL towers, respectively

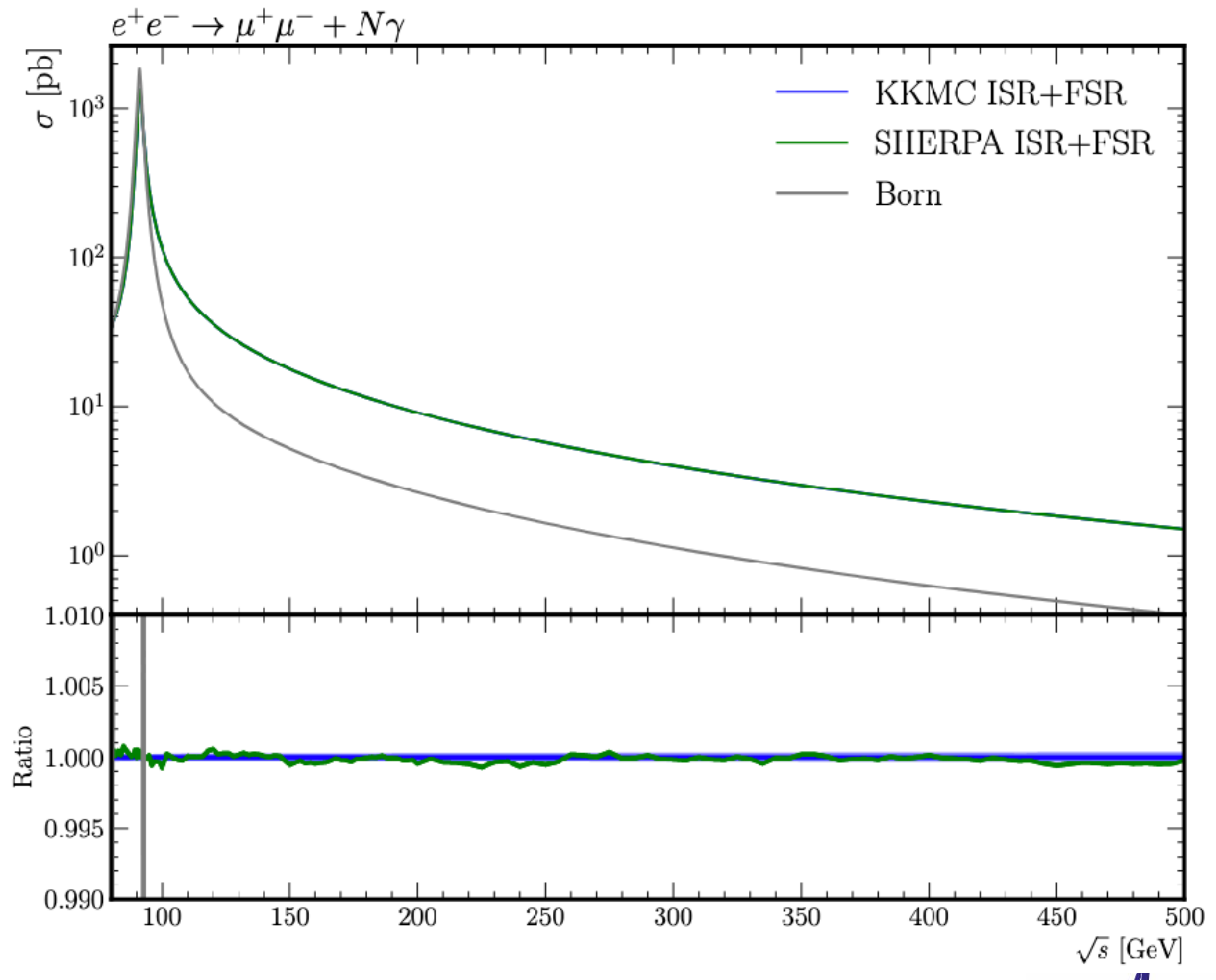

Exclusive photons

K. Mękała/D. Jeans/JRR/J. Tian/A.F. Żarnecki, arXiv:2504.11365

QED ISR [+FSR], QED shower + matching

- Why is the exact theoretical modelling of explicit photons important?

Detector optimization

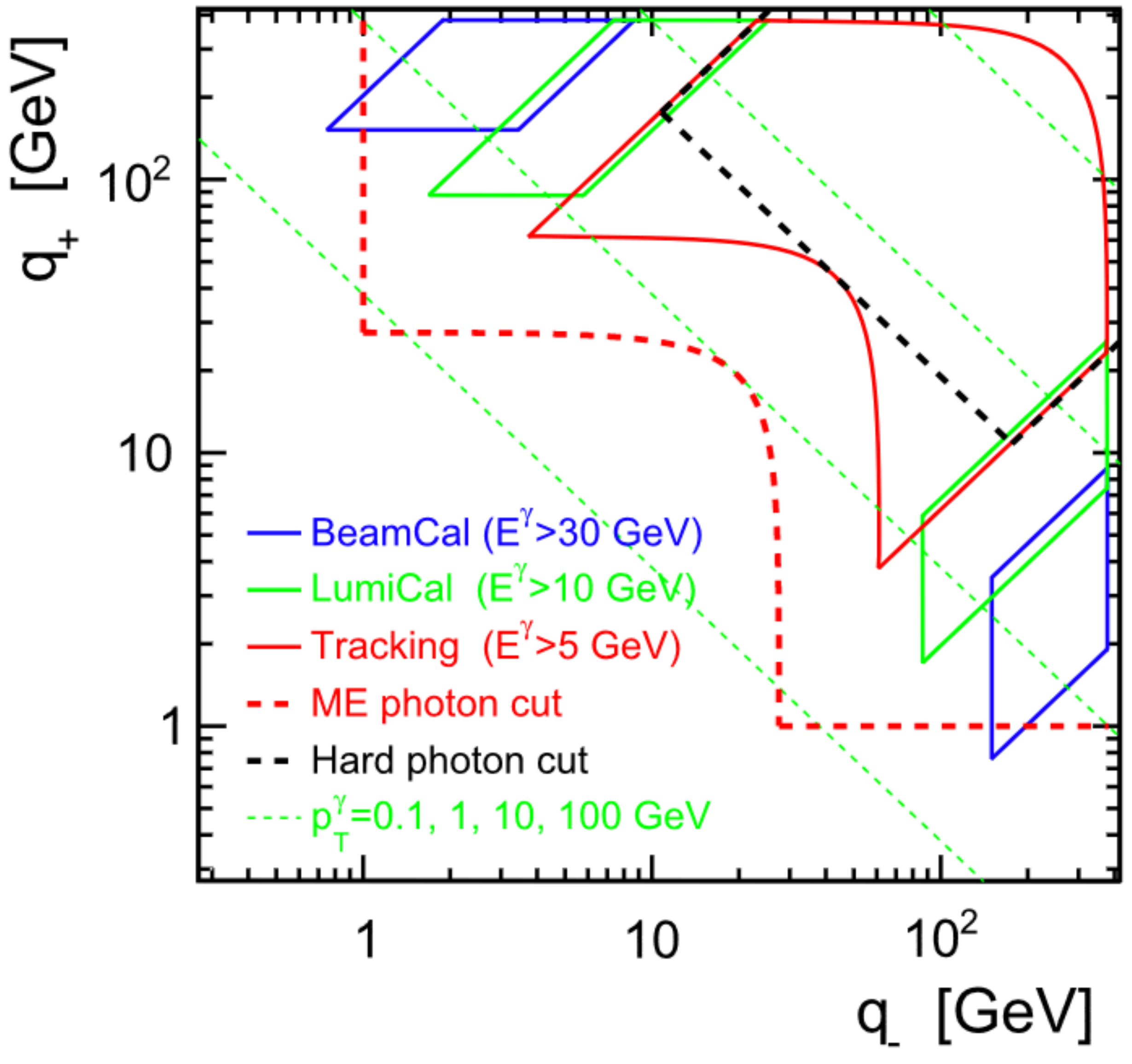

Light-quark tagging

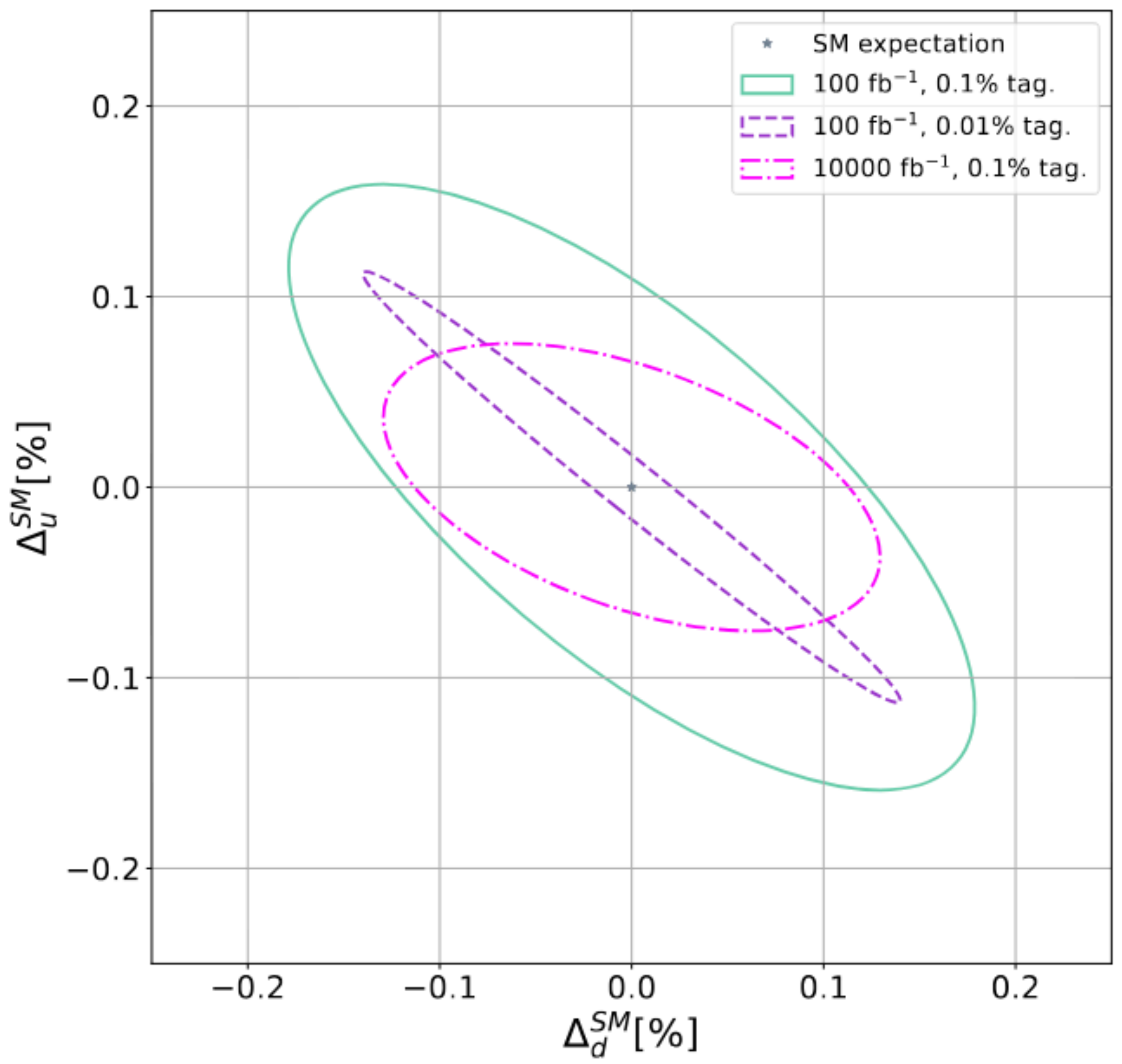

Monophoton searches

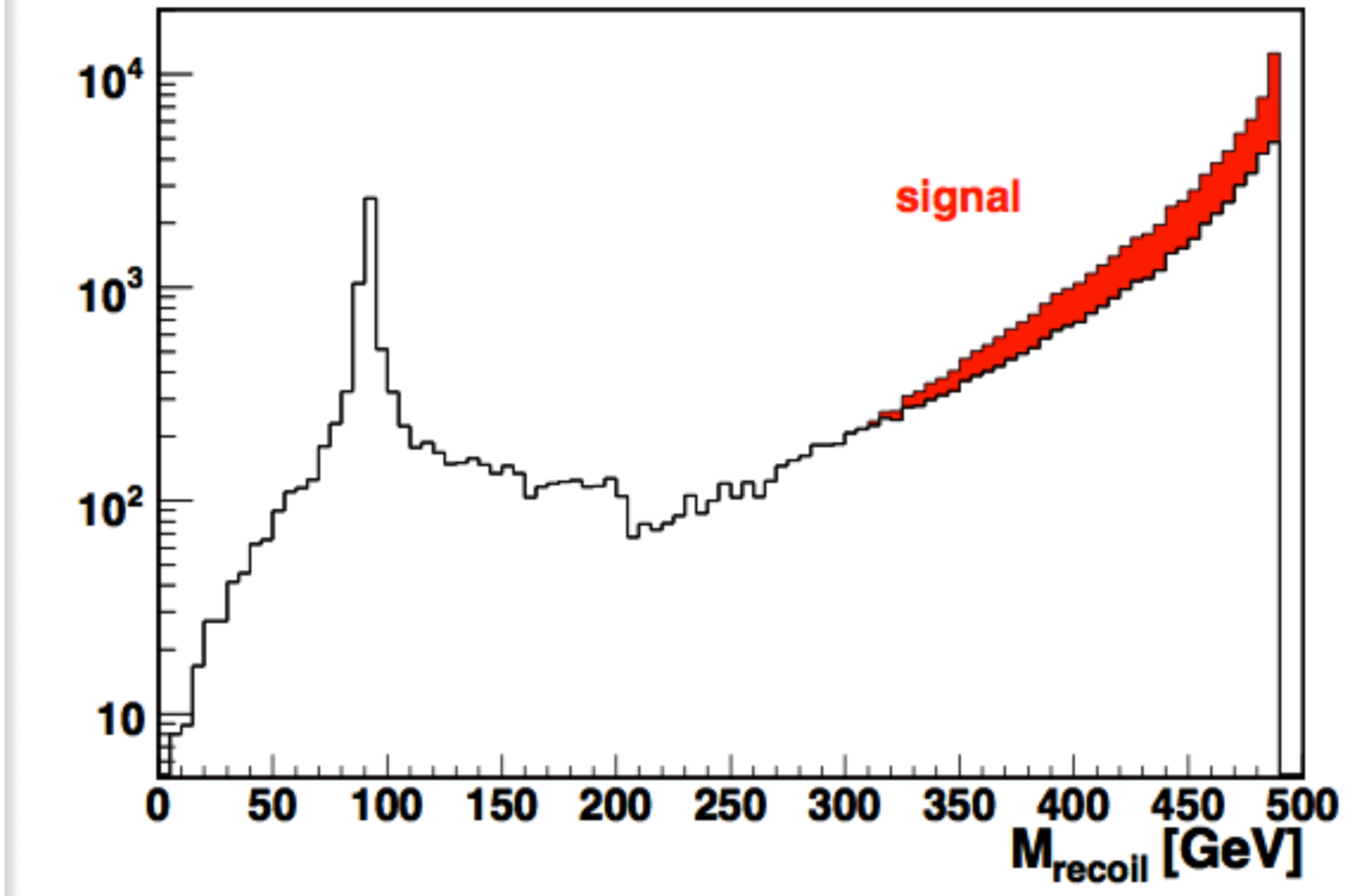

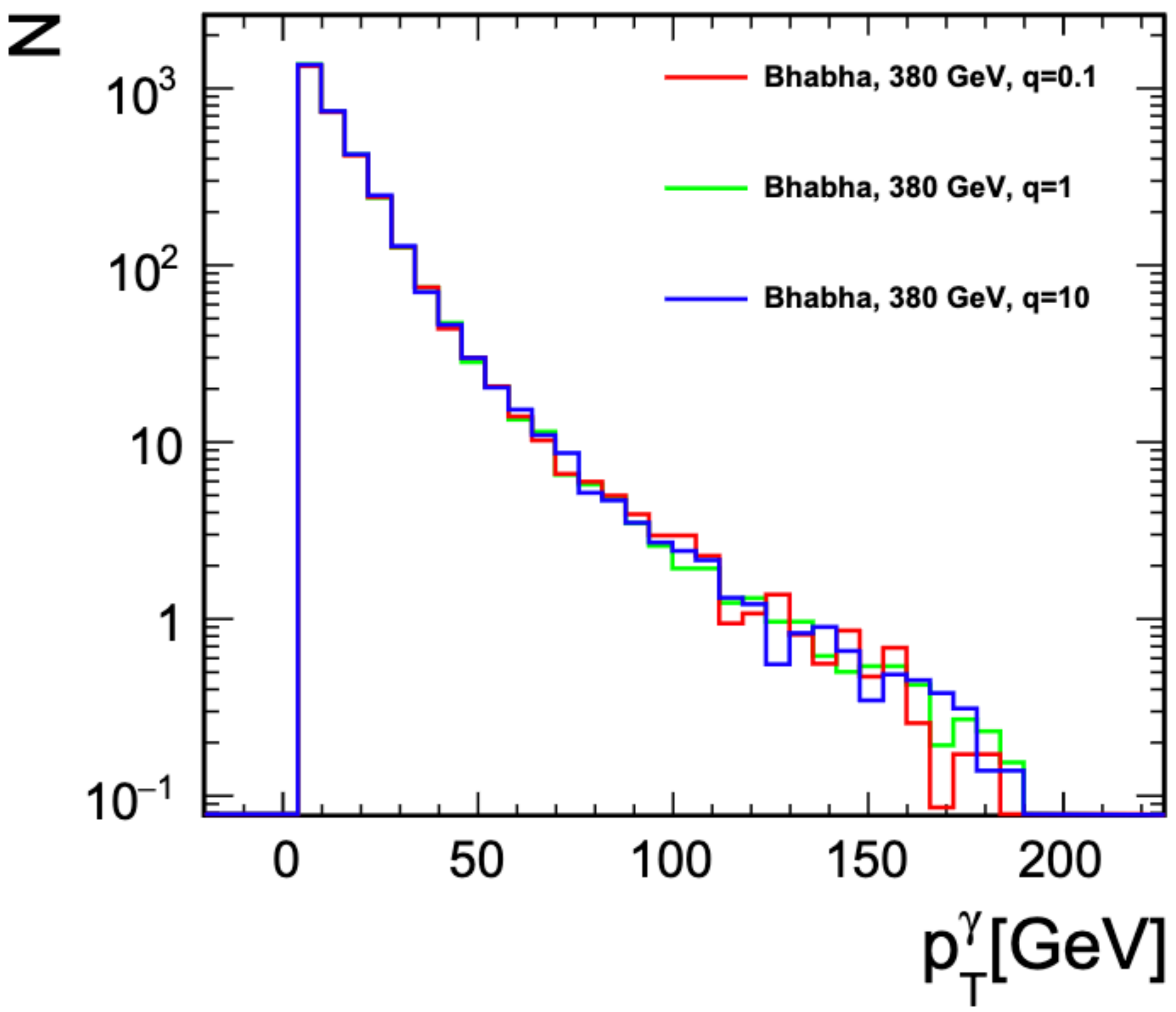

J. Kalinowski/W. Kotlarski/P. Sopicki/A.F. Zarnecki, 2020

Exclusive photons & QED showers

Different algorithms for exclusive photons

- Explicit photon from fix-order (LO/NLO/NNLO) matrix element (best description)
  - "Shower-recoil approach": generate $p_\perp$ according to $\frac{\alpha}{\pi} \cdot \log \frac{p_\perp^2}{m_e^2}$
  - Boost according to the generated $p_\perp$ (avail. for for ISR, EPA or ISR+EPA)
  - Generalizable as recursive algorithm with *n* exclusive photons
- YFS: explicit generation of (arbitrary multiplicities) of soft photons
  - Automatically matched to soft emissions in the hard matrix elements
  - Needs to be properly matched with collinear and hard photons

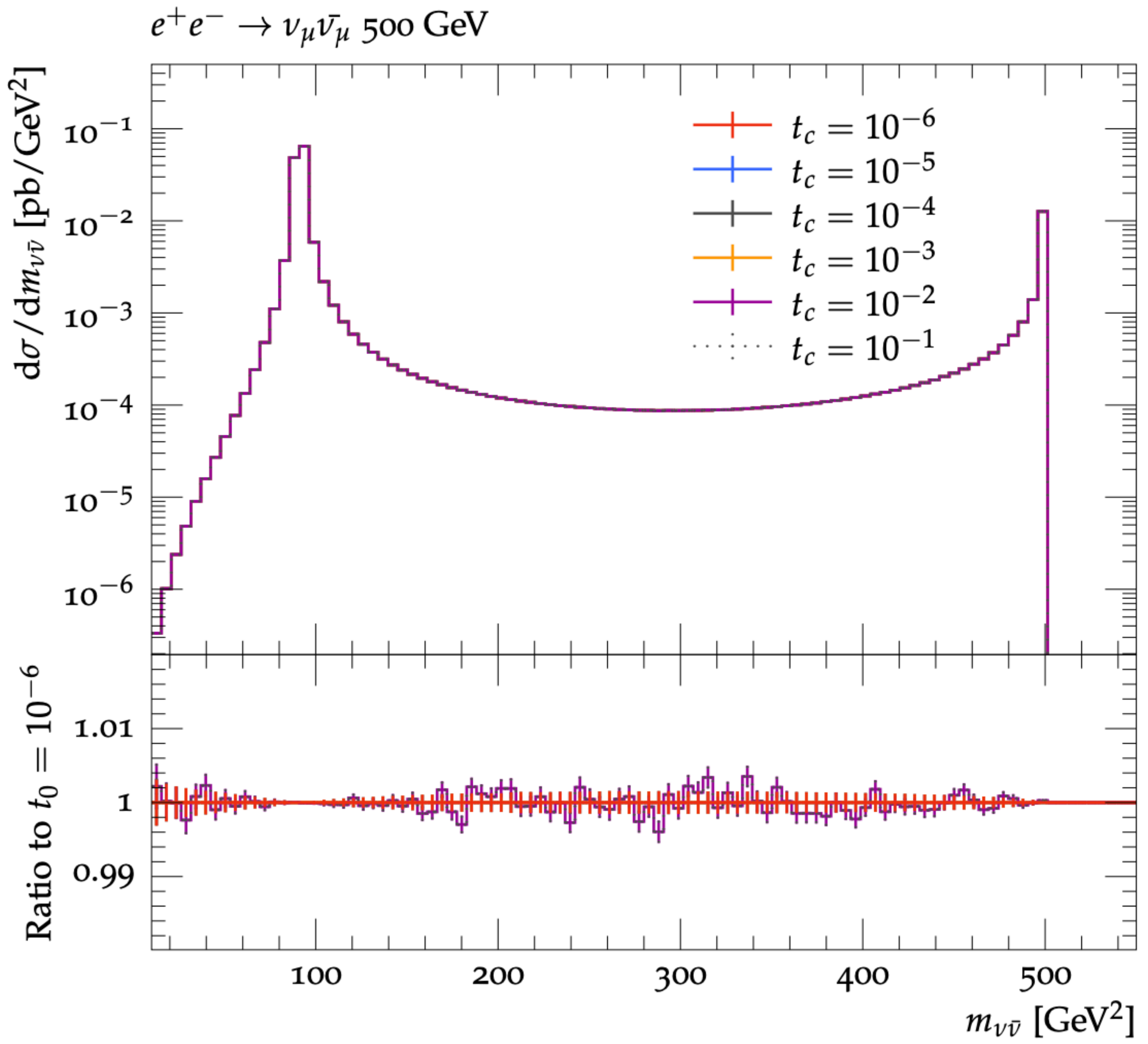

Schönherr, Graz EW Workshop, 2026

- QED showers based on (collinear) splitting kernels
  - QED is simpler (Abelian) and more complicated (no large-NC limit, all charged partons equally important)
  - Nasty interplay (algorithmic and numerical) between ISR QED shower and QED ePDF
  - Again beware of resonances: $q^2 \lesssim \Gamma^2$ coherent emission (photon radiation does not resolve resonance)

    $q^2 \gtrsim \Gamma^2$ incoherent emission (photon radiation can resolve the resonance)

Thresholds @ FCC-ee: $W^+W^-, t\bar{t}$

- LHC threshold production: kinematic behavior shadowed by proton PDFs [now top threshold visible]
- FCC-ee very precise energy scans: highest precision measurements of M_W ($\Delta M_W \sim$ 0.3 MeV), M_t ($\Delta M_t \sim$ 7 MeV)
- FCC-ee very precise energy scans: huge QED ISR effects (30% for *Z*, 15-20% for *WW*, *ZH*, *tt*)
- In addition: full off-shell processes and resummation of large QED (*WW*) or QCD logarithms (*tt*) needed
- Proper matching necessary to N(N)LO fixed-order calculation (and to corresponding showers)

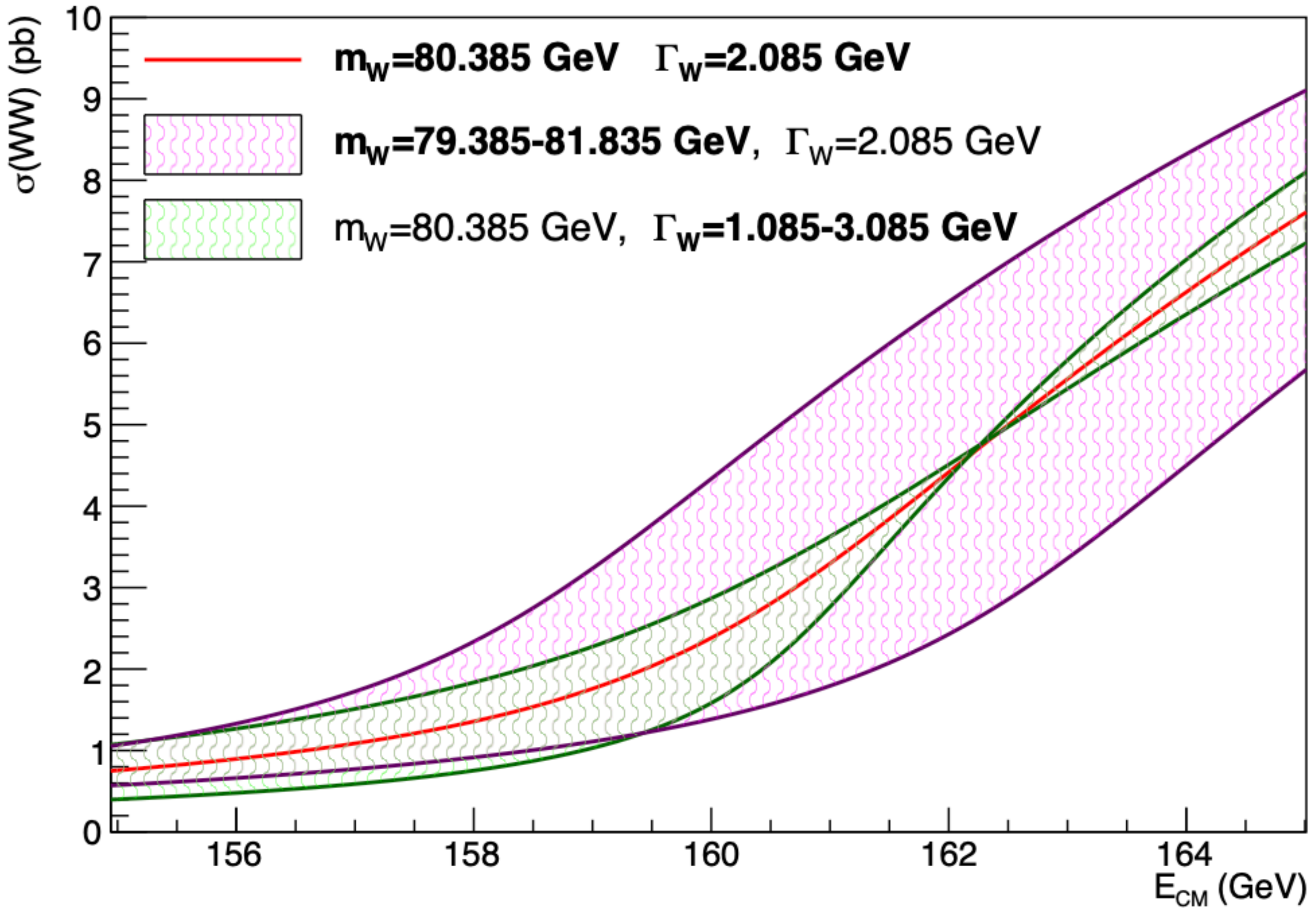

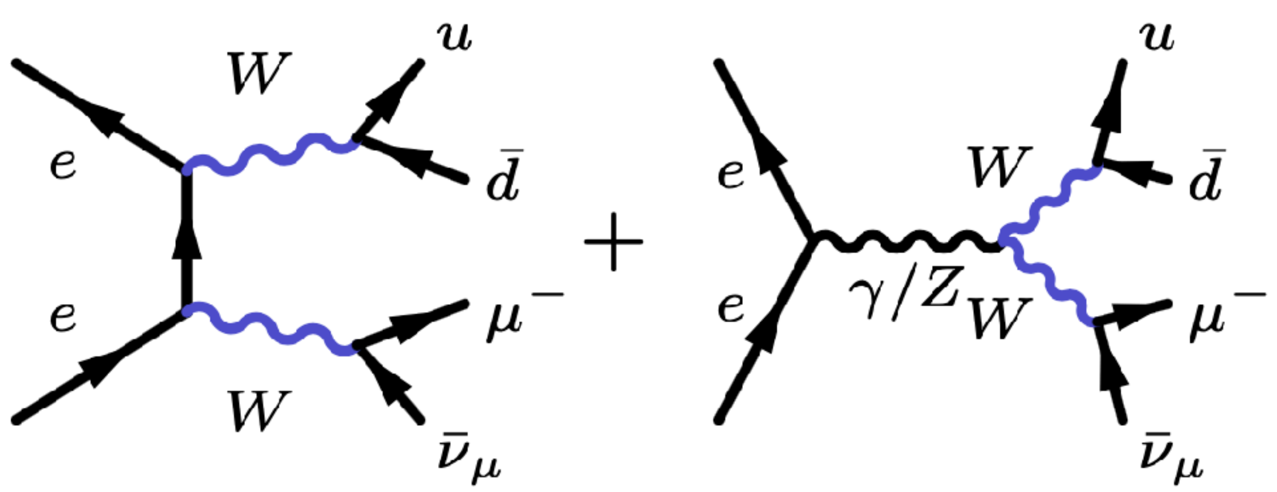

$$\sigma_{WW} = C\alpha^2\beta\Big[\, 1 + c^{(0)}\beta \qquad \text{LO}$$

$$+\,\alpha\left(\frac{c_1^{(1)}}{\beta} + c_2^{(1)}\ln\beta L_e + c_3^{(1)} L_e + c_4^{(1)} + c_5^{(1)}\beta\right) \qquad \text{NLO}$$

$$+\,\alpha^2\underbrace{\left(\frac{c_1^{(2)}}{\beta^2} + \frac{c_2^{(2)}}{\beta} + c_3^{(2)}\ln^2\beta L_e^2 + c_4^{(2)}\ln\beta L_e^2 + \ldots\right)}_{\text{leading NNLO parts known}} + \ldots\Big] \qquad \text{NNLO}$$

NNLO ↓ required for FCC-ee

Top threshold: importance and how to handle it in MC

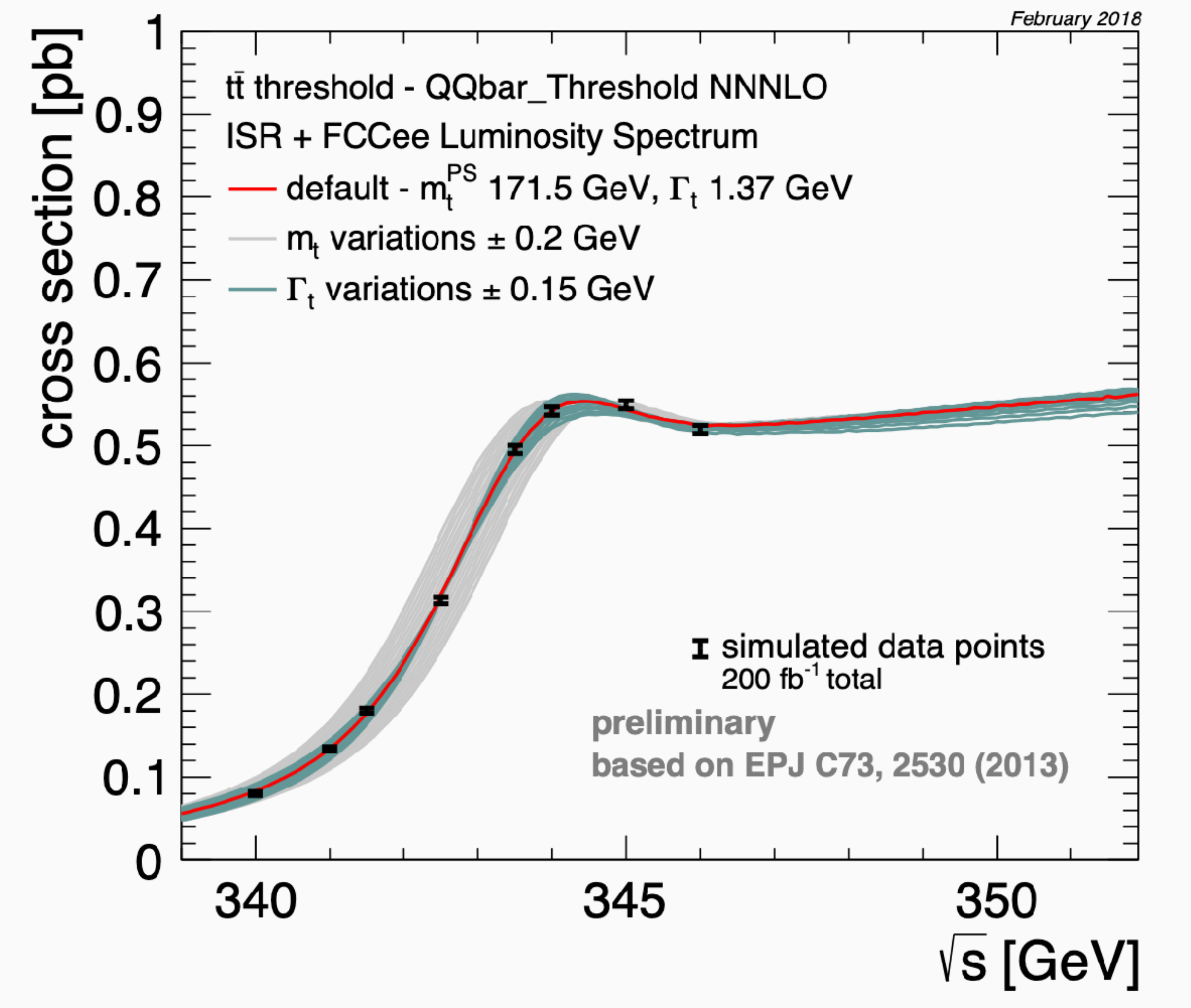

- ☑ Position and shape of threshold depends on M_{top}
- ☑ Top threshold uses well-defined (short-distance) mass definition
- ☑ Top mass uncertainty possible: ~ 7 MeV [exp.] ⊕ 35 MeV [th.]

from: Defranchis/de Blas/Mekta/Selvaggi/Vos: 2503.18713

Uncertainty source	Impact on σ_{WbWb} [%]		
	340 GeV	345 GeV	365 GeV
Integrated luminosity	0.12	0.11	0.02
b tagging	0.11	0.06	0.01
ZZ had. norm.	0.46	0.19	0.04
ZZ semihad. norm.	0.23	0.07	0.03
WW had. norm.	0.17	0.09	0.02
WW semihad. norm.	0.06	0.04	0.03
q$\bar{q}$ had. norm.	0.12	0.09	0.02
q$\bar{q}$ semihad. norm.	0.18	0.06	0.01
WWZ norm.	0.03	0.01	0.01
Total (incl. stat)	2.31	0.89	0.12

Uncertainty source	m_t^{PS} [MeV]	Γ_t [MeV]	Input values
Experimental (stat. ×1.2)	4.3	10.4	$L = 410\,\mathrm{fb}^{-1}$ (FCC-ee)
Parametric y_t	4.2	3.6	$\delta y_t = 3\%$
Parametric α_S	2.2	1.7	$\delta\alpha_S(m_Z^2) = 10^{-4}$
Luminosity calibration (uncorr.)	0.5	1.0	$\delta L/L = 0.1\%$
Luminosity calibration (corr.)	0.4	0.4	$\delta L/L = 0.05\%$
Beam energy calibration (uncorr.)	1.2	1.8	$\delta\sqrt{s} = 5$ MeV [41, 42]
Beam energy calibration (corr.)	1.2	0.1	$\delta\sqrt{s} = 2.5$ MeV
Beam energy spread (uncorr.)	0.3	0.8	$\delta\Delta E = 1\%$ [41]
Beam energy spread (corr.)	0.1	1.1	$\delta\Delta E = 0.5\%$
Total profiled	6.8	11.5	
Theory, unprofiled (scale)	35	25	N^{3}LO NR-QCD [11]

Top threshold: importance and how to handle it in MC

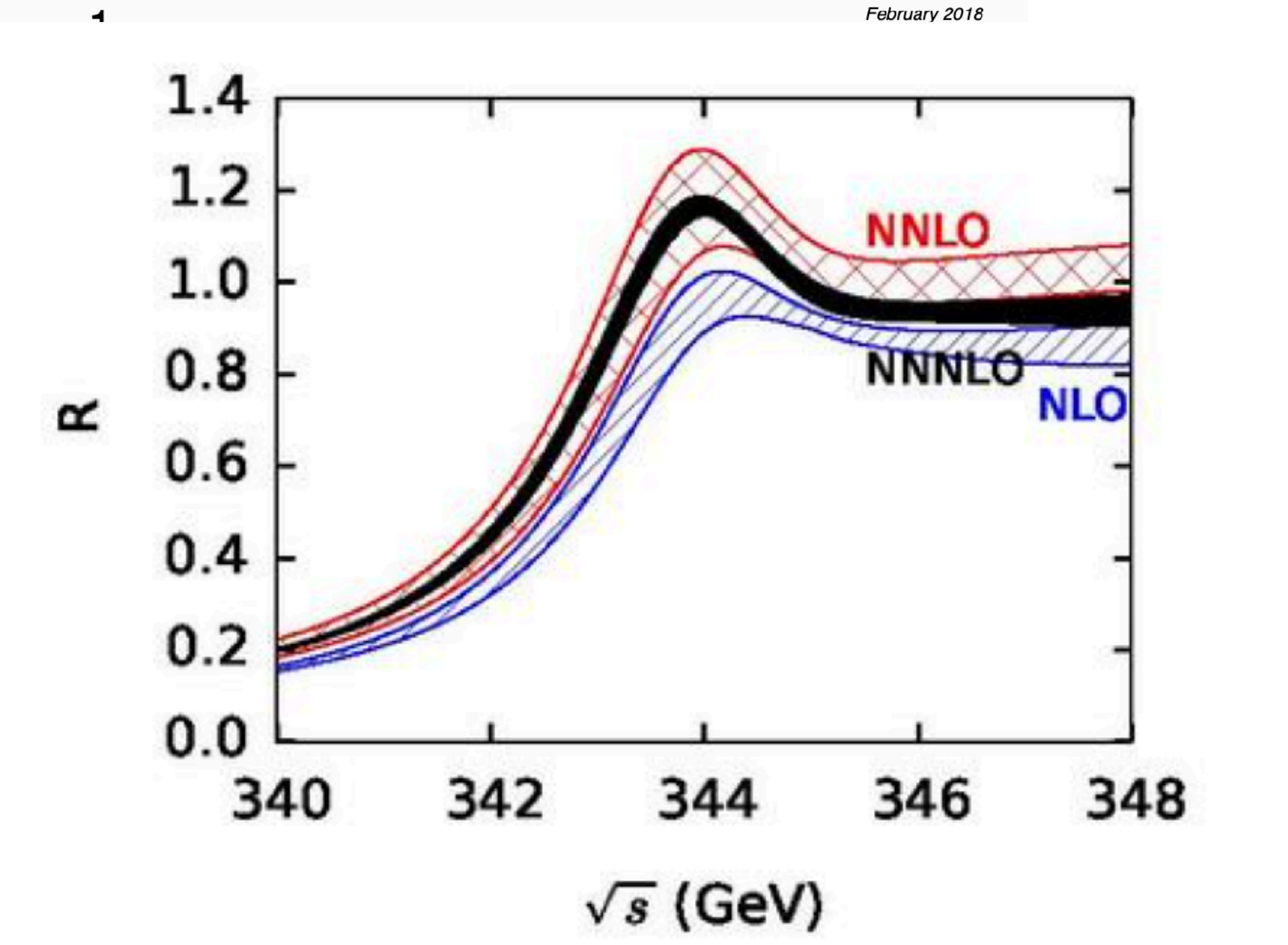

- ☑ Position and shape of threshold depends on M_{top}
- ☑ Top threshold uses well-defined (short-distance) mass definition
- ☑ Top mass uncertainty possible: ~ 7 MeV [exp.] ⊕ 35 MeV [th.]

from: Defranchis/de Blas/Mekta/Selvaggi/Vos: 2503.18713

Uncertainty source	Impact on σ_{WbWb} [%]		
	340 GeV	345 GeV	365 GeV
Integrated luminosity	0.12	0.11	0.02
b tagging	0.11	0.06	0.01
ZZ had. norm.	0.46	0.19	0.04
ZZ semihad. norm.	0.23	0.07	0.03
WW had. norm.	0.17	0.09	0.02
WW semihad. norm.	0.06	0.04	0.03
$q\bar{q}$ had. norm.	0.12	0.09	0.02
$q\bar{q}$ semihad. norm.	0.18	0.06	0.01
WWZ norm.	0.03	0.01	0.01
Total (incl. stat)	2.31	0.89	0.12

Uncertainty source	m_t^{PS} [MeV]	Γ_t [MeV]	Input values
Experimental (stat. ×1.2)	4.3	10.4	$L = 410\,\mathrm{fb}^{-1}$ (FCC-ee)
Parametric y_t	4.2	3.6	$\delta y_t = 3\%$
Parametric α_S	2.2	1.7	$\delta\alpha_S(m_Z^2) = 10^{-4}$
Luminosity calibration (uncorr.)	0.5	1.0	$\delta L/L = 0.1\%$
Luminosity calibration (corr.)	0.4	0.4	$\delta L/L = 0.05\%$
Beam energy calibration (uncorr.)	1.2	1.8	$\delta\sqrt{s} = 5$ MeV [41, 42]
Beam energy calibration (corr.)	1.2	0.1	$\delta\sqrt{s} = 2.5$ MeV
Beam energy spread (uncorr.)	0.3	0.8	$\delta\Delta E = 1\%$ [41]
Beam energy spread (corr.)	0.1	1.1	$\delta\Delta E = 0.5\%$
Total profiled	6.8	11.5	
Theory, unprofiled (scale)	35	25	N^3LO NR-QCD [11]

Top threshold: from inclusive to differential

- NRQCD is EFT for non-relativistic quark-antiquark systems: separate scales $\mu_h = h \cdot m_t \qquad \mu_s = f \cdot m_t v$
- Resummation of singular terms close to threshold @ NNNLO/NNLL Hoang et al. '99-'01; Beneke et al., '13-'14

Solve non-relativistic Schrödinger equation for Green's function:

$$\left[(E + i\Gamma_t) - \left\{-\frac{\nabla^2}{m_t} + V^{(c)}_{\rm QCD}(r)\right\}\right] G^{(c)}(\vec{x}; E) = \delta^3(\vec{x})$$

QCD potential:

$$V_{\rm pQCD}(r) = -\frac{C_F\,\alpha_s(\mu_R)}{r}\left\{1 + \frac{\alpha_s(\mu_R)}{4\pi}[a_1 + 2\gamma_E\beta_0] + \left(\frac{\alpha_s(\mu_R)}{4\pi}\right)^2\left[a_2 + \left(\frac{\pi^2}{3} + 4\gamma_E^2\right)\beta_0^2 + 2\gamma_E(2a_1\beta_0 + \beta_1)\right]\right\}$$

Top threshold: from inclusive to differential

- NRQCD is EFT for non-relativistic quark-antiquark systems: separate scales $\mu_h = h \cdot m_t \qquad \mu_s = f \cdot m_t v$
- Resummation of singular terms close to threshold @ NNNLO/NNLL Hoang et al. '99-'01; Beneke et al., '13-'14

Solve non-relativistic Schrödinger equation for Green's function:

$$\left[(E + i\Gamma_t) - \left\{-\frac{\nabla^2}{m_t} + V^{(c)}_{\mathrm{QCD}}(r)\right\}\right] G^{(c)}(\vec{x}; E) = \delta^3(\vec{x})$$

QCD potential:

$$V_{\mathrm{pQCD}}(r) = -\frac{C_F\,\alpha_s(\mu_R)}{r}\left\{1 + \frac{\alpha_s(\mu_R)}{4\pi}[a_1 + 2\gamma_E\beta_0] + \left(\frac{\alpha_s(\mu_R)}{4\pi}\right)^2\left[a_2 + \left(\frac{\pi^2}{3} + 4\gamma_E^2\right)\beta_0^2 + 2\gamma_E(2a_1\beta_0 + \beta_1)\right]\right\}$$

can be mapped onto effective *ttV* vertex

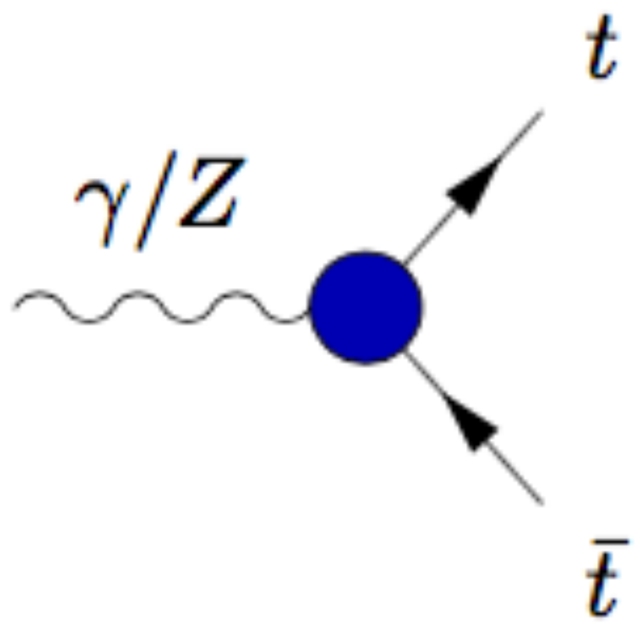

$$\sim \sqrt{R^{v/a}_{\mathrm{(N)LL}}} \sim \frac{\mathcal{G}^{v/a}_{\mathrm{(N)LL}}}{\mathcal{G}^{v/a}\big|_{\alpha_s=0}} \longrightarrow 1$$

far away from threshold

$$\mathbb{C} \ni \mathcal{G}^{v/a}_{\mathrm{(N)LL}} = \mathcal{G}^{v/a}_{\mathrm{(N)LL}}(\alpha_s, M_t^{\mathrm{pole}}, \sqrt{s}, |\vec{p}_t|, \Gamma_t)$$

differential in off-shell *tt* phase space

Top threshold: validation & matching

- Transition region between relativistic and resummation effects

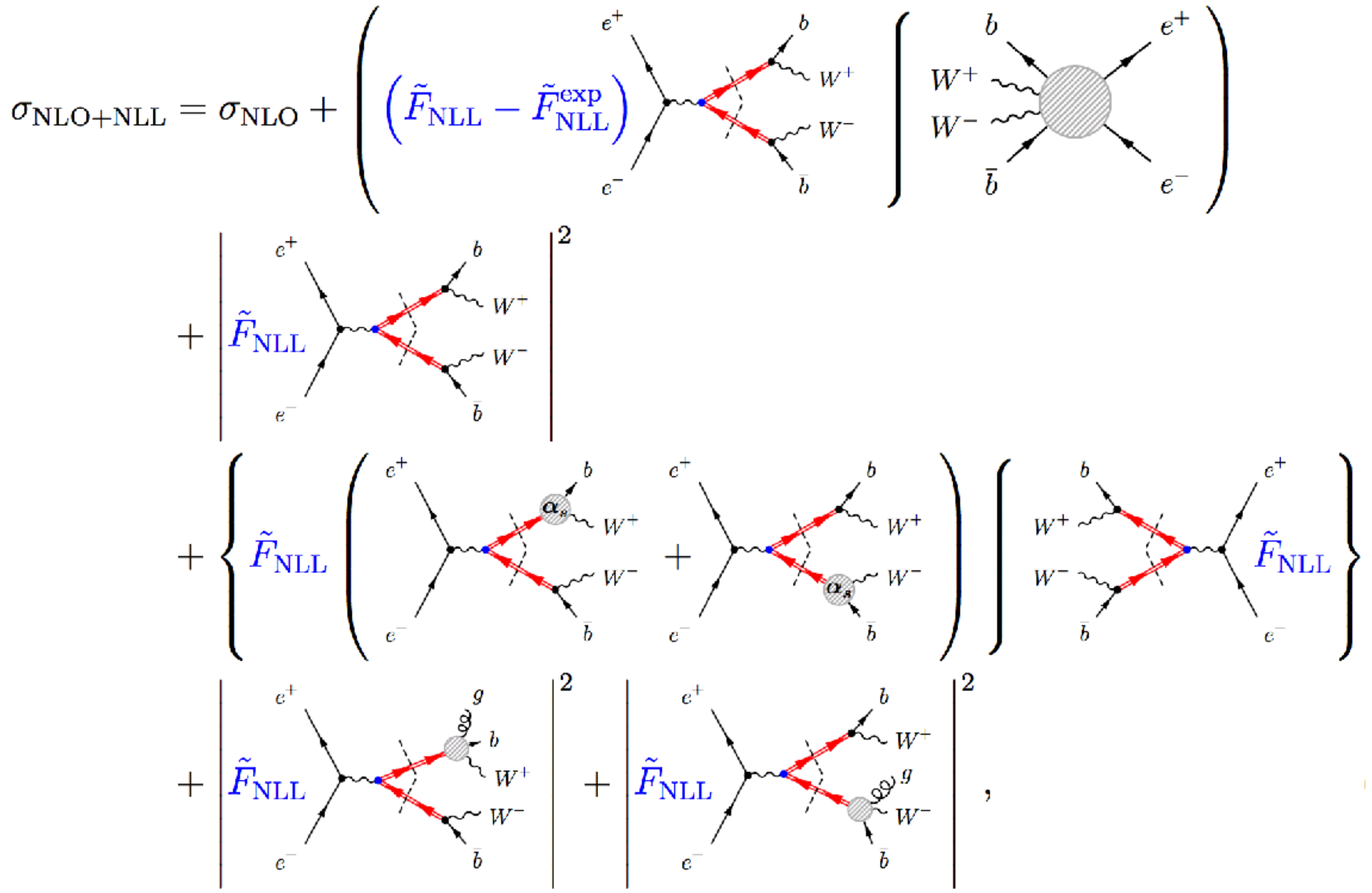

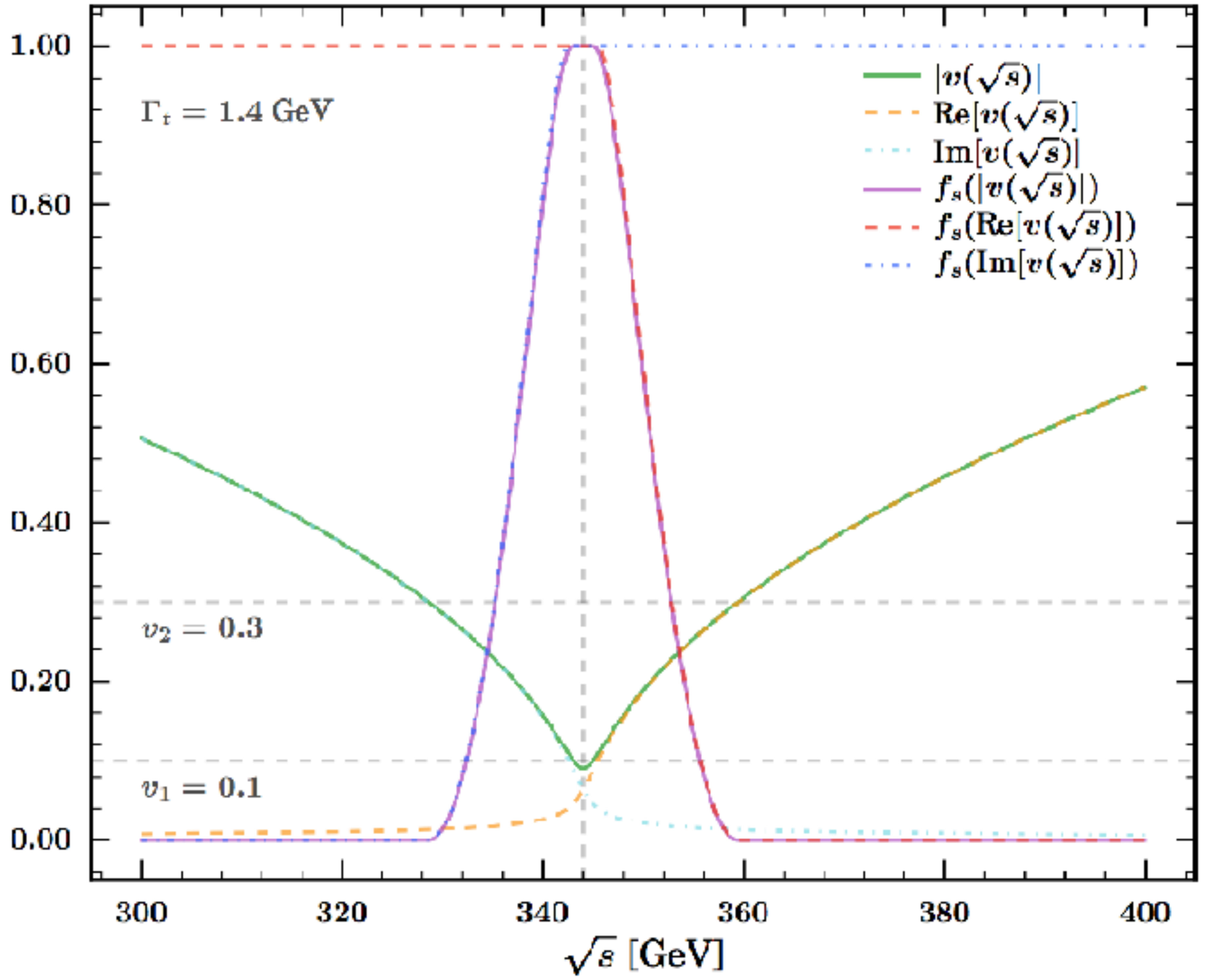

$$\sigma_{\rm matched} = \sigma_{\rm FO}\,[\alpha_{\rm H}] + \sigma^{\rm full}_{\rm NRQCD}\,[f_s\,\alpha_{\rm H},\ f_s\,\alpha_{\rm S},\ f_s\,\alpha_{\rm US}] - \sigma^{\rm expanded}_{\rm NRQCD}\,[f_s\,\alpha_{\rm H},\ f_s\,\alpha_{\rm H}]\ ,$$

$$\alpha_{\rm H} = \alpha_s\left[\mu_{\rm H} = h M_t^{\rm 1S}\right]\ , \qquad \alpha_{\rm F} = \alpha_s\left[\mu_{\rm F} = h M_t^{\rm 1S}\sqrt{\nu_*}\right]\ ,$$

$$\alpha_{\rm S} = \alpha_s\left[\mu_{\rm S} = h M_t^{\rm 1S} f\nu_*\right]\ , \qquad \alpha_{\rm U} = \alpha_s\left[\mu_{\rm US} = h M_t^{\rm 1S}(f\nu_*)^2\right]$$

Smoothstep matching function (inspired from SCET profile scales):

$$f_s(v) = \begin{cases} 1 & v < v_1 \\ 1 - 3\left(\frac{v-v_1}{v_2-v_1}\right)^2 - 2\left(\frac{v-v_1}{v_2-v_1}\right)^3 & v_1 \le v \le v_2 \\ 0 & v > v_2 \end{cases}$$

Matching threshold NLL to continuum NLO

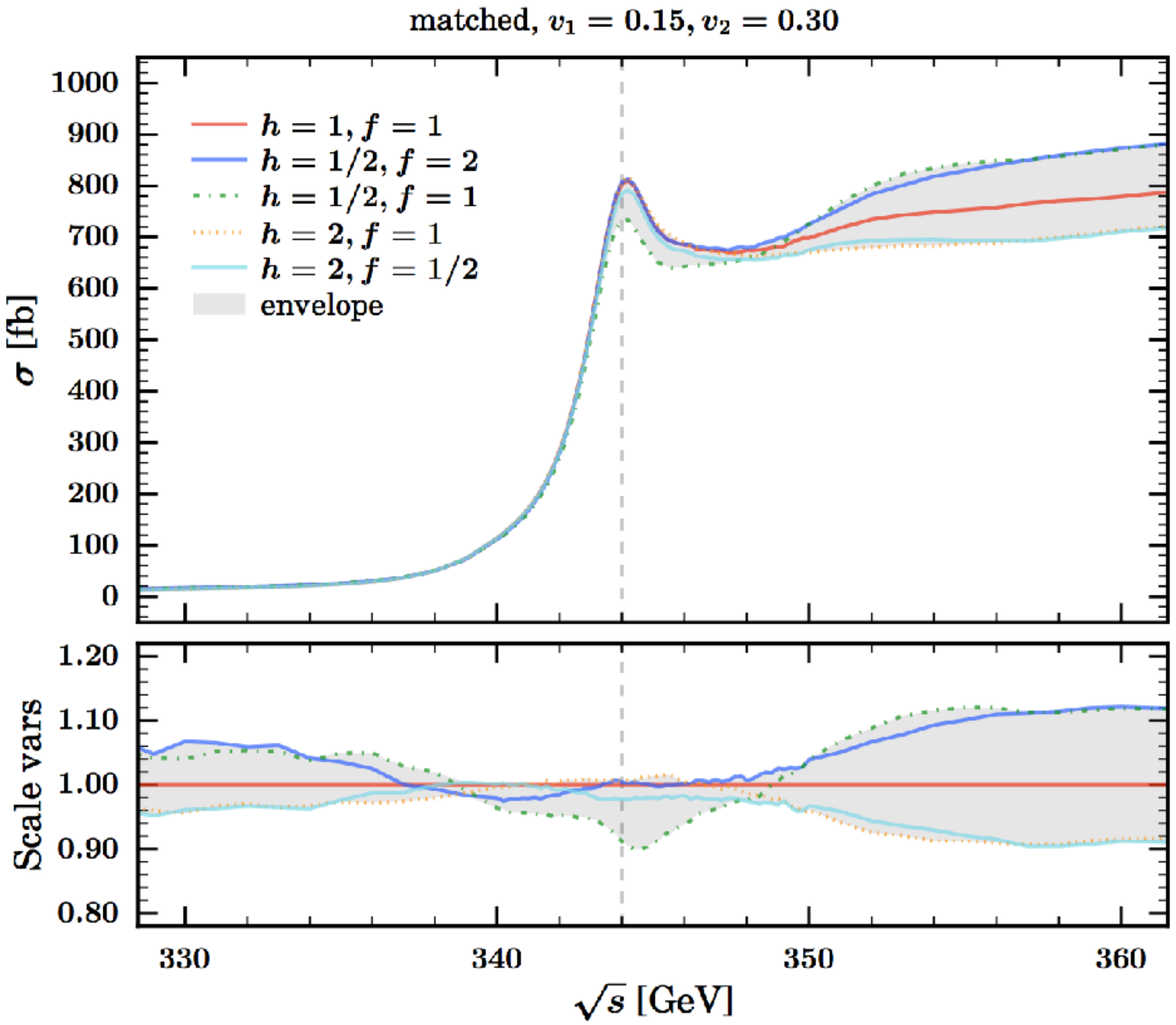

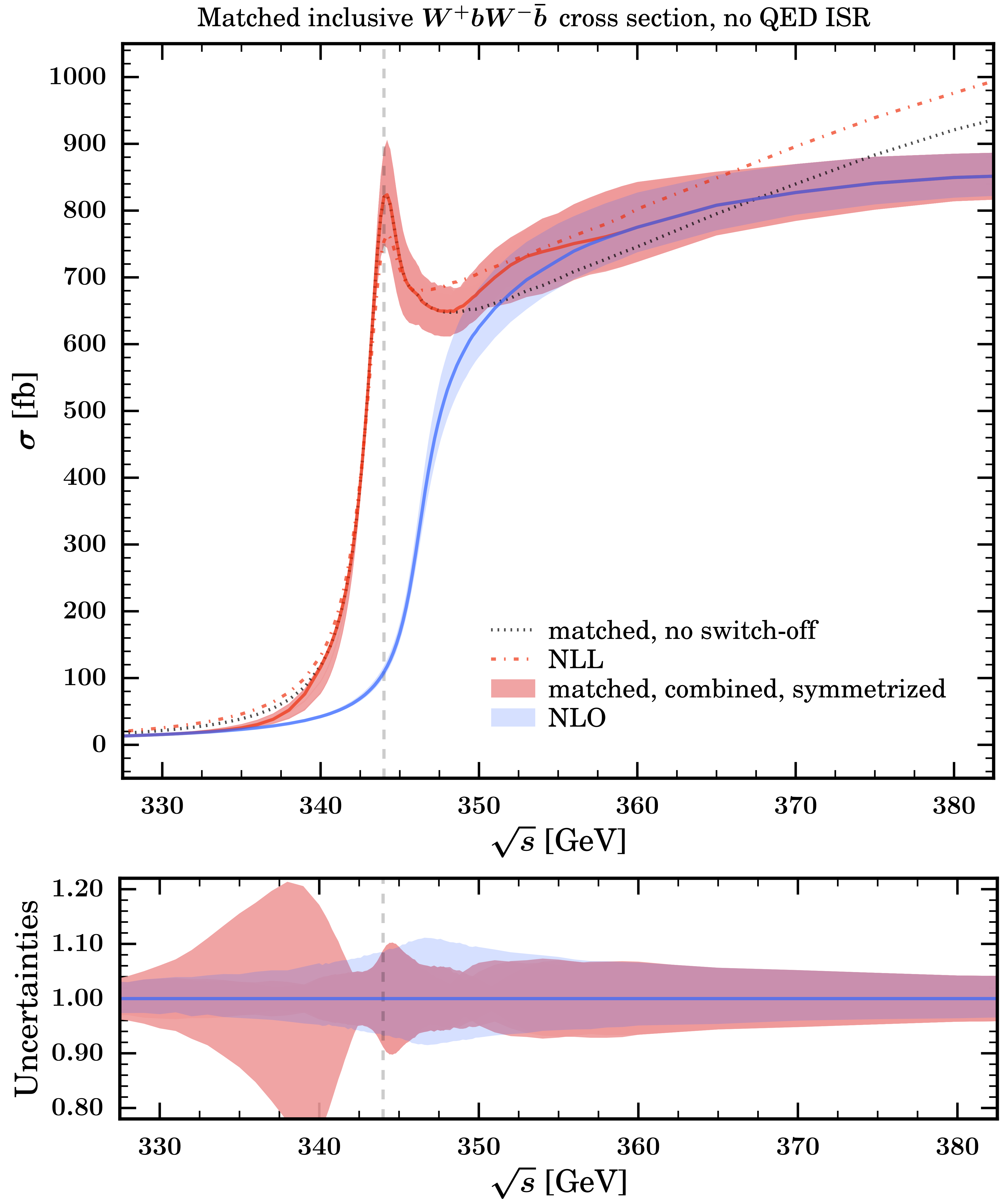

Total uncertainty: ***h-f* variation band and matching [switch-off function]**

Symmetrization of error bands:

$$\sigma_{\max} = \max\left[\max_{i\in\text{HF}} \sigma_i \;,\; \sigma_0 + (\sigma_0 - \min_{i\in\text{HF}} \sigma_i)\right]$$

$$\sigma_{\min} = \min\left[\min_{i\in\text{HF}} \sigma_i \;,\; \sigma_0 - (\max_{i\in\text{HF}} \sigma_i - \sigma_0)\right]$$

Bach/Chokoufé/Hoang/Kilian/JRR/
Stahlhofen/Teubner/Weiss, 1712.02220

Threshold matching with QED ISR

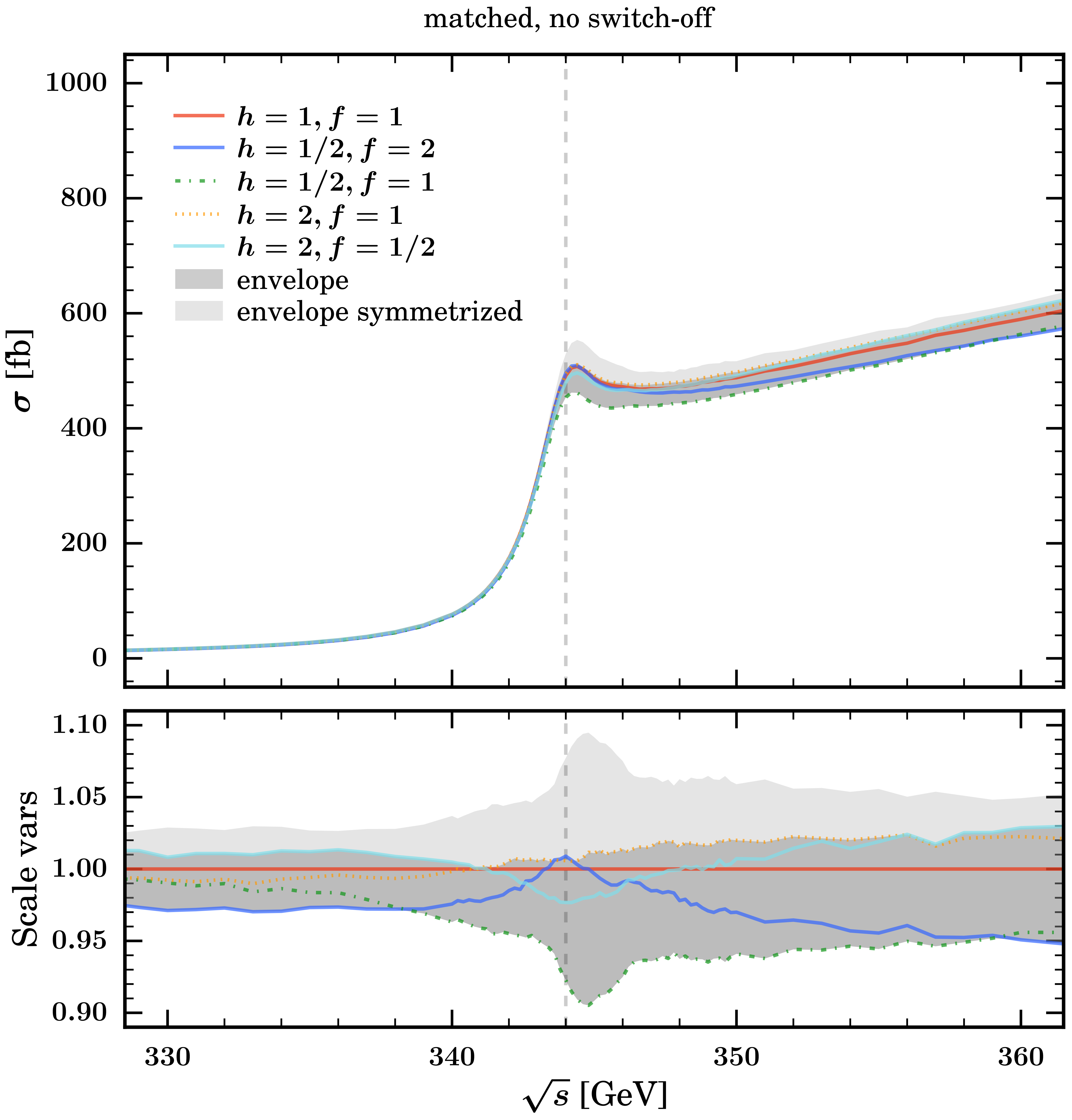

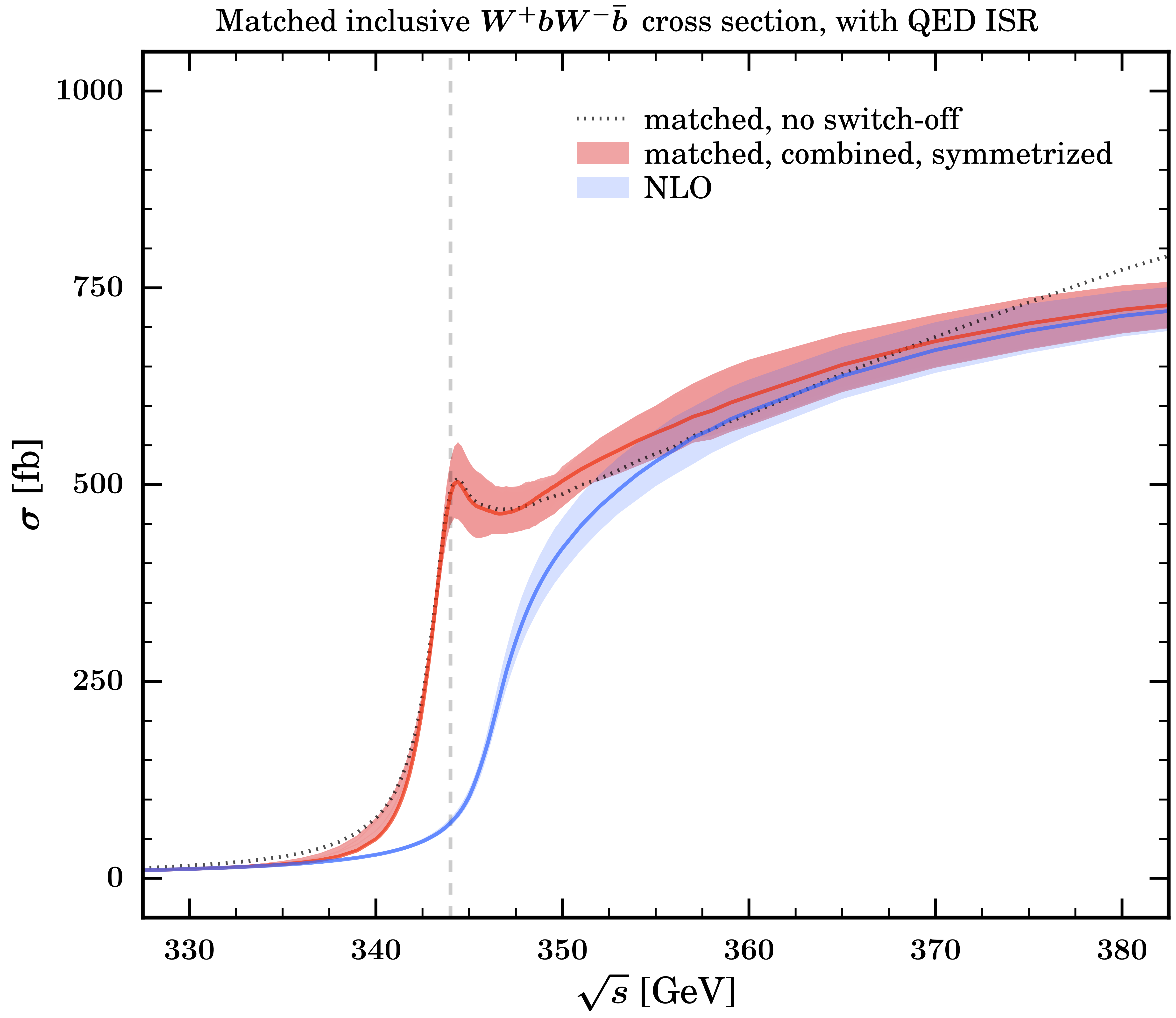

Bach/Chokoufé/Hoang/Kilian/JRR/Stahlhofen/Teubner/Weiss, 1712.02220

Matched threshold differential distributions

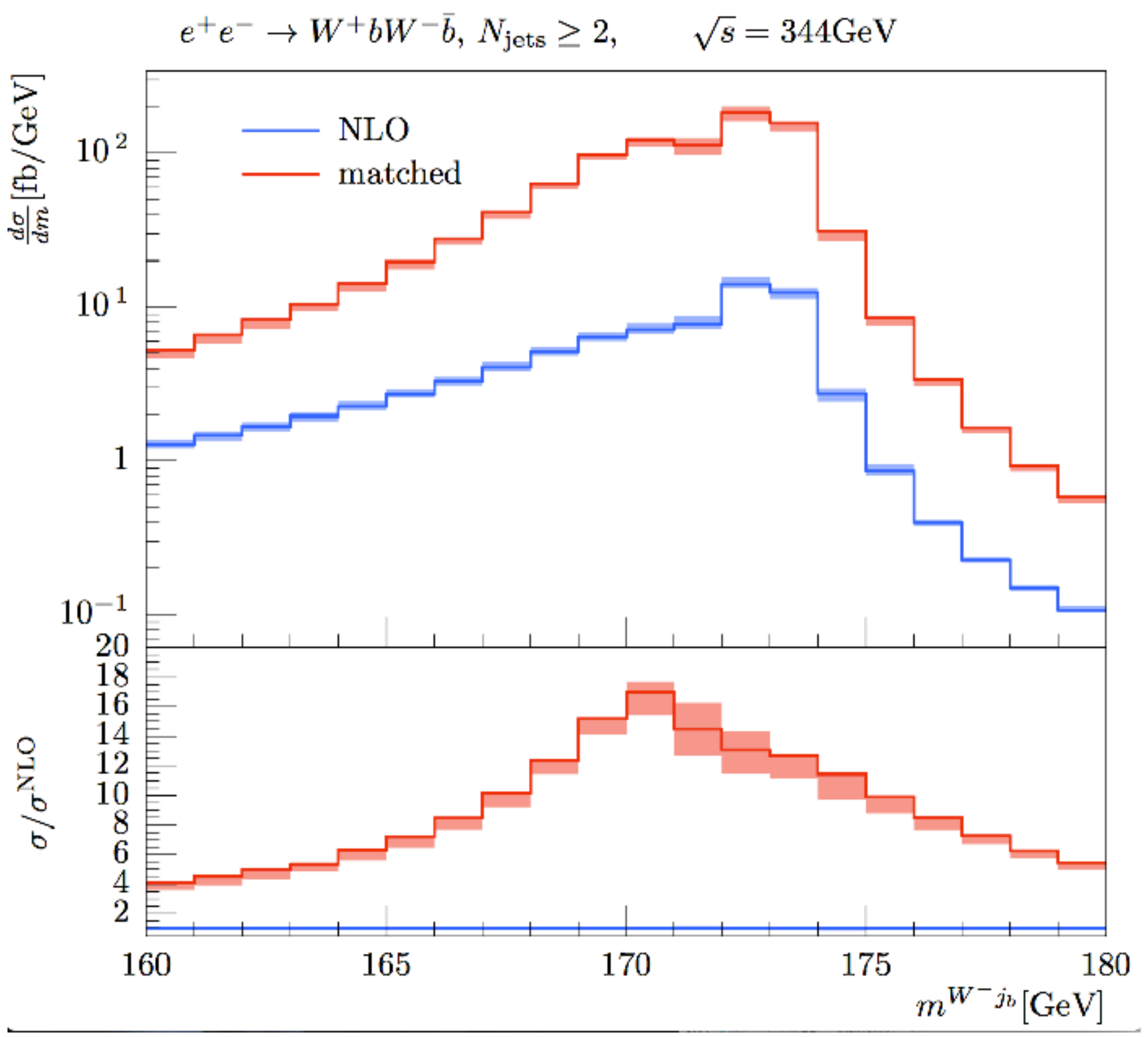

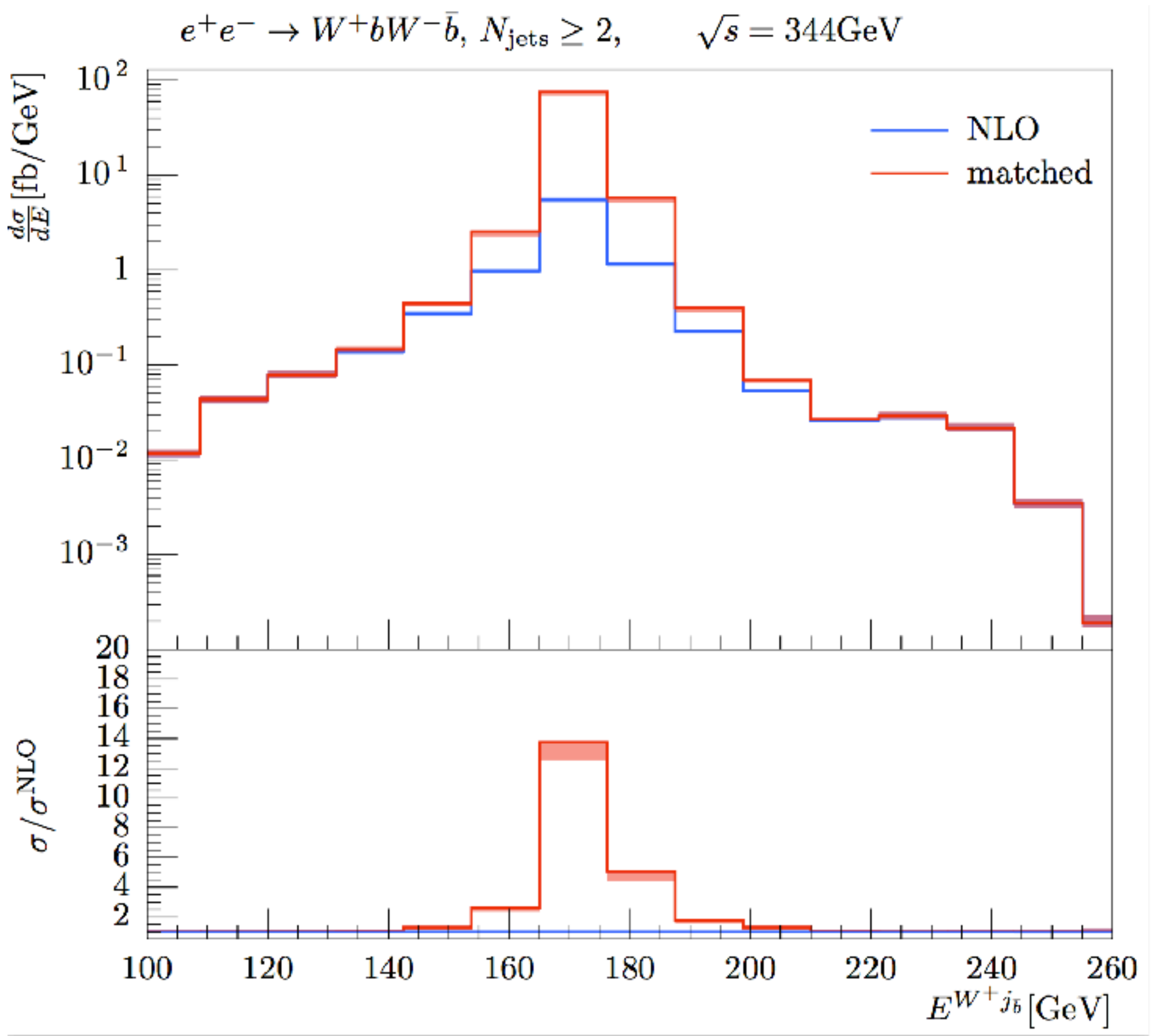

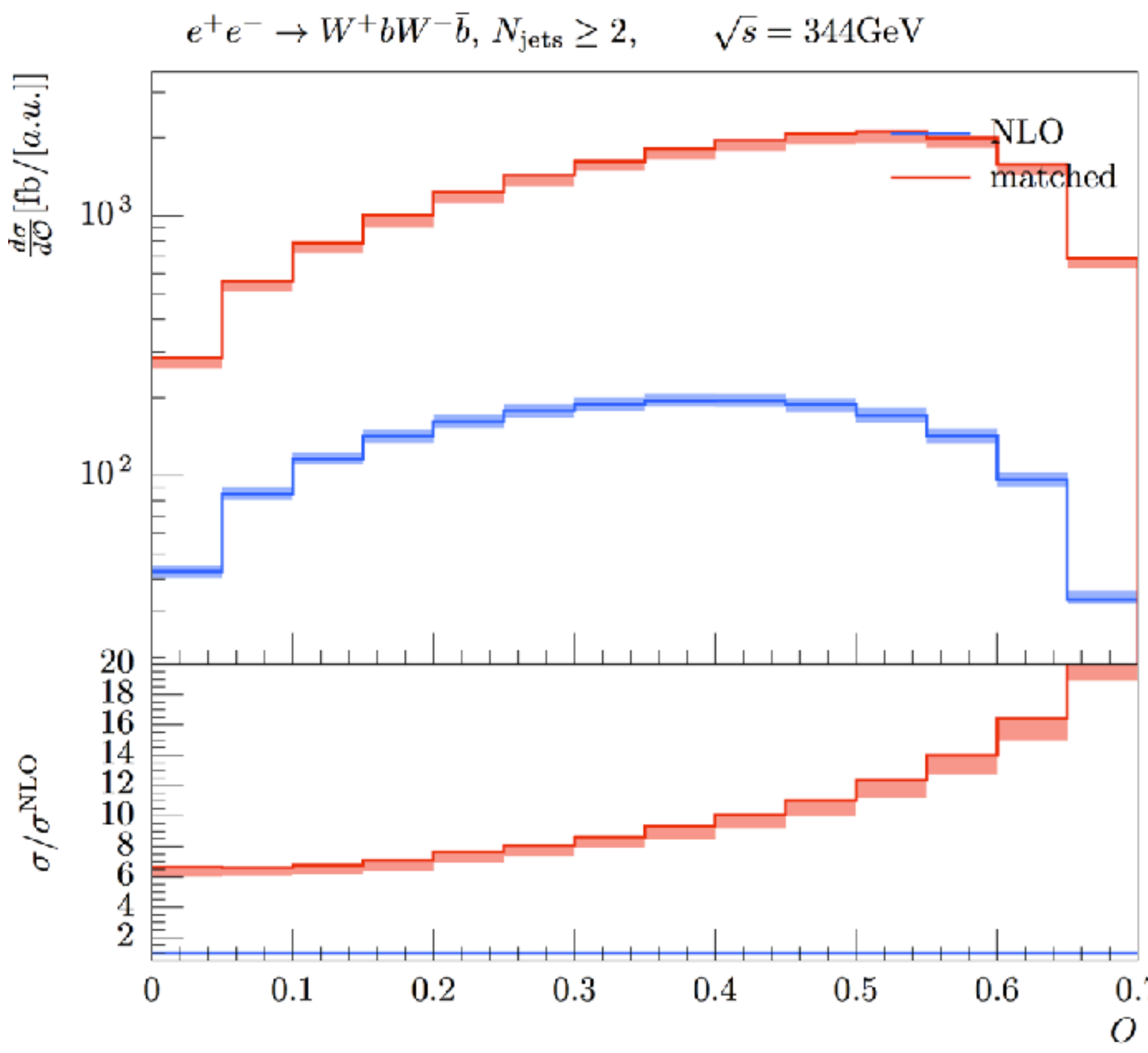

Matched threshold differential distributions

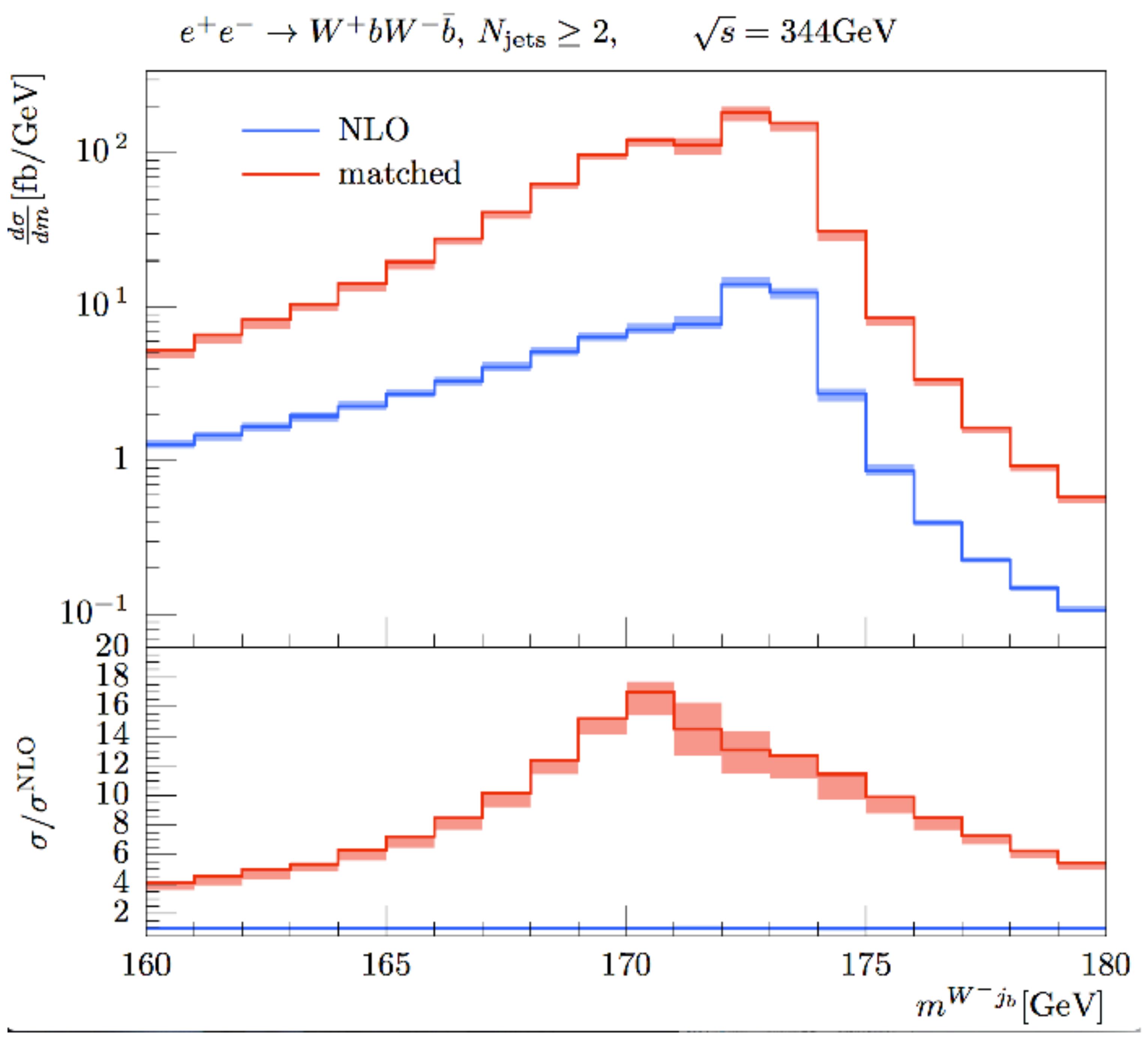

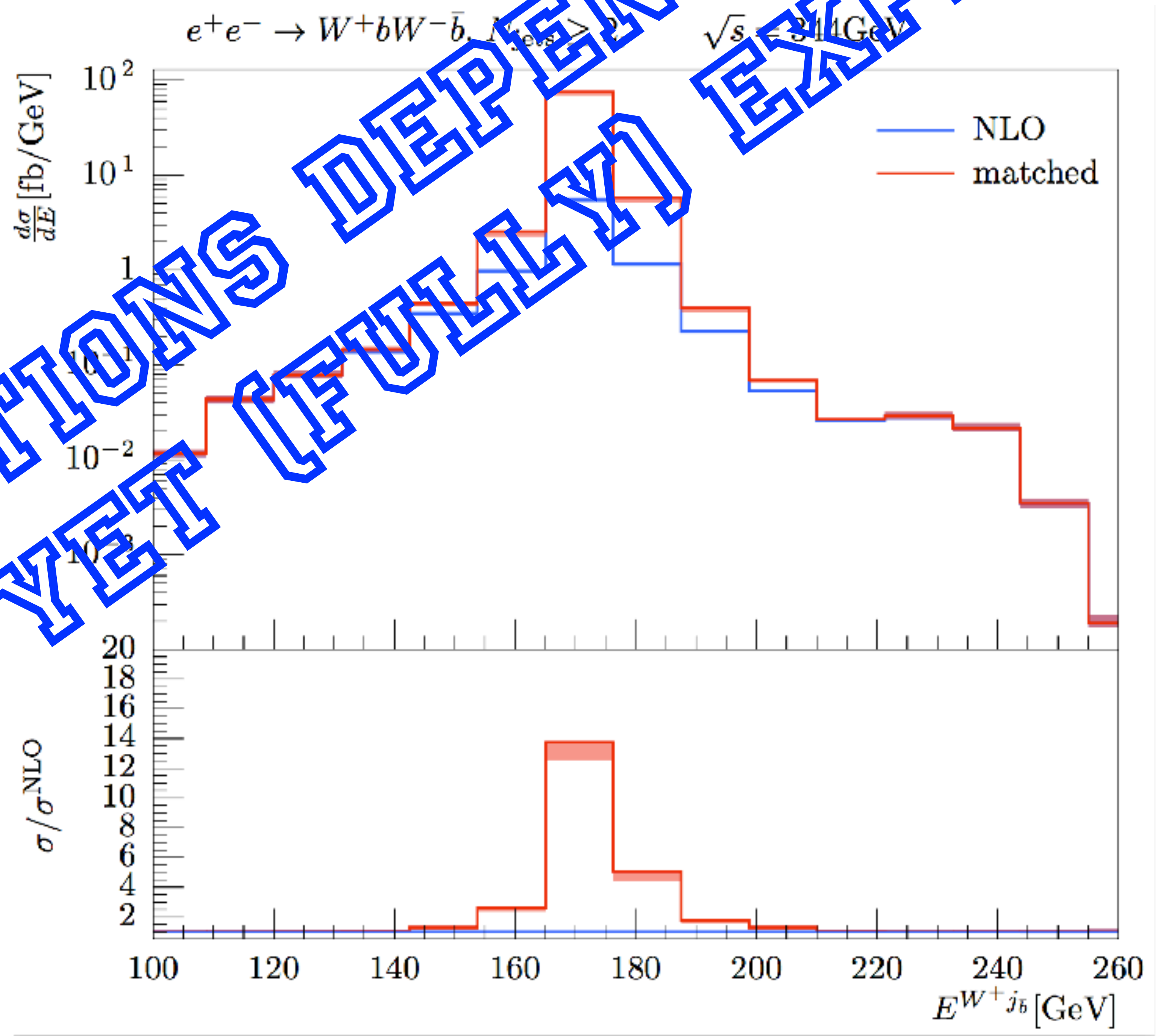

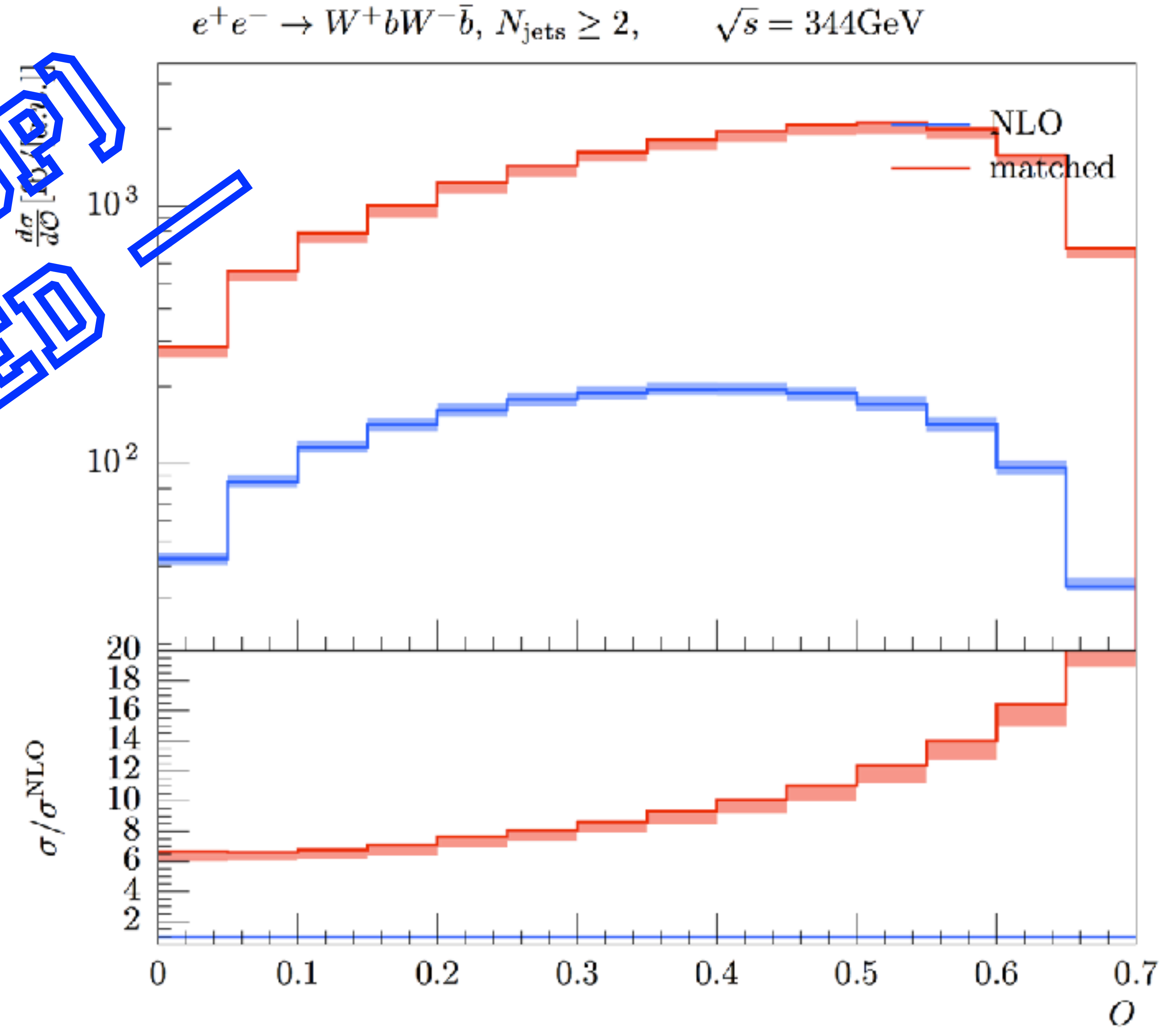

DISTRIBUTIONS DEPEND ON M(TOP) — NOT YET (FULLY) EXPLOITED —

Challenges for the top threshold ...

Theory improvements needed: higher QCD order, EW corrections (ISR matching!!), soft gluons ... ...

$e^+e^- \to W^+bW^-\bar{b}$ $\Longrightarrow$ plenty of opportunities for future projects

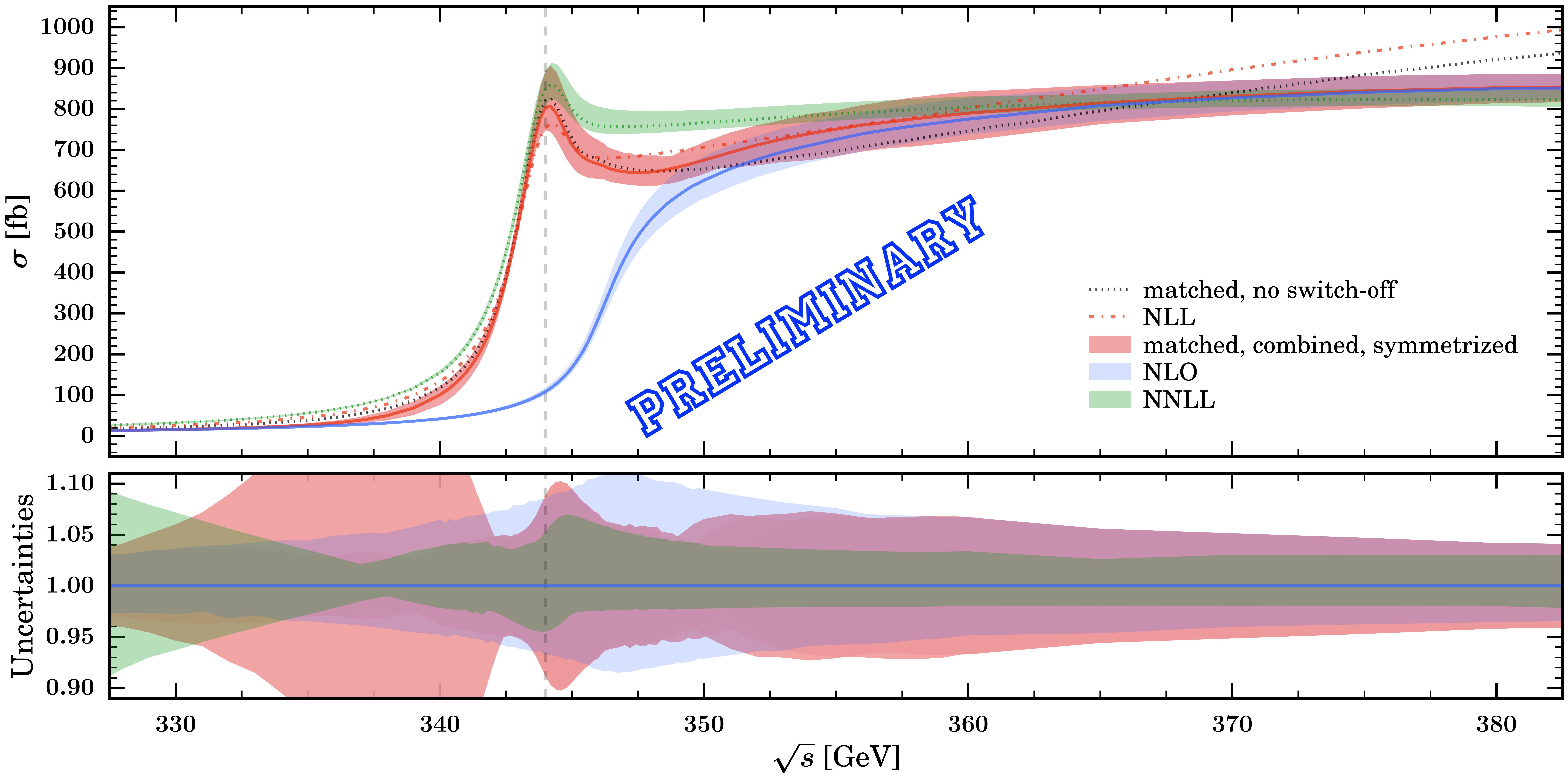

Beam simulations

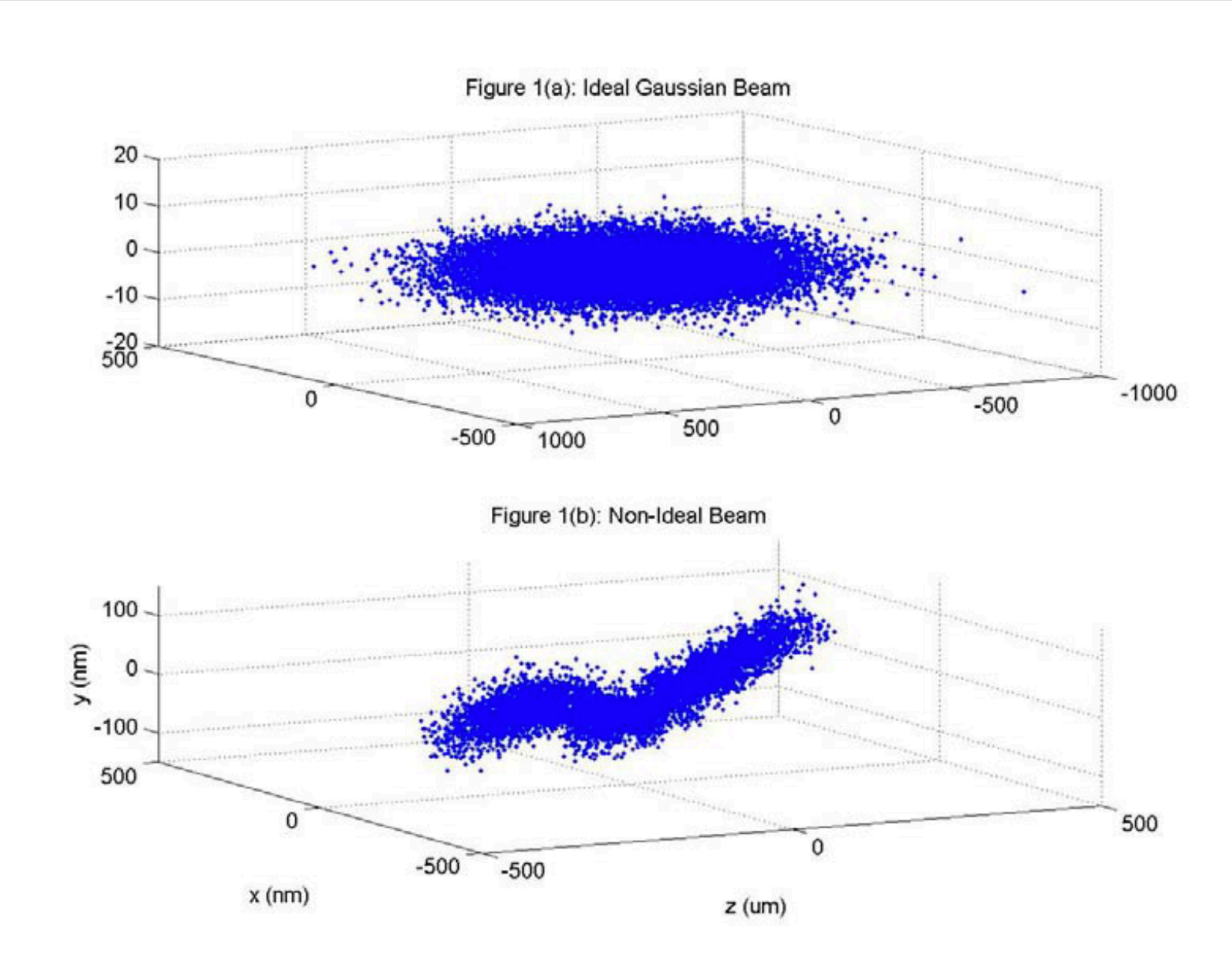

- Micro-scale bunches create beam structure/-strahlung
- Machine simulation tools like `GuineaPig`, `CAIN`, `Fluka`, `XSuite`
- Has to be folded into realistic (fast!) MC simulations

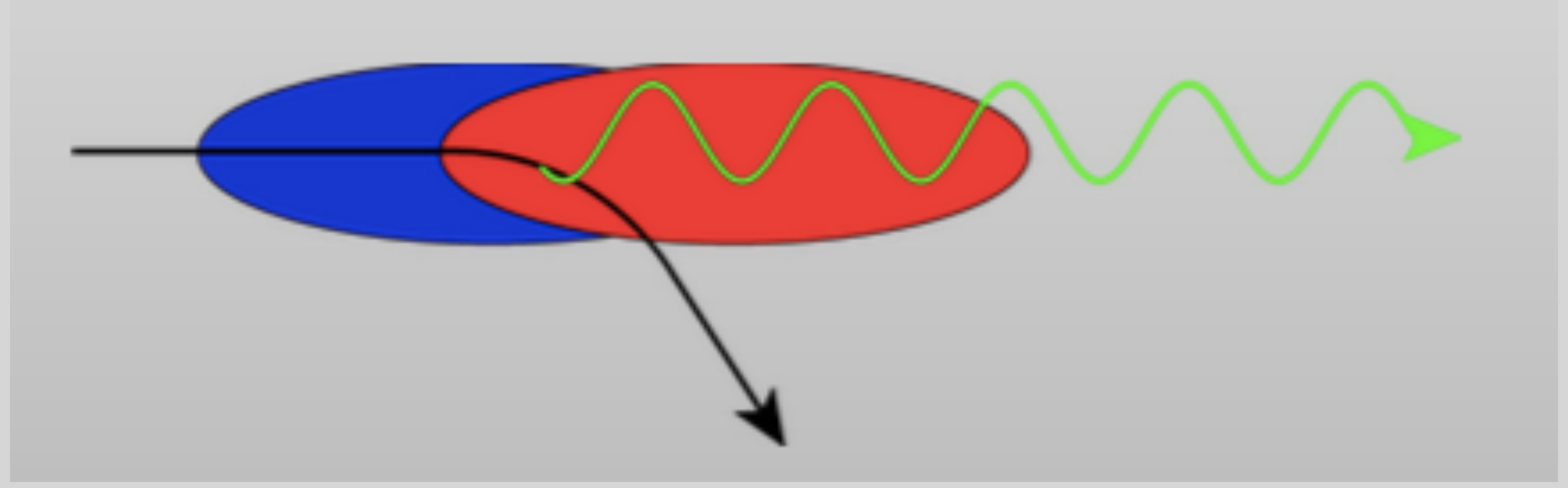

$$L \approx \frac{N}{4\pi\sigma_x\sigma_y} \frac{\eta P_{AC}}{E_{CM}}$$

Luminosity smearing is a convolution of:

- Natural beam energy spread (~ 0.02 — 0.1%) [machine design]
- Beamstrahlung (classical ED) [beam optics]
- Initial state radiation (QED) [physics sim.]

FCC-ee beam spectra

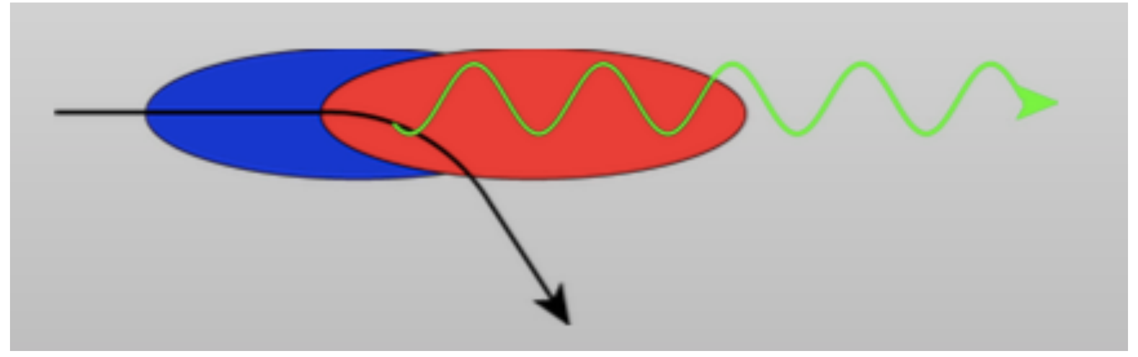

$$L \approx \frac{N}{4\pi\sigma_x\sigma_y}\,\frac{\eta P_{AC}}{E_{CM}}$$

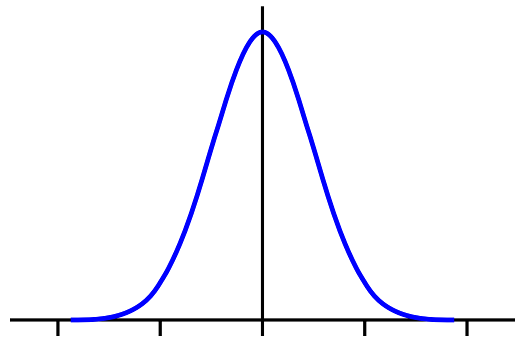

$$\begin{aligned} D_{\ell_1\ell_2}(x_1,x_2) &= D_{\ell_1}(x_1)\cdot D_{\ell_2}(x_2) \\ D_{\ell_i}(x_i) &= \delta(1-x_i) + \gamma_i\, x_i^{\alpha_i}\cdot(1-x_i)^{\beta_i} \end{aligned}$$

1. Gaussian shape with specific spreads
2. Parameterized (delta peak ⊕ power law)
3. Generator for 2D histogrammed fit (most versatile)

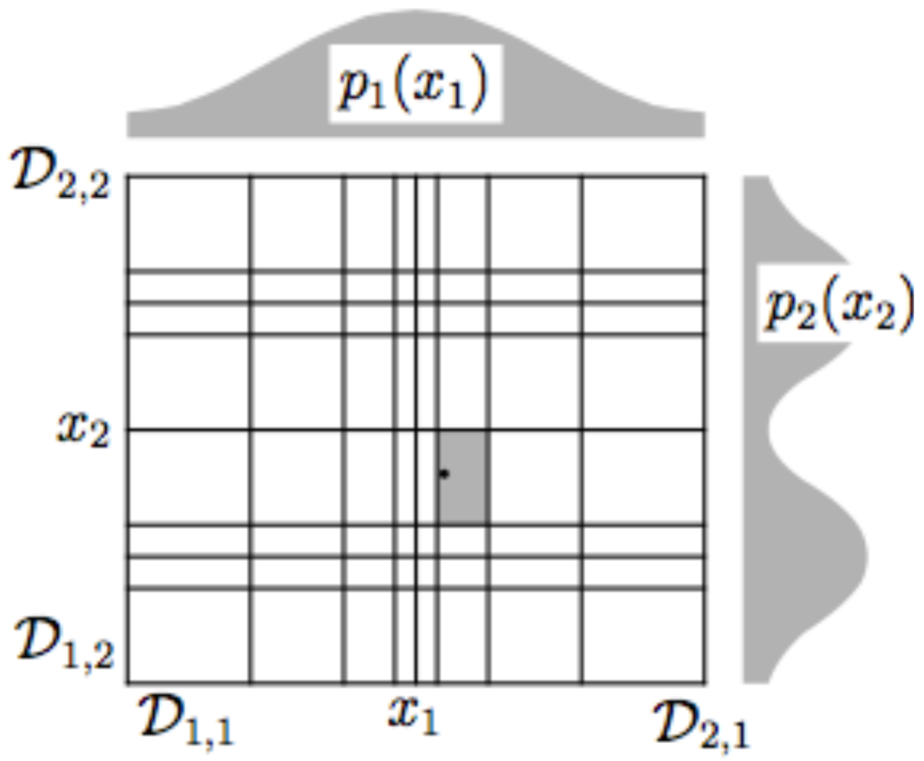

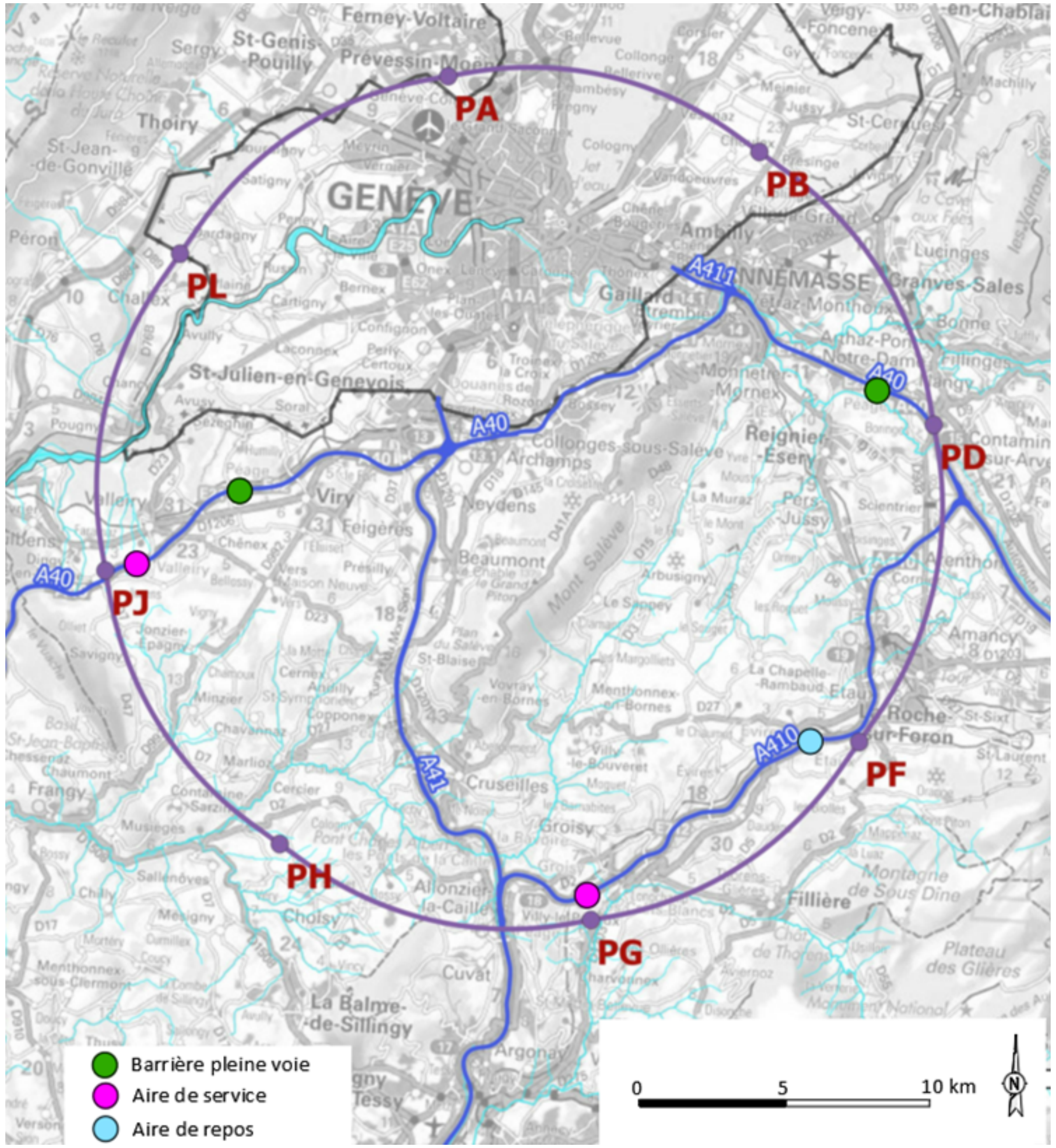

FCC-ee beam spectra

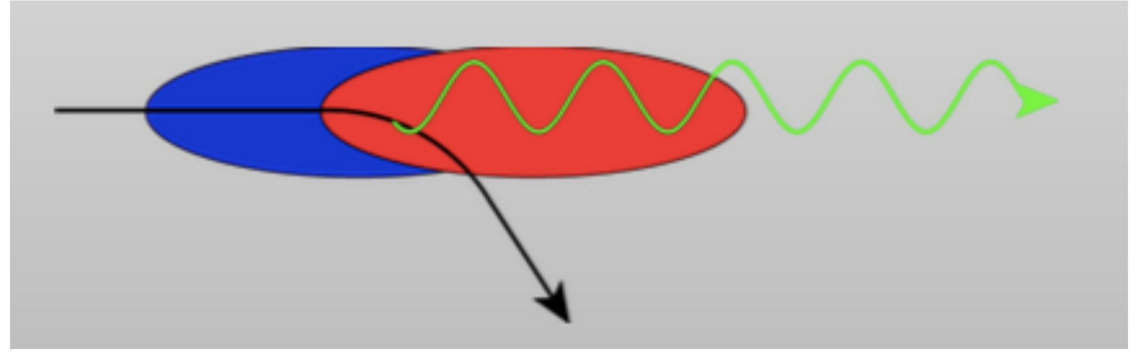

$$L \approx \frac{N}{4\pi\sigma_x\sigma_y}\,\frac{\eta P_{AC}}{E_{CM}}$$

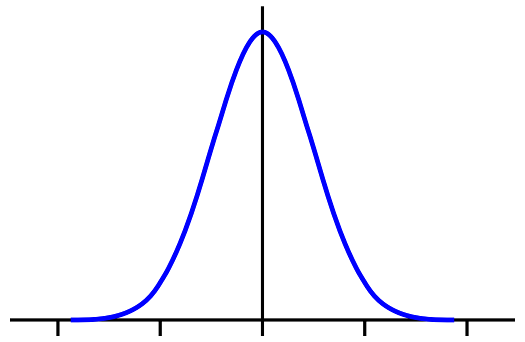

$$\begin{aligned} D_{\ell_1\ell_2}(x_1,x_2) &= D_{\ell_1}(x_1)\cdot D_{\ell_2}(x_2) \\ D_{\ell_i}(x_i) &= \delta(1-x_i)+\gamma_i\, x_i^{\alpha_i}\cdot(1-x_i)^{\beta_i} \end{aligned}$$

1. Gaussian shape with specific spreads
2. Parameterized (delta peak ⊕ power law)
3. Generator for 2D histogrammed fit (most versatile)

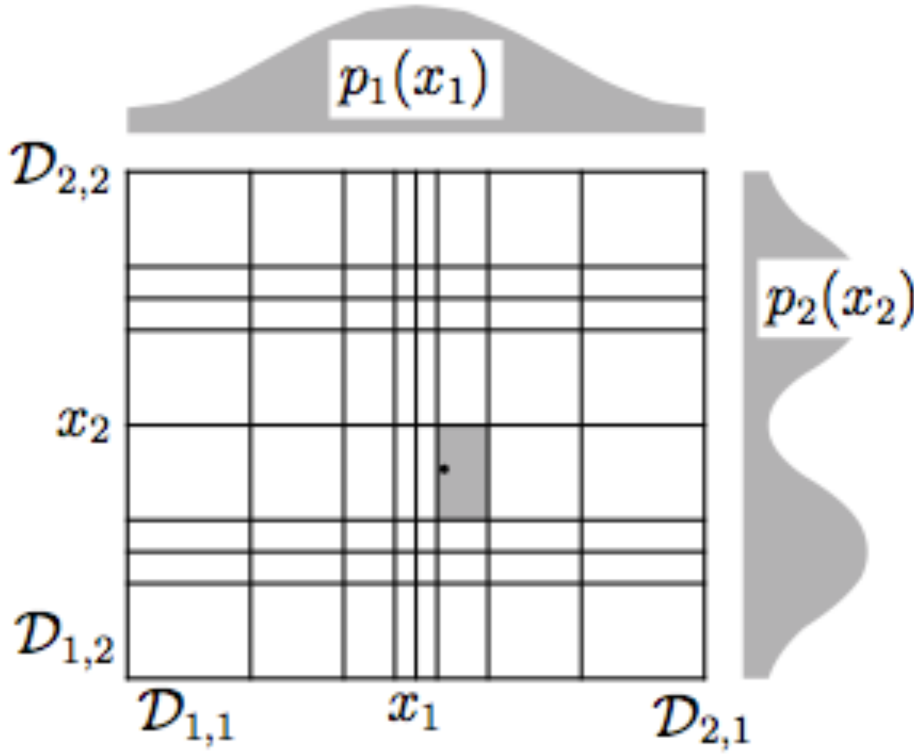

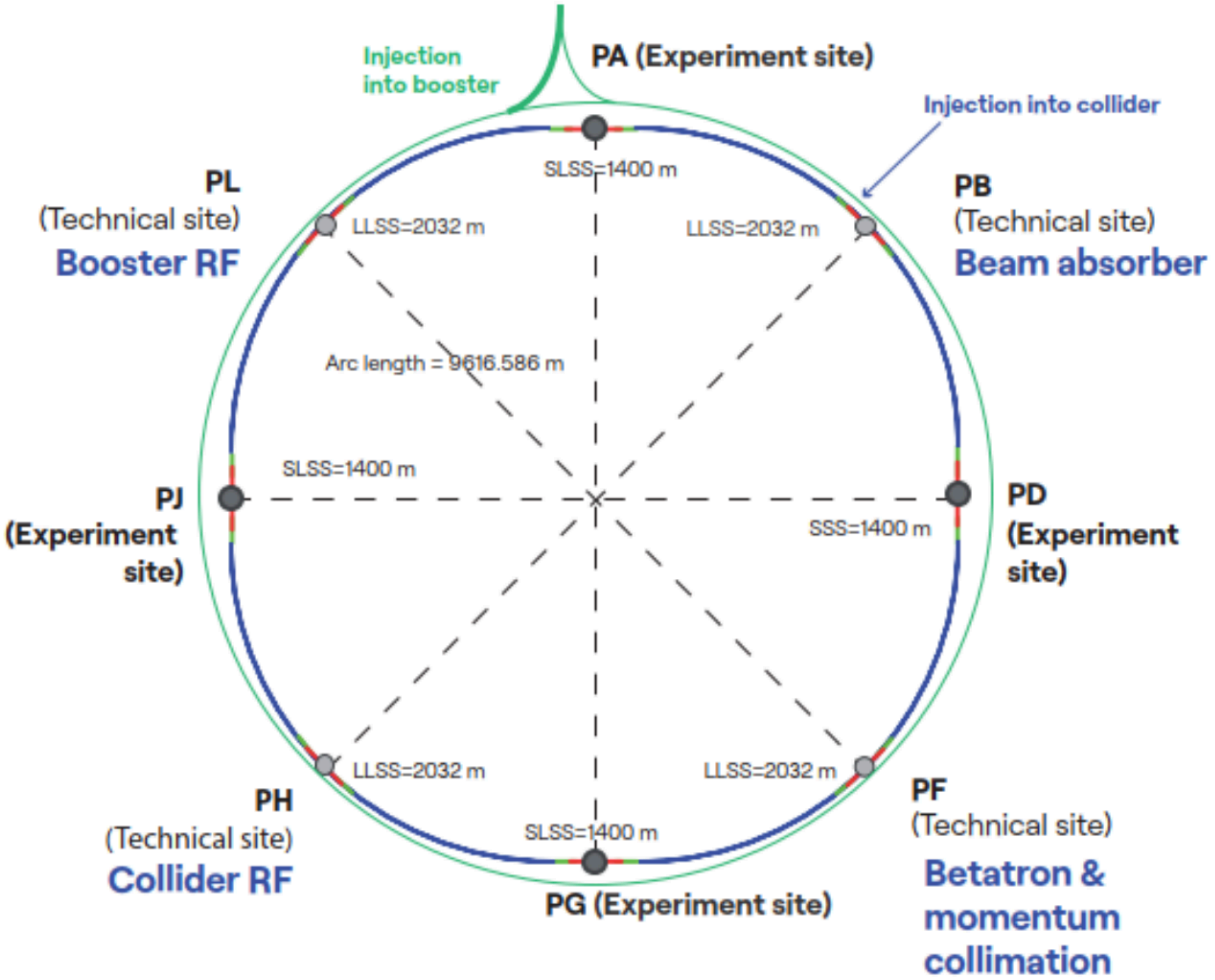

FCC-ee beam spectra

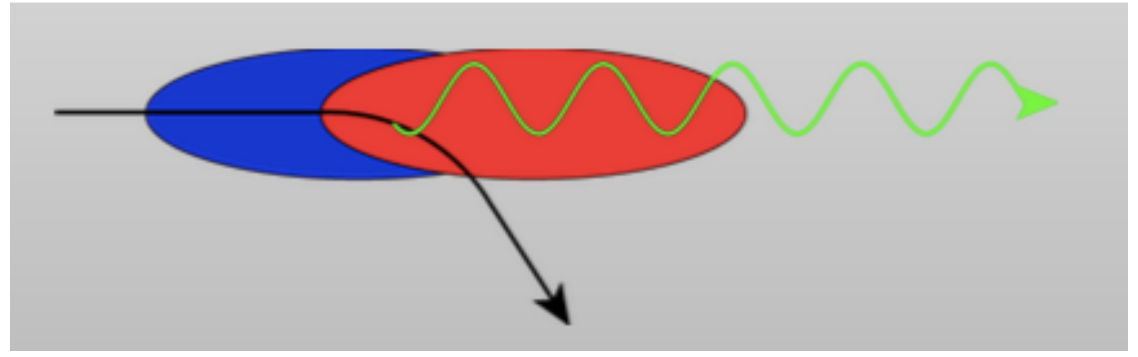

$$L \approx \frac{N}{4\pi\sigma_x\sigma_y}\,\frac{\eta P_{AC}}{E_{CM}}$$

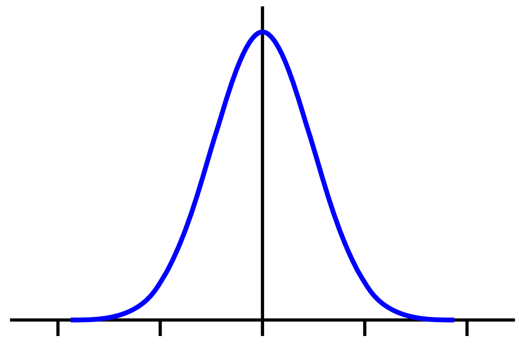

$$\begin{aligned} D_{\ell_1\ell_2}(x_1,x_2) &= D_{\ell_1}(x_1)\cdot D_{\ell_2}(x_2) \\ D_{\ell_i}(x_i) &= \delta(1-x_i) + \gamma_i\, x_i^{\alpha_i}\cdot(1-x_i)^{\beta_i} \end{aligned}$$

1. Gaussian shape with specific spreads
2. Parameterized (delta peak ⊕ power law)
3. Generator for 2D histogrammed fit (most versatile)

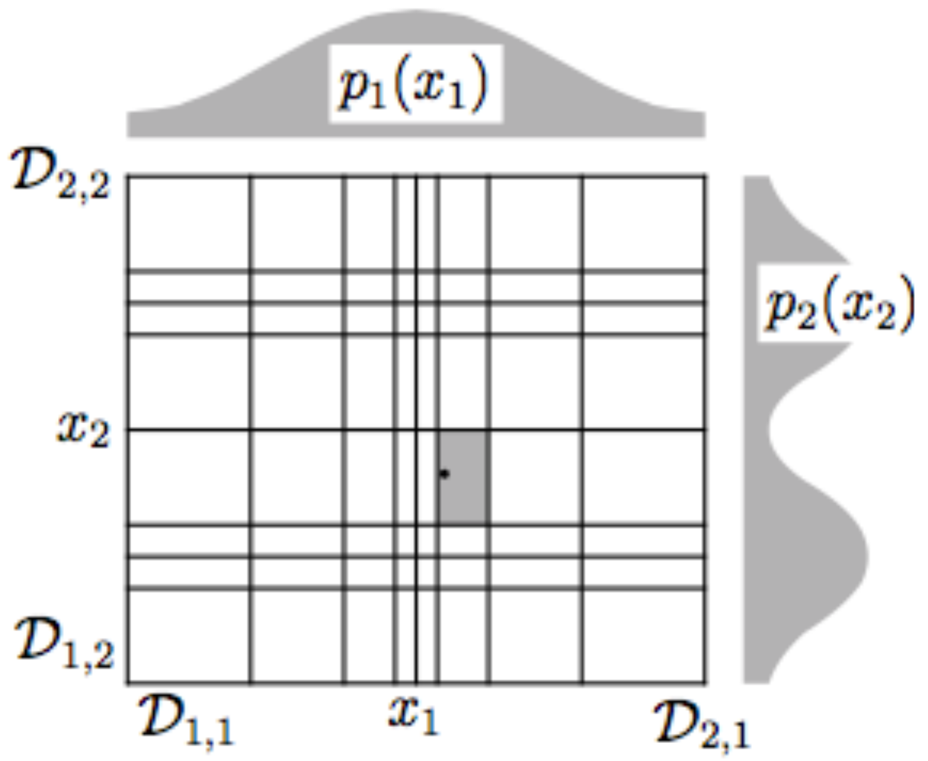

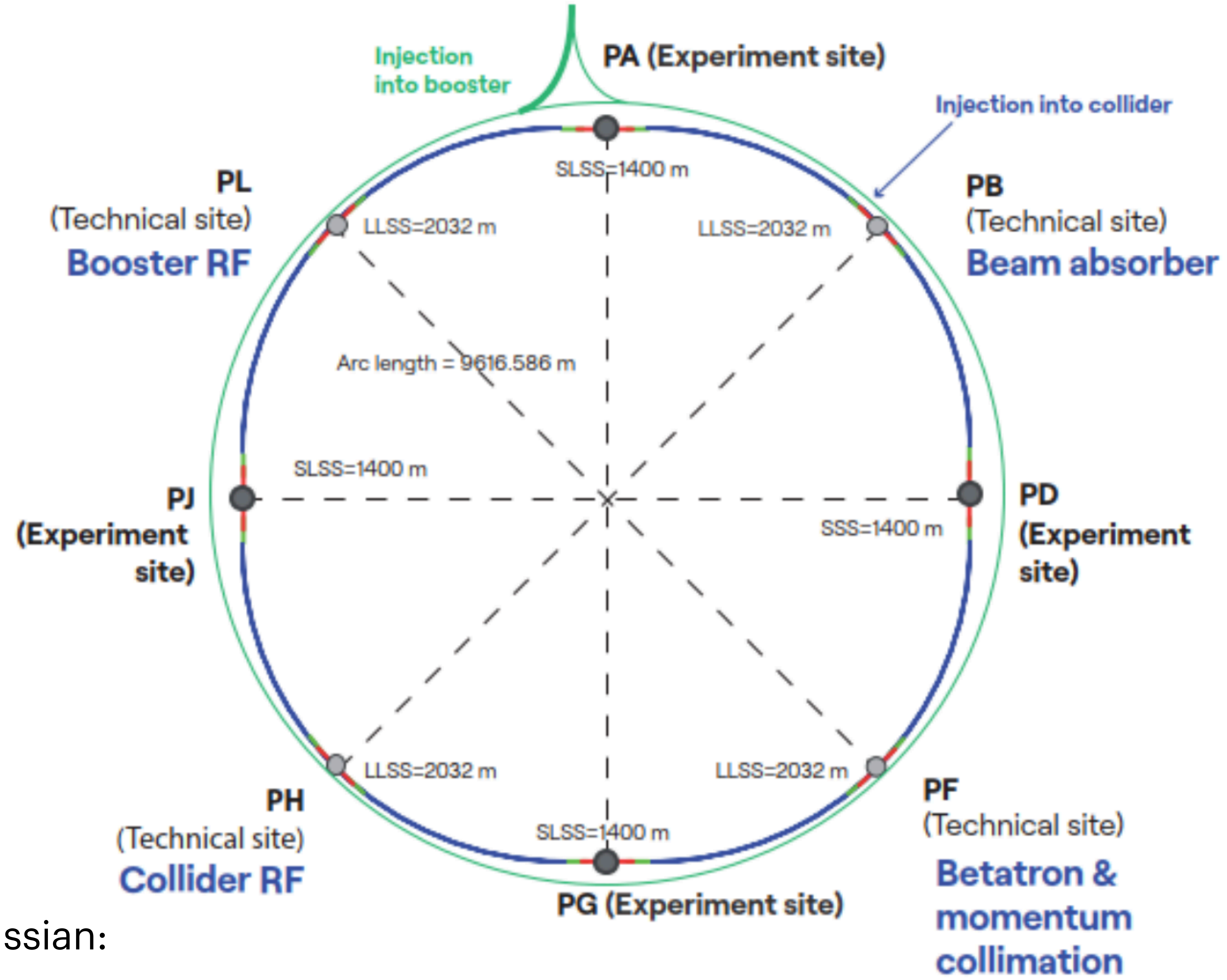

Parameterized spectra/Gaussian:

fast evaluation, easy(ier) unfolding

Fitting FCC-ee spectra w/ CIRCE algorithm

- Circular collider: bunches pass each other many times, energy losses do not accumulate (due to beam optics)
- Simulation well described by Gaussian spread [data from Katsunobo Oide, 2023/24]

Fitting FCC-ee spectra w/ CIRCE algorithm

- Circular collider: bunches pass each other many times, energy losses do not accumulate (due to beam optics)
- Simulation well described by Gaussian spread [data from Katsunobo Oide, 2023/24]

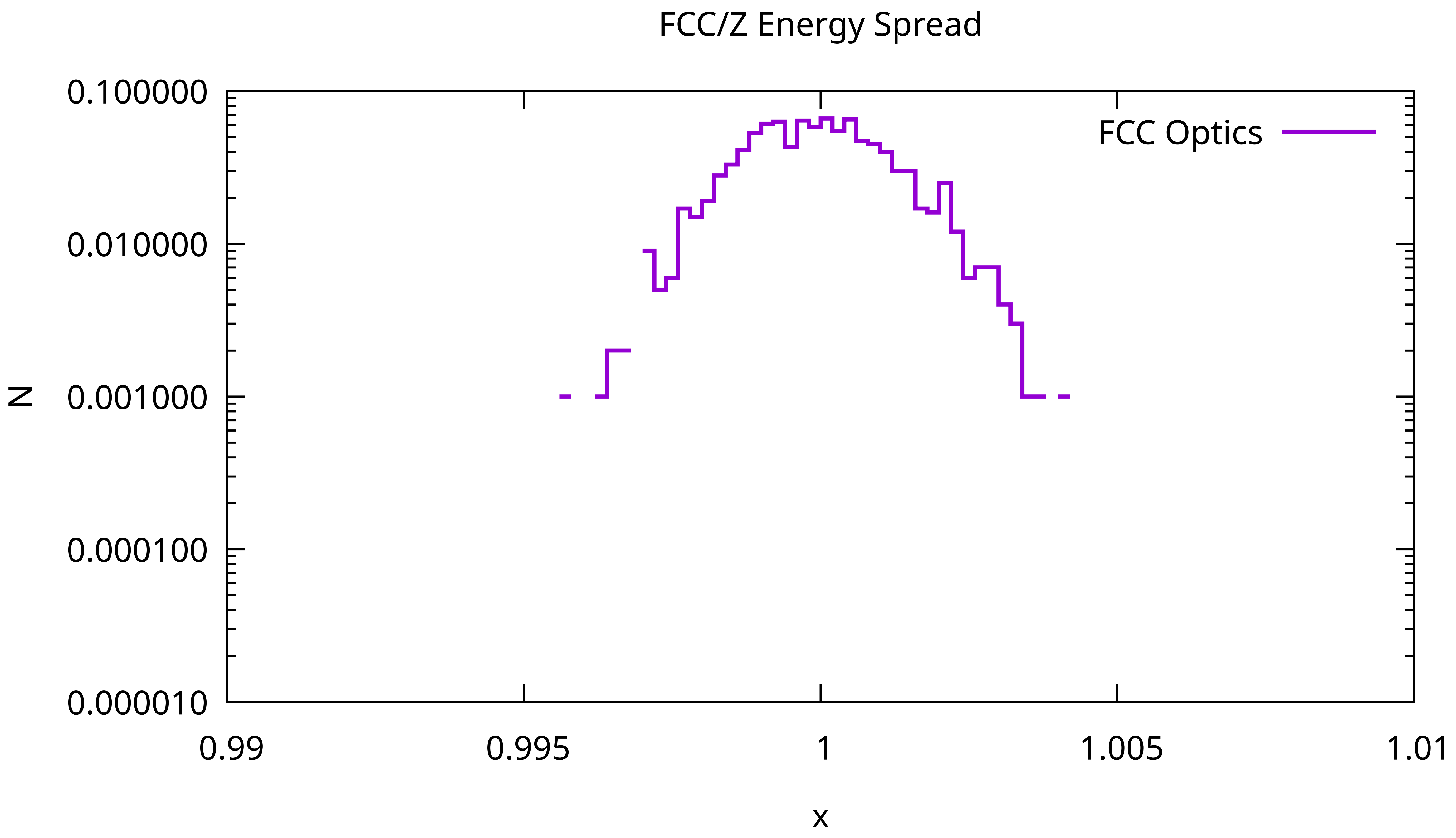

Fitting FCC-ee spectra w/ CIRCE algorithm

- Circular collider: bunches pass each other many times, energy losses do not accumulate (due to beam optics)
- Simulation well described by Gaussian spread [data from Katsunobo Oide, 2023/24]

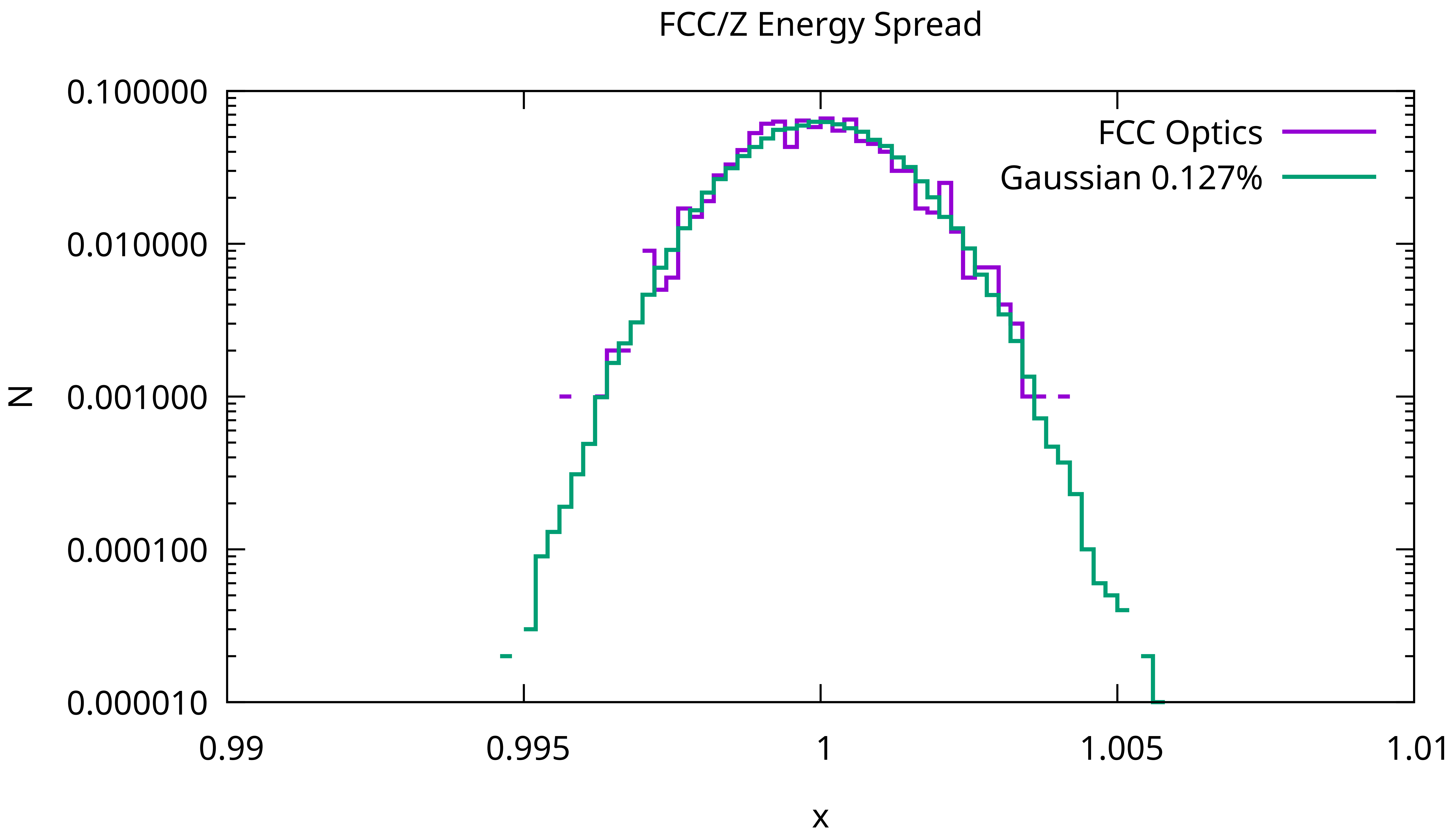

Distributions fit by CIRCE

Fitting FCC-ee spectra w/ CIRCE algorithm

- Circular collider: bunches pass each other many times, energy losses do not accumulate (due to beam optics)
- Simulation well described by Gaussian spread [data from Katsunobo Oide, 2023/24]
- Deviations from Gaussian only visible at the highest energies (240 / 365 GeV)

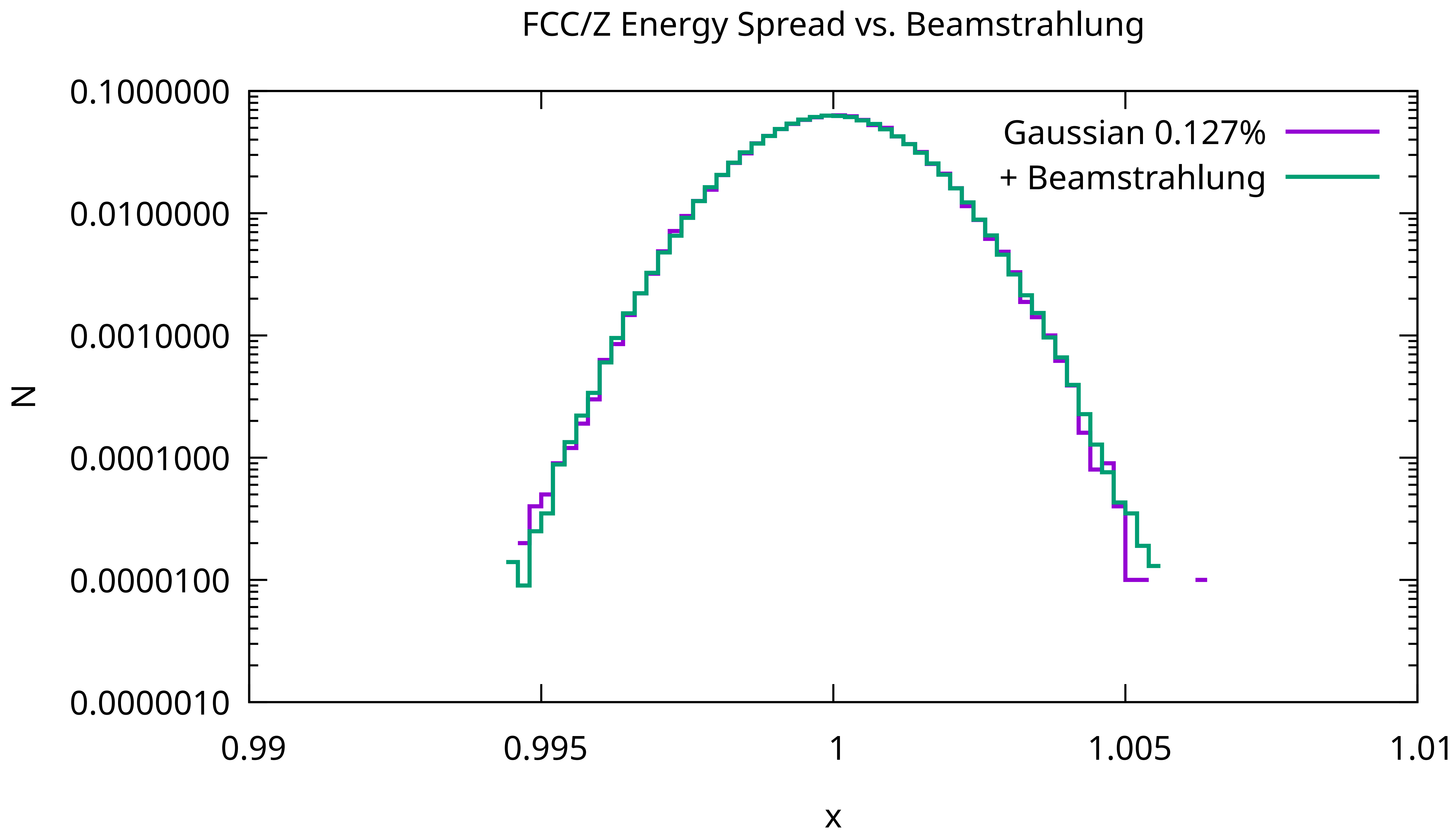

FCC 2024	$\Delta_{BS} E_{e^\pm}$/Gev	$\langle E_\gamma \rangle_{BS}$/Gev	$0.15\% \cdot E_{e^\pm}$/Gev
Z	0.0012	0.0016	0.07
WW	0.0039	0.0059	0.12
ZH	0.0140	0.0189	0.18
Top	0.0329	0.0531	0.27

Distributions fit by CIRCE

Fitting FCC-ee spectra w/ CIRCE algorithm

- Circular collider: bunches pass each other many times, energy losses do not accumulate (due to beam optics)
- Simulation well described by Gaussian spread   [data from Katsunobo Oide, 2023/24]

- Deviations from Gaussian only visible at the highest energies (240 / 365 GeV)

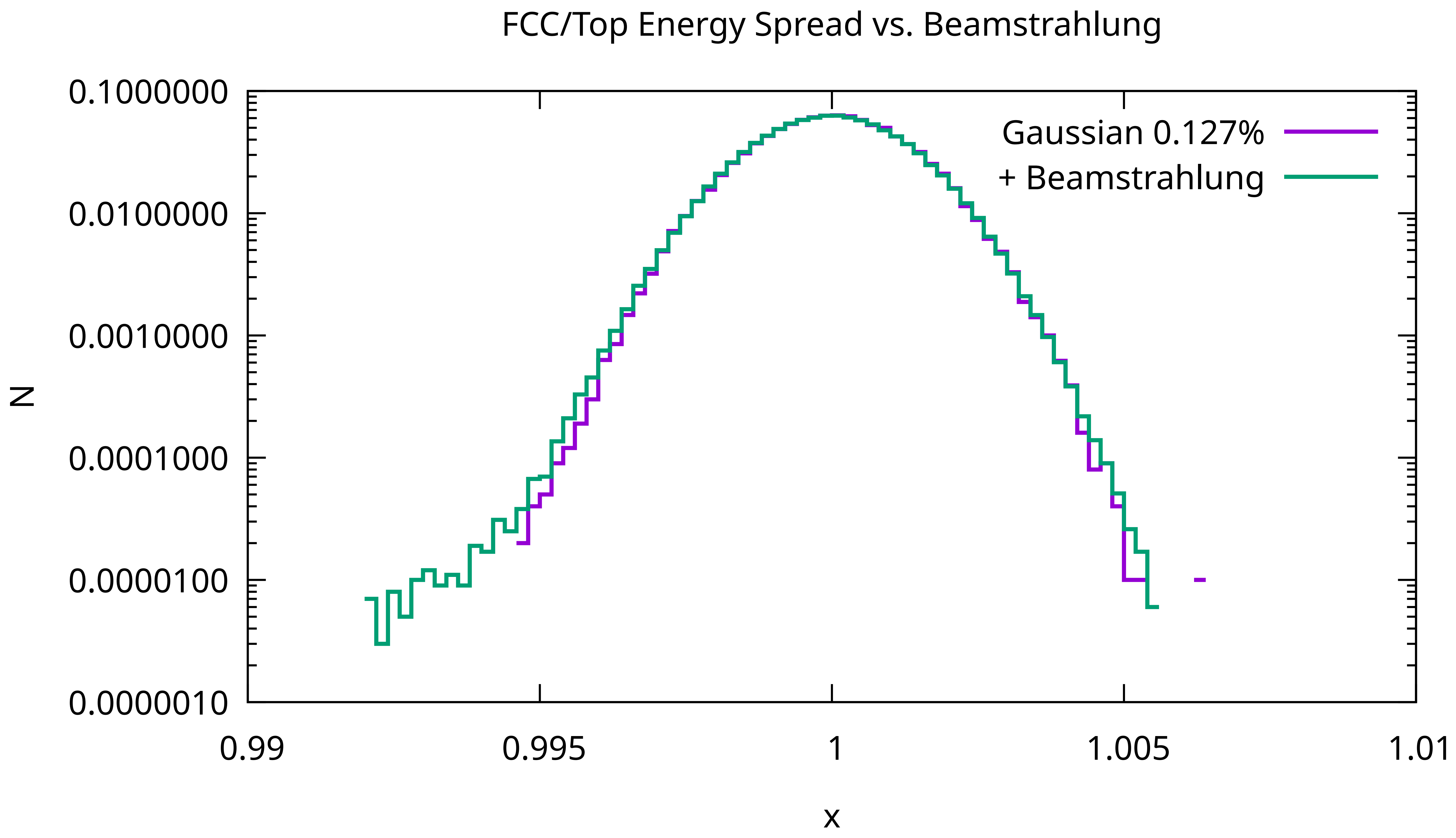

FCC 2024	$\Delta_{BS} E_{e^\pm}$/Gev	$\langle E_\gamma \rangle_{BS}$/Gev	$0.15\% \cdot E_{e^\pm}$/Gev
Z	0.0012	0.0016	0.07
WW	0.0039	0.0059	0.12
ZH	0.0140	0.0189	0.18
Top	0.0329	0.0531	0.27

Distributions fit by CIRCE

FCC-ee beam spectra

Four asymmetric interaction points (PA, PD, PG, PJ)

One (fictitious) symmetric point (PB)

37 Rapidity (asymmetric energy loss)

$e^+e^- \to \mu^+\mu^-$ at FCC_{ee} in $t\bar{t}$-threshold mode at interaction point PD.

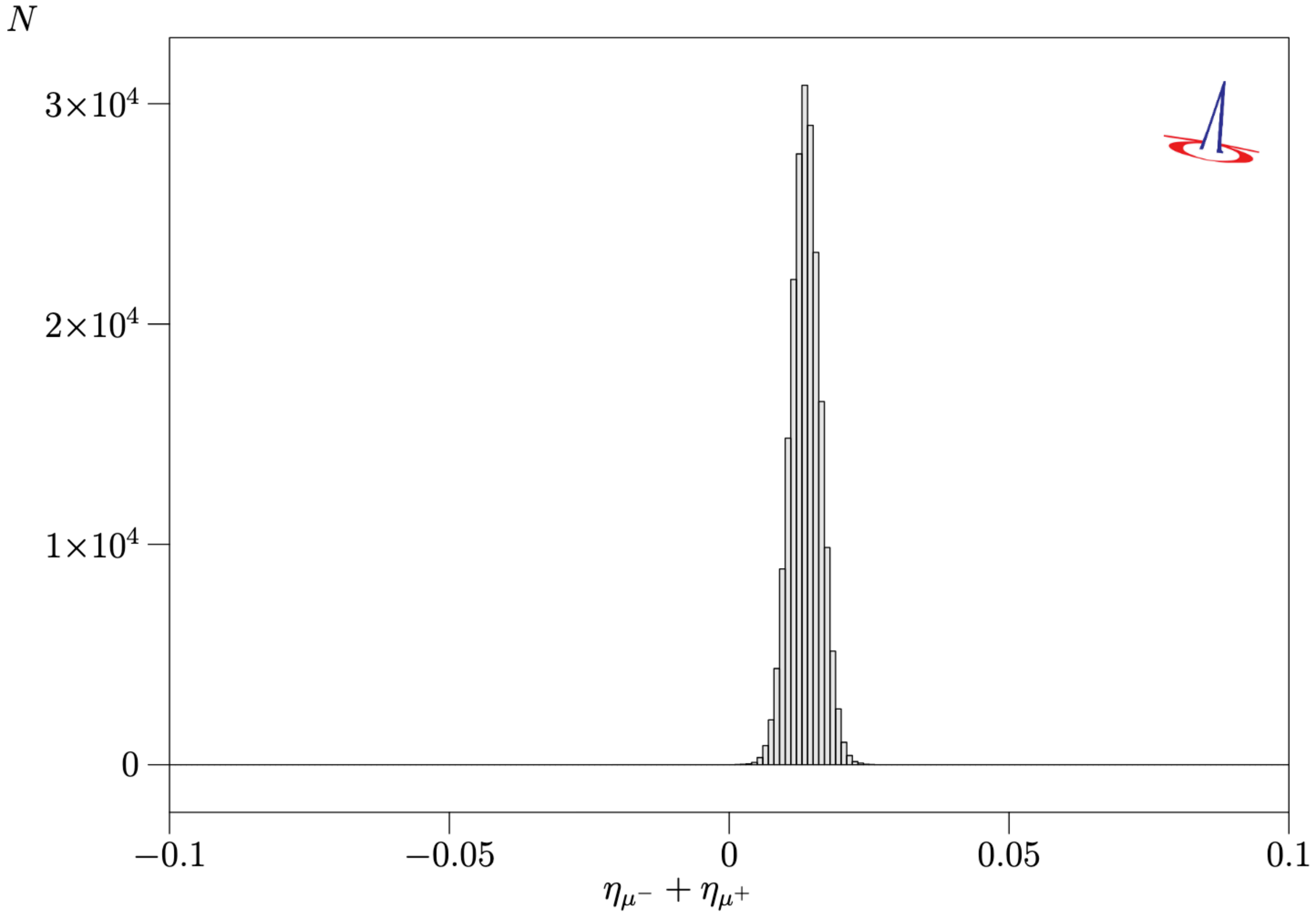

38 Invariant mass (energy spread)

$e^+e^- \to \mu^+\mu^-$ at FCC_{ee} in $t\bar{t}$-threshold mode at interaction point PD.

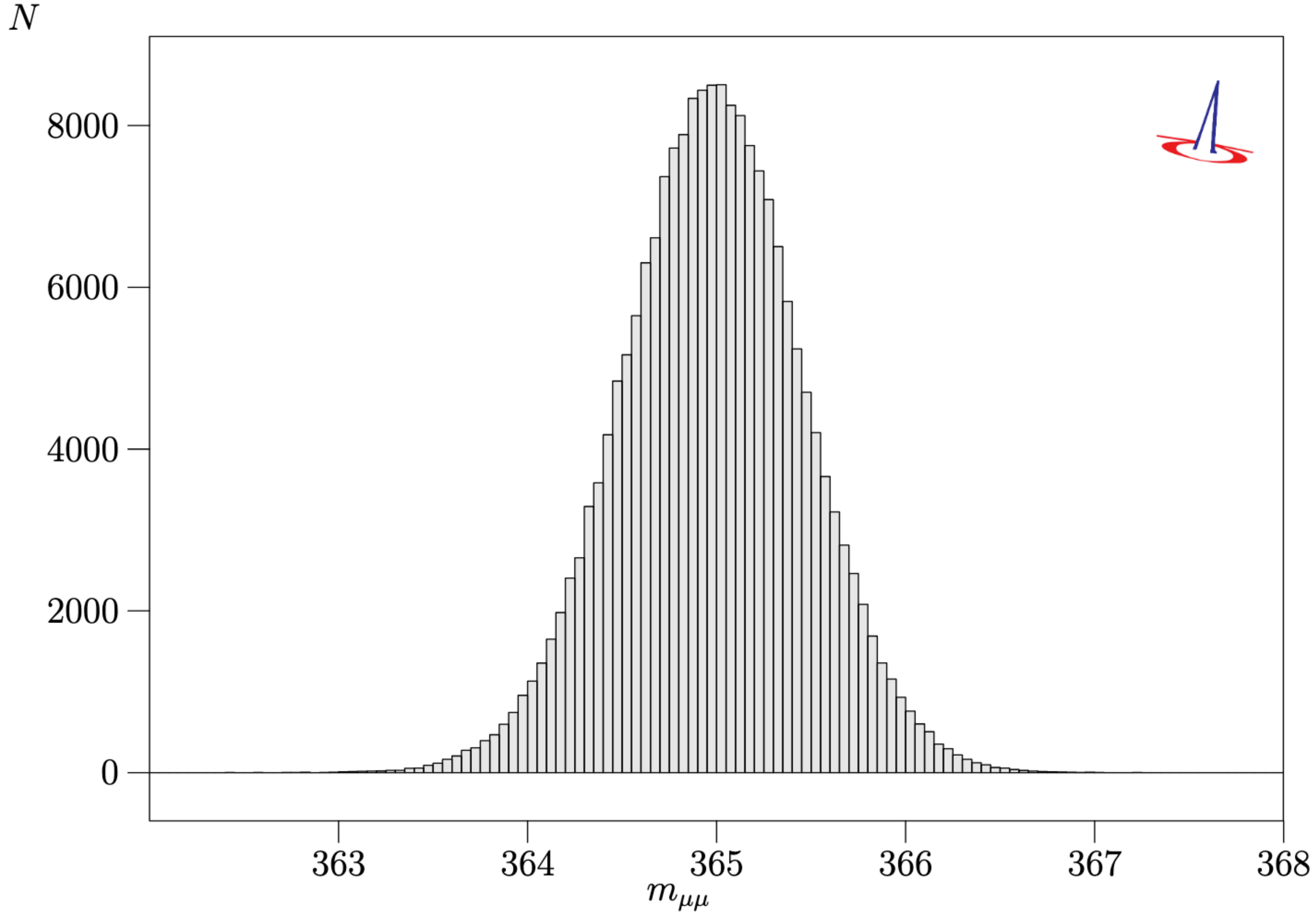

Conclusions & Outlook

- Building upon huge success of MC generators in the LHC era
- Automation of NLO QCD + EW for SM (and partially for BSM); matching to (N)LL parton shower + hadronization
- Much higher precision demands: improvements for parton showers and hadronization needed
- FCC-ee will be dominated by N(N)LO EW
- QED logarithms dominate normalisations and shape of differential distributions
- Exclusive photons are important in *all* event selections
- Two major paradigms: collinear vs. YFS resummation // collinear ePDFs vs. YFS radiator functions
- Crucial to have at least 1—2 generators frameworks for each algorithm
- FCC-ee has several important thresholds: W^+W^-, ZH, and $t\bar{t}$, special implementations/treatmetns needed
- Many topics omitted due to time reasons: luminometry, spin correlations, special processes, efficiency and modern algorithms …

Be cautious with generative AI

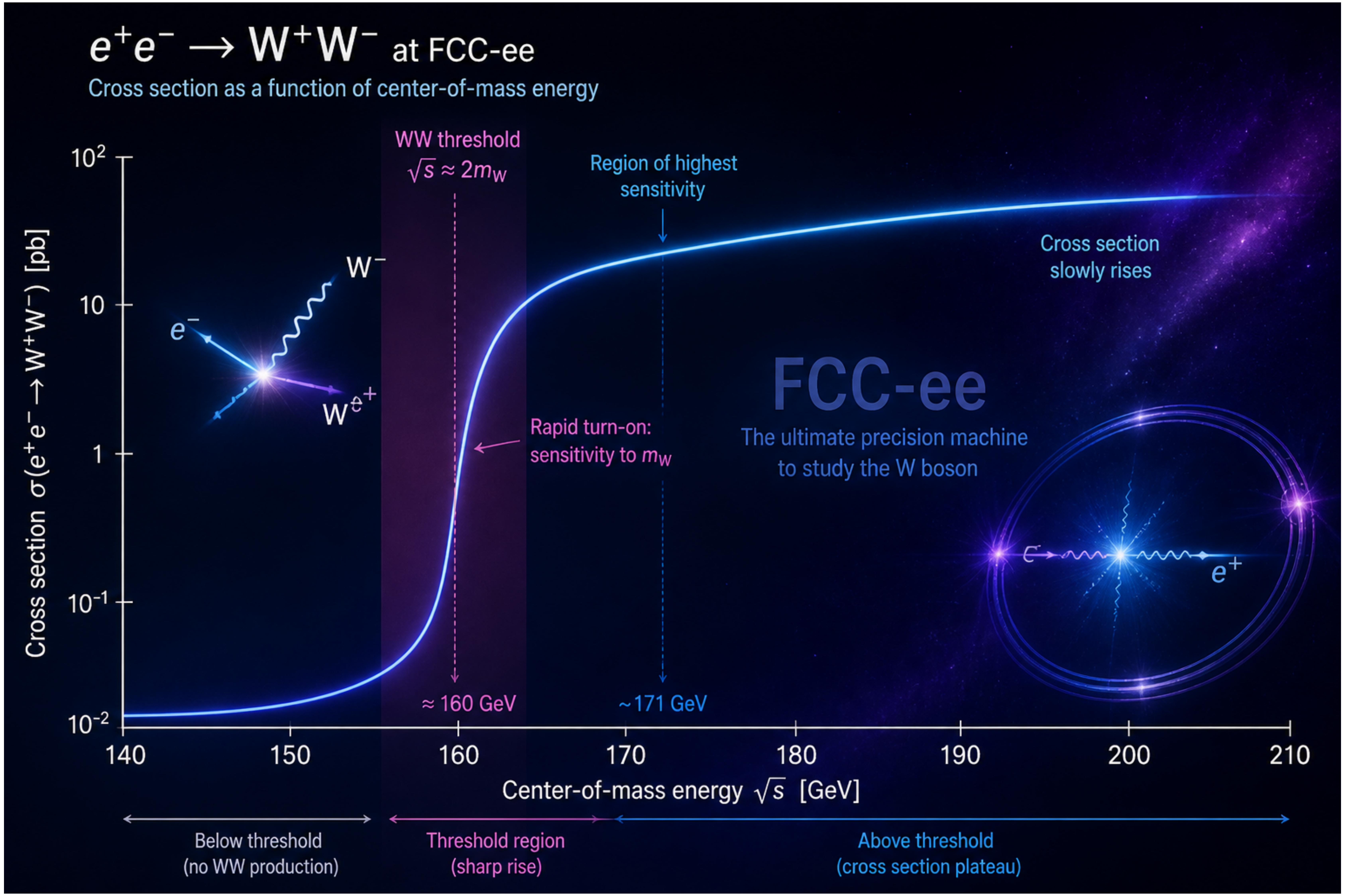

Find the error ...

chatgpt.com

BACKUP

Beam spectra at FCC-ee

- Harder spectra at higher energy designs:

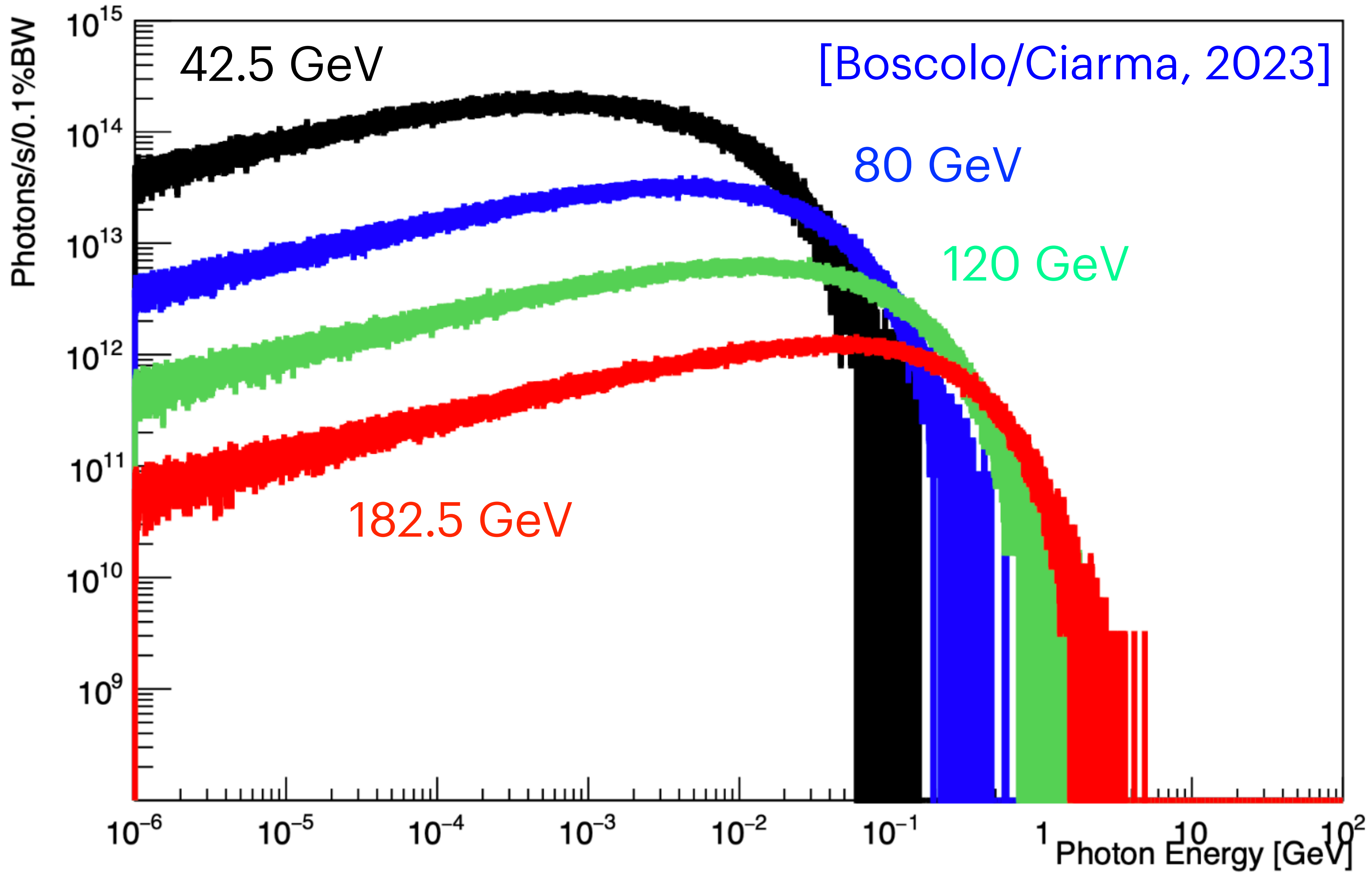

Beam spectra at FCC-ee

- Harder spectra at higher energy designs:
- Spectra become harder even as fractions of nominal beam energies: $z := \sqrt{\frac{E_{e^-}}{E_{beam}} \cdot \frac{E_{e^+}}{E_{beam}}}$

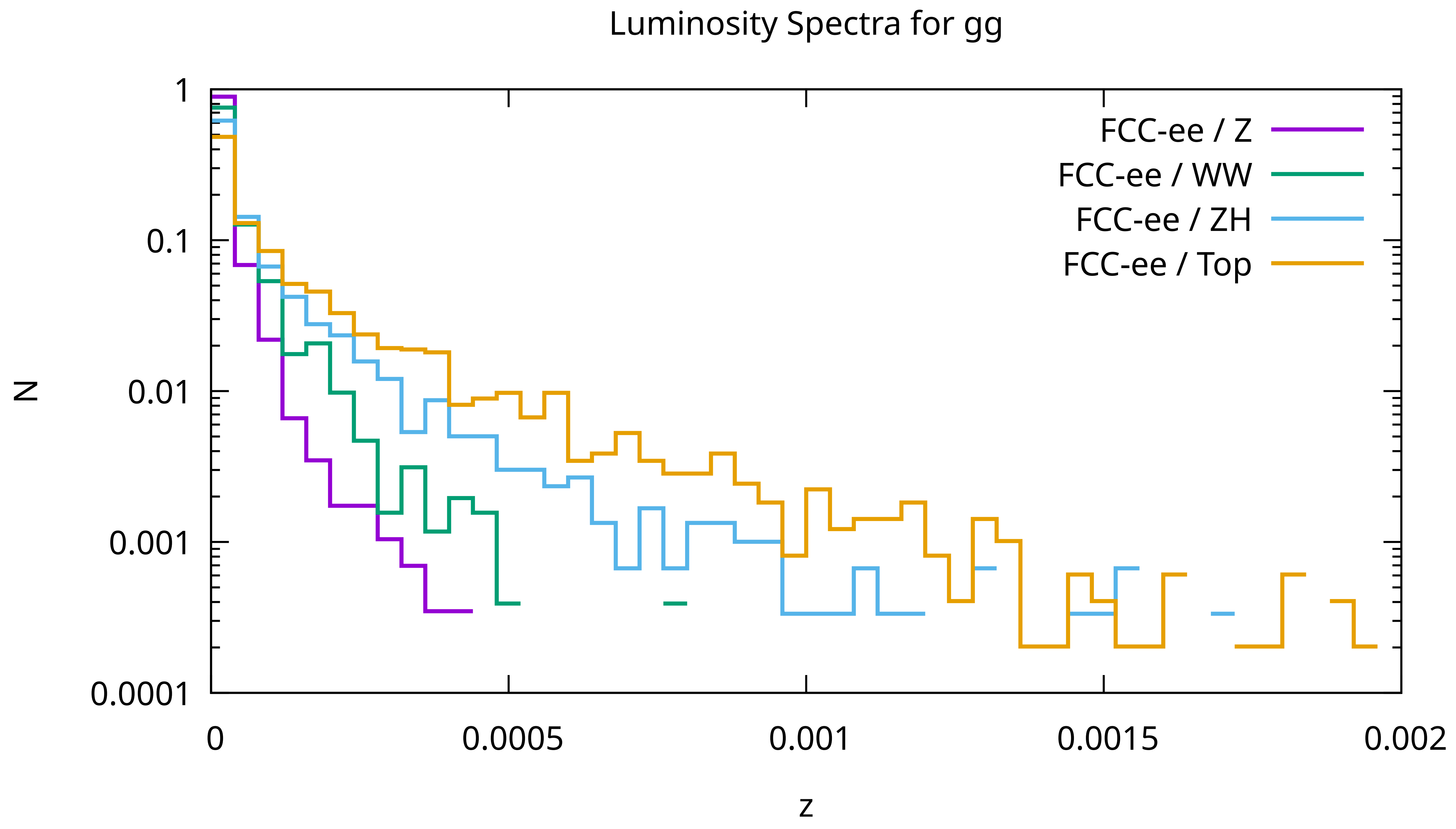

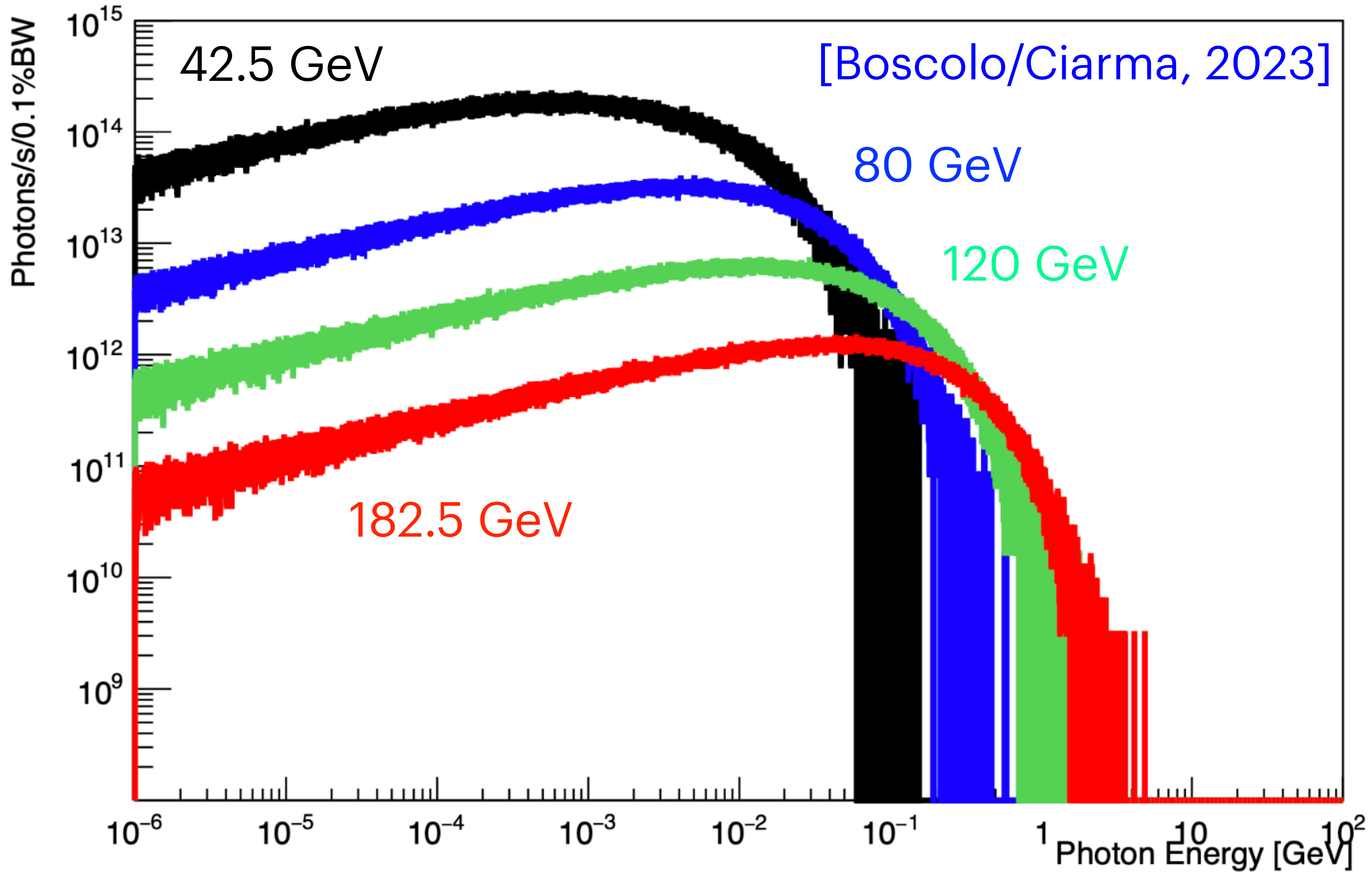

Beam spectra at FCC-ee

- Harder spectra at higher energy designs:
- Luminosity spectra for e^+e^- very steep, especially on the Z pole : $z := \sqrt{\frac{E_{e^-}}{E_{beam}} \cdot \frac{E_{e^+}}{E_{beam}}}$

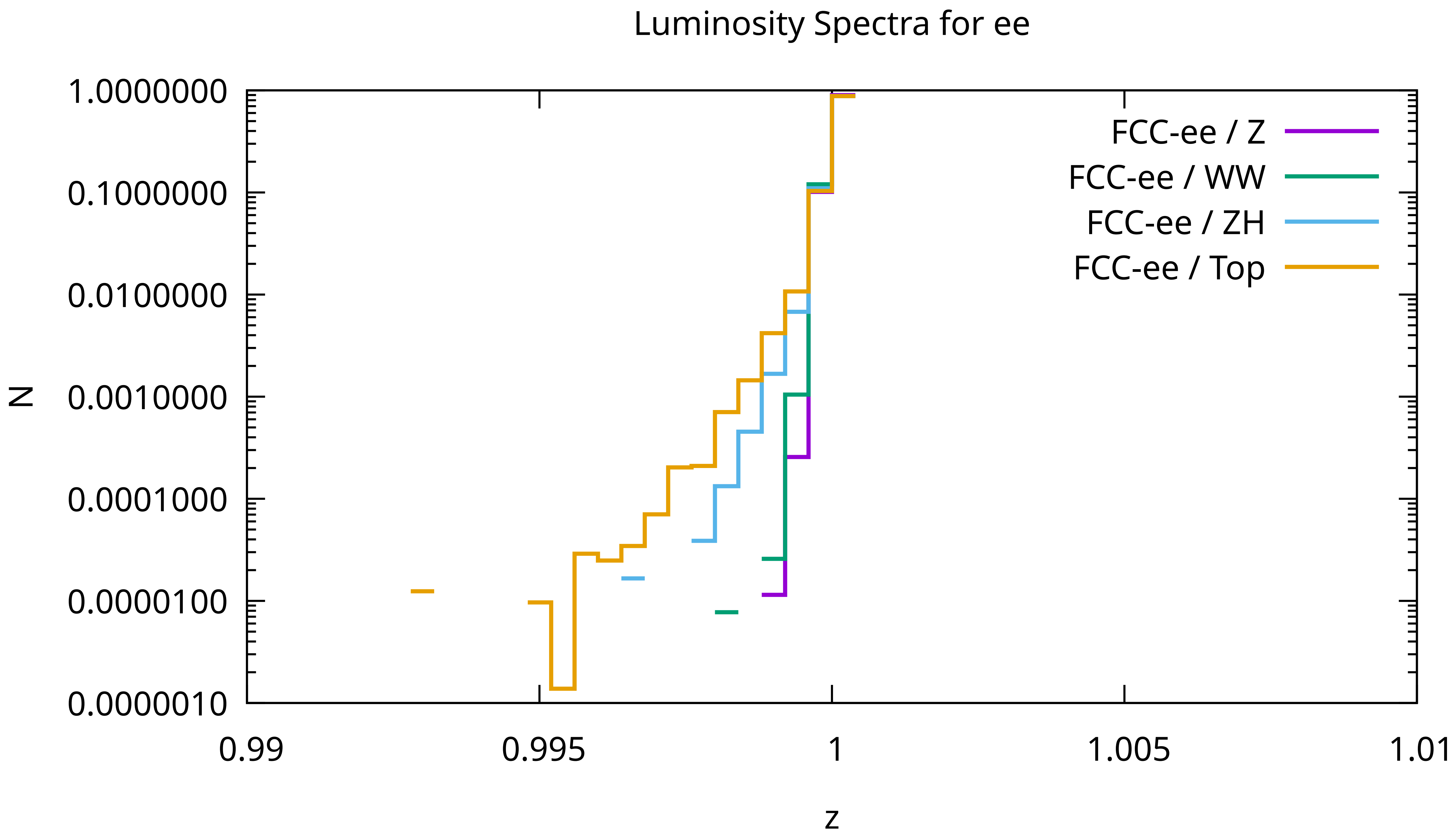

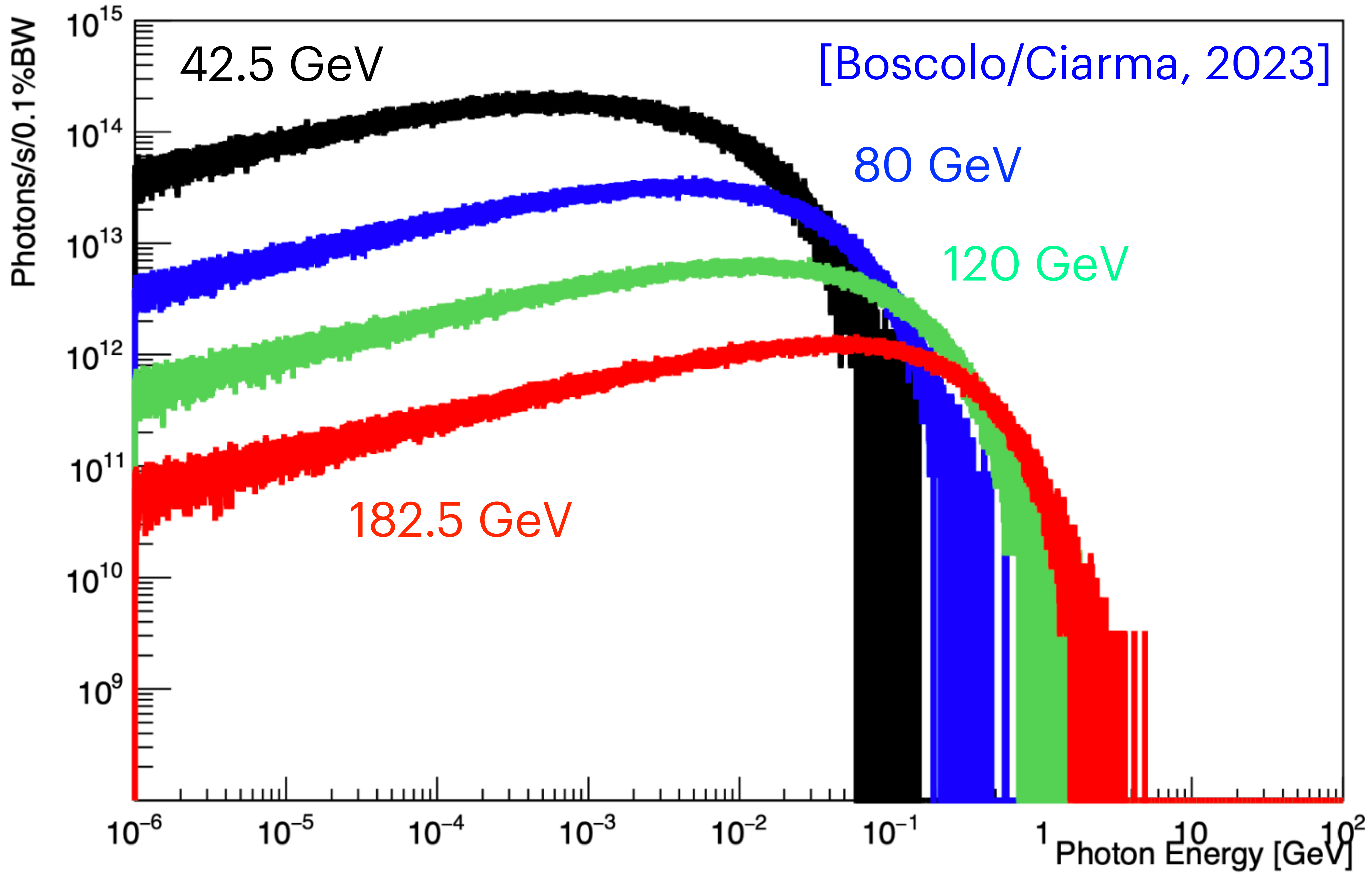

Fitting FCC-ee spectra w/ CIRCE algorithm

Fitting modified Gaussian at Z pole easy [Thorsten Ohl, 2024/25]

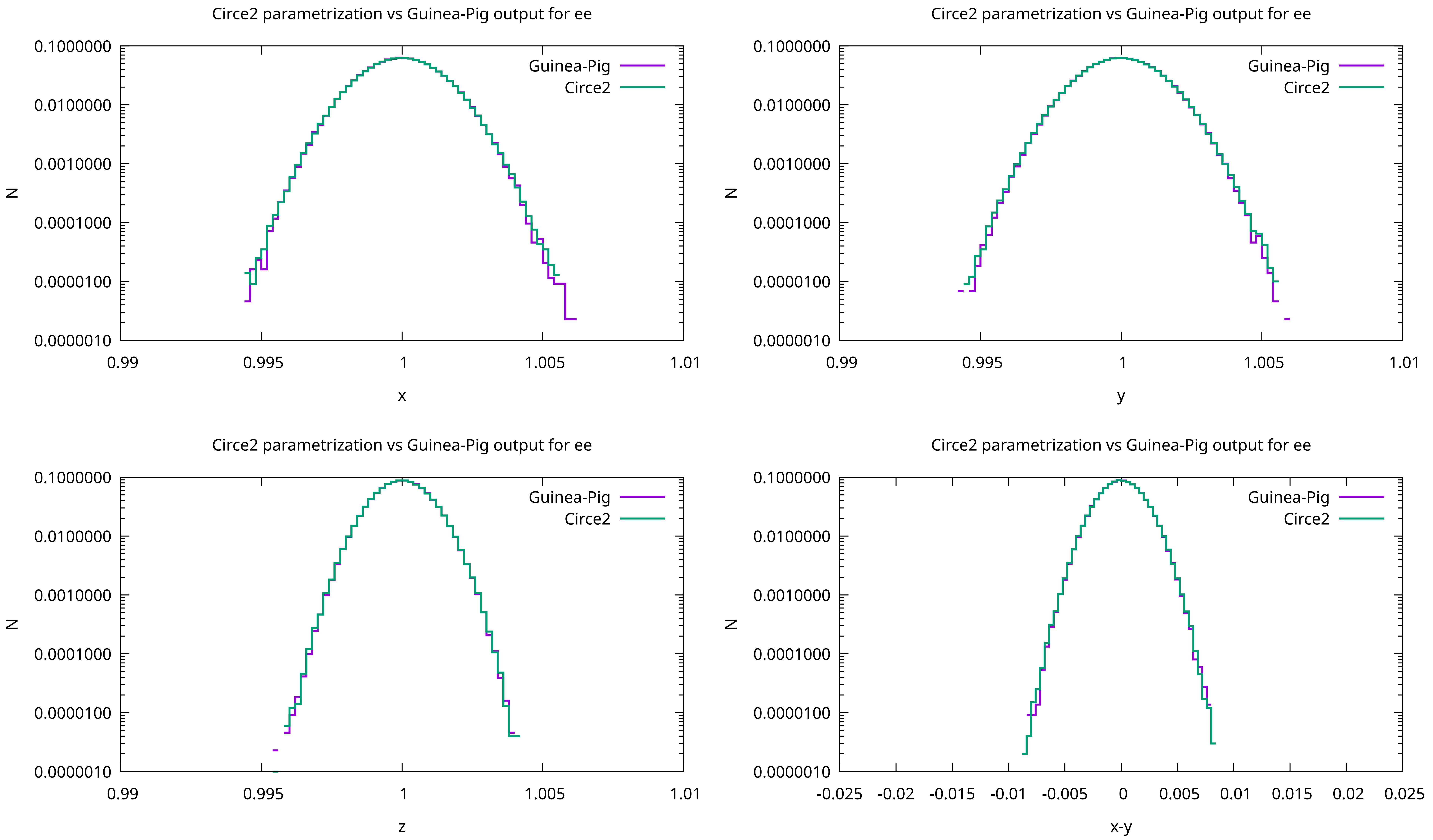

Fitting FCC-ee spectra w/ CIRCE algorithm

Fitting e^+e^- spectrum at tt [Thorsten Ohl, 2024/25]

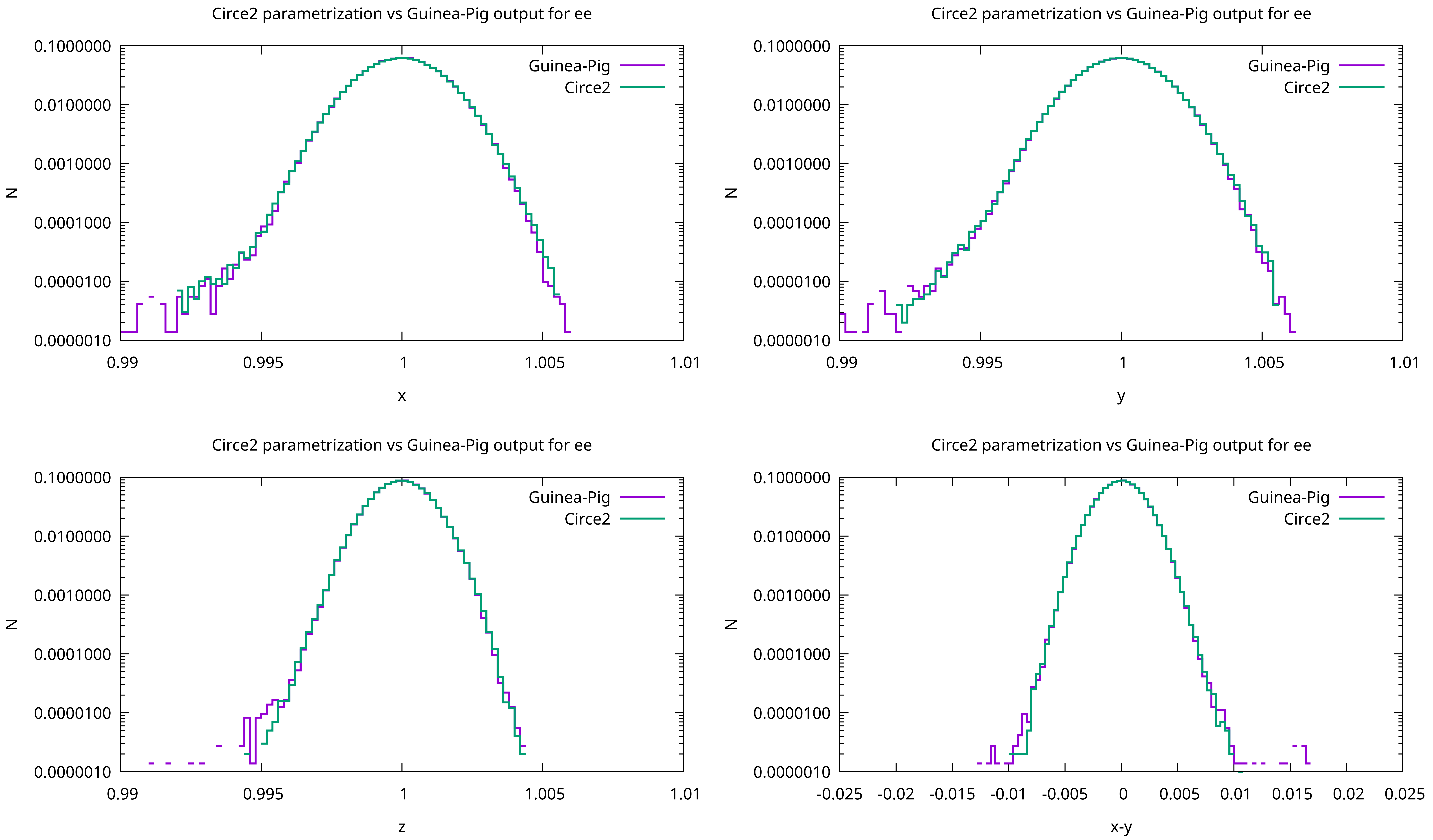

Fitting FCC-ee spectra w/ CIRCE algorithm

Fitting $\gamma\gamma$ spectrum at tt [Thorsten Ohl, 2024/25]

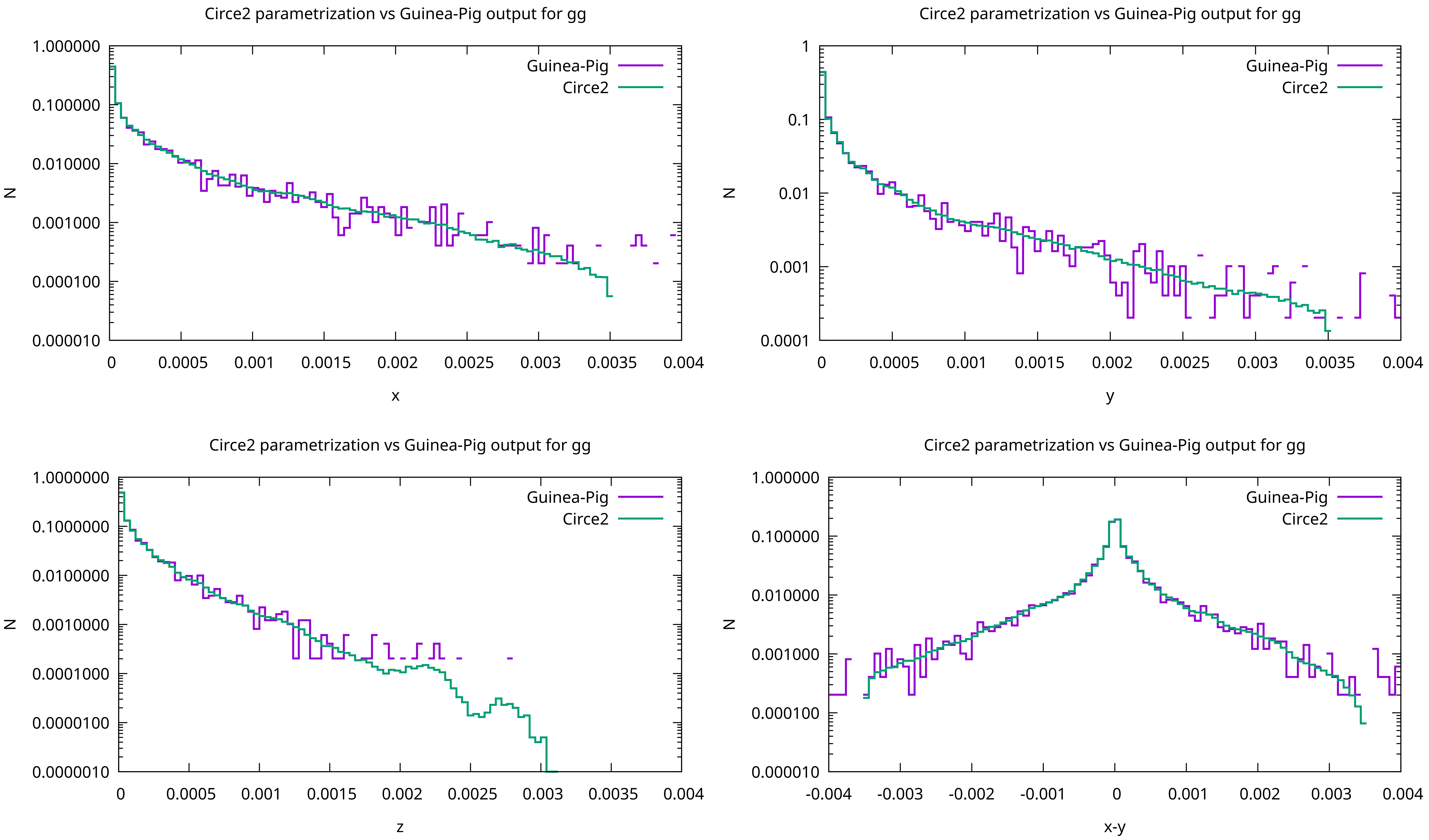

Machine Learning Framework for Phase Space Sampling

VAMP = Whizard's built-in ML algorithm for phase space

1. Invertible, parameterized mappings with adaptive optimization (⇒ normalizing-flow ansatz)
2. Multi-channel decomposition with adaptive optimization for weights (⇒ attention / transformer ansatz)
3. Initial setup not from random noise ⇒ use ME singularity structure and phase-space topology

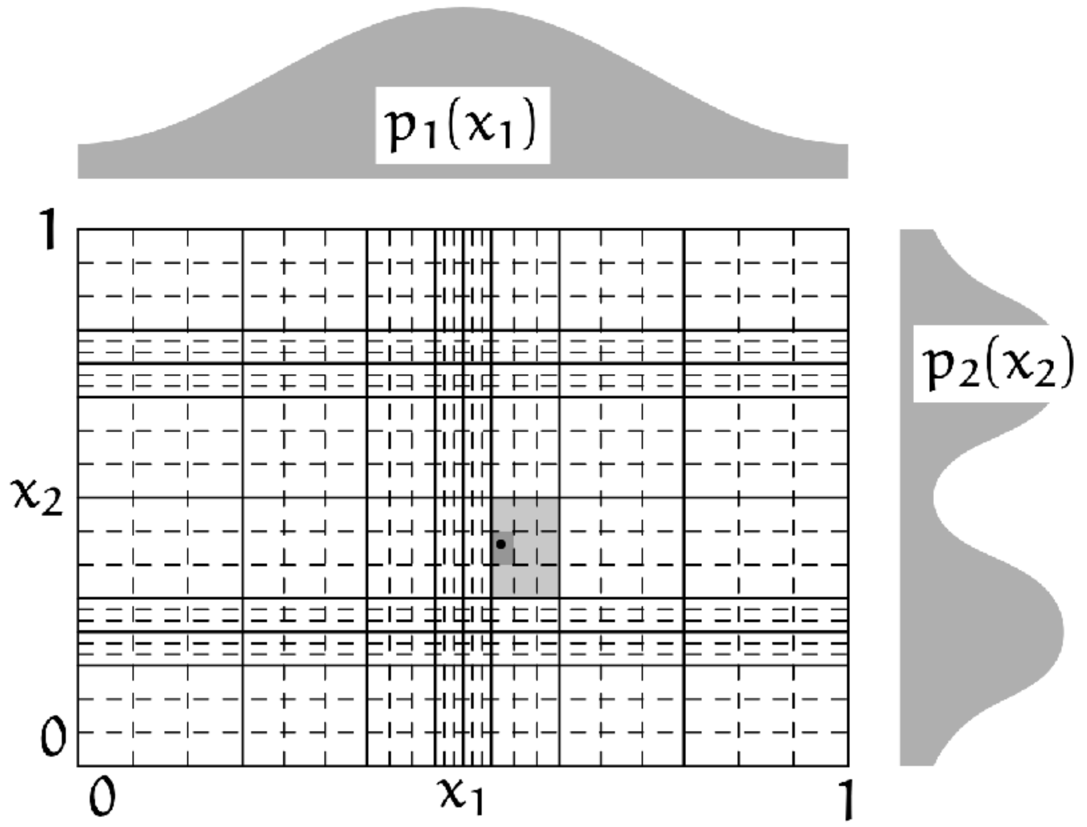

Machine Learning Framework for Phase Space Sampling

VAMP = Whizard's built-in ML algorithm for phase space

1. Invertible, parameterized mappings with adaptive optimization
   (⇒ normalizing-flow ansatz)
2. Multi-channel decomposition with adaptive optimization for weights
   (⇒ attention / transformer ansatz)
3. Initial setup not from random noise
   ⇒ use ME singularity structure and phase-space topology

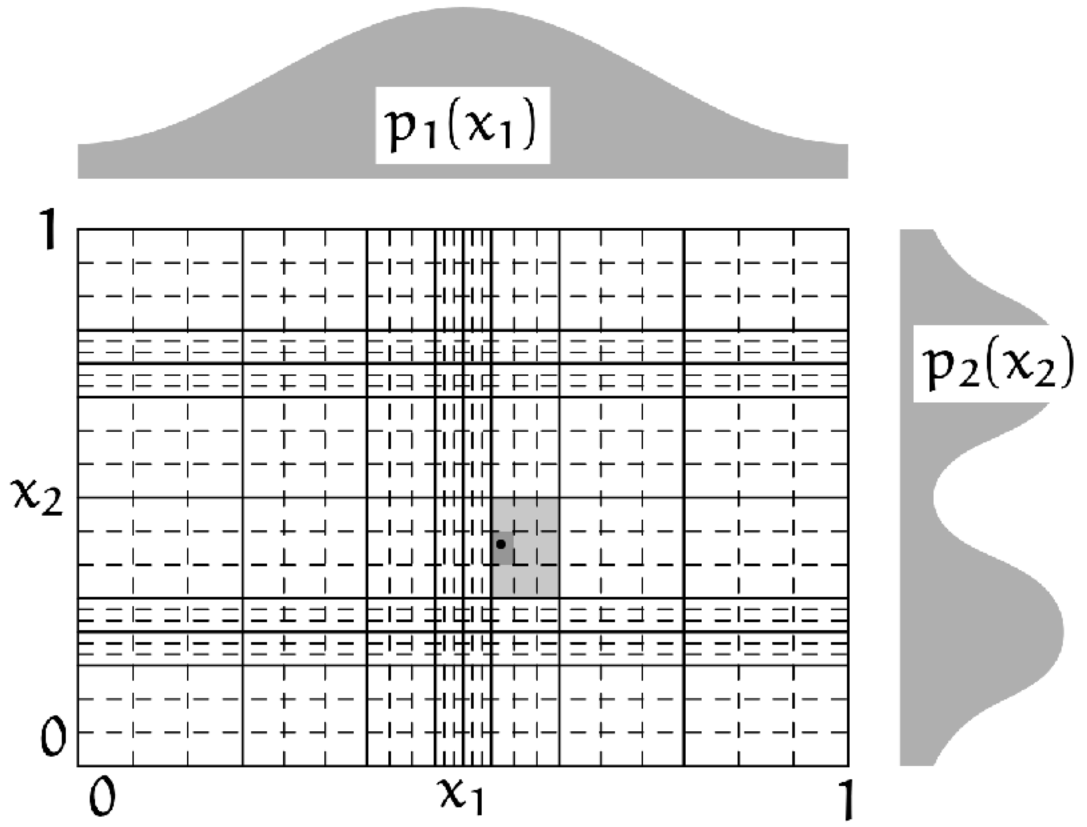

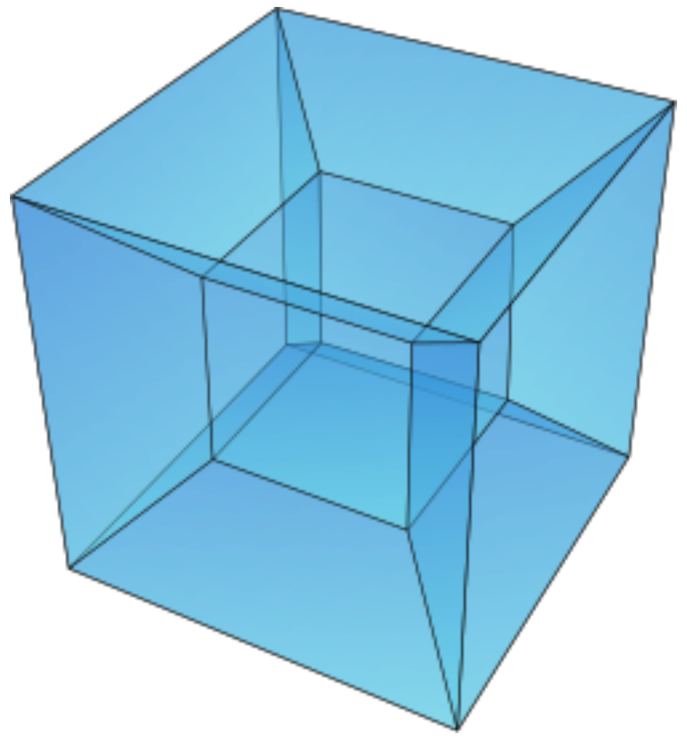

$U = (0,1)^{\otimes n}$

$g(U)$

physics-inspired invertible
diff. mappings from unit hypercube
to cut-constrained phase space
manifold

$g^{-1}(\phi)$

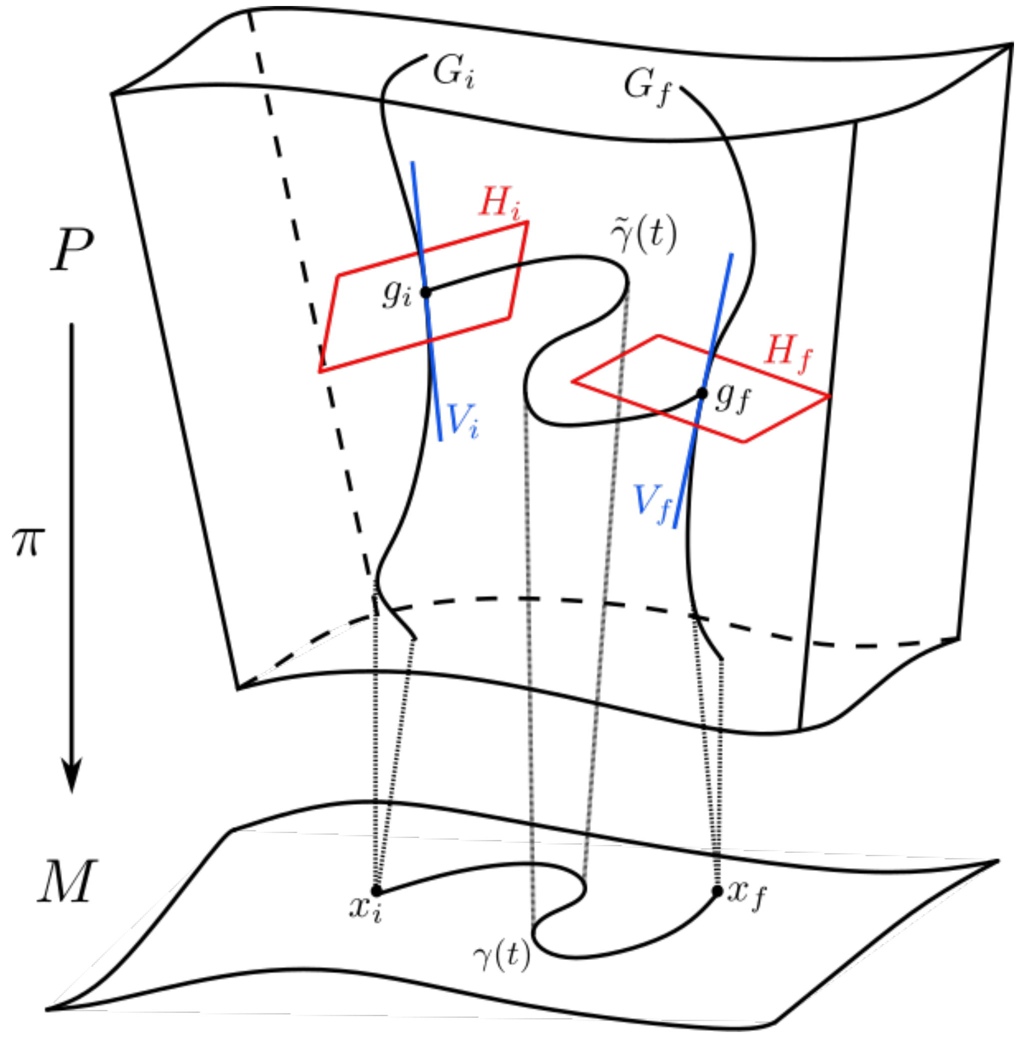

Machine Learning Framework for Phase Space Sampling

VAMP = Whizard's built-in ML algorithm for phase space

1. Invertible, parameterized mappings with adaptive optimization
   (⇒ normalizing-flow ansatz)
2. Multi-channel decomposition with adaptive optimization for weights
   (⇒ attention / transformer ansatz)
3. Initial setup not from random noise
   ⇒ use ME singularity structure and phase-space topology

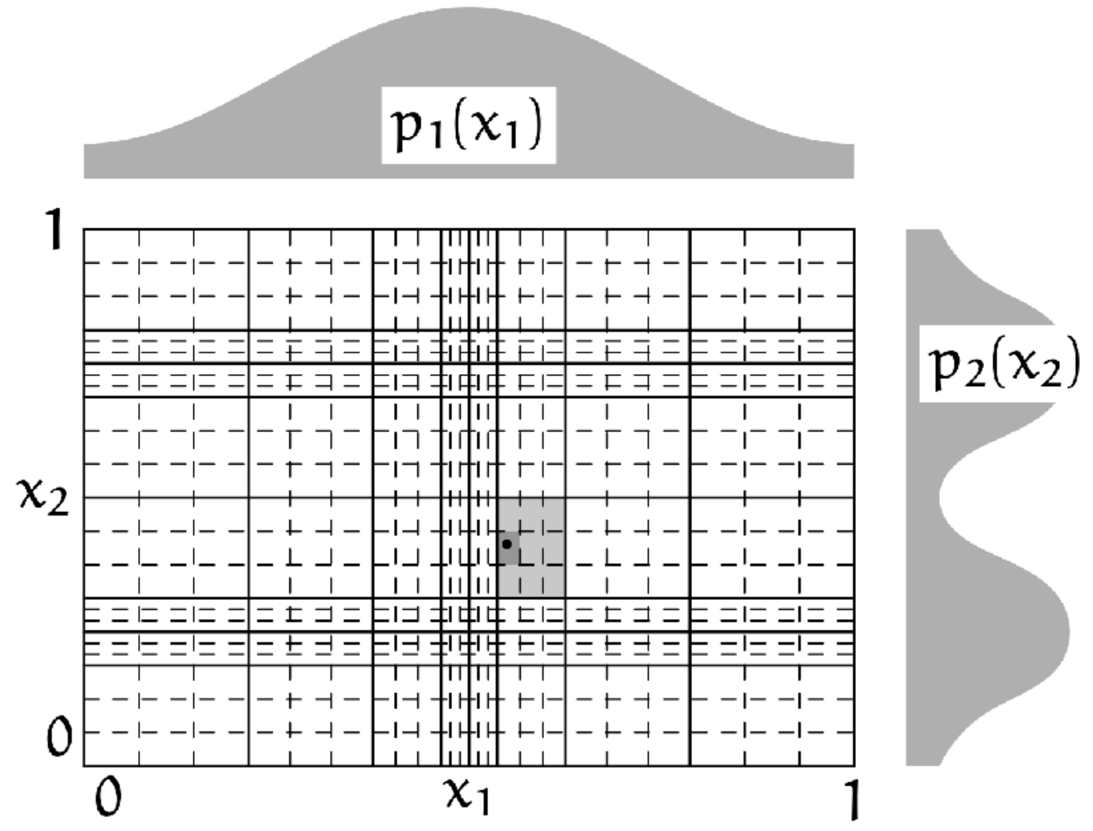

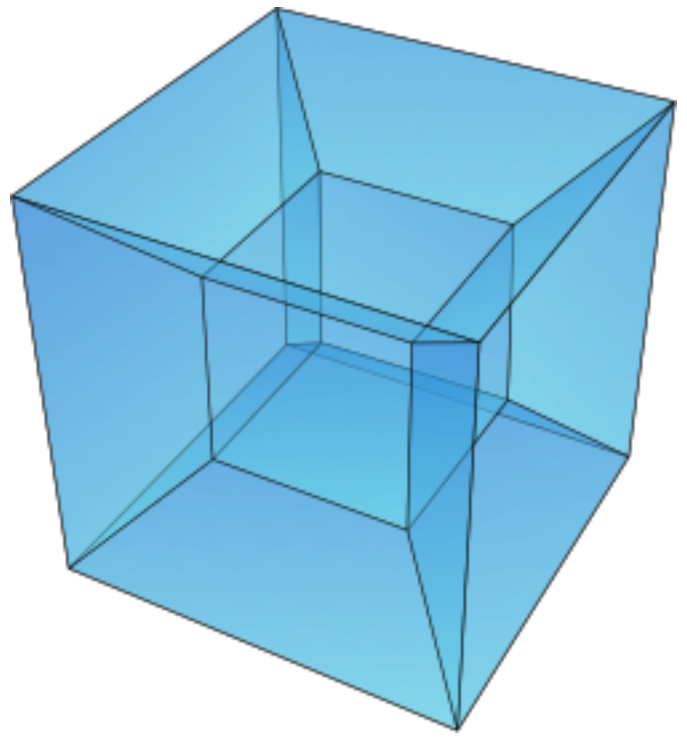

$U = (0,1)^{\otimes n}$

$g(U)$

physics-inspired invertible diff. mappings from unit hypercube to cut-constrained phase space manifold

$g^{-1}(\phi)$

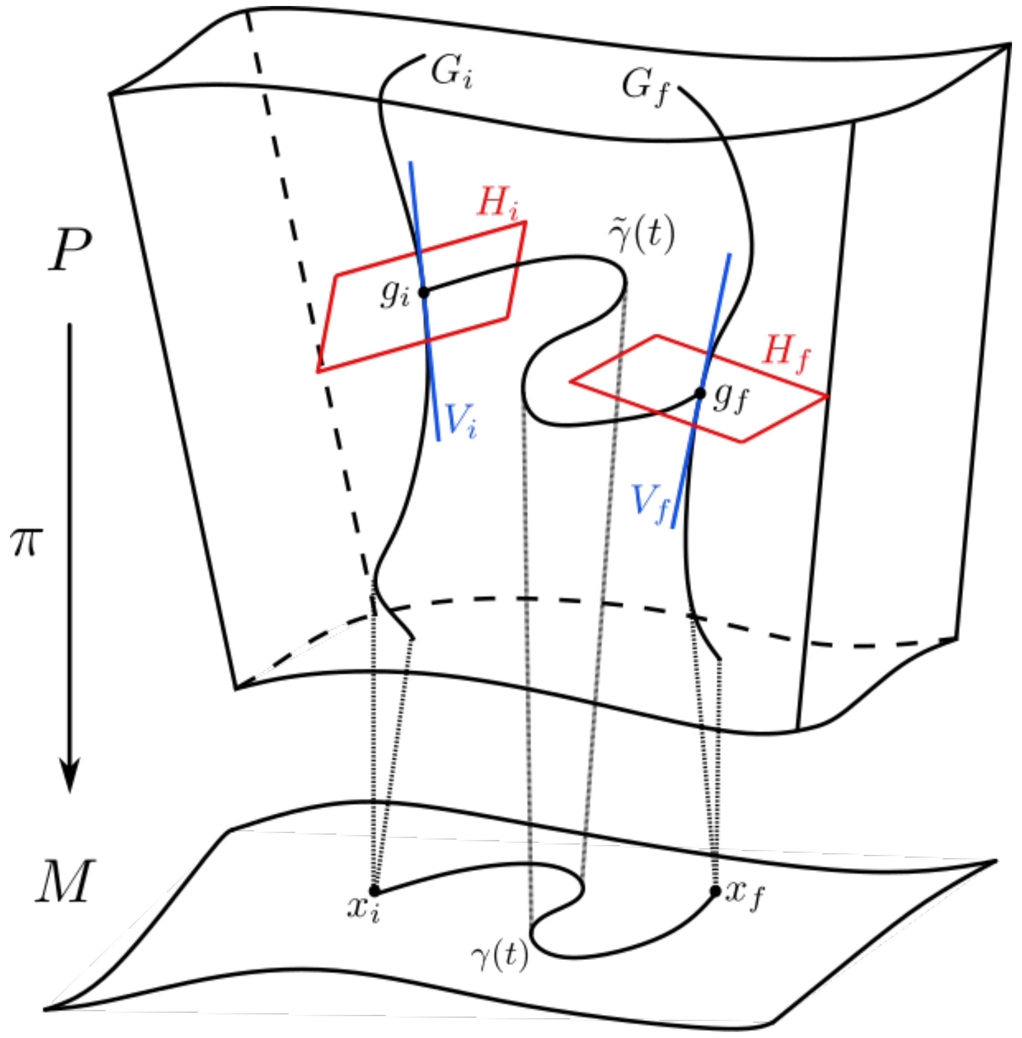

$$\int_{s_0}^{s_1} f(s)ds = \sum_i \alpha_i \int_{s_0}^{s_1} \frac{f(s)}{g(s)} g_i(s) ds$$

channel weights

channel mappings

Machine Learning Framework for Phase Space Sampling

VAMP = Whizard's built-in ML algorithm for phase space

1. Invertible, parameterized mappings with adaptive optimization
   (⇒ normalizing-flow ansatz)
2. Multi-channel decomposition with adaptive optimization for weights
   (⇒ attention / transformer ansatz)
3. Initial setup not from random noise
   ⇒ use ME singularity structure and phase-space topology

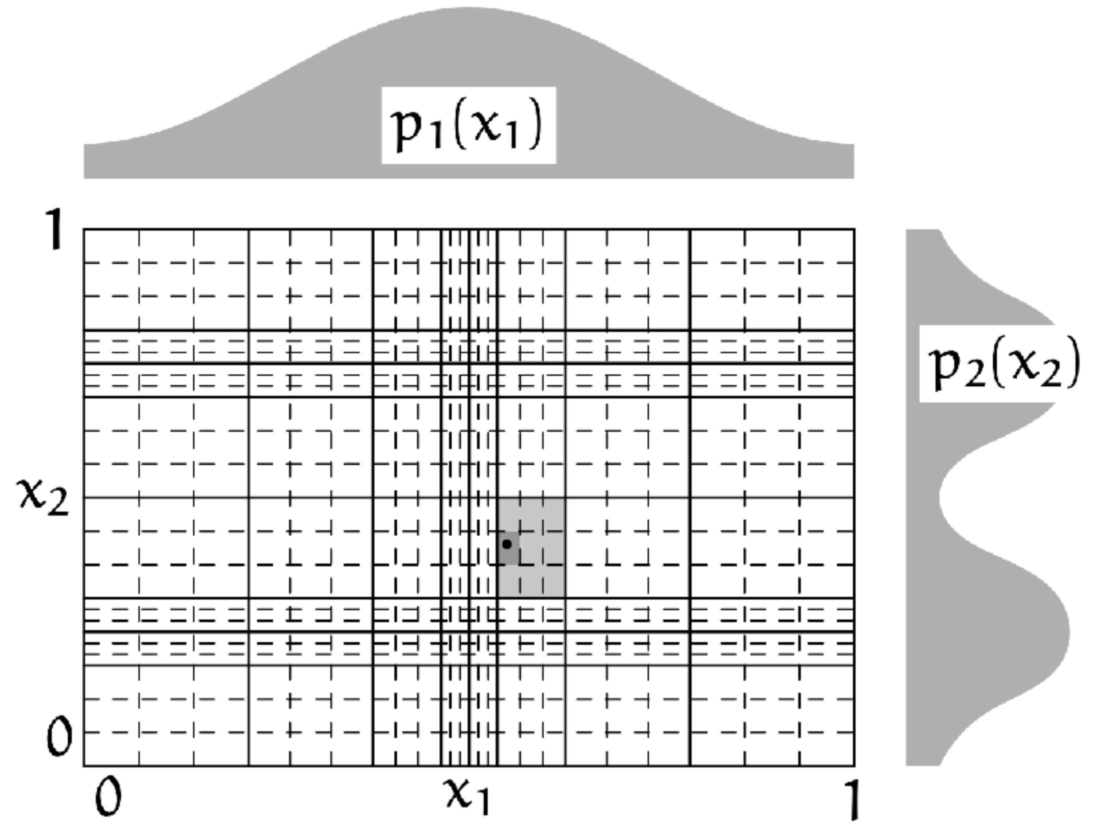

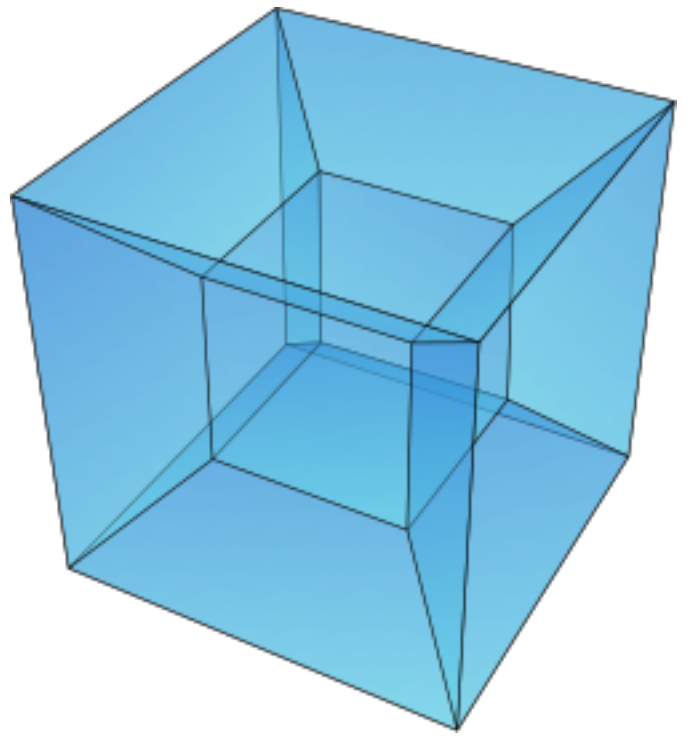

$U = (0,1)^{\otimes n}$

$g(U)$

physics-inspired invertible diff. mappings from unit hypercube to cut-constrained phase space manifold

$g^{-1}(\phi)$

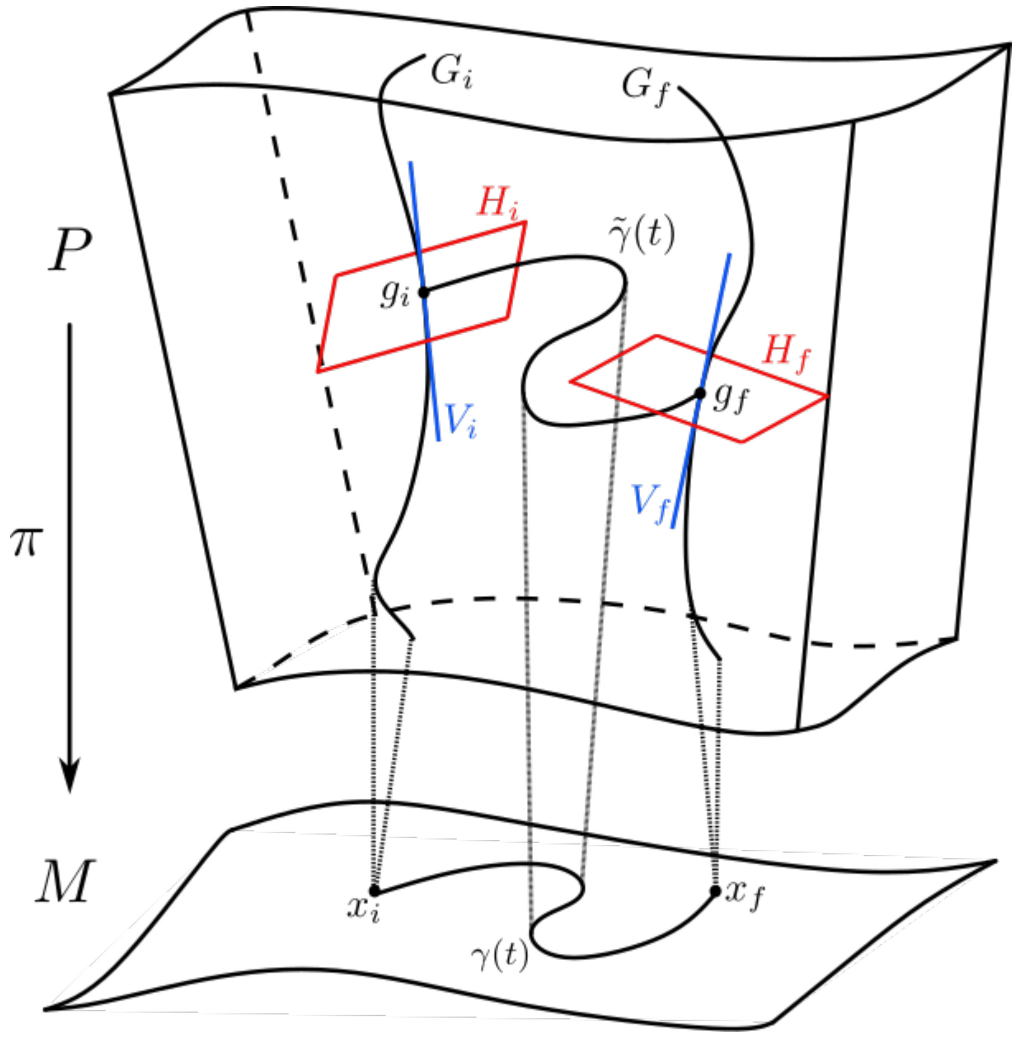

$$\int_{s_0}^{s_1} f(s)ds = \sum_i \alpha_i \int_{s_0}^{s_1} \frac{f(s)}{g(s)} g_i(s) ds$$

channel weights

channel mappings

Parameterized lenses in category theory

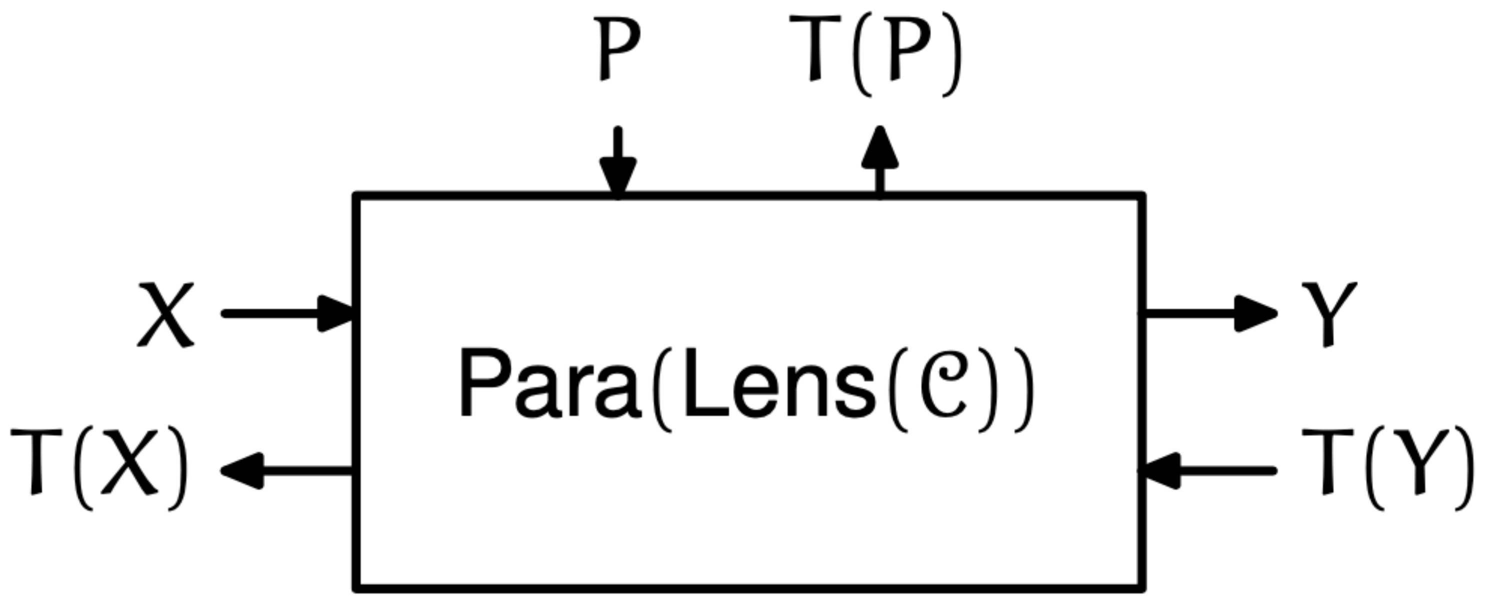

Cruttwell, Gavranović ea., 1910.07065; 2103.01931; 2203.12478; 2403.13001; 2404.00408

Machine Learning Framework for Phase Space Sampling

VAMP = Whizard's built-in ML algorithm for phase space

1. Invertible, parameterized mappings with adaptive optimization
   (⇒ normalizing-flow ansatz)
2. Multi-channel decomposition with adaptive optimization for weights
   (⇒ attention / transformer ansatz)
3. Initial setup not from random noise
   ⇒ use ME singularity structure and phase-space topology

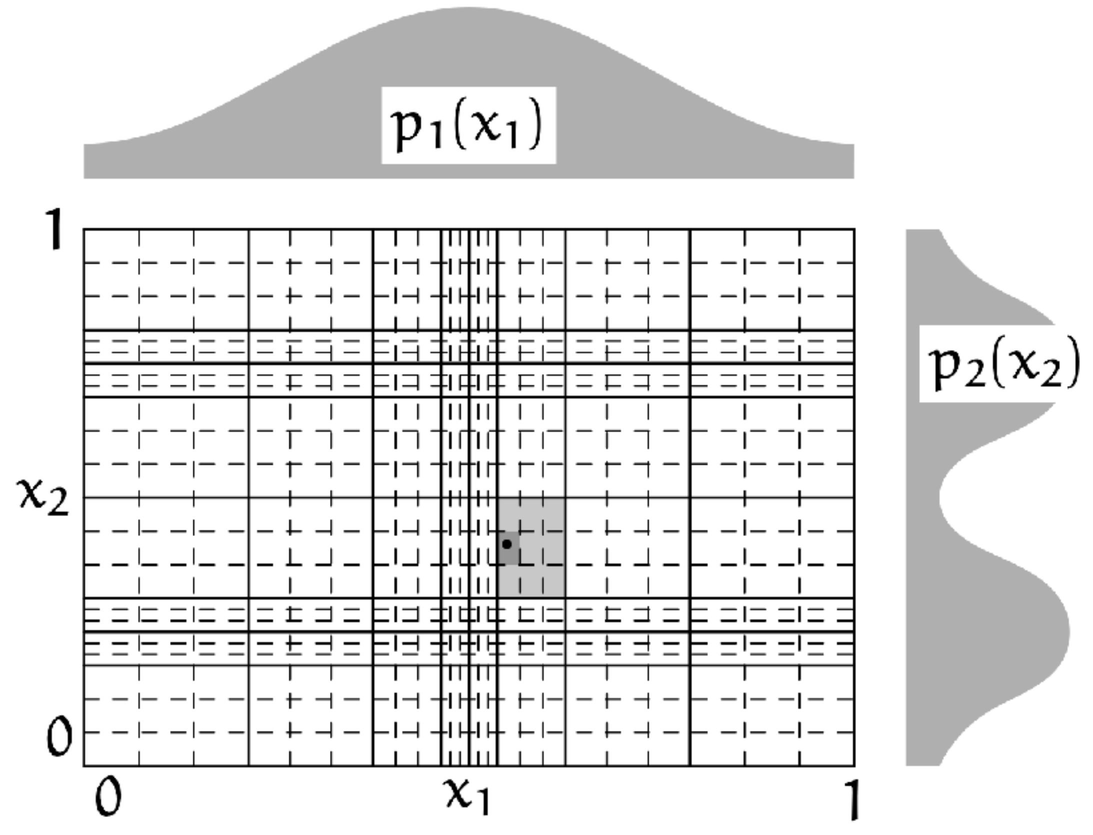

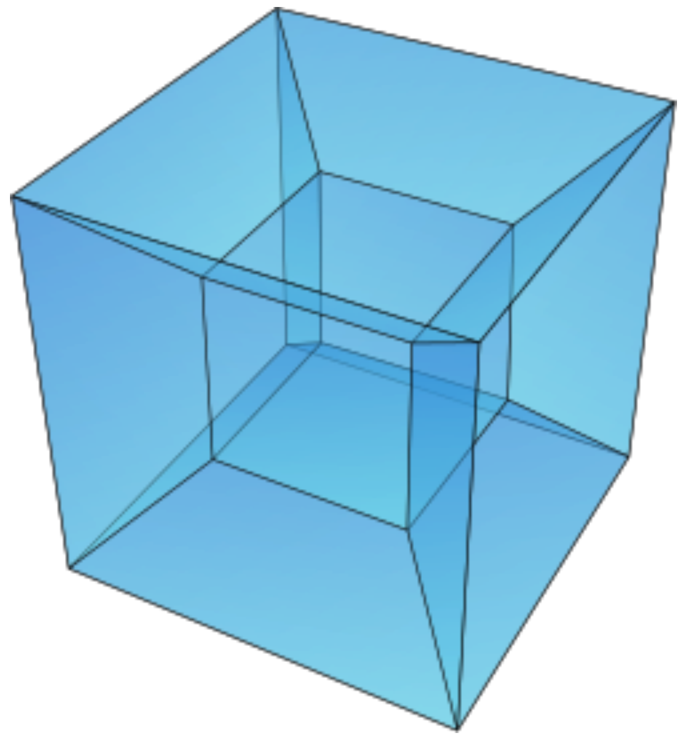

$U = (0,1)^{\otimes n}$

$g(U)$

physics-inspired invertible
diff. mappings from unit hypercube
to cut-constrained phase space
manifold

$g^{-1}(\phi)$

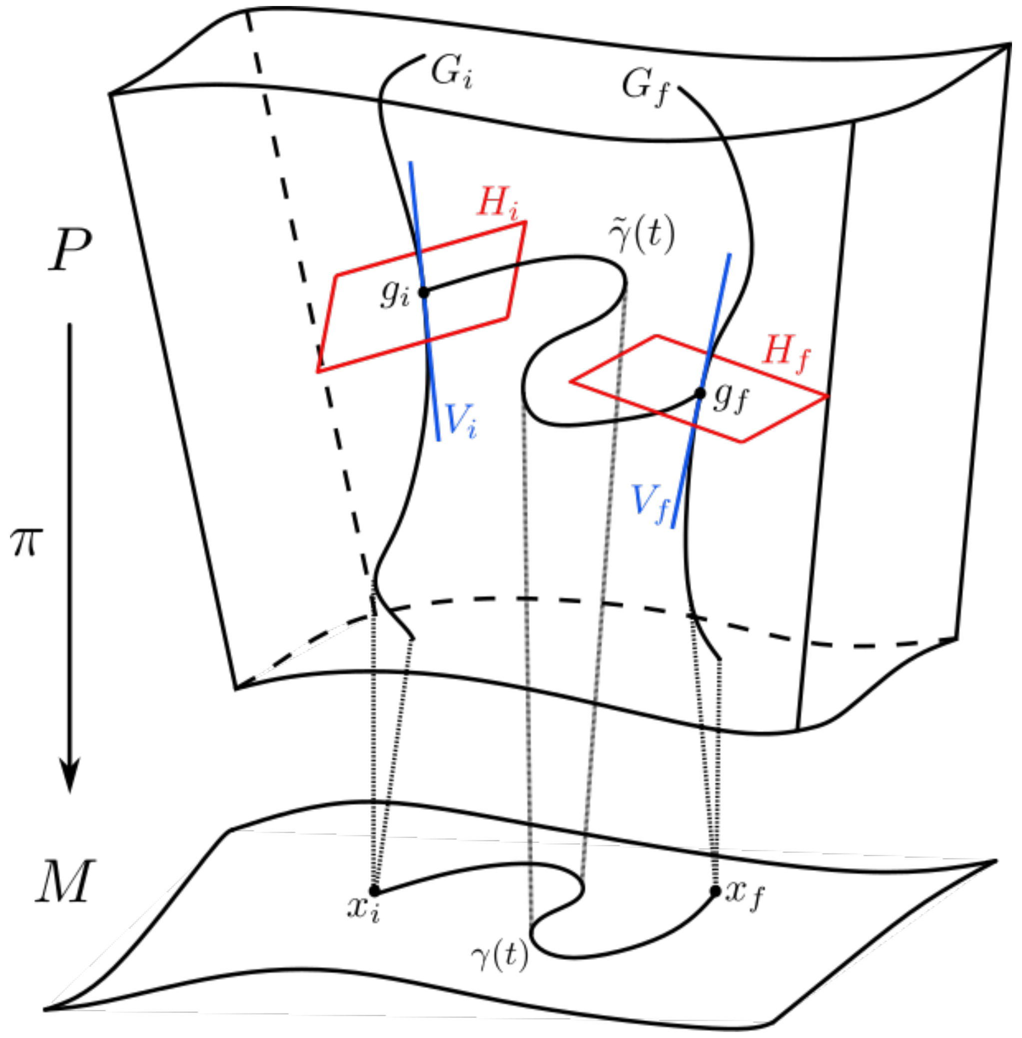

$$\int_{s_0}^{s_1} f(s)ds = \sum_i \alpha_i \int_{s_0}^{s_1} \frac{f(s)}{g(s)} g_i(s) ds$$

channel weights

channel mappings

Latent space
(Integrator
variables)

Parameterized lenses in category theory

Channel weights / other parameters

Target space
(Physical PS
variables)

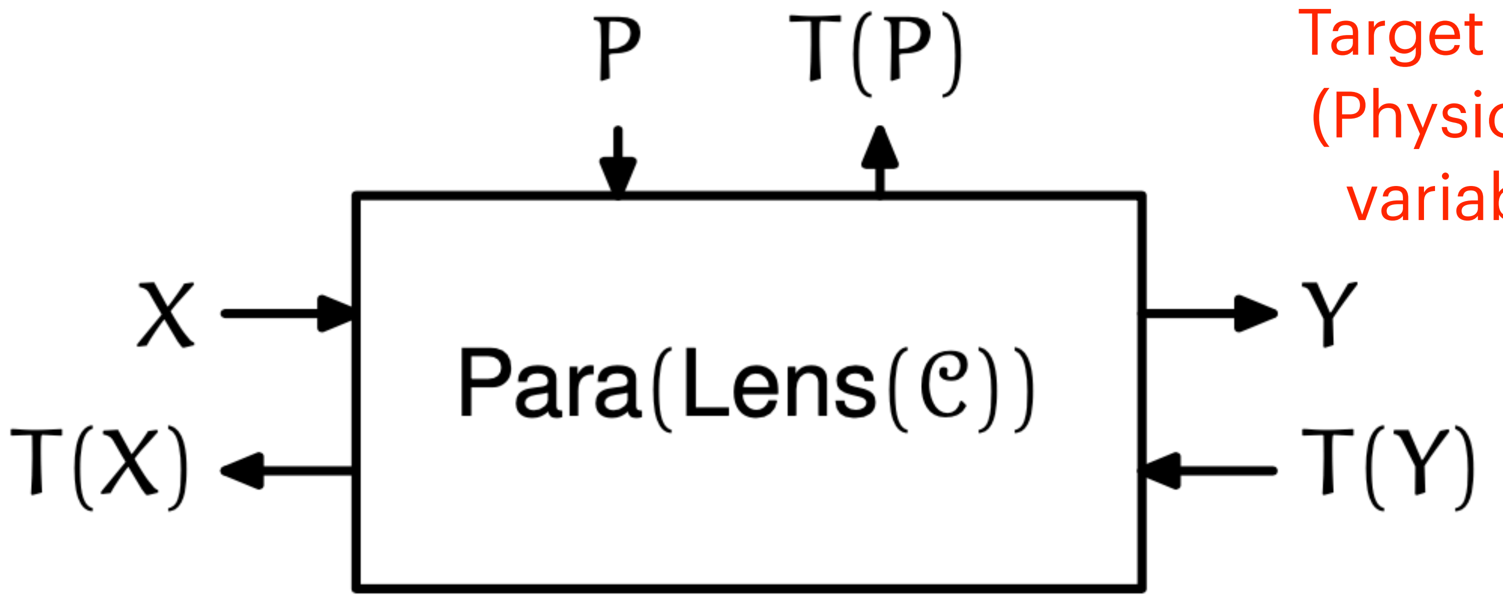

Cruttwell, Gavranović ea., 1910.07065; 2103.01931;
2203.12478; 2403.13001; 2404.00408

Top threshold: parametric uncertainties

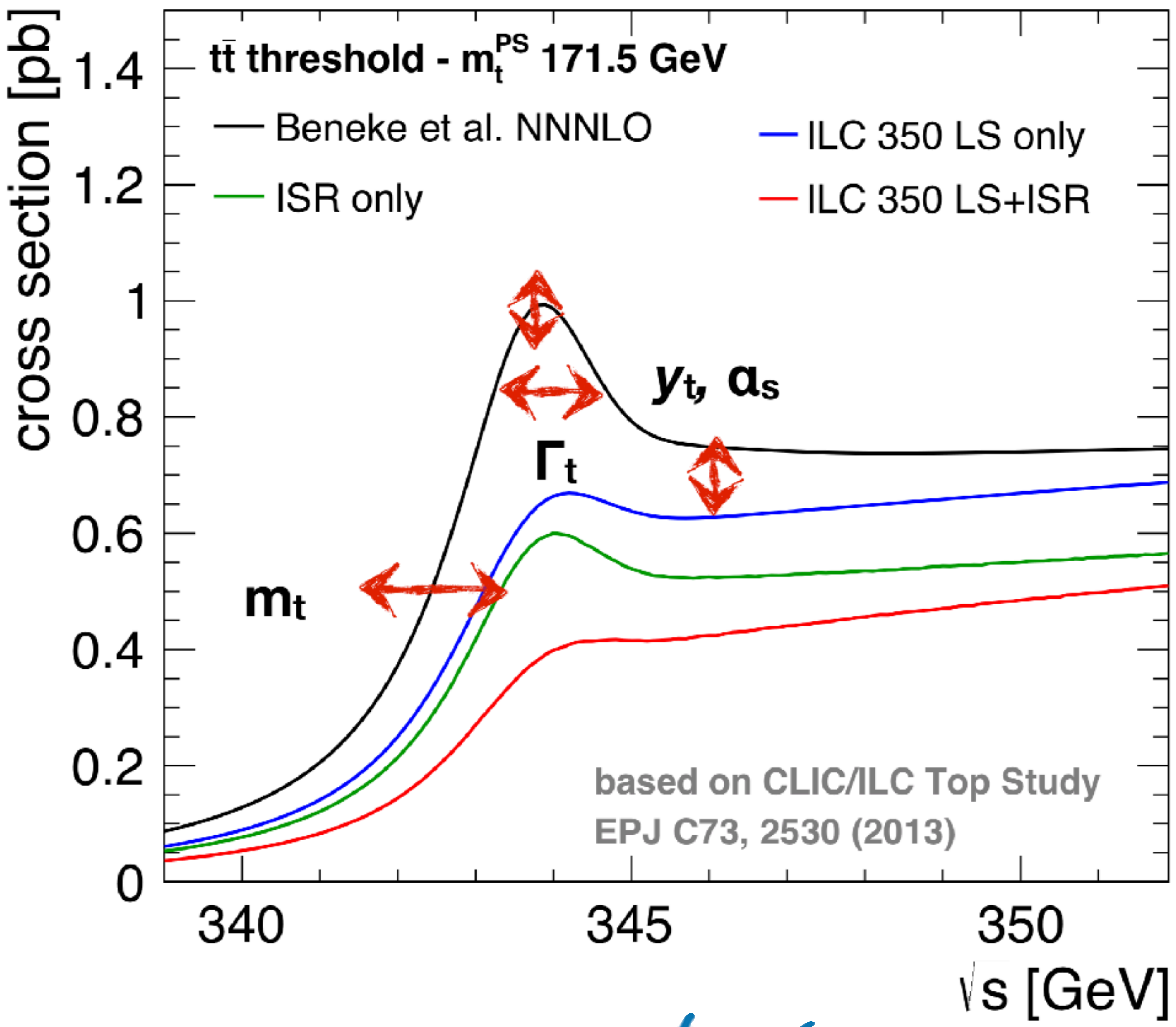

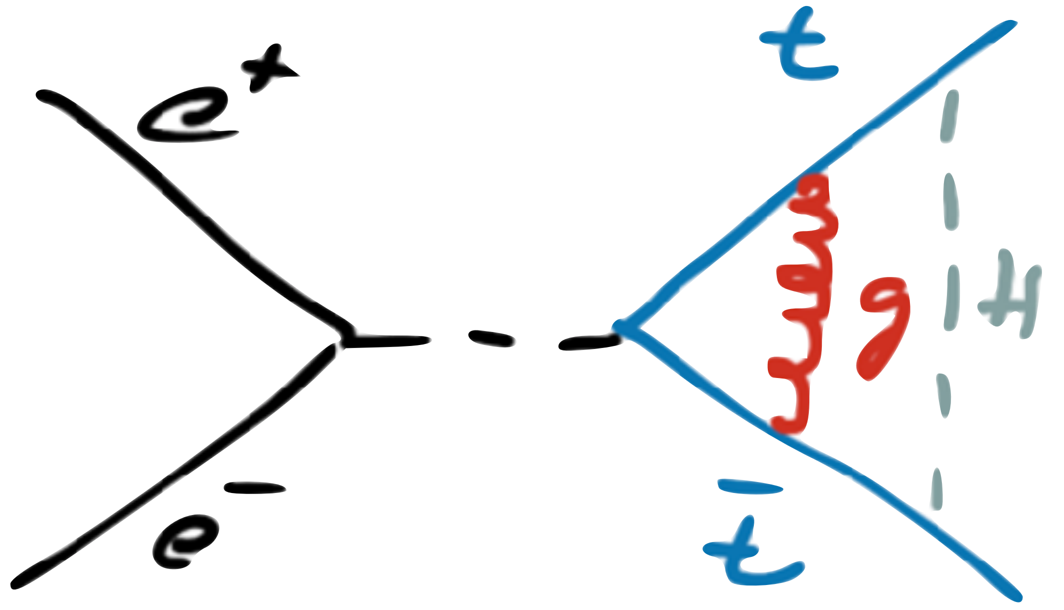

Dependence on M_t, Γ_t, α_s, y_t

based on:

Beneke/Maier/Piclum/Rauh, 2015

Defranchis/de Blas/Mekta/Selvaggi/Vos: 2503.18713

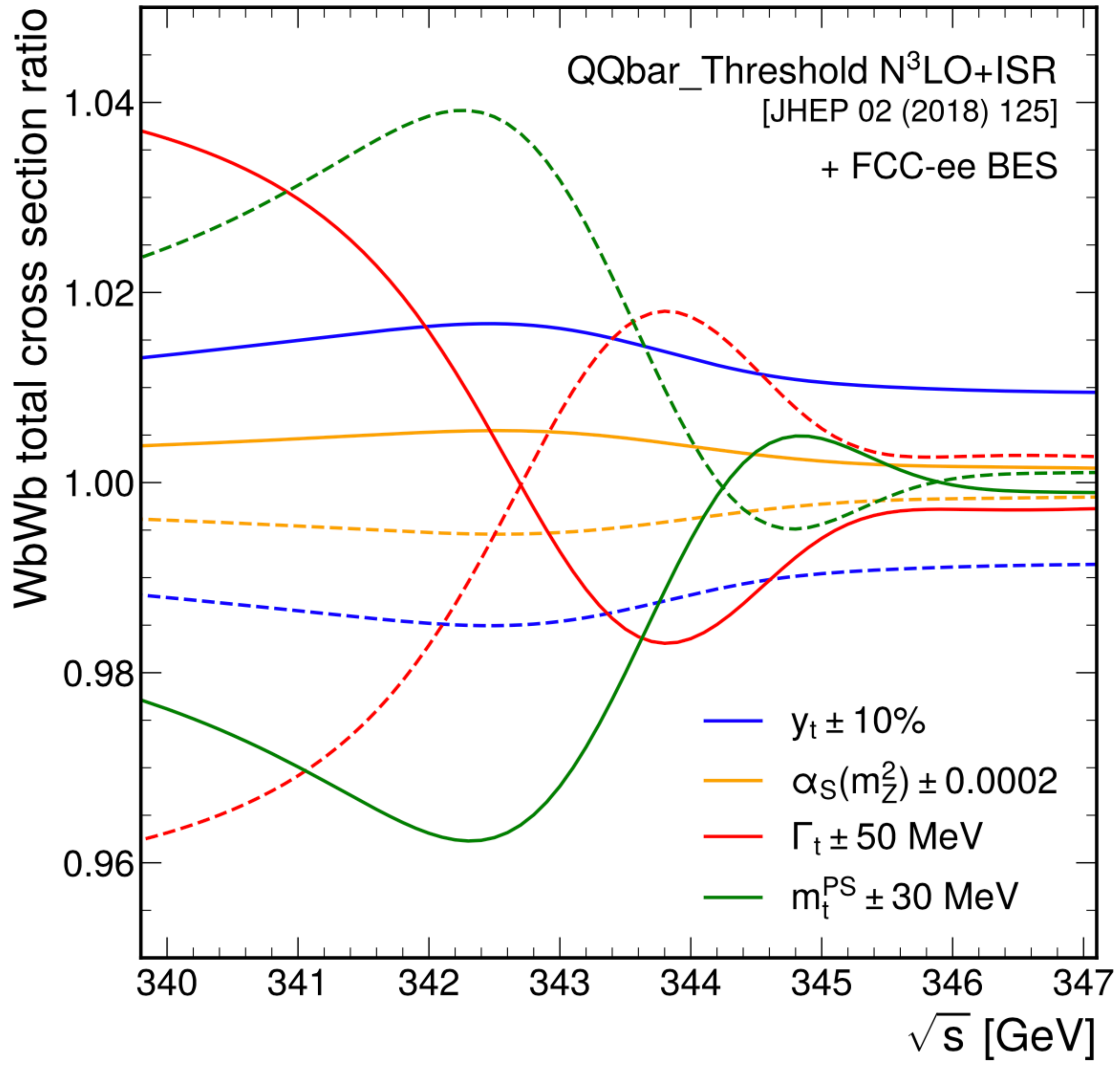

Fixed-order vs. resummation uncertainties

NRQCD NNNLO fixed order + α_s logarithms

Kiyo et al., 2005; Beneke et al., 2008-2015

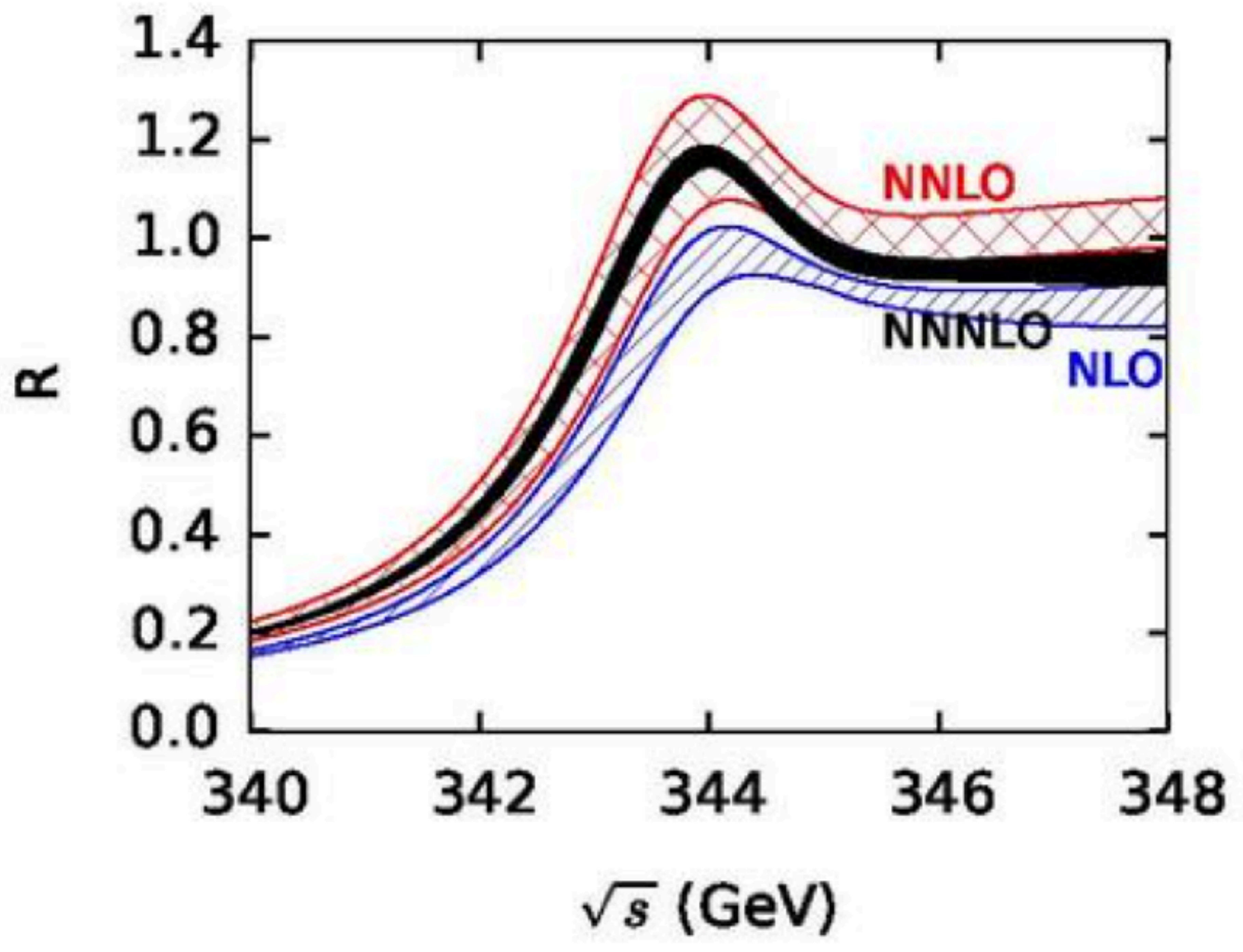

Fixed-order vs. resummation uncertainties

NRQCD NNNLO fixed order + α_s logarithms

Kiyo et al., 2005; Beneke et al., 2008-2015

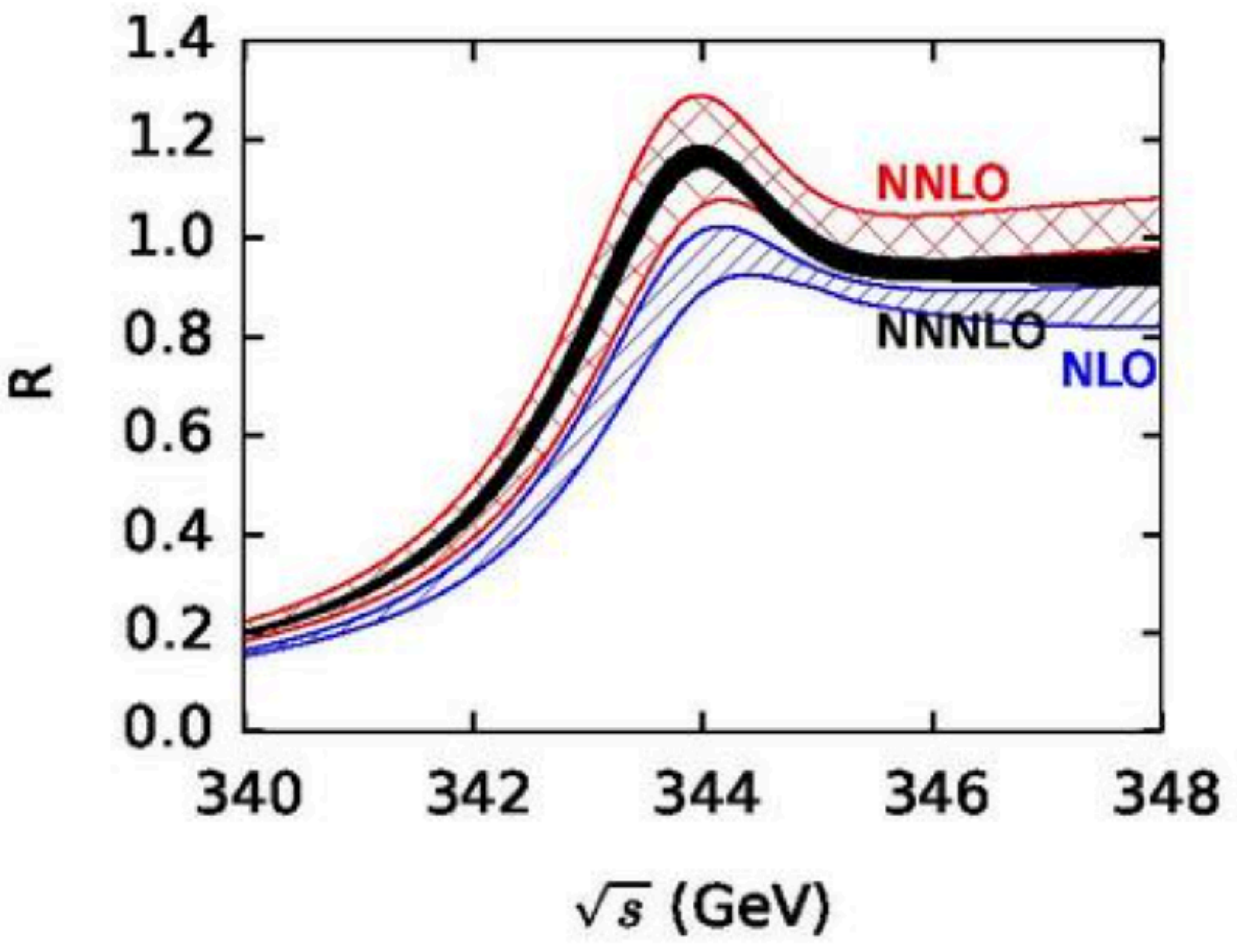

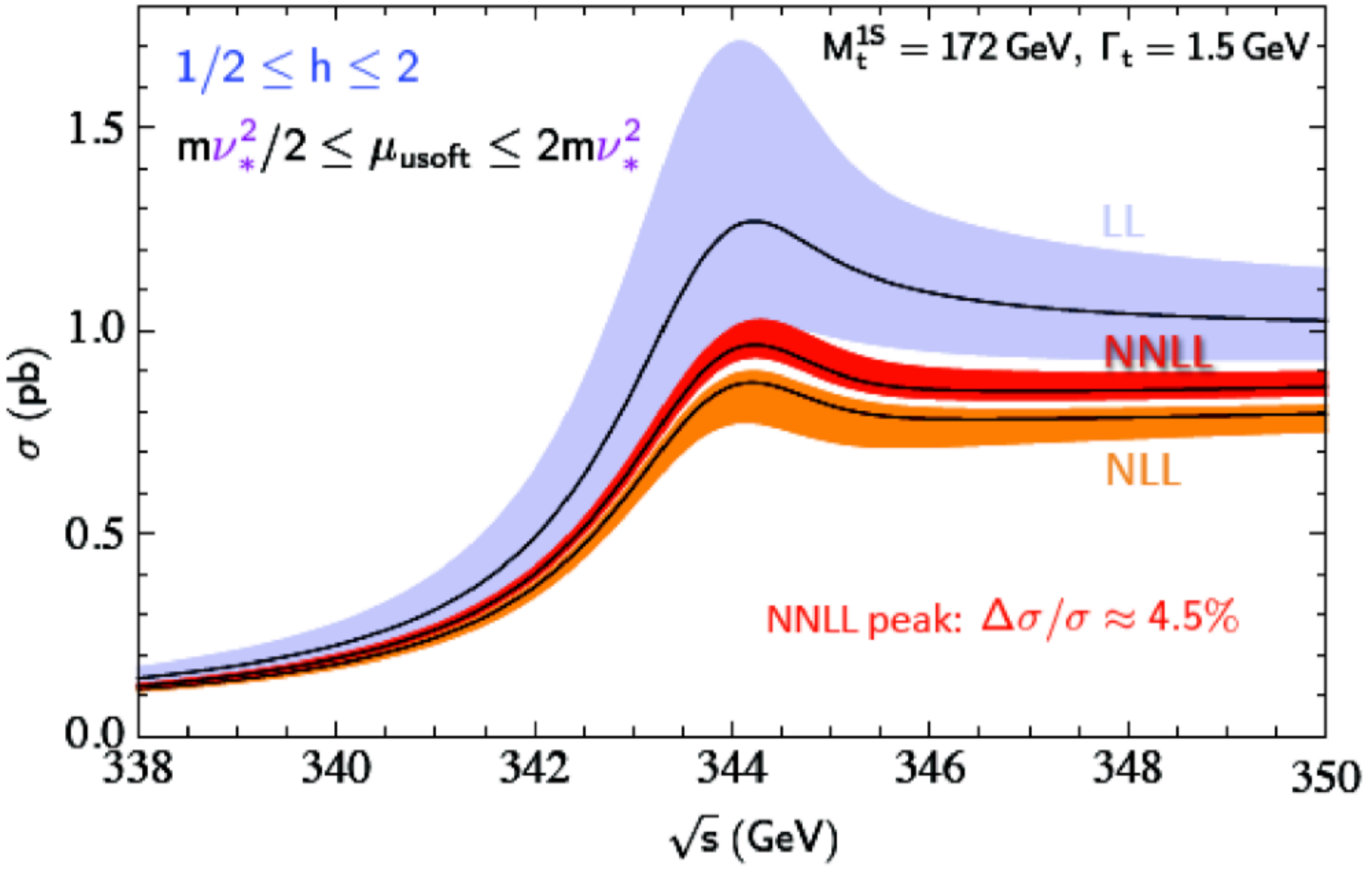

Resummation of velocity logarithms

Hoang/Stahlhofen, 2012

$$\mu_h = h \cdot m_t \qquad \mu_s = f \cdot m_t v$$

Fixed-order vs. resummation uncertainties

NRQCD NNNLO fixed order + α_s logarithms

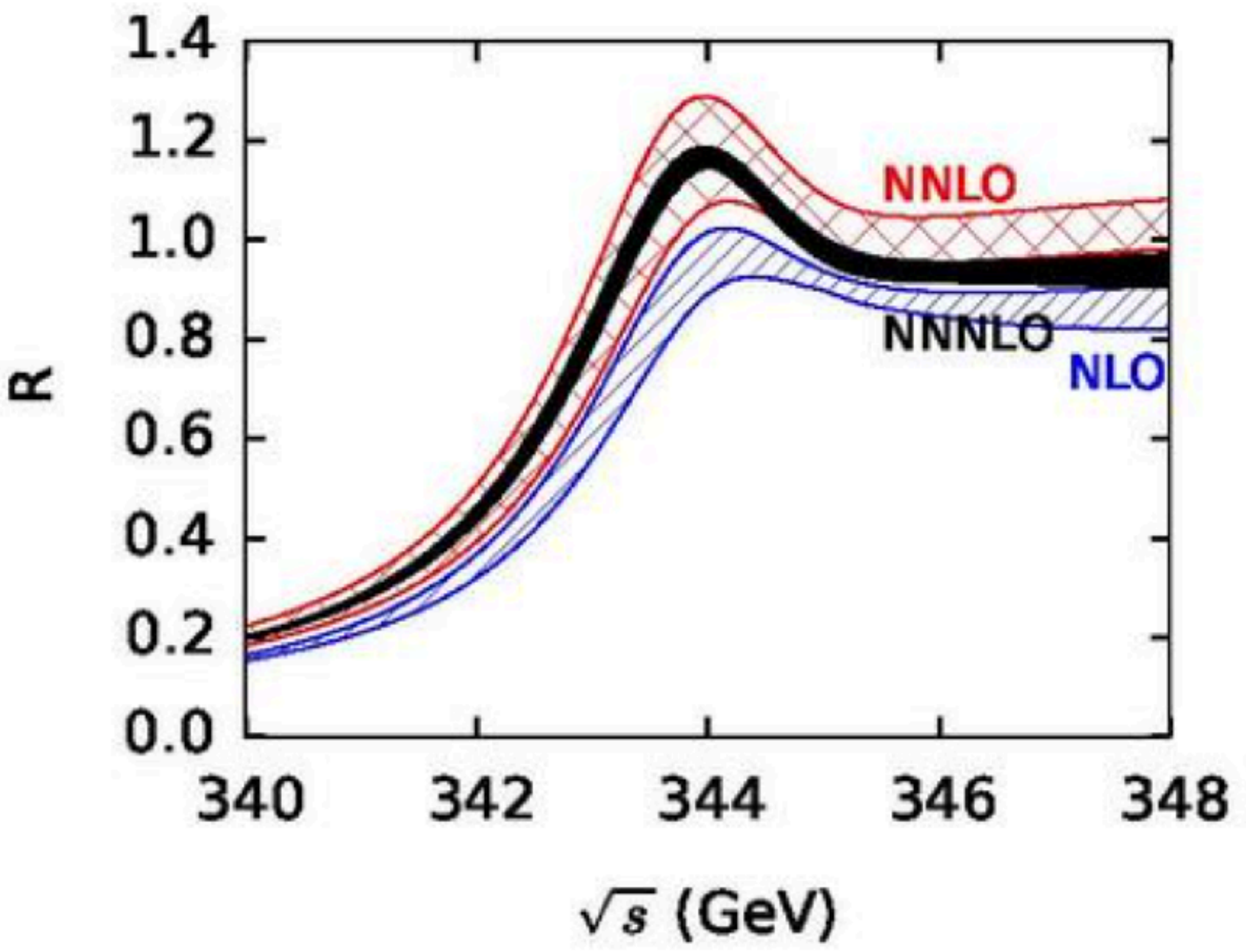

Kiyo et al., 2005; Beneke et al., 2008-2015

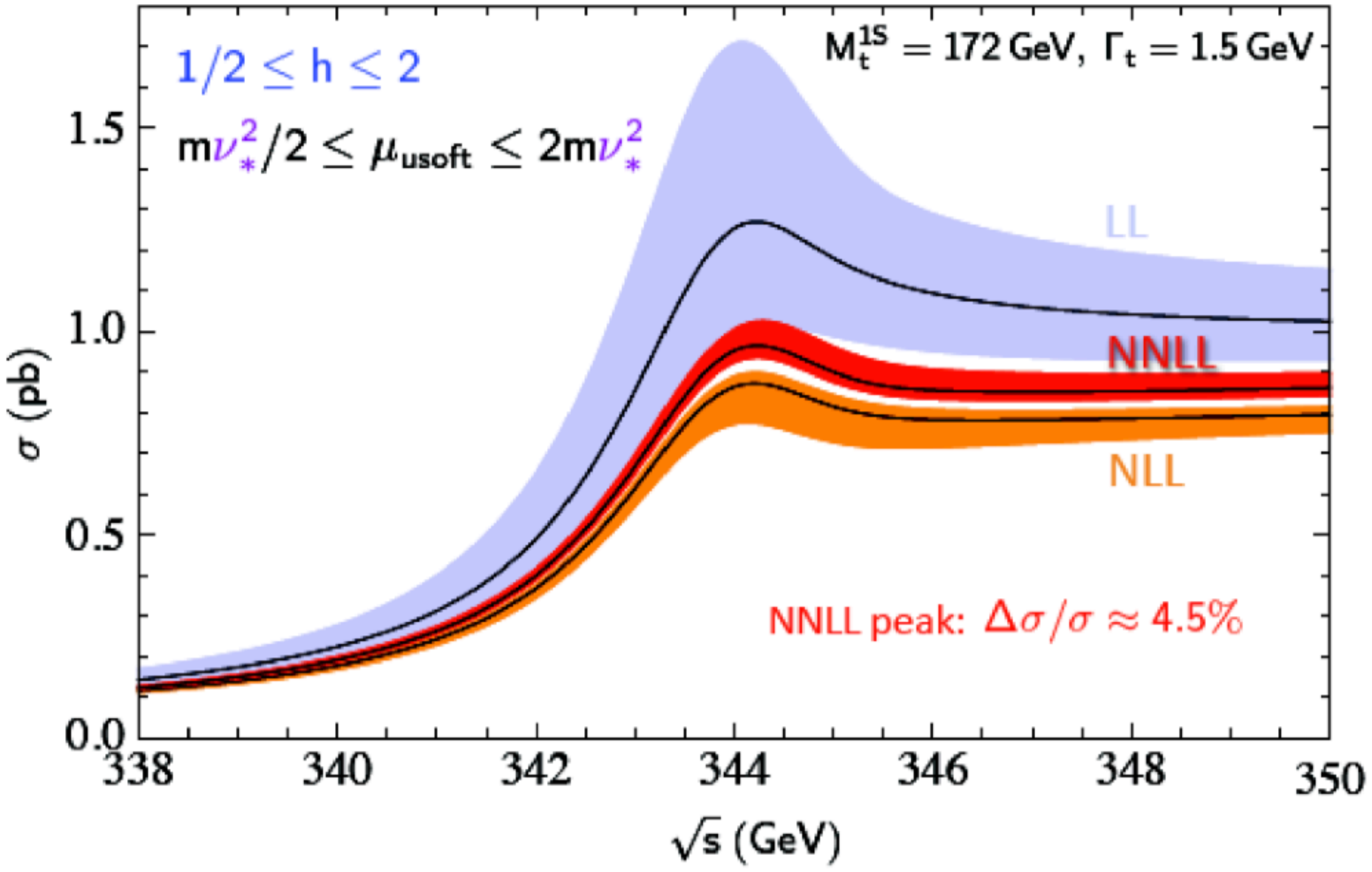

[Hoang & Stahlhofen '13]

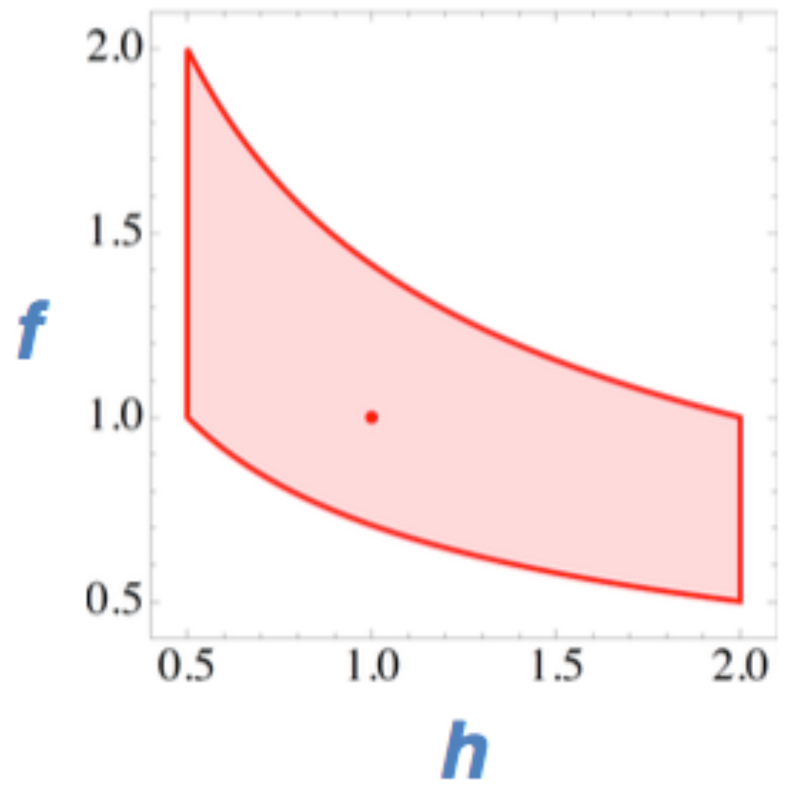

Resummation of velocity logarithms

Hoang/Stahlhofen, 2012

$$\mu_h = h \cdot m_t \qquad \mu_s = f \cdot m_t v$$

Top threshold: validation & matching

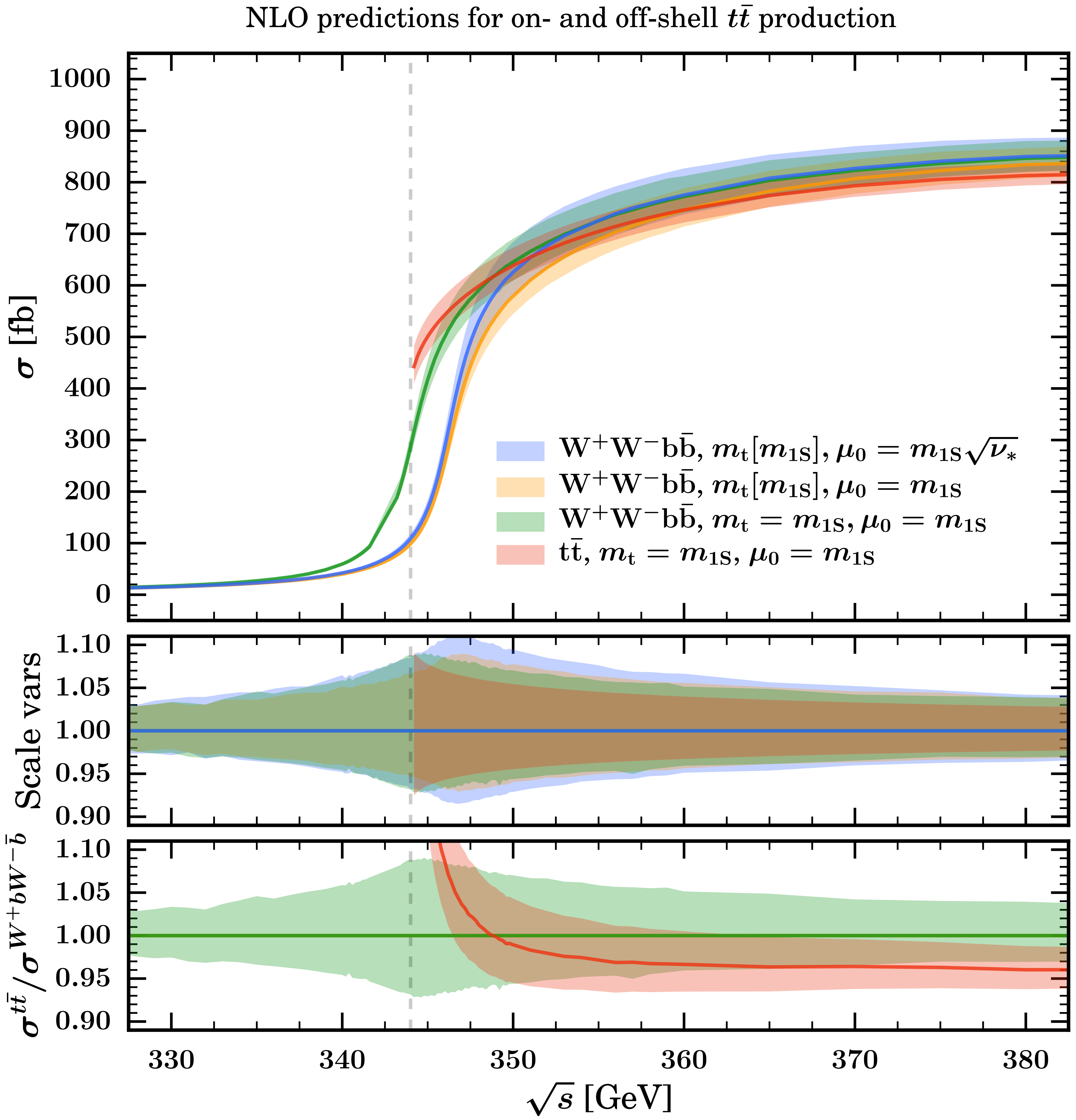

Top threshold: validation & matching

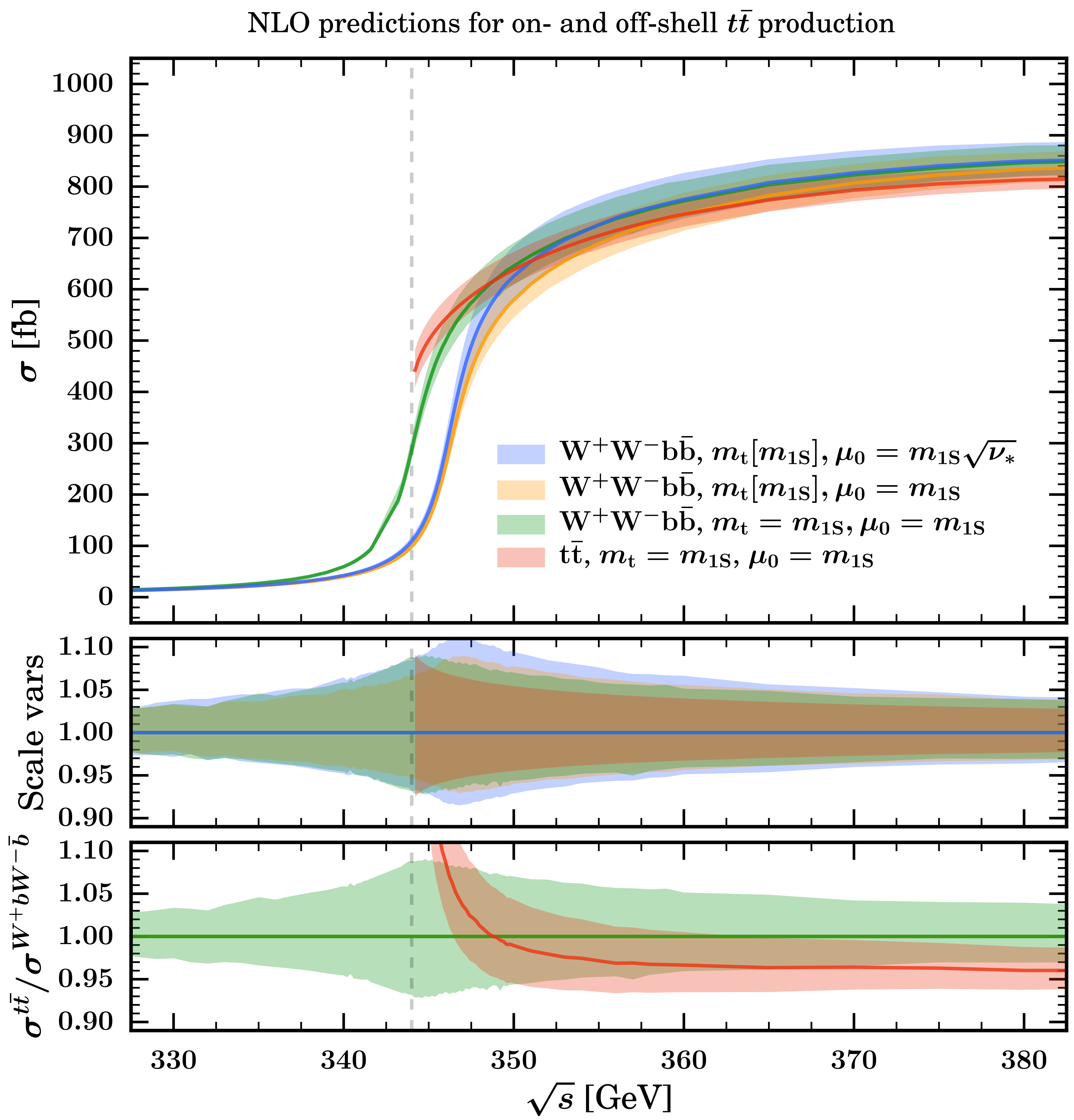

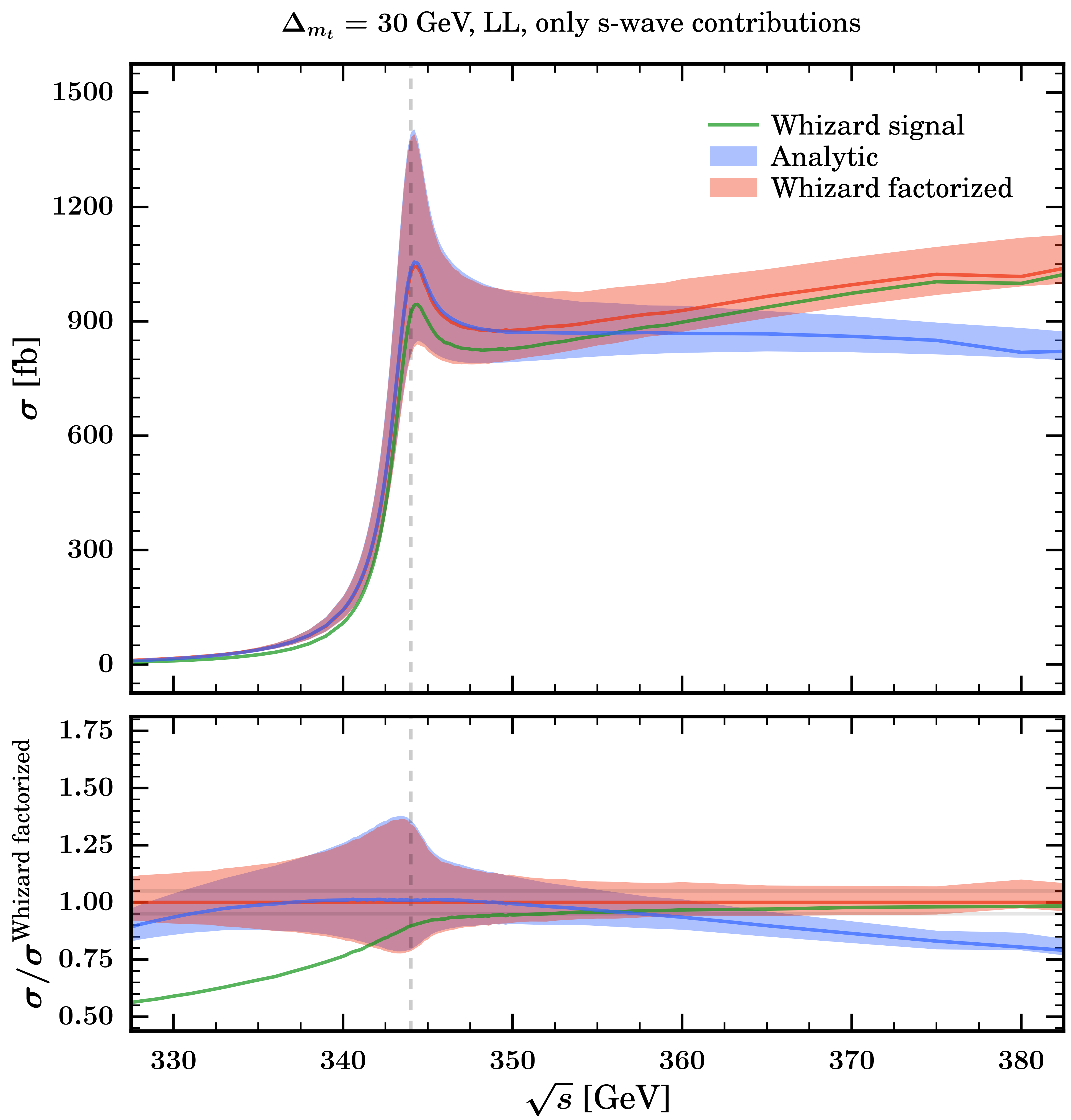

Top threshold: validation & matching

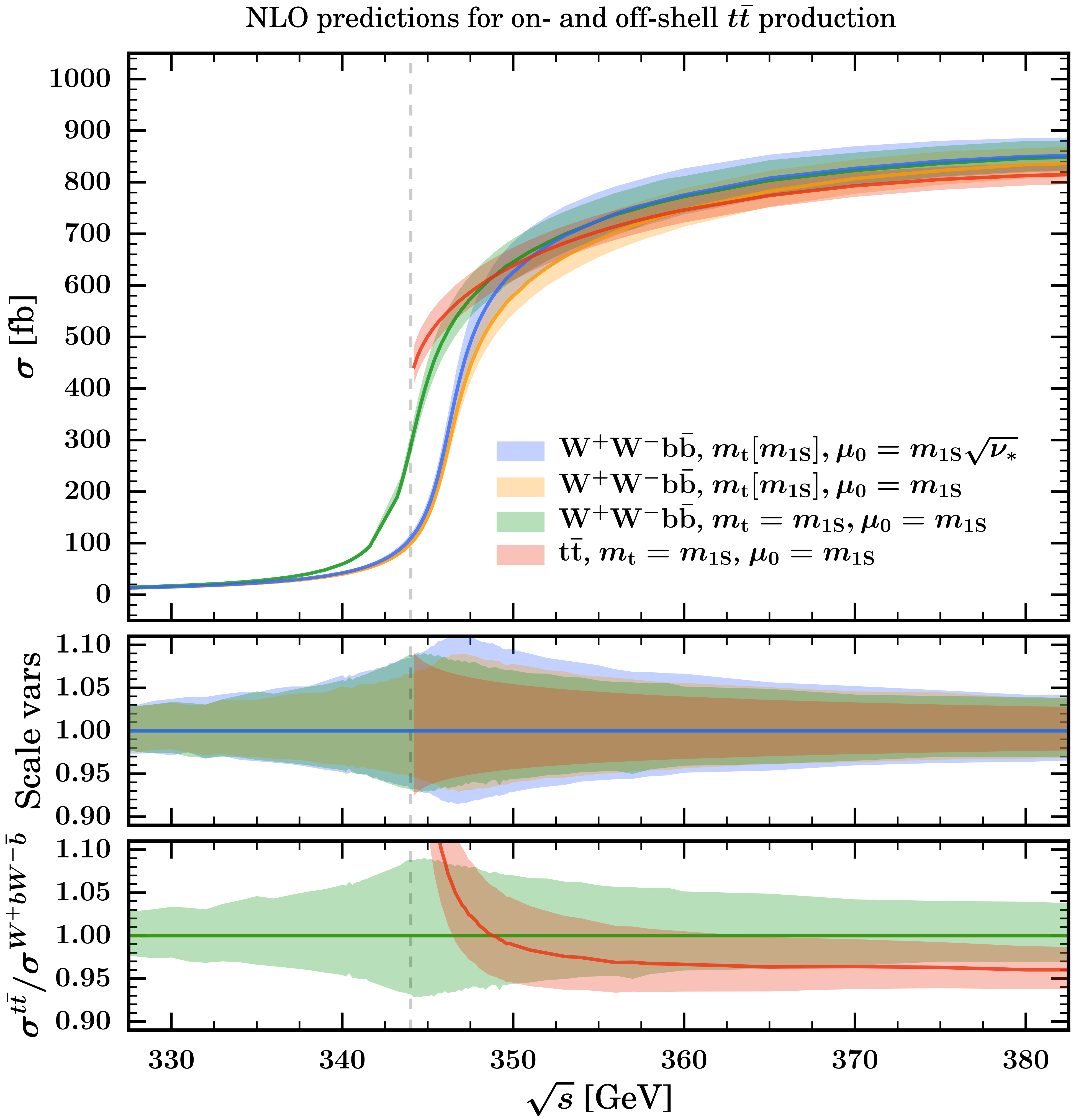

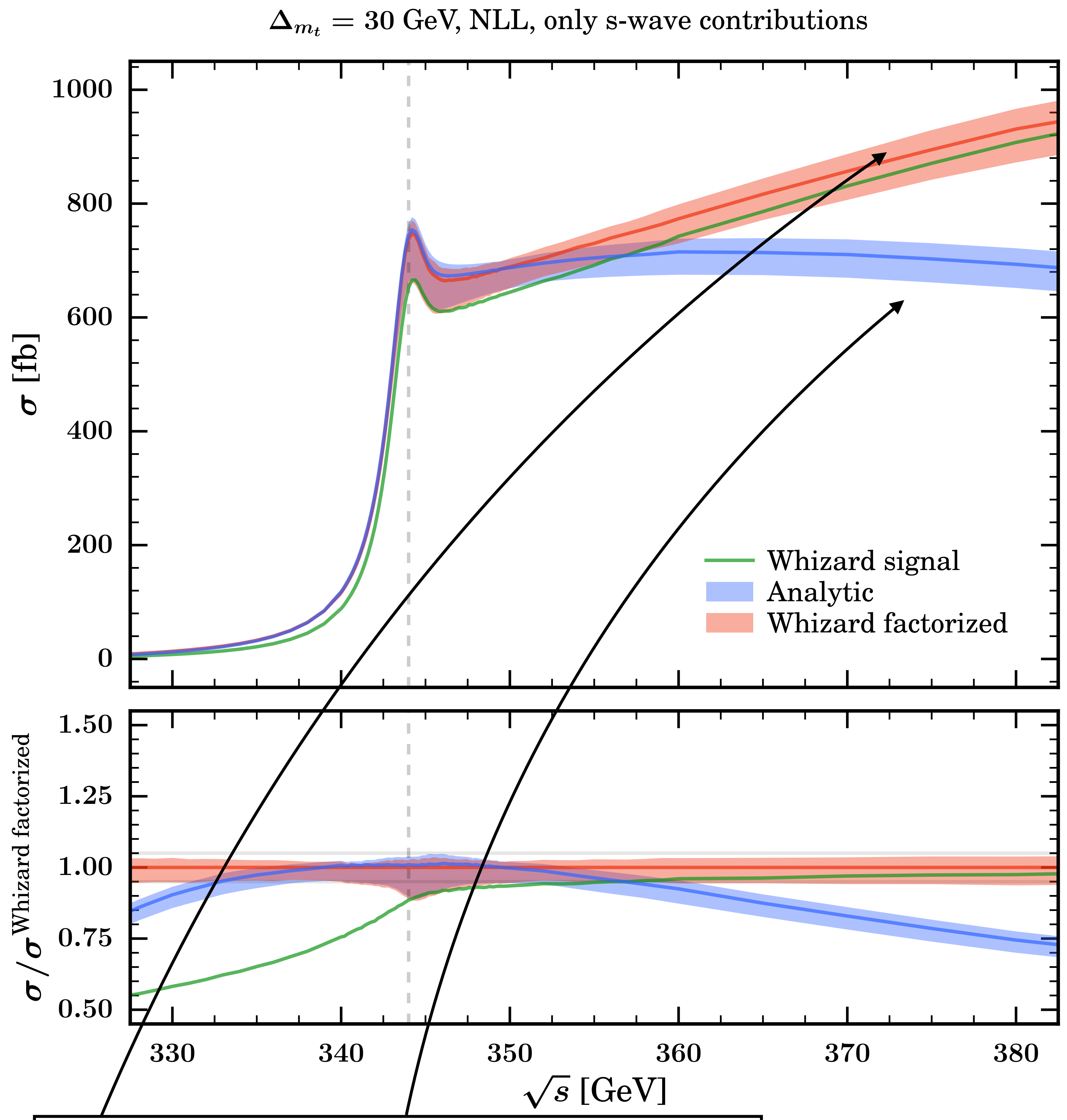

NRQCD result invalid away from threshold

Electron PDFs: some details

P. Bredt/T. Striegl, 2025

```
* Full NLL electron PDFs:
* Q = 1.0000E+00 GeV, NLL, alpha fixed:

  ePDF (x =    1.000000000000000E-44, S/NS/ELE/POS/GAM) =      1.131183E+42     1.290173E+06     5.655916E+41     5.655916E+41     5.078808E+43
  ePDF (x =    1.000000000000000E-44, e- - [S + NS]/2) = 0.00000000
  ePDF (x =    1.000000000000000E-44, e+ - [S - NS]/2) = 0.00000000
  ePDF (x =    1.000000000000000E-43, S/NS/ELE/POS/GAM) =      1.106221E+41     7.885546E+04     5.531106E+40     5.531106E+40     4.968602E+42
  ePDF (x =    1.000000000000000E-43, e- - [S + NS]/2) = 0.00000000
  ePDF (x =    1.000000000000000E-43, e+ - [S - NS]/2) = 0.00000000
  ePDF (x =    1.000000000000000E-42, S/NS/ELE/POS/GAM) =      1.081259E+40    -8.861889E+03     5.406296E+39     5.406296E+39     4.858498E+41
  ePDF (x =    1.000000000000000E-42, e- - [S + NS]/2) = 0.00000000
  ePDF (x =    1.000000000000000E-42, e+ - [S - NS]/2) = 0.00000000
  ePDF (x =    1.000000000000000E-41, S/NS/ELE/POS/GAM) =      1.056297E+39     1.200275E+03     5.281486E+38     5.281486E+38     4.748496E+40
  ePDF (x =    1.000000000000000E-41, e- - [S + NS]/2) = 0.00000000
  ePDF (x =    1.000000000000000E-41, e+ - [S - NS]/2) = 0.00000000
  ePDF (x =    1.000000000000000E-40, S/NS/ELE/POS/GAM) =      1.031335E+38     2.082260E+02     5.156676E+37     5.156676E+37     4.638596E+39
  ePDF (x =    1.000000000000000E-40, e- - [S + NS]/2) = 0.00000000
  ePDF (x =    1.000000000000000E-40, e+ - [S - NS]/2) = 0.00000000
  ePDF (x =    1.000000000000000E-39, S/NS/ELE/POS/GAM) =      1.006373E+37     1.717684E+01     5.031866E+36     5.031866E+36     4.528797E+38
  ePDF (x =    1.000000000000000E-39, e- - [S + NS]/2) = 0.00000000
  ePDF (x =    1.000000000000000E-39, e+ - [S - NS]/2) = 0.00000000
  ePDF (x =    1.000000000000000E-38, S/NS/ELE/POS/GAM) =      9.814112E+35     7.520304E-01     4.907056E+35     4.907056E+35     4.419100E+37
  ePDF (x =    1.000000000000000E-38, e- - [S + NS]/2) = 0.00000000
  ePDF (x =    1.000000000000000E-38, e+ - [S - NS]/2) = 0.00000000
  ePDF (x =    1.000000000000000E-37, S/NS/ELE/POS/GAM) =      9.564492E+34    -4.189107E-01     4.782246E+34     4.782246E+34     4.309505E+36
  ePDF (x =    1.000000000000000E-37, e- - [S + NS]/2) = 0.00000000
  ePDF (x =    1.000000000000000E-37, e+ - [S - NS]/2) = 0.00000000
  ePDF (x =    1.000000000000000E-36, S/NS/ELE/POS/GAM) =      9.314872E+33    -2.591904E-01     4.657436E+33     4.657436E+33     4.200012E+35
  ePDF (x =    1.000000000000000E-36, e- - [S + NS]/2) = 0.50000000
  ePDF (x =    1.000000000000000E-36, e+ - [S - NS]/2) = 0.50000000
  ePDF (x =    1.000000000000000E-35, S/NS/ELE/POS/GAM) =      9.065252E+32    -2.549587E-01     4.532626E+32     4.532626E+32     4.090620E+34
  ePDF (x =    1.000000000000000E-35, e- - [S + NS]/2) = 0.00000000
  ePDF (x =    1.000000000000000E-35, e+ - [S - NS]/2) = 0.00000000
  ePDF (x =    1.000000000000000E-34, S/NS/ELE/POS/GAM) =      8.815632E+31    -2.321432E-01     4.407816E+31     4.407816E+31     3.981331E+33
  ePDF (x =    1.000000000000000E-34, e- - [S + NS]/2) = 0.01562500
  ePDF (x =    1.000000000000000E-34, e+ - [S - NS]/2) = 0.00000000
  ePDF (x =    1.000000000000000E-33, S/NS/ELE/POS/GAM) =      8.566012E+30    -2.133651E-01     4.283006E+30     4.283006E+30     3.872143E+32
```

$$
\begin{aligned}
\hat{J}^{\rm NLL}_{\rm S,2,an} = \frac{1}{108 b_0 z\left(z^2-1\right)} \times \Big(& 608 b_0 N_F^2 z^5 + 192 b_0 L_0 N_F^2 z^5 - 432 b_0 N_F z^5 + 96 b_0 N_F \pi^2 z^5 - 960 b_0^2 N_F \pi z^5 + \\
& 1152 b_1 N_F \pi z^5 + 1152 b_0^2 L_0 N_F \pi z^5 + 144 b_0 N_F^2 z^4 + 144 b_0 L_0 N_F^2 z^4 - 486 b_0 z^4 - 405 b_0 L_0 z^4 - 3852 b_0 N_F z^4 + \\
& 1656 b_0 L_0 N_F z^4 + 360 b_0^2 \pi^3 z^4 + 432 b_0^3 \pi^2 z^4 + 324 b_0 \pi^2 z^4 - 432 b_0 b_1 \pi^2 z^4 - 432 b_0^3 L_0 \pi^2 z^4 + 216 b_0 L_0 \pi^2 z^4 + \\
& 120 b_0 N_F \pi^2 z^4 + 432 b_1 \pi z^4 + 432 b_0^2 L_0 \pi z^4 - 3984 b_0^2 N_F \pi z^4 + 864 b_1 N_F \pi z^4 + 864 b_0^2 L_0 N_F \pi z^4 - 1328 b_0 N_F^2 z^3 - \\
& 336 b_0 L_0 N_F^2 z^3 + 1350 b_0 z^3 - 1539 b_0 L_0 z^3 + 4092 b_0 N_F z^3 - 1656 b_0 L_0 N_F z^3 - 360 b_0^2 \pi^3 z^3 - 432 b_0^3 \pi^2 z^3 - \\
& 504 b_0 \pi^2 z^3 + 432 b_0 b_1 \pi^2 z^3 + 432 b_0^3 L_0 \pi^2 z^3 - 216 b_0 L_0 \pi^2 z^3 - 216 b_0 N_F \pi^2 z^3 - 1080 b_0^2 \pi z^3 + 1296 b_1 \pi z^3 + \\
& 1296 b_0^2 L_0 \pi z^3 + 3504 b_0^2 N_F \pi z^3 - 2016 b_1 N_F \pi z^3 - 2016 b_0^2 L_0 N_F \pi z^3 - 176 b_0 N_F^2 z^2 - 336 b_0 L_0 N_F^2 z^2 + \\
& 486 b_0 z^2 + 405 b_0 L_0 z^2 + 5004 b_0 N_F z^2 - 1656 b_0 L_0 N_F z^2 - 648 b_0^2 \pi^3 z^2 - 432 b_0^3 \pi^2 z^2 + 108 b_0 \pi^2 z^2 + \\
& 432 b_0 b_1 \pi^2 z^2 + 432 b_0^3 L_0 \pi^2 z^2 - 216 b_0 L_0 \pi^2 z^2 - 216 b_0 N_F \pi^2 z^2 - 432 b_1 \pi z^2 - 432 b_0^2 L_0 \pi z^2 + 6672 b_0^2 N_F \pi z^2 - \\
& 2016 b_1 N_F \pi z^2 - 2016 b_0^2 L_0 N_F \pi z^2 + 720 b_0 N_F^2 z + 144 b_0 L_0 N_F^2 z - 1350 b_0 z + 1539 b_0 L_0 z - 3660 b_0 N_F z + \\
& 1656 b_0 L_0 N_F z + 864 b_0 (z-1) \Big((\log(z+1) - \log(1-z)) z^2 + \log(1-z) - \log(z+1) - 5\log(2) \Big) \mathrm{Li}_2\left(\frac{1-z}{2}\right) z - \\
& 4z \Big(\log(z) z^3 + \log(1-z) z - \log(1-z) + \log(z) + (z(z+6)-5)\log(z+1) \Big) \Big) \mathrm{Li}_2(-z) + 8z \Big((z-1) \Big(- \\
& 4z^2 + 2z - 6\log(1-z) + 6 b_0 \pi + 3 \Big) - 2\left(z^3 + 5z - 4\right) \log(z+1) \Big) \mathrm{Li}_2\left(\frac{1}{z+1}\right) + 4\left(z^2-1\right)(z(5z-8) + \\
& 10(z-1) z \log(z+1) - 6) \mathrm{Li}_2\left(\frac{z}{z+1}\right) + 8z\left(z^2-1\right)(3z + 4N_F(z+1) + 8) \mathrm{Li}_3(1-z) - 8z(6N_F + z) \Big(z^2 - \\
& 1 \Big) \mathrm{Li}_3\left(\frac{z-1}{z}\right) + 8z(z+1)(z(7z-16)+7) \mathrm{Li}_3(-z) + 4z(8zN_F + 20N_F + 3z + 9)\left(z^2-1\right) \mathrm{Li}_3(z) + 16z(z + \\
& 1)(z(3z-4)+3) \mathrm{Li}_3\left(\frac{1}{z+1}\right) - z(16 N_F (z-1)(z+1)(2z+5) + z(z(21z+67)+99) - 107)\zeta(3) \Big) \Big) - \\
& 216 b_0 (z-1)(z+1)(z(9z+7)+3) \log^2(2) + 96 b_0 N_F \pi^2 - 2688 b_0^2 N_F \pi + 1152 b_1 N_F \pi + 1152 b_0^2 L_0 N_F \pi \Big)
\end{aligned}
$$

Electron PDFs: some details

P. Bredt/T. Striegl, 2025

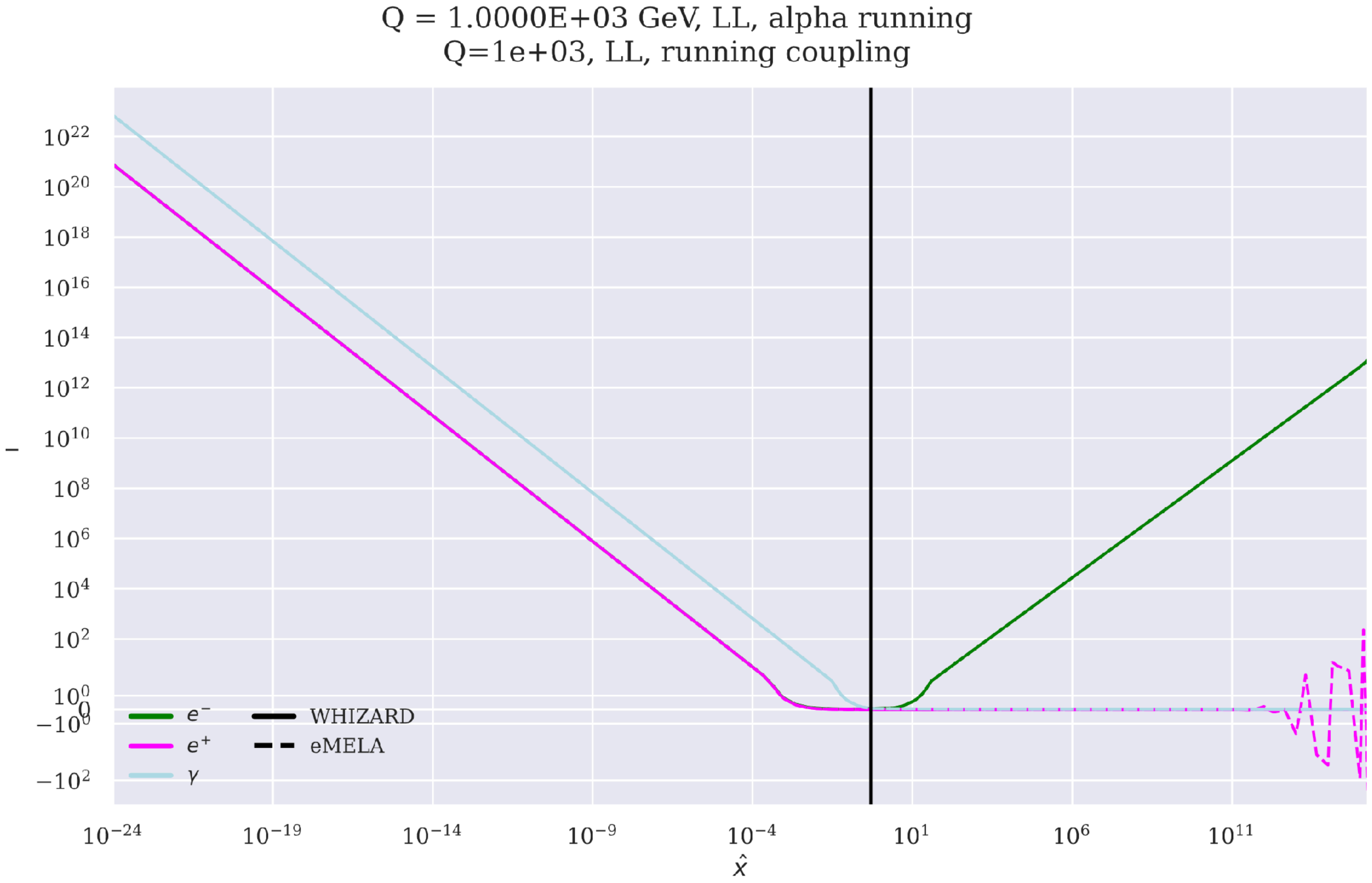

$$
\begin{aligned}
\hat{J}^{\rm NLL}_{\rm S,2,an} = {} & \frac{1}{108 b_0 z\bigl(z^2-1\bigr)} \times \Bigl(608 b_0 N_F^2 z^5 + 192 b_0 L_0 N_F^2 z^5 - 432 b_0 N_F z^5 + 96 b_0 N_F \pi^2 z^5 - 960 b_0^2 N_F \pi z^5 + \\
& 1152 b_1 N_F \pi z^5 + 1152 b_0^2 L_0 N_F \pi z^5 + 144 b_0 N_F^2 z^4 + 144 b_0 L_0 N_F^2 z^4 - 486 b_0 z^4 - 405 b_0 L_0 z^4 - 3852 b_0 N_F z^4 + \\
& 1656 b_0 L_0 N_F z^4 + 360 b_0^2 \pi^3 z^4 + 432 b_0^3 \pi^2 z^4 + 324 b_0 \pi^2 z^4 - 432 b_0 b_1 \pi^2 z^4 - 432 b_0^3 L_0 \pi^2 z^4 + 216 b_0 L_0 \pi^2 z^4 + \\
& 120 b_0 N_F \pi^2 z^4 + 432 b_1 \pi z^4 + 432 b_0^2 L_0 \pi z^4 - 3984 b_0^2 N_F \pi z^4 + 864 b_1 N_F \pi z^4 + 864 b_0^2 L_0 N_F \pi z^4 - 1328 b_0 N_F^2 z^3 - \\
& 336 b_0 L_0 N_F^2 z^3 + 1350 b_0 z^3 - 1539 b_0 L_0 z^3 + 4092 b_0 N_F z^3 - 1656 b_0 L_0 N_F z^3 - 360 b_0^2 \pi^3 z^3 - 432 b_0^3 \pi^2 z^3 - \\
& 504 b_0 \pi^2 z^3 + 432 b_0 b_1 \pi^2 z^3 + 432 b_0^3 L_0 \pi^2 z^3 - 216 b_0 L_0 \pi^2 z^3 - 216 b_0 N_F \pi^2 z^3 - 1080 b_0^2 \pi z^3 + 1296 b_1 \pi z^3 + \\
& 1296 b_0^2 L_0 \pi z^3 + 3504 b_0^2 N_F \pi z^3 - 2016 b_1 N_F \pi z^3 - 2016 b_0^2 L_0 N_F \pi z^3 - 176 b_0 N_F^2 z^2 - 336 b_0 L_0 N_F^2 z^2 + \\
& 486 b_0 z^2 + 405 b_0 L_0 z^2 + 5004 b_0 N_F z^2 - 1656 b_0 L_0 N_F z^2 - 648 b_0^2 \pi^3 z^2 - 432 b_0^3 \pi^2 z^2 + 108 b_0 \pi^2 z^2 + \\
& 432 b_0 b_1 \pi^2 z^2 + 432 b_0^3 L_0 \pi^2 z^2 - 216 b_0 L_0 \pi^2 z^2 - 216 b_0 N_F \pi^2 z^2 - 432 b_1 \pi z^2 - 432 b_0^2 L_0 \pi z^2 + 6672 b_0^2 N_F \pi z^2 - \\
& 2016 b_1 N_F \pi z^2 - 2016 b_0^2 L_0 N_F \pi z^2 + 720 b_0 N_F^2 z + 144 b_0 L_0 N_F^2 z - 1350 b_0 z + 1539 b_0 L_0 z - 3660 b_0 N_F z + \\
& 1656 b_0 L_0 N_F z + 864 b_0 (z-1)\Bigl((\log(z+1) - \log(1-z)) z^2 + \log(1-z) - \log(z+1) - 5\log(2)\Bigr)\mathrm{Li}_2\Bigl(\frac{1-z}{2}\Bigr) z - \\
& 4z\Bigl(\log(z) z^3 + \log(1-z) z - \log(1-z) + \log(z) + (z(z+6)-5)\log(z+1)\Bigr)\Bigr)\mathrm{Li}_2(-z) + 8z\Bigl((z-1)\Bigl(- \\
& 4z^2 + 2z - 6\log(1-z) + 6 b_0 \pi + 3\Bigr) - 2\Bigl(z^3 + 5z - 4\Bigr)\log(z+1)\Bigr)\mathrm{Li}_2\Bigl(\frac{1}{z+1}\Bigr) + 4\Bigl(z^2-1\Bigr)(z(5z-8) + \\
& 10(z-1) z \log(z+1) - 6)\mathrm{Li}_2\Bigl(\frac{z}{z+1}\Bigr) + 8z\Bigl(z^2-1\Bigr)(3z + 4N_F(z+1) + 8)\mathrm{Li}_3(1-z) - 8z(6N_F + z)\Bigl(z^2 - \\
& 1\Bigr)\mathrm{Li}_3\Bigl(\frac{z-1}{z}\Bigr) + 8z(z+1)(z(7z-16)+7)\mathrm{Li}_3(-z) + 4z(8zN_F + 20N_F + 3z + 9)\Bigl(z^2-1\Bigr)\mathrm{Li}_3(z) + 16z(z + \\
& 1)(z(3z-4)+3)\mathrm{Li}_3\Bigl(\frac{1}{z+1}\Bigr) - z(16N_F(z-1)(z+1)(2z+5) + z(z(21z+67)+99) - 107)\zeta(3)\Bigr)\Bigr) - \\
& 216 b_0 (z-1)(z+1)(z(9z+7)+3)\log^2(2) + 96 b_0 N_F \pi^2 - 2688 b_0^2 N_F \pi + 1152 b_1 N_F \pi + 1152 b_0^2 L_0 N_F \pi\Bigr)
\end{aligned}
$$

Electron PDFs: some details

P. Bredt/T. Striegl, 2025

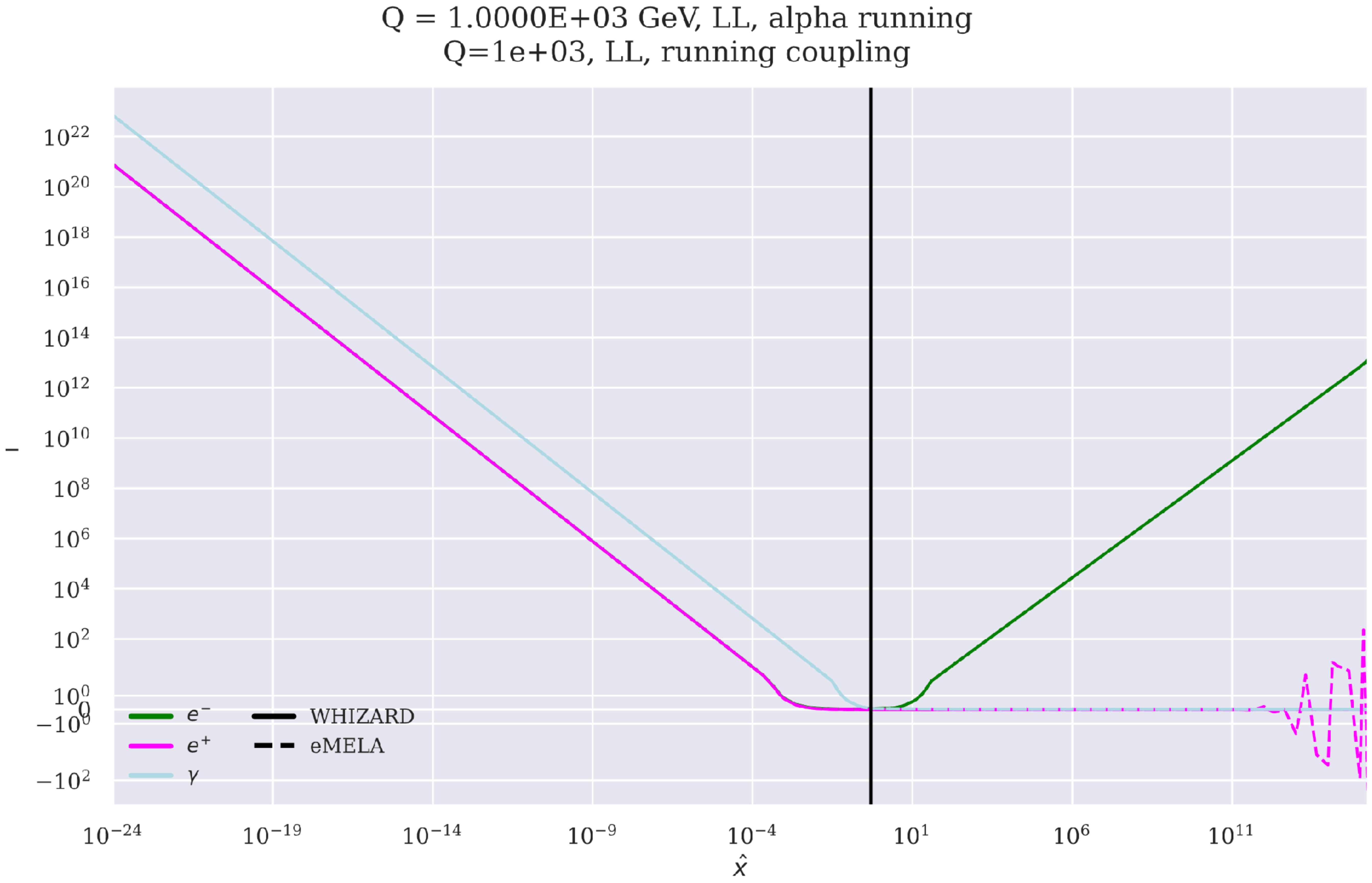

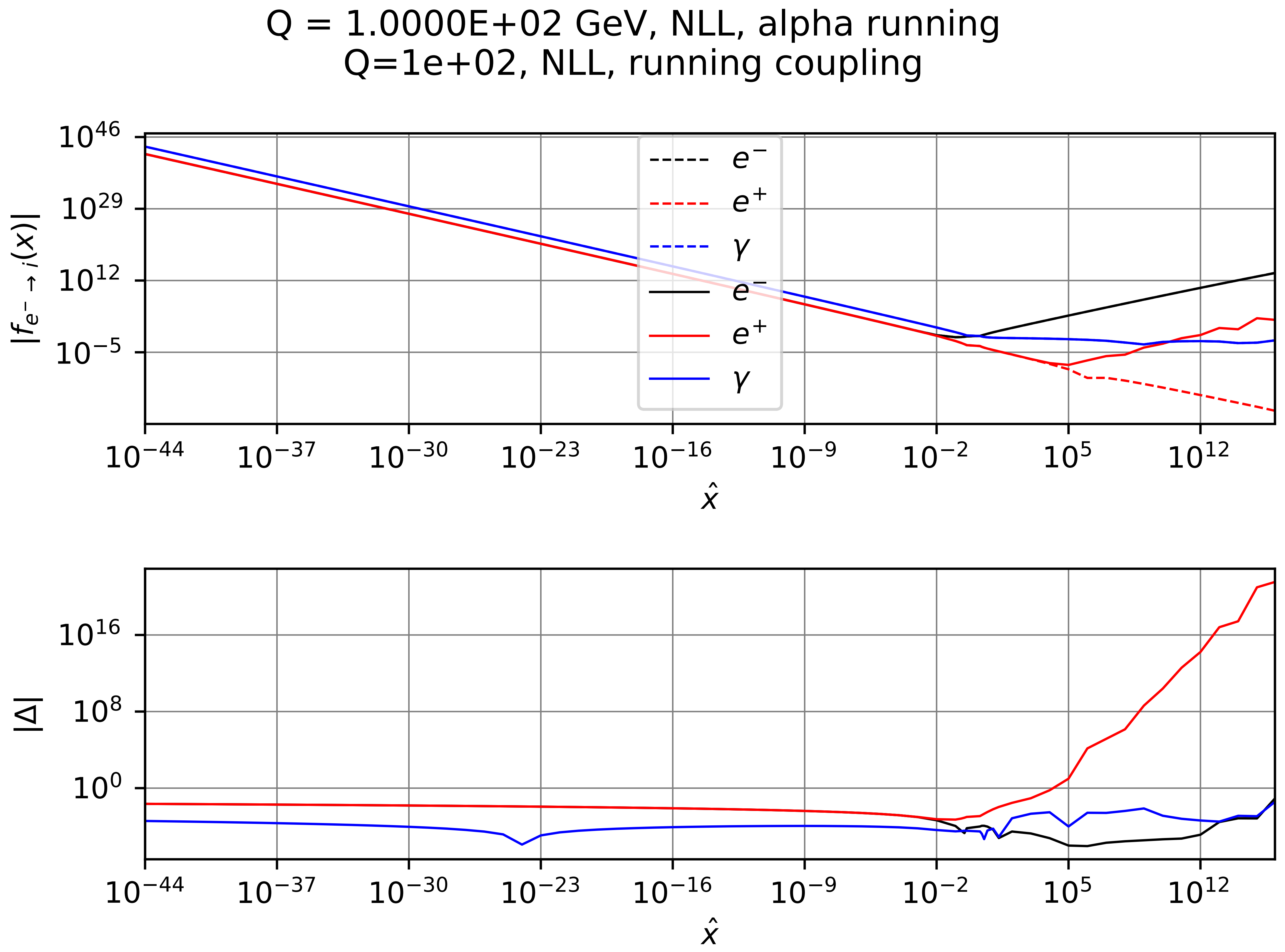

$\hat{x} = x$ for $x < 0.5$, $\hat{x} = 1/(1-x)$ for $x > 0.5$

[Maciej Skrzypek; Brussels Topical Workshop]

[Francesco Ucci, this workshop]

Luminometry

Bhabha cross sect. depends on detector acceptance angles

$$\sigma_{Bh} \simeq 4\pi\alpha^2\left(\frac{1}{t_{\min}} - \frac{1}{t_{\max}}\right) = 4\pi\alpha^2\left(\frac{t_{\max} - t_{\min}}{\bar{t}^2}\right), \quad \bar{t} = \sqrt{t_{\min} t_{\max}}$$

Machine	$\theta_{\min} \div \theta_{\max}$ [mrad]	$\sqrt{s}$ [GeV]	$\bar{t}/s \simeq \bar{\theta}^2/4$	$\sqrt{\bar{t}}$ [GeV]
LEP	28÷50	M_Z	3.5×10^{-4}	1.70
FCCee	64÷86	M_Z	13.7×10^{-4}	3.37
FCCee	64÷86	240	13.7×10^{-4}	8.9
FCCee	64÷86	350	13.7×10^{-4}	13.0
ILC	31÷77	500	6.0×10^{-4}	12.2
ILC	31÷77	1000	6.0×10^{-4}	24.4
CLIC	39÷134	3000	13.0×10^{-4}	108

Current BHLUMI precision forecast for FCCee

Type of correction / Error	M_Z (2019) [1]	240 GeV	350 GeV [2]
(a) Photonic $\mathcal{O}(L_e\alpha^2)$	0.027%	0.032%	0.033%
(b) Photonic $\mathcal{O}(L_e^3\alpha^3)$	0.015%	0.026%	0.028%
(c) Vacuum polariz.	0.009%	0.020%	0.022%
(d) Light pairs	0.010%	0.015%	0.015%
(e) Z and s-channel γ exchange	0.09%	0.25% (0.034%)	0.5% (0.07%)
(f) Up-down interference	0.009%	0.010%	0.010%
(g) Technical Precision	[0.027%]		
Total	10×10^{-4}	25×10^{-4} (6×10^{-4})	50×10^{-4} (8.7×10^{-4})

Forecast

Type of correction / Error	FCCee_{M_Z} [1]	FCCee_{240}	FCCee_{350}
(a) Photonic $\mathcal{O}(L_e^2\alpha^3)$	0.10×10^{-4}	0.10×10^{-4}	0.13×10^{-4}
(b) Photonic $\mathcal{O}(L_e^4\alpha^4)$	0.06×10^{-4}	$0.26 \times 10^{-4(a)}$	$0.27 \times 10^{-4(a)}$
(c) Vacuum polariz.	0.6×10^{-4}	1.0×10^{-4}	1.1×10^{-4}
(d) Light pairs	0.5×10^{-4}	0.4×10^{-4}	0.4×10^{-4}
(e) Z and s-channel γ exch.	0.1×10^{-4}	$1.0 \times 10^{-4(*)}$	$1.0 \times 10^{-4(*)}$
(f) Up-down interference	0.1×10^{-4}	0.09×10^{-4}	0.1×10^{-4}
Total	1.0×10^{-4}	1.5×10^{-4}	1.6×10^{-4}

Luminometry

Bhabha cross sect. depends on detector acceptance angles

$$\sigma_{Bh} \simeq 4\pi\alpha^2 \left(\frac{1}{t_{\min}} - \frac{1}{t_{\max}} \right) = 4\pi\alpha^2 \left(\frac{t_{\max} - t_{\min}}{\bar{t}^2} \right), \quad \bar{t} = \sqrt{t_{\min} t_{\max}}$$

Machine	$\theta_{\min} \div \theta_{\max}$ [mrad]	$\sqrt{s}$ [GeV]	$\bar{t}/s \simeq \bar{\theta}^2/4$	$\sqrt{\bar{t}}$ [GeV]
LEP	28÷50	M_Z	3.5×10^{-4}	1.70
FCCee	64÷86	M_Z	13.7×10^{-4}	3.37
FCCee	64÷86	240	13.7×10^{-4}	8.9
FCCee	64÷86	350	13.7×10^{-4}	13.0
ILC	31÷77	500	6.0×10^{-4}	12.2
ILC	31÷77	1000	6.0×10^{-4}	24.4
CLIC	39÷134	3000	13.0×10^{-4}	108

Current BHLUMI precision forecast for FCCee			
Type of correction / Error	M_Z (2019) [1]	240 GeV	350 GeV [2]
(a) Photonic $\mathcal{O}(L_e\alpha^2)$	0.027%	0.032%	0.033%
(b) Photonic $\mathcal{O}(L_e^3\alpha^3)$	0.015%	0.026%	0.028%
(c) Vacuum polariz.	0.009%	0.020%	0.022%
(d) Light pairs	0.010%	0.015%	0.015%
(e) Z and s-channel γ exchange	0.09%	0.25% (0.034%)	0.5% (0.07%)
(f) Up-down interference	0.009%	0.010%	0.010%
(g) Technical Precision	[0.027%]		
Total	10×10^{-4}	25×10^{-4} (6×10^{-4})	50×10^{-4} (8.7×10^{-4})

Forecast			
Type of correction / Error	FCCee$_{M_Z}$[1]	FCCee$_{240}$	FCCee$_{350}$
(a) Photonic $\mathcal{O}(L_e^2\alpha^3)$	0.10×10^{-4}	0.10×10^{-4}	0.13×10^{-4}
(b) Photonic $\mathcal{O}(L_e^4\alpha^4)$	0.06×10^{-4}	$0.26 \times 10^{-4(a)}$	$0.27 \times 10^{-4(a)}$
(c) Vacuum polariz.	0.6×10^{-4}	1.0×10^{-4}	1.1×10^{-4}
(d) Light pairs	0.5×10^{-4}	0.4×10^{-4}	0.4×10^{-4}
(e) Z and s-channel γ exch.	0.1×10^{-4}	$1.0 \times 10^{-4(*)}$	$1.0 \times 10^{-4(*)}$
(f) Up-down interference	0.1×10^{-4}	0.09×10^{-4}	0.1×10^{-4}
Total	1.0×10^{-4}	1.5×10^{-4}	1.6×10^{-4}

- Technical precision needs 2nd code: `BHLumi` vs. `BabaYaga` (NNLO in hard process possible)
- Major ingredients: hadronic vacuum polarization, EW corrections, light fermion pairs
- Inclusion of 4f, 4f + γ, 5f, 6f backgrounds necessary at matrix element level

Spin correlations in MC

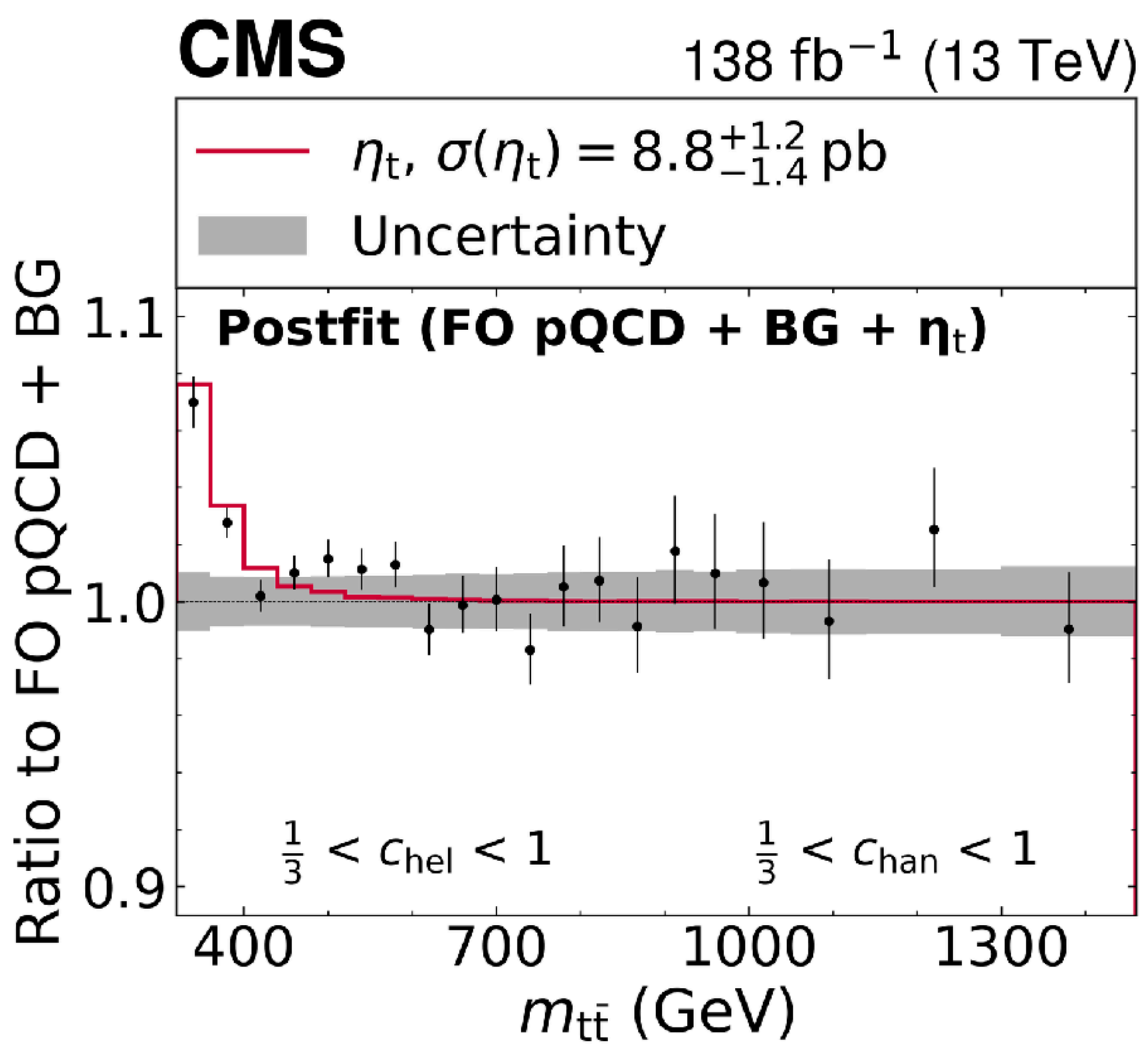

Spin correlations have proven very beneficial for the LHC top analyses CMS, 2503.22382

Top spin aligned through production and reconstructible from final state leptons

$$\rho^{\rm f}_{(\lambda'_F,\lambda'_{\bar F}),(\lambda_F,\lambda_{\bar F})} = \frac{1}{\mathcal{N}} \sum_{\lambda_l,\lambda_{\bar l}} \rho^{\rm in}_{(\lambda_l,\lambda_{\bar l})}(\mathcal{P},\overline{\mathcal{P}}) \mathcal{M}^{\lambda_l,\lambda_{\bar l}}_{\lambda'_F,\lambda'_{\bar F}}(\sqrt{s},\Theta) \left[\mathcal{M}^{\lambda_l,\lambda_{\bar l}}_{\lambda_F,\lambda_{\bar F}}(\sqrt{s},\Theta)\right]^*$$

Observables described via spin-density matrices, directly constructed in MC event generators

Durupt/Maltoni/Mattelaer, 2510.17730. Ohl/Wüst, 26xx.xxxxx

Spin correlations in MC

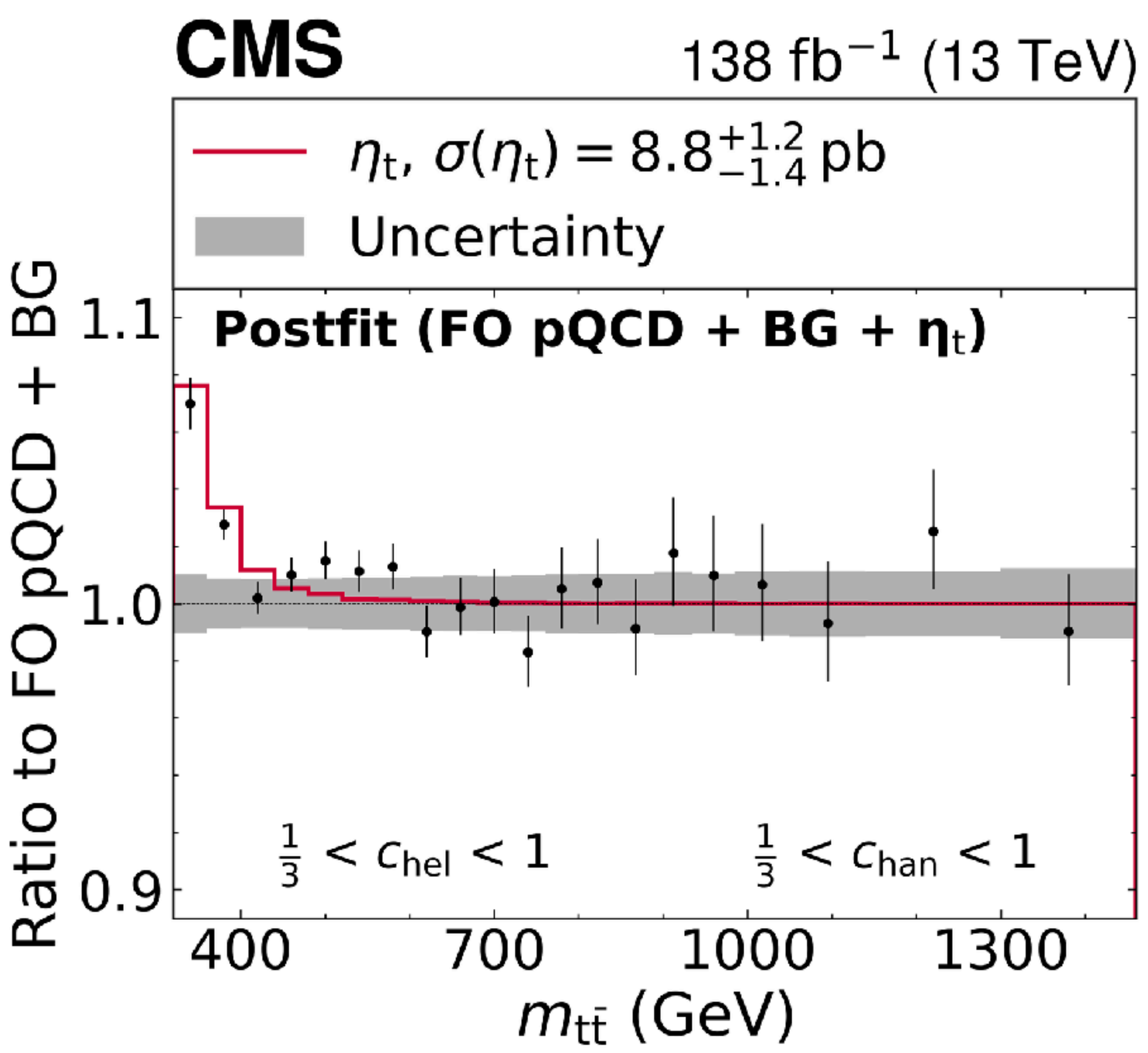

Spin correlations have proven very beneficial for the LHC top analyses CMS, 2503.22382

Top spin aligned through production and reconstructible from final state leptons

$$\rho^{\rm f}_{(\lambda'_F,\lambda'_{\bar F}),(\lambda_F,\lambda_{\bar F})} = \frac{1}{\mathcal{N}} \sum_{\lambda_l,\lambda_{\bar l}} \rho^{\rm in}_{(\lambda_l,\lambda_{\bar l})}(\mathcal{P},\overline{\mathcal{P}}) \mathcal{M}^{\lambda_l,\lambda_{\bar l}}_{\lambda'_F,\lambda'_{\bar F}}(\sqrt{s},\Theta) \left[\mathcal{M}^{\lambda_l,\lambda_{\bar l}}_{\lambda_F,\lambda_{\bar F}}(\sqrt{s},\Theta)\right]^*$$

Observables described via spin-density matrices, directly constructed in MC event generators

Durupt/Maltoni/Mattelaer, 2510.17730. Ohl/Wüst, 26xx.xxxxx

Spin-density matrix for di-top (2 qubit) for entanglement variables:

$$\rho(\alpha,\beta,\gamma) = \frac{1}{4}\left(\mathbf{1} + \alpha_i\sigma_i \otimes \mathbf{1} + \beta_j \mathbf{1} \otimes \sigma_j + \gamma_{ij}\sigma_i \otimes \sigma_j\right)$$

Purity: $\frac{1}{4} \leq \quad \Gamma[\rho] := \mathrm{Tr}\left[\rho^2\right] \quad \leq 1$

Concurrence: $\max(0, \lambda_1 - \lambda_2 - \lambda_3 - \lambda_4)$

for matrix $\sqrt{\sqrt{\rho}(\sigma_y \otimes \sigma_y)\rho^*(\sigma_y \otimes \sigma_y)\sqrt{\rho}}$

density matrix of spin-flipped state

cf. e.g. Altakach/Lambda/Maltoni/Sakurai, 2601.09558

Spin correlations in MC

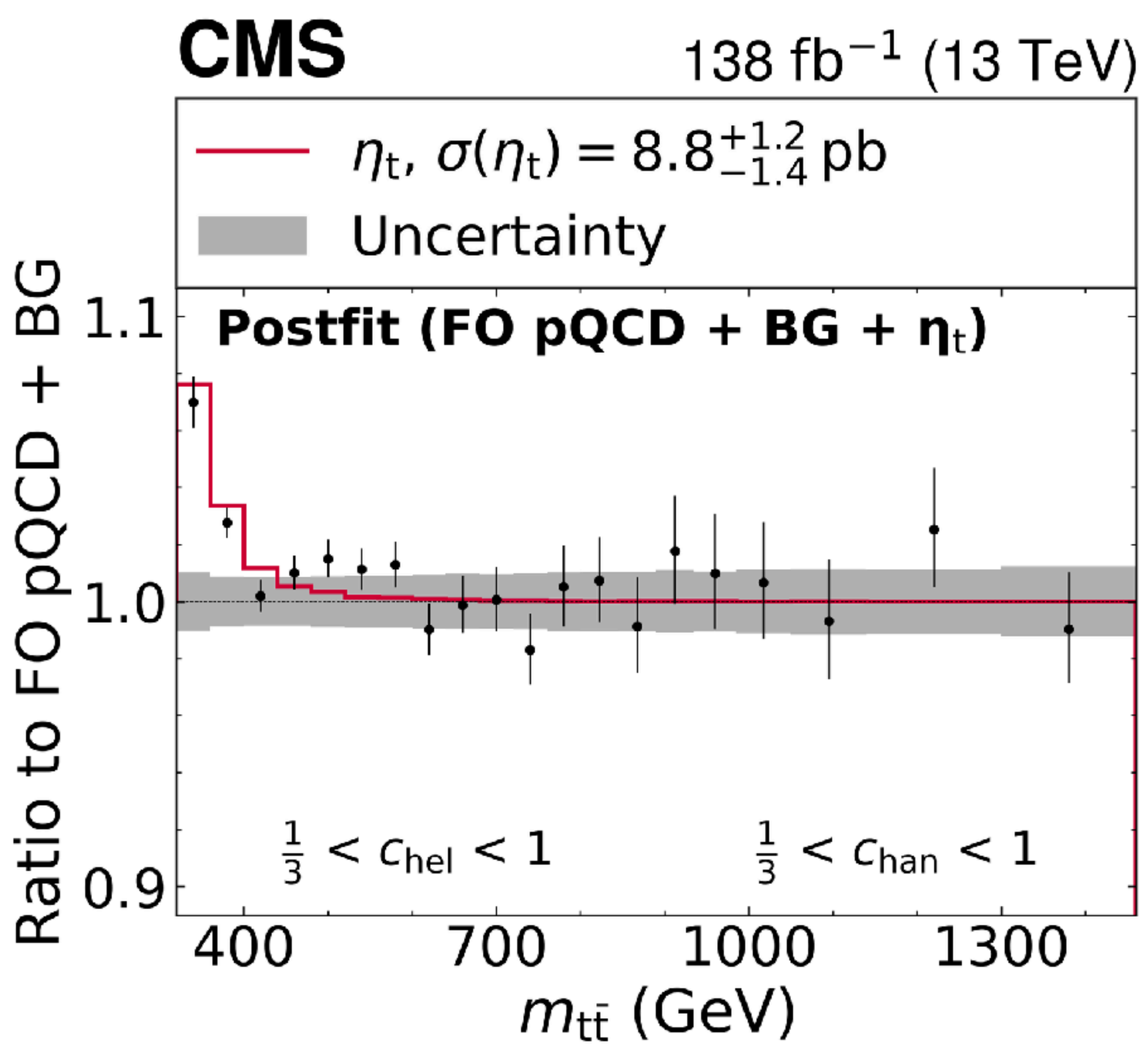

Spin correlations have proven very beneficial for the LHC top analyses CMS, 2503.22382

Top spin aligned through production and reconstructible from final state leptons

$$\rho^{f}_{(\lambda'_F,\lambda'_{\bar{F}}),(\lambda_F,\lambda_{\bar{F}})} = \frac{1}{\mathcal{N}} \sum_{\lambda_l,\lambda_{\bar{l}}} \rho^{in}_{(\lambda_l,\lambda_{\bar{l}})}(\mathcal{P},\overline{\mathcal{P}}) \mathcal{M}^{\lambda_l,\lambda_{\bar{l}}}_{\lambda'_F,\lambda'_{\bar{F}}}(\sqrt{s},\Theta) \left[\mathcal{M}^{\lambda_l,\lambda_{\bar{l}}}_{\lambda_F,\lambda_{\bar{F}}}(\sqrt{s},\Theta)\right]^*$$

Observables described via spin-density matrices, directly constructed in MC event generators

Durupt/Maltoni/Mattelaer, 2510.17730. Ohl/Wüst, 26xx.xxxxx

Spin-density matrix for di-top (2 qubit) for entanglement variables:

$$\rho(\alpha,\beta,\gamma) = \frac{1}{4}\left(\mathbf{1} + \alpha_i\sigma_i \otimes \mathbf{1} + \beta_j \mathbf{1} \otimes \sigma_j + \gamma_{ij}\sigma_i \otimes \sigma_j\right)$$

Purity: $\frac{1}{4} \leq \quad \Gamma[\rho] := \mathrm{Tr}\left[\rho^2\right] \quad \leq 1$

Concurrence: $\max(0, \lambda_1 - \lambda_2 - \lambda_3 - \lambda_4)$

for matrix $\sqrt{\sqrt{\rho}(\sigma_y \otimes \sigma_y)\rho^*(\sigma_y \otimes \sigma_y)\sqrt{\rho}}$

density matrix of spin-flipped state

cf. e.g. Altakach/Lambda/Maltoni/Sakurai, 2601.09558

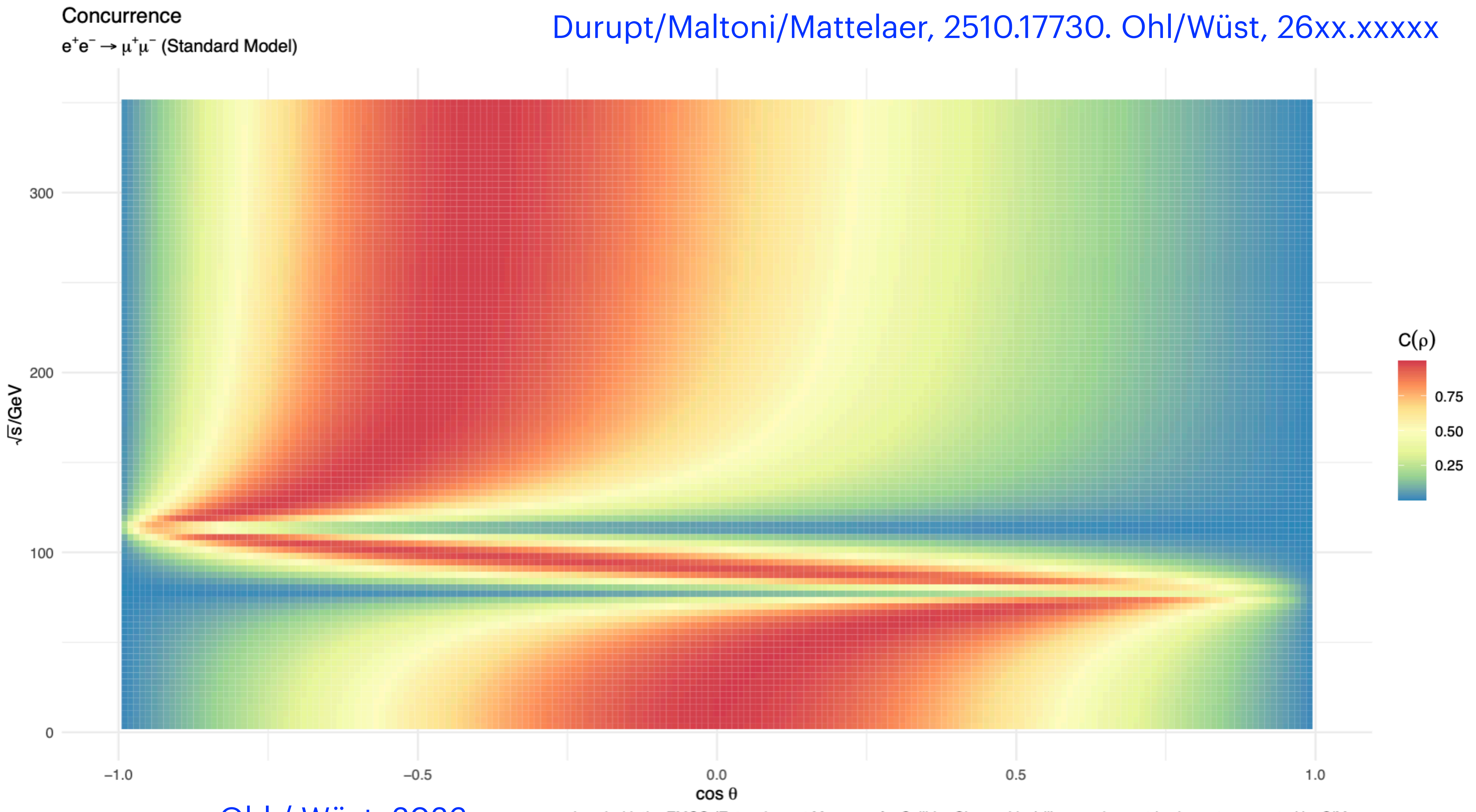

Ohl / Wüst, 2026